A transgenic approach to investigate the role of Epstein-Barr virus encoded RNA1 in lymphomagenesis

by

Claire E. Repellin

A THESIS PRESENTED FOR THE DEGREE OF DOCTOR OF PHILOSOPHY IN THE FACULTY OF BIOMEDICAL AND LIFE SCIENCES AT THE UNIVERSITY OF GLASGOW

IBLS Division of Molecular Genetics
Dumbarton road
Glasgow
G11 6NU

December 2005

In the memory of my grand-father Jean

Abstract

Epstein-Barr Virus (EBV) is associated with several human cancers including Burkitt's lymphoma (BL), Hodgkin's disease and nasopharyngeal carcinoma amongst others. In these cancers, a different subset of the viral latent genes are expressed, but all express the EBV small encoded RNAs: EBER1 and EBER2. The EBERs are polymerase III (pol III) genes but do not fall neatly into any of the 3 promoter types as they combine both pol II (Sp1, ATF and TATA-like box) and pol III elements (A and B boxes). The EBERs have been shown to confer resistance to interferon (IFN)-α-induced apoptosis via binding of the IFN-inducible, double-stranded (ds) RNA-activated protein kinase PKR and inhibition of its activation by phosphorylation. Evidence has also suggested an oncogenic role of the EBERs in BL cells, indicating their possible contribution to the disease process of EBV-associated tumours.

In order to investigate the potential role of EBER1 as an oncogenic RNA *in vivo*, 13 lines of transgenic mice designed to express EBER1 in lymphoid cells using three variant transgenes were generated. The transgenes incorporate a novel combination of tissue-specific RNA pol II and pol III elements. The efficacy of transgene expression was confirmed in culture. Mice of 10 of the transgenic lines were shown to express EBER1 in lymphoid tissues and the expression varied between the lines. The phenotypic consequences of EBER1 expression *in vivo* were examined and lymphoid expansion in mice of several lines was observed at a young age as well as the development of B-cell lymphoma in one of the lines. Cross-breeding programmes were undertaken and have shown that EBER1 does not cooperate in lymphomagenesis with EBNA1. However cooperation was observed in B-cell lymphomagenesis between EBER1 and N-myc although not with c-Myc. This might suggest that the oncogenic mechanism is elicited through cell survival.

The role of EBER1 in response to dsRNA stimulation was analysed *in vivo* and results indicate an inhibition of Stat1 expression and activation by EBER1, This might reflect downstream actions of blockade of the IFN pathway or a new pathway.

The results in this study support the hypothesis that EBER1 has oncogenic properties, the first pol III RNA described as such. This implicates the RNA in the pathogenesis of EBV associated lymphoma in addition to its role in immune evasion.

Acknowledgements

First of all I would like to thank Joanna Wilson my supervisor for her guidance and advice throughout this project, for all our inspiring conversations, for her suggestions and her proof-reading this thesis.

A big thank you to past and present members of the JBW lab, including David, Donald, Chrystalla, Liz, Nooshin and Yazeed. To Monica for her help, her presence during the long microinjection and dissection sessions, her support and most of all for her friendship. To Mark, for making sure my English vocabulary broaden itself whenever possible, and all his words of wisdom. To Adele, for being my fellow PhD lab friend and sharing a lot of the PhD life ups and moans, and being such a good friend. A thank you to Joanna, Mark, David and Adele for the Wednesday badminton sessions, loved them.

I would like to thank my assessors Sheila and Pam for their comments and suggestions throughout my PhD. I am grateful to the people in the Prep and wash rooms and also to Jane, Alexis, Joanne and Wendy for their efficiencies. I would also like to acknowledge the animal house staff for all their help during this project.

A huge thank you to my fellow French friends in Glasgow, especially Leila, Mario, Hubert, Aoibhinn, Sébastien and Audrey, for making life here look a little like home.

A massive acknowledgement to my family, especially to my parents and wee brother, who have always believed in me during all these years and pushed me in the right direction. Thank you for your support throughout my studies.

Finally to my husband, Vincent, who has been my rock during these last four years in Glasgow. Thank you for sharing my joys and pains and for your encouragements and support.

This work was supported by the Wellcome Trust.

Unless otherwise stated, all results were obtained by the author's own efforts.

Table of contents

Chapter 7. Discussion

List of figures

List of tables

Abbreviations

AAF	IFN-α-associated factor
ALNs	Axillary lymph nodes
APS	Ammonium persulfate
ATF	Activating transcription factor
BCR	B cell receptor
β-Me	β-mercaptoethanol
bp	Base pair
BSA	Bovine serum albumin
BL	Burkitt's Lymphoma
°C	Degree celsius
cDNA	Complementary DNA
Ci	Curie
CLNs	Cervical lymph nodes
CMV	Cytomegalovirus
CTARs	C terminal-activating regions
dCTP	Deoxycytosine triphosphate
DEPC	Diethyl pyrocarbonate
DMSO	Dimethylsulphoxide
DNA	Deoxyribonucleic acid
dNTP	Deoxynucleotide triphosphate
ds	Double stranded
DSE	Distal sequence element
DTT	Dithiotreitol
EAP	EBER-associated protein
EBERs	Epstein-Barr small encoded RNAs
EBNA	Epstein-Barr nuclear antigen
EBV	Epstein Barr Virus
E. coli	*Escherichia coli*

EDTA	Ethylenediaminetetra-acetic acid
eIF2α	α subunit of protein synthesis initiation factor
Eμ	Immunoglobulin heavy chain intronic enhancer
ETAB	EBER TATA box
EtBr	Ethidium bromide
EtOH	Ethanol
FACS	Fluorescence activated cell sorting
FBS	Foetal bovine serum
FITC	Fluorescein isothiocyanate
FSH	Follicule stimulating hormone
g	Gram or gravity
GAF	γ-activated factor
GAS	IFNγ-activated site
gDNA	Genomic DNA
H_2O	Distilled water
hCG	Human chorionic gonadotropin
HD	Hodgkin's disease
HHV	Human herpes virus
HRP	Horseradish peroxidase
HVP	Herpesvirus Papio
IFN	Interferon
IL	Interleukin
Ig	Immunoglobulin
IgH	Immunoglobulin heavy chain
IRF	Interferon responsive factor
ISGF3	IFN-stimulated gene factor 3
ISRE	IFN-stimulated response element
kb	kilobase
kDa	kilodalton
LB	Luria broth
L	Liver

LCL	Lymphoblastoid cell line
LH	Luteinizing hormone
LMP	Latent membrane protein
LN	Lymph node
mA	Milli Ampere
mg	Milligram
Mg	Magnesium
MLNs	Mesentheric lymph nodes
miRNA	MicroRNA
ml	Millilitre
µl	Microlitre
mM	millimolar
MMLV	Moloney Murine Leukemia Virus
MOPS	3-N-morpholinopropanesulphonic acid
mRNA	Messenger RNA
MCS	Multiple cloning site
ng	Nanograms
nm	Nanometres
NFAT	Nuclear factor activating transcription
NK	Natural killer
NP40	Nonidet P40
NPC	Nasopharyngeal carcinoma
OAS	Olygoadenylate synthase
OD	Optical density
PAGE	Polyacrylamide gel electrophoresis
PBS	Phosphate buffer saline
PCR	Polymerase chain reaction
PE	Phycoerythrin
pg	Picogram
pIC	Polyinosinic-polycytidilic acid

PKR	Interferon-inducible double-stranded RNA-activated protein
PLNs	Peripheral lymph nodes
pmol	picomol
PMS	Pregnant mare's serum gonadotropin
PMSF	Phenylmethylsulphonyl fluoride
pol III	RNA polymerase III
PP	Peyer's patches
PSE	Proximal sequence element
QPCR	Quantitative PCR
RBC	Red blood cell
RNA	Ribonucleic acid
RNAi	RNA interference
RNase	Ribonuclease
RNP	Ribonucleoprotein
rpm	Revolutions per minute
rRNA	Ribosomal RNA
RPMI	Roswell Park Memorial Institute
RT	Reverse transcription
S	Spleen
SDS	Sodium dodecyl sulfate
Ser	Serine
SFM	Serum Free Medium
shRNA	Small hairpin RNA
SILNs	Superficial inguinal lymph nodes
siRNA	Small interfering RNA
TCR	T cell receptor
spf	Specific pathogen free
Stat	Signal transducers and activators of transcription
Tyr	Tyrosine

U	Unit
UTR	Untranslated region
UV	Ultra violet
V	Volt
VA	Virus associated
v/v	Volume per volume
Wt	Wild type
w/v	Weight per volume

Chapter 1. Introduction

1.1. Epstein-Barr Virus

1.1.1. Discovery of the virus

Members of the *herpesviridae* family are classified into three subfamilies: alpha, beta and gamma on the basis of their biological properties. Epstein-Barr virus (EBV), also called Human Herpesvirus 4, is a ubiquitous gamma-herpes virus, which was discovered in 1964 in B lymphocytes cultured from an African Burkitt's lymphoma. Its presence was detected by electron microscopy (Epstein *et al.*, 1964) and it was the first time that this technique was used to confirm the presence of a virus.

EBV has a large double-stranded DNA genome, which encodes 87 genes (Kieff and Rickinson, 2001, Young and Rickinson, 2004, for reviews), including 11 latent genes (Figure 1.1). Two EBV types circulate in most populations, which are designated type 1, which is the most common type, and type 2. The main difference between the 2 genomes lies in the genes which encode the EBV nuclear proteins.

1.1.2. Primary infection, latent and lytic viral life cycles

More than 90 % of the world-wide population is estimated to be infected by EBV. The virus is normally contracted asymptomatically at an early age, via saliva and persists as a life-long infection in a latent state.

EBV infection takes place in the oropharynx of an individual. The virus infects naive B cells in the lymphoid tissue of Waldeyer's ring. However, there is increasing evidence that the epithelium at the site of infection has a role in primary infection and in virus shedding (Borza and Hutt-Fletcher, 2002). EBV enters the B cells via CD21, the EBV receptor. Monoclonal antibodies directed against CD21 can block EBV infection. The infection correlates with the expression of CD21 during B cell development (Fingeroth *et al.*, 1984). The crystal structure of CD21 has now been determined and a possible region

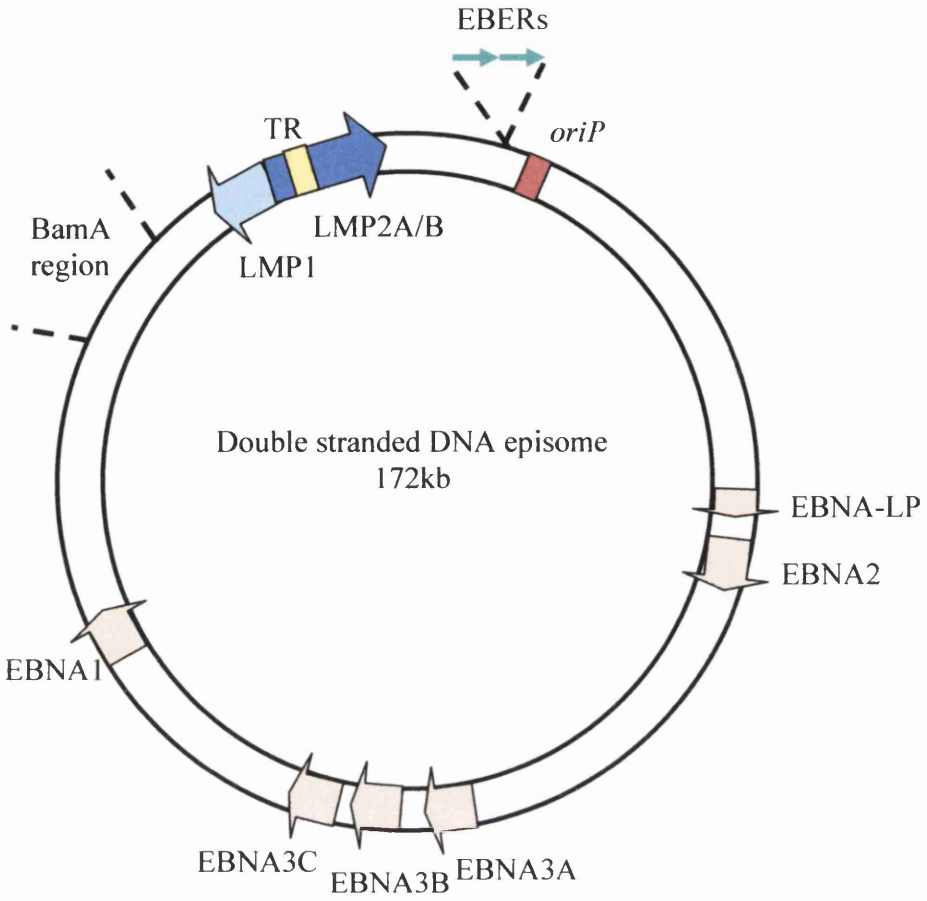

Figure 1.1: The EBV genome and the latent genes

This figure is a schematic diagram of the double stranded EBV episome showing the location of the different latent genes. The open reading frames of the latent proteins are indicated with block arrows (EBNA in light orange, LMP in blue) showing the transcriptional orientation of each gene. BamA region signifies *Bam*HI A region and includes the BARF0 and BARF1 genes. The EBNA genes include: EBNA-LP, EBNA2, EBNA3A, EBNA3B, EBNA3C and EBNA1. The LMP genes include LMP1, LMP2A and LMP2B. The terminal repeats are shown in the yellow box and the origin of replication (*oriP*) in a red box. The location and orientation of the EBERs (EBER1 and EBER2) are shown with green arrows. The figure is not to scale. EBNA: EBV nuclear antigen, LMP: latent membrane protein, EBER: EBV encoded RNA. This figure was modified from Murray and Young, 2001.

for EBV attachment was identified (Prota *et al.*, 2002). The most abundant glycoprotein of EBV, gp350/220, was shown to be the CD21 ligand (Nemerov *et al.*, 1987, Nemerov *et al.*, 1989) (Kieff and Rickinson, 2001, for review). Adsorption of gp350/220 to CD21 on the B-lymphocyte plasma membrane initiates infection of primary B lymphocytes. The interaction between gp42 and HLA class II, which functions as a co-receptor, is also required for infection (Wang and Hutt-Fletcher, 1998, Li *et al.*, 1997a). This step is followed by aggregation of CD21 in the plasma membrane and internalization of EBV into cytoplasmic vesicles (Carel *et al.*, 1990).

Once the virus enters the naive B cells, it switches on the growth programme leading to the activation of B cells, which can enter germinal center reactions without the presence of an antigen. Germinal center B cells will then differentiate into memory B cells (Thorley-Lawson and Gross, 2004, for review). Through the differentiation process, different sets of the latent genes are expressed (Babcock *et al.*, 2000). For instance, during the growth programme all of the latent genes are expressed (Joseph *et al.*, 2000), whereas germinal center B cells express only EBNA1, LMP1 and LMP2A. In the memory B cells, the virus enters the latency programme where it is thought that no viral protein is expressed (Hochberg *et al.*, 2004), unless the memory cell divides in which case EBNA1 will be expressed to ensure viral DNA replication. The replication of viral DNA during the latent phase occurs only once per cell cycle (Adams, 1987). Memory B cells are the perfect hosts for the virus as they are long lived cells and therefore EBV can persist for long periods of time and also remain undetected by the immune system as no viral proteins are expressed.

Reactivation and replication occur within healthy carriers in order to produce new virions, which can then infect new hosts (Amon and Farrell, 2005 for review). In tissue culture assays, it was shown that the virus can be induced to enter the lytic cycle by cross-linking IgG to the B cell receptor (BCR). In order to induce reactivation, the virus needs a latency programme where no LMPs are expressed as LMP2A has been shown to block reactivation of the lytic cycle following IgG cross-linking (Miller *et al.*, 1994). During lytic replication several rounds of replication are initiated from the origin (*oriLyt*) (Hammerschmidt and Sugden, 1988). Lytic gene expression follows a specific order starting first with the immediate early genes, BZLF1 and BRLF1 (Biggin *et al.*, 1987), then the early genes and finally the late genes (Tsurumi *et al.*, 2005, for review). It was shown that the expression of BZLF1 alone can transactivate the early promoter and therefore

induce the lytic cycle (Rooney *et al.*, 1989). BZLF1 was shown to activate its own expression as well as that of BRLF1 (Speck *et al.*, 1997). The gene product of BRLF1 is also a transactivator and activates various viral and cellular promoters. BRLF1 was shown to bind the retinoblastoma protein *in vivo* early after reactivation (Zacny, *et al.*, 1998). This interaction initiates cell cycle progression and thus production of viral DNA during the lytic cycle. The early genes are involved in DNA replication whereas the late genes encode the viral structural proteins.

1.1.3. The different diseases associated with EBV

As mentioned previously, infection usually occurs at an early age. However, if the primary infection occurs post-puberty, this can result in infectious mononucleosis (IM), also called glandular fever (Steven, 1996, for review).

EBV is also associated with several malignancies (Rickinson and Kieff, 2001, Baumforth *et al.*, 1999, Kuppers, 2003, for reviews) including Hodgkin's disease (HD) (about 50% of cases) (Kuppers and Rajewsky, 1998, for review), Burkitt's lymphoma (BL) (Magrath, 1990, for review), nasopharyngeal carcinoma (NPC) (Raab-Traub, 1992, Spano *et al.*, 2003, for reviews) and some rare T cell lymphomas (Meijer *et al.*, 1996, for review). In immune-deficient individuals EBV can cause lymphoproliferative disease (Gaidano *et al.*, 1998). EBV has also been linked to post-transplant lymphoproliferative disease (PTLD) (Nalesnik, 1998).

Different subsets of the latent genes are expressed in the different EBV associated tumour cells. For instance, in BL only EBNA1 and the EBERs, are expressed, which is termed latency I, whereas in HD and NPC, EBNA1, LMP1, LMP2 and the EBERs are expressed, which is termed latency II (Table 1.1).

1.1.4. Burkitt's lymphoma

Denis Burkitt, who was a surgeon working in East Africa, identified a new tumour occurring in children, which is now known as Burkitt's lymphoma (BL) (Burkitt, 1962). There are two forms of BL an endemic form (eBL), which is 100% associated with EBV,

Latency stage	EBV latent genes expressed	Associated malignancies
I	EBNA1, EBERs and *Bam*HI A	Burkitt's lymphoma
II	EBNA1, LMP1, LMP2A, LMP2B, EBERs and *Bam*HI A	Nasopharyngeal carcinoma, Hodgkin's disease, Peripheral T-cell lymphoma
III	EBNA1, EBNA3, EBNA4, EBNA5, EBNA6, LMP1, LMP2A, LMP2B, EBERs and *Bam*HI A	Lymphoproliferative disease, Post-transplant lymphoproliferative disease, infectious mononucleosis

Table 1.1: The latent genes expressed in the different EBV associated malignancies

and a sporadic form (sBL). The endemic regions include equatorial Africa and coastal New Guinea and are coincident with the malaria belt. It has been suggested that the immunosuppression resulting from the malarial infection increases the chances of BL occurring. The sBL form is found world-wide at an incidence 50 to 100 times lower than the eBL. In Europe and the United States 15% to 25% of sBL tumors are EBV genome positive. A third form of BL is found in AIDS patients and 30% to 40% are associated with EBV.

Both eBL and sBL are characterised by chromosome translocations of chromosome 8 and either chromosomes 2, 14 or 22. The translocation results in the juxtaposition of the *c-myc* locus (on chromosome 8) to one of the immunoglobulin (Ig) heavy or light chain loci and leads to the abnormal overexpression of c-Myc in B cells. The most common translocation in BL is t(8;14) and the break points were shown to be different in eBL and sBL forms. In eBL, the breaks in chromosome 8 occur outside the *c-myc* locus whereas in sBL the breaks occur either 5' to the first non-coding exon, within the first exon or within the first intron of myc (Pelicci *et al.*, 1986). The breaks in chromosome 14 occur 5' to or within the heavy chain joining region for eBL whereas in sBL the breaks occur near the μ switch region (Neri *et al.*, 1988). The t(8;14) translocation is found in 80% of cases, the remaining translocations t(8;2) and t(8;22) account for 10% each and result in translocation of the light chain genes to the 3' region of the *c-myc* sequence.

Other genetic and epigenetic changes are observed in BL following tumour progression (Lindstrom and Wiman, 2002, for review). p53 is often mutated in BL (Farrell *et al.*, 1991) and the mutations are clustered in the core domain of p53 (Vousden *et al.*, 1993). In other cases of BL, MDM2 is overexpressed which leads to inactivation of wild-type p53 (Capoulade *et al.*, 1998). p16*INK4*α was found inactivated by promoter methylation in 42% of the primary BL tumours and 89.5% of the BL cell lines examined (Klangby *et al.*, 1998). This leads to the inactivation of the retinoblastoma protein (pRb) pathway. p14ARF loss has been detected in BL at a much lower frequency (6%), which leads to inactivation of p53, as p14ARF was shown to stabilise p53. Some of these tumours carried wild-type p53 and overexpression of MDM2 (Klangby *et al.*, 1998, Lindstrom *et al.*, 2001).

In BL, EBV appears to be a contributing factor rather than an essential factor as sBL can arise without the presence of EBV. Only two of the latent genes are expressed in this B cell malignancy and these are EBNA1 and the EBERs. The expression of LMP1 and EBNA2 has been reported in less than 1% of eBL (Niedobitek *et al.*, 1995) and in more than 1% of non-endemic BL (Carbone and Gloghini, 1996). EBNA1 was first suggested to supply an oncogenic function following the generation of EμEBNA1 transgenic mice (Wilson and Levine, 1992, Wilson *et al.*, 1996). A subsequent study on the EμEBNA1 suggested a survival function for EBNA1 in this model (Tsimbouri *et al.*, 2002). It has been shown that inhibition of EBNA1 using a dominant negative approach in cultured BL cells leads to decreased survival and induction of apoptosis in EBV positive BL cells. It was therefore suggested that EBNA1 is a critical factor for survival of EBV positive BL (Kennedy *et al.*, 2003). The EBERs could also provide a survival factor as they have been reported to confer resistance to apoptosis (Komano *et al.*, 1999). This will be described in more detail in section 1.3.5.

1.2. The different latent protein encoding genes of EBV

1.2.1. The EBV nuclear antigens

1.2.1.1. EBV nuclear antigen 1

EBV nuclear antigen 1 (EBNA1) is the only viral protein expressed in all the disease states of EBV. However, it has been shown that EBNA1 is not essential for transformation of B-cells in culture but enhances this process (Humme *et al.*, 2003). EBNA1 is a sequence specific DNA binding protein (Rawlins *et al.*, 1985) and has a critical role in the maintenance and replication of the EBV genome (Yates *et al.*, 1985). This is achieved by binding to the episomal origin of replication, *oriP* (Kieff and Rickinson, 2001, for review). *OriP* is composed of 20 copies of the EBNA1 binding site in tandem repeats, called the family of repeats (FR), localised 1kb away from the dyad symmetry element (DS), which comprises four copies of the EBNA1 binding site. Upon binding to DNA, EBNA1 brings FR and DS in close proximity. Using a yeast two-hybrid approach, it was shown that a human cellular protein, termed EBNA1 binding protein 2 (EBP2), binds EBNA1 and is important for plasmid maintenance (Shire *et al.*, 1999). It

was recently demonstrated that repression of EBP2 expression lead to a decrease in the EBNA1 capacity to bind mitotic chromosomes and that EBP2 was regulated by a kinase from the Aurora B kinase family (Kapoor *et al.*, 2005). Aurora kinases phosphorylate histone H3 providing a direct path to the nucleosome and are regulators of cytokenesis during mitosis.

EBNA1 is composed of three different domains: a short N-terminal domain followed by a glycine-alanine (gly/ala) repeat domain and a C-terminal domain. The gly/ala domain varies in its number of repeats depending upon the EBV strain, which leads to a variation in the size of the protein (Kieff and Rickinson, 2001). This domain stabilises the mature protein preventing it being degraded by the proteasome (Levitskaya *et al.*, 1997) and also enables the protein to escape from immune surveillance. It does this by preventing antigen processing and thus presentation through MHCI; as a consequence the protein cannot be recognised through cytolytic $CD8^+$ interactions (Levitskaya *et al.*, 1995). Furthermore, this region limits "self" expression also helping in immune detection by limiting protein levels. The C-terminal domain of EBNA1 comprises the dimerisation domain, as EBNA1 binds to DNA as a dimer (Bochkarev *et al.*, 1995), the DNA binding domain, a transcriptional activation domain and a nuclear localisation domain.

1.2.1.2. EBV nuclear antigen 2

EBV nuclear antigen 2 (EBNA2) is a transcription factor of both viral genes (LMP1 and LMP2B) and cellular genes (CD21, CD23 and others) (Wang *et al.*, 1987, Wang *et al.*, 1990, Abbot *et al.*, 1990, Cordier *et al.*, 1990). EBNA2 does not bind to DNA directly, instead it interacts with a sequence-specific DNA binding protein RBP-Jκ to regulate gene expression (Grossman *et al.*, 1994).

EBNA2 plays a crucial role in the transformation process of B-cells *in vitro* by EBV. This was demonstrated by the EBV P3HR-1 strain, which has a deletion in the EBNA2 gene and the last two exons of EBNA-LP and is unable to transform B cells *in vitro* (Cohen *et al.*, 1989). Cellular proteins whose expression was up or down regulated by EBNA2 were recently identified using a proteomics approach and were shown to be similar to those observed following EBV infection (Schlee *et al.*, 2004). c-Myc was also

shown to be directly activated by EBNA2 (Kaiser *et al.*, 1999) and thus could be an important factor for EBV induced B cell proliferation.

1.2.1.3. EBV nuclear antigen 3 family

The EBNA3 genes are adjacent on the viral genome (figure 1.1) and are termed EBNA3A (or EBNA3) (Hennessy *et al.*, 1986), EBNA3B (or EBNA4) and EBNA3C (or EBNA6). EBNA3A and 3C have been shown to have an essential role in B cell transformation *in vitro* using EBV recombinant viruses (Tomkinson *et al.*, 1993) whereas EBNA3B was found to be dispensable (Tomkinson and Kieff, 1992). However, EBNA3B has been shown to induce expression of CD40 and vimentin when stably transfected into EBV negative B cells (Silins and Sculley, 1994). EBNA3A was also shown to be important for the growth maintenance of LCLs (Maruo *et al.*, 2003, Maruo *et al.*, 2005). EBNA3C functions as a transactivator (Subramanian *et al.*, 2002, for review) as its expression in Raji cells (which have a deletion in EBNA3C) increases the expression of LMP1 (Allday and Farrell, 1994). EBNA3C was also shown to repress the Cp promoter, and therefore can negatively regulate the expression of EBNA proteins including itself (Radkov *et al.*, 1997). *In vitro* translated EBNA3C binds pRb, which is dependent on the pocket domain of pRb (Parker *et al.*, 1996). The EBNA3 proteins (like EBNA2) interact with RBP-Jκ (Robertson *et al.*, 1996). This disrupts RBP-Jκ binding to EBNA2 thus repressing EBNA2 mediated transactivation. The binding of EBNA3A to RBPJκ was shown to be important for LCL growth (Maruo *et al.*, 2005).

1.2.1.4. EBV nuclear antigen leader protein

EBNA-leader protein (LP) is also termed EBNA5. It is encoded by the 5' leader of each of the EBNA mRNAs (Kieff and Rickinson, 2001), and thus is a protein of variable size. Along with EBNA2 it is one of the first latent proteins expressed. EBNA-LP in cooperation with EBNA2 induces the G_o to G_1 transition of resting B cells, which is measured by an increase in cyclin D2 expression (Sinclair *et al.*, 1994). EBNA-LP also cooperates with EBNA2 in upregulating transcriptional targets of EBNA2, including LMP1 (Nitsche *et al.*, 1997). EBNA-LP has been shown to co-localise with the retinoblastoma protein (pRb) in LCLs and it was shown *in vitro* that it binds both pRB and

p53 (Szekely *et al.*, 1993). EBNA-LP is not required for immortalisation of cultured B-cells; however mutants of EBNA-LP genes show an impaired ability to transform primary B cells (Mannick *et al.*, 1991, Allan *et al.*, 1992).

1.2.2. The latent membrane proteins

1.2.2.1. Latent membrane protein 1

Latent membrane protein 1 (LMP1) is thought to be the main transforming protein of EBV due to its classic oncogene activity in the ability to transform rodent fibroblasts in culture and lead to a tumourigenic phenotype of these cells in nude mice (Wang *et al.*, 1985). LMP1 is essential for EBV immortalisation of B cells in culture (Kaye *et al.*, 1993). Furthermore in transgenic mice, LMP1 expression under the control of a polyomavirus or viral L2 promoter leads to the early stages of epithelial neoplasia (Wilson *et al.*, 1990, Stevenson *et al.*, 2005) and with an IgH enhancer predisposes mice to B cell neoplasia (Kulwichit *et al.*, 1998, and our laboratory unpublished observations). LMP1 is a transmembrane protein composed of a short cytoplasmic N-terminal domain, six hydrophobic transmembrane domains and a long C-terminal domain (Eliopoulos and Young, 2001, Li and Chang, 2003, for reviews). LMP1 is a constitutively active receptor-like molecule, which simulates an activated CD40 (Gires *et al.*, 1997, Kilger *et al.*, 1998). LMP1 exerts its function via its C-terminal domain, which encompasses three different regions termed C-terminal-activating regions (CTAR) 1, 2 and 3. CTAR1 binds the complex of cellular proteins belonging to the family of tumour necrosis factor receptor associated factors (TRAFs) whereas CTAR2 binds tumour necrosis factor-receptor death domain proteins (TRADDs). Through these associations, several signaling pathways are activated including the NFκB pathway (Huen *et al.*, 1995), MAPK pathways (Eliopoulos *et al.*, 1999b), JNK pathway (Eliopoulos *et al.*, 1999a), and PI3K, Akt pathways (Dawson *et al.*, 2003). The Jak-Stat pathway is activated via CTAR3 (Gires *et al.*, 1999). The oligomerisation of LMP1 at the plasma membrane is essential for activation of cell signaling (Liebowitz *et al.*, 1992) and it has recently been shown that LMP1 is associated with lipid rafts (Rothenberger *et al.*, 2002).

1.2.2.2. Latent membrane proteins 2A and 2B

Two distinct proteins are encoded by the latent membrane protein 2 (LMP2) gene: LMP2A and LMP2B (Sample *et al.*, 1989). With differential promoter usage LMP2A incorporates an additional 5' exon and hence N-terminal sequence compared to LMP2B. They both have 12 transmembrane domains and a short C-terminal domain. LMP2A also has a long Nt domain (Longnecker and Kieff, 1990). The use of EBV recombinants with mutations in different LMP2 parts demonstrated that the LMP2 proteins are not essential for EBV transformation of B-cells (Longnecker *et al.*, 1993a, Longnecker *et al.*, 1993b, Longnecker, 2000). They were also shown to be dispensable for *in vivo* growth of EBV infected B-cells following injection in SCID mice (Rochford *et al.*, 1997). LMP2A was shown to associate with LMP1 in the plasma membrane of latently infected cells (Longnecker *et al.*, 1991) and like LMP1, LMP2A associates with lipid rafts (Dykstra *et al.*, 2001). The N-terminal domain of LMP2A contains an immunoreceptor tyrosine-based activation motif (ITAM) (Fruehling and Longnecker, 1997), which can be phosphorylated and is usually found on the B cell receptor (BCR) complex. The Src family of protein kinases (PTKs) and Syk interact with phosphorylated ITAM, usually following BCR stimulation, and with LMP2A. As mentioned previously, in tissue culture assays the virus can be induced to enter the lytic cycle by cross-linking IgG to BCR. As LMP2A was shown to mimic BCR signalling in transgenic mice (Caldwell *et al.*, 1998), it was thought that LMP2A could also induce the lytic cycle. Unexpectedly, following IgG cross-linking, LMP2A prevented activation of the lytic cycle in B-cells. This was shown to occur via blocking of BCR-stimulated calcium mobilization and phosphorylation of signalling molecules through LMP2A's association with Lyn and Syk (Miller *et al.*, 1994, Miller *et al.*, 1995). LMP2A was also shown to block BCR from entering lipid rafts and thus subsequent signalling from the receptor (Dykstra *et al.*, 2001). Recently, a dual role for LMP2A in reactivation was suggested. In permissive B-cells, LMP2A was shown to induce the lytic cycle when acting alone, whereas following stimulation of BCR LMP2A was shown to inhibit reactivation (Schaadt *et al.*, 2005).

1.3. The EBV encoded RNAs

The EBV encoded RNAs (EBERs) encode two small non-polyadenylated RNAs called EBER1 and EBER2 (Clemens, 1993, Clemens, 2006, for reviews). The EBERs are transcribed by RNA polymerase III (RNA pol III) (Rosa *et al.*, 1981, Howe and Shu, 1989) and are the most abundant viral transcripts in some latently EBV-infected cells; for instance the EBER1 level has been estimated to be as high as 10^7 molecules per cell (Lerner *et al.*, 1981). EBER1 is usually more abundant by 10 fold than EBER2, which is due to a faster turnover of EBER2 (0.75 hours) compared to that of EBER1 (8-9 hours) (Clarke *et al.*, 1992). Their abundance varies in different cell lines and may be related to the copy number of EBV DNA (Lerner *et al.*, 1981, Arrand and Rymo, 1982). Their abundance allows them to be readily used as target molecules for detection of EBV-infected cells in tissues by *in situ* hybridization, and their detection is considered a highly reliable marker of the presence of EBV (Wu *et al.*, 1991).

1.3.1. Structure of the EBERs

The EBERs are encoded by the right-hand 1000 base pairs of the *Eco*RI J fragment (Figure 1.2) of the EBV genome (Lerner *et al.*, 1981, Arrand and Rymo, 1982) and are transcribed from left to right on the EBV genome map (Arrand and Rymo, 1982). The EBER1 and EBER2 transcripts are 167 and 172 nucleotides long respectively and are separated in the genome by 161 bp (Rosa *et al.*, 1981).

The primary sequence of the *Eco*RI J fragment has been compared between five different EBV strains, which were isolated from different pathologies and in different geographical locations. No variation in the EBER1 sequence was observed between the different strains, whereas two single base pair changes were observed for the EBER2 gene at positions 68 (G to A) and 168 (A to G). Several base pair changes were observed in the region between EBER1 and EBER2 (Arrand *et al.*, 1989). A single base pair change was observed in the region 5' of the EBER1 promoter and two substitutions were observed in the region 3' of the EBER2 gene. These minor changes grouped the strains into two families, which corresponds with the two EBV types. This study suggests that a precise

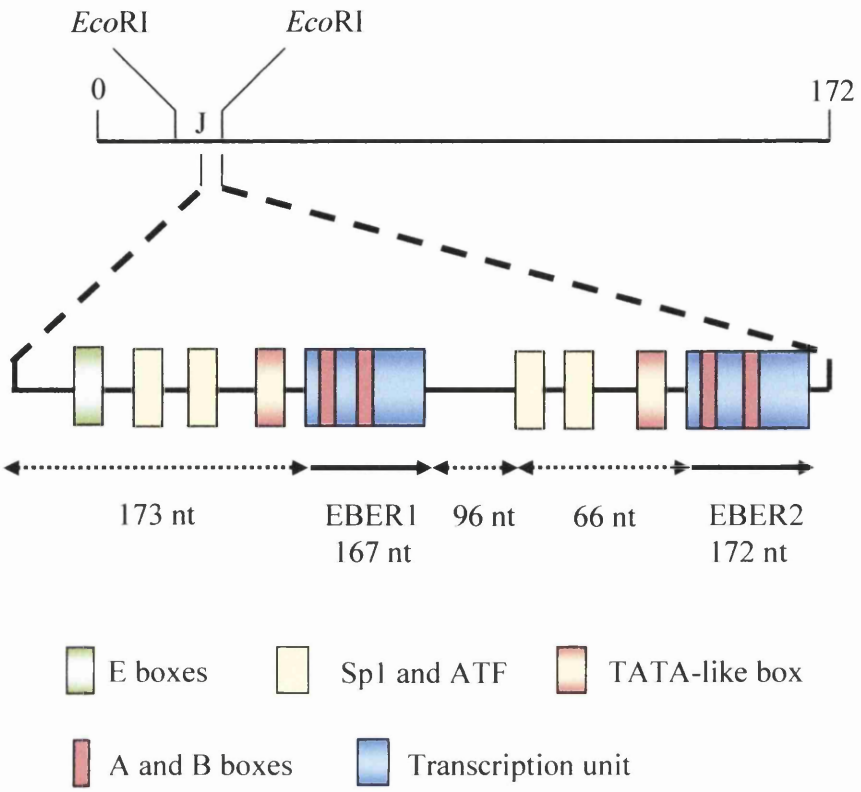

Figure 1.2: Diagrammatic representation of the EBER genes

The top line indicates the linear EBV genome (172kb) with the relative location of the *Eco*RI J fragment (see also figure 1.1). The bottom line indicates the EBER1 and EBER2 genes along with their promoter elements. The c-Myc binding sites (E boxes) on the EBER1 promoter is shown in green and white. The upstream elements are shown in yellow and in yellow and red for the TATA-like element. The internal elements are shown in red. The transcriptional regions of the EBERs are shown in blue and the transcriptional direction of the two genes is indicated by an arrow. This diagram is not to scale. The figure is modified from Clemens 1993.

sequence is important for the function of these RNAs. This could be needed for the secondary structure of the EBERs, since both EBER1 and EBER2 are predicted to form extensively base-paired structures containing a number of short stem loops (Figure 1.3) (Rosa *et al.*, 1981, Glickman *et al.*, 1988). Herpesvirus Papio (HVP) is a baboon virus whose genome is co-linear with that of EBV and its small RNAs were shown to cross-hybridise with the EBER sequence. The secondary structure of the HVP RNAs is also conserved (Howe and Shu, 1988). Therefore, the structure of the EBERs is likely to be critical for their interaction with specific proteins and thus for their function *in vivo*.

1.3.2. Expression of the EBERs by RNA polymerase III

1.3.2.1. The RNA polymerase III

The eukaryotic RNA pol III synthesizes 5s rRNA, tRNAs, 7 spliced leader (SL) RNA, U6 small nuclear (Sn) RNA and a few other small stable RNAs and small viral RNAs such as the EBERs and the virus-associated (VA) RNAs of Adenovirus (Mathews and Shenk, 1991, for review). The VA RNAs are two small highly structured pol III RNAs. One of the features of pol III action is that some of the promoters of pol III genes require sequence elements downstream of the transcription start within the transcribed region (Paule and White, 2000, for review). The promoters of pol III genes are divided into three types (Figure 1.4). Type I promoter is unique to 5s RNA and is composed of three internal elements: an A block, an intermediate element and a C block. The type II promoter is the most common type and is found in tRNA genes. This promoter contains two internal elements, the A and B blocks. The A blocks from type I and II promoters are homologous and interchangeable (Ciliberto *et al.*, 1983). The location of block B is variable as well as the space between A and B blocks. On type II promoters, the transcription complex assembly first involves binding of transcription factor (TF) IIIC to A and B blocks. TFIIIC then recruits TFIIIB, containing the TATA-binding protein (TBP), which in turn recruits pol III (Geiduschek and Kassavetis, 2001, for review). In *Saccharomyces cerevisiae*, it was shown that TFIIIB alone recruits pol III (Kassavetis *et al.*, 1990). It was recently shown that c-Myc is also involved in activation of pol III transcription by binding to TFIIIB (Gomez-Roman *et al.*, 2003). With type I promoters, the transcription complex assembly is similar to that of type II promoters, except for the binding of TFIIIA on A and C blocks, which then recruits TFIIIC. The third promoter type (type III) does not require internal

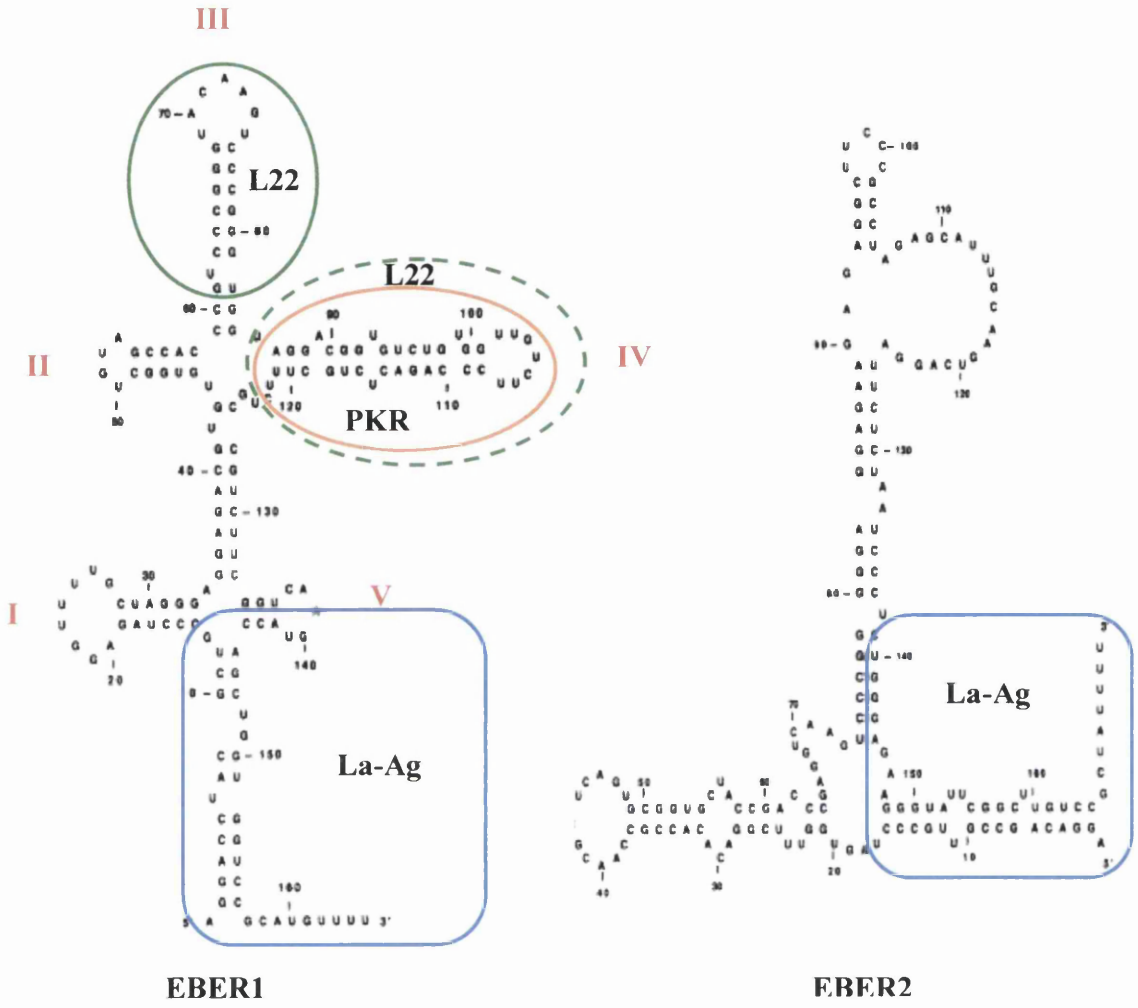

Figure 1.3: The protein binding sites of EBER1 and EBER2

The EBER1 and EBER2 secondary structures are presented (as modified from Howe and Shu, 1988) in this figure along with their identified protein binding sites. The La-antigen (La-Ag) binding site of both EBER1 and EBER2 is presented in a blue box. The PKR binding site of EBER1 is presented in an orange circle. The L22 major binding site is presented as a green circle and the minor binding site as a dashed green circle. The stem-loop number of EBER1 is presented in red and with Roman characters.

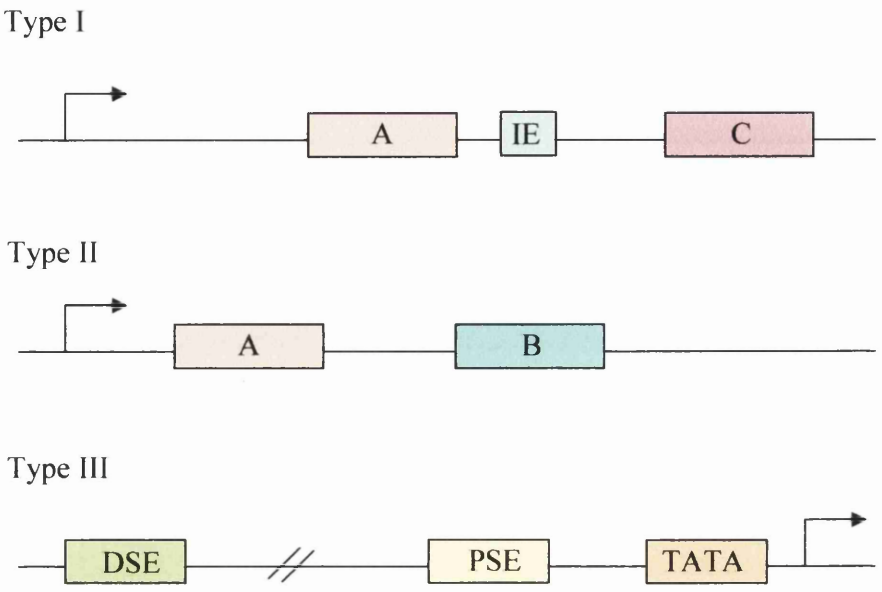

Figure 1.4: The three types of promoters used by RNA polymerase III

The arrow on each promoter indicates the transcription start. The positions of the various promoter elements are also indicated and include the A (orange), B (blue) or C (pink) blocks, the intermediate element (IE) (light blue), TATA box (light orange), proximal sequence element (PSE) (light yellow) and distal sequence element (DSE) (light green).

The figure was adapted from Paule and White, 2000.

promoter elements, instead it has three upstream elements: a TATA box, a proximal sequence element (PSE) and a distal sequence element (DSE). The factors that bind these elements are different from types I and II except for the binding of TFIIIB on the TATA box. Proximal element transcription factor (PTF) binds PSE and Oct1 binds DSE. Both these factors interact and this interaction stabilises their binding to DNA. PTF also interacts with TBP (Geiduschek and Kassavetis, 2001, for review). RNA pol III, unlike pol I and II, does not require the presence of various factors to terminate transcription. Instead, pol III recognizes a stretch of T (four or more) as the termination signal. The polymerase then releases the transcript.

1.3.2.2. The EBER promoter

The EBER genes are pol III genes but do not fall neatly into any of the 3 promoter types as they combine both pol II and pol III elements (Figure 1.5). They have internal A and B blocks which are characteristic of type II promoters and are essential for pol III transcription (Figure 1.5A, red) (Howe and Shu, 1989). However, the efficient transcription of the EBER genes also requires 3 upstream elements: a TATA-like box (TGTA, -28 to -23, relative to the start site for transcription for EBER1), activating transcription factor (ATF) binding site (-51 to -47 for EBER1) and Sp1 binding site (-65 to -60 for EBER1) which are usually associated with sequences transcribed by RNA polymerase II (Howe and Shu, 1988, 1989) (Figure 1.5A, in yellow and in yellow and orange).

The deletion of all three upstream elements from either the EBER1 or EBER2 promoter reduces transcription levels by more than 95% compared to a wild-type promoter in transfection assays (Howe and Shu, 1989). The deletion of both Sp1 and ATF elements showed a similar reduction in EBER2 transcription. However, sequences upstream of Sp1 in the EBER2 promoter are not essential for transcription, as their deletion did not affect the transcription of EBER2. The promoter of EBER2 was studied in more detail by testing mutated promoters in transfection assays. A mutation in the ATF binding sequence decreased transcription by 50% compared to a wild-type promoter, whereas mutation in either Sp1 or the TATA-like box decreased transcription by 80%. The authors also showed that the internal elements (A and B box) were essential for transcription of EBER2 as deletion of either element led to a drastic decrease in EBER2 expression.

A

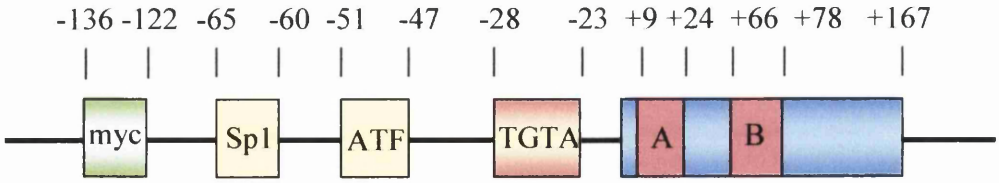

B

```
6301 gaaaggtcag cctgcaaggt ggatggcgtg ttttctgagg ttatccccgc tacgtgcagt
6361 gctgggtgat agagacccta gaatgtgtcg aaatgaccaa gcgtccccgc agcggggctc
6421 ccaacacggg ttcccagaga gggtaaaaga gggggccata aagcccaggg tgtaaaacac
6481 cgaccgcgcc accagatggc acacgtgggg gaaatgaggg ttagcatagg caacccccgc
6541 ctacacacca actatagcaa accccgcccc gtcacggtga cgtagtctgt cttgaggaga
6601 tgtagacttg tagacactgc aaaacctcag gacctacgct gccctagagg ttttgctagg
6661 gaggagacgt gtgtggctgt agccacccgt cccgggtaca agtcccgggt ggtgaggacg
6721 gtgtctgtgg ttgtcttccc agactctgct ttctgccgtc ttcggtcaag taccagctgg
6781 tggtccgcat gtttt
```

Figure 1.5: The EBER1 promoter and sequence

A diagram of the EBER1 promoter is presented in panel A. The c-Myc E boxes (myc) are shown in green and white. The three upstream elements are shown in yellow (Sp1 and ATF sites) and in yellow and orange (TATA-like box). The A and B boxes are shown in red. The nucleotide position of the different promoter elements is indicated where +1 is the start of the EBER1 gene. Panel B shows the nucleotide sequence of the EBER1 promoter and gene. The Sp1 and ATF binding sites are shown in blue and bold. The TATA-like box is shown in dark purple and bold and the A and B boxes are in red and bold. The EBER1 transcribed sequence is underlined. The nucleotide position is indicated on the left hand-side and is relative to the B95.8 sequence.

A study similar to this was undertaken to characterise the EBER1 promoter further (Wensing *et al.*, 2001). Successive deletion mutants of the different upstream elements of the EBER1 promoter were transiently transfected into 293 cells and EBER1 expression was compared to wild-type by northern blot. The results showed that like EBER2, the sequences upstream of the Sp1 site are not required for efficient transcription in this system. Deletion of the Sp1 site reduced transcription by 50%. Deletion of both Sp1 and ATF resulted in very little EBER1 expression. No additional effect was observed when the three upstream elements were deleted. The authors also showed that the presence of *oriP* (the sequence immediately 3' to the EBER2 gene) and EBNA1 (which binds to and transactivates this sequence) increased EBER1 expression by two to four fold.

Several new binding sites were identified on the EBER promoters by genomic footprinting: one additional Sp1 site and two other binding sites (W and X) for EBER1, and two additional binding sites (Y and Z) for EBER2. Site X of EBER1 has two E boxes and it was demonstrated that c-Myc binds this element (Figures 1.2 and 1.5A) (Niller *et al.*, 2003). This finding suggests a direct role and contribution between EBER1 and c-Myc.

The TATA-like box of EBER2 was studied in more detail and was termed EBER TATA box or ETAB (Howe and Shu, 1993). The ETAB element is located at a pol II TATA box position (-28 -23). However, its consensus sequence is different from that of a TATA box (TGTAGA compared to TATAA). The ETAB promoter element does not function as a pol II TATA box and does not substitute for a TATA box *in vitro*. Different nucleotides in the EBER2 ETAB were mutated and the constructs were transfected into BJAB cells (an EBV negative BL cell line). When ETAB was mutated to a consensus TATA box, EBER2 transcription was inhibited. The results from the various ETAB mutants suggested that the correct ETAB sequence is necessary for EBER2 transcription. In *in vitro* transcription assays, it was shown that by replacing the ETAB element by a consensus TATA box followed by two G nucleotides instead of a thymidine doublet EBER2 could be transcribed by both pol II and pol III. This suggested that the ETAB confers pol III specificity for EBER2 transcription. As EBER1 and EBER2 have similar ETABs, one can hypothesise that this also applies for the EBER1 TATA-like box and that the presence of this element is necessary for EBER1 transcription by RNA pol III.

1.3.3. Subcellular localisation of the EBERs

Low resolution *in situ* hybridisation data initially suggested that these RNAs have a nuclear location in Raji cells (Howe and Steitz, 1986). However, high resolution confocal laser scanning microscopy combined with *in situ* hybridisation using fluorescent probes has shown that both RNAs occur abundantly in both the cytoplasm and the nucleus of exponentially growing Raji cells (Schwemmle *et al.*, 1992). The nuclear localisation of the La antigen was also confirmed (an EBER1 binding protein, section 3.4.1), suggesting that this protein does not interact with the EBERs in the cytoplasm. It was also demonstrated that in the cytoplasm DAI (also known as PKR, another EBER1 binding protein, section 3.4.3) co-localises with EBER1 in the rough ER region. However, during mitosis, the staining generated with the EBER probes was different than that obtained during interphase, and showed that during this phase the EBERs are not associated with either the La antigen or PKR. It seems likely that the EBERs exist in both nucleus and cytoplasm.

1.3.4. Interaction of the EBERs with cellular and viral proteins

To date, the EBERs has been shown to bind four host cell proteins: the La antigen, the small EBER-associated protein (EAP)/L22, the interferon-inducible protein kinase PKR, 2'5' oligoadenylate synthase (2'5'OAS) and one viral protein: EBNA1.

1.3.4.1. The La antigen

The La protein was first identified as an autoantigen from patients with Systemic lupus erythematosus and Sjogren's syndrome. Anti-La antibodies were used to immunoprecipitate La ribonucleoproteins (RNPs) from radioactive cell extracts, which showed that La was associated with a number of small RNAs (Maraia and Intine, 2001, for review). The La antigen was also shown to associate with viral small RNAs, such as adenovirus VAI and VAII (Rosa *et al.*, 1981), the EBERs (Lerner *et al.*, 1981) and the HVP RNAs (Howe and Shu, 1988).

The La antigen is a phosphoprotein, whose main function is to bind the oligouridylate stretch at the 3' termini of all mammalian RNA pol III transcripts (Mathews and Francoeur, 1984). The binding is usually transient and is thought to stabilise the nascent RNAs from 3' exonuclease degradation before they undergo maturation. However, for the EBERs the association was shown to be stable (Howe and Shu, 1988). The La antigen is also thought to be implicated in internal ribosome entry site-mediated translation in mammalian cells and in the processing of a subset of pol II 3'-processed snRNA containing a uridylate stretch. The La binding site on the EBER transcripts has been identified (Glickman *et al.*, 1988) and is shown in figure 1.3. The findings confirmed that La binds to the U stretch at the 3' end of the EBERs. The functional significance of this interaction remains to be determined. It has been hypothesised that the binding of La to EBERs could act to retain the EBERs in the nucleus as it is a nuclear protein.

1.3.4.2. The small EBER-associated protein/ L22

A second protein was shown to be present in the EBER-RNP and was termed the small EBER-associated protein (EAP) (Toczyski and Steitz, 1991). This protein was also shown to be associated with the HVP RNAs (Toczyski and Steitz, 1991). In patients suffering from different forms of leukemia, a chromosomal translocation t(3;21) was shown to result from the joining of the acute myeloid leukemia (AML) 1 gene and the EAP gene (Nucifora *et al.*, 1993); however the joining of the two genes did not maintain the reading frame of EAP. EBER1 stem loop III was later identified as the EAP binding site and nearly all the nucleotides in the stem loop were shown to be important for binding (Figure 1.3). Stem loop IV was identified as a weaker binding site using EBER1 deletion mutants (Toczyski and Steitz, 1993). It was subsequently demonstrated that EAP was the same protein as the ribosomal protein L22 (Toczyski *et al.*, 1994). L22 is a component of the ribosome and is thought to have a role in organising the ribosome. Toczyski *et al.*, (1994) indicated that in addition to the cytoplasmic and nucleolar localisation of L22, it also exhibited a nucleoplasmic signal in EBV positive cells unlike negative cells. As EBER1 also exhibits a strong nuclear signal (Howe and Steitz, 1986), it was concluded that the redistribution of L22 to the nucleus was due to the presence of EBER1 in EBV positive cells. This association was thought to occur before ribosome assembly. Therefore this could lead to a depletion of L22 from ribosomes and could alter translation.

1.3.4.3. The interferon-inducible, double-stranded RNA-activated protein kinase PKR

The interferon (IFN)-inducible, double-stranded (ds) RNA-activated protein kinase PKR (previously known as p68, DAI, dsI, P1 and PK_{ds}) is one of the first proteins to be activated following any viral infection. Upon binding of dsRNA, PKR becomes activated and undergoes autophosphorylation. Once activated it can phosphorylate the α subunit of protein synthesis initiation factor eIF2 (eIF2α) leading to inhibition of translation at the level of initiation (Clemens, 1997, Williams, 1999, for reviews). This and the role of PKR will be described in more detail in section 1.5.3.1. In this section the EBER1-PKR interaction is described.

In vitro assays have demonstrated that EBER1 binds to PKR (Clarke *et al.*, 1991) and inhibits activation of PKR (Sharp *et al.*, 1993). EBER2 was also shown to bind to PKR but was less efficient than EBER1 at rescuing protein synthesis following dsRNA treatment (Sharp *et al.*, 1993). The interaction between the EBERs and PKR was also demonstrated *in vivo* (Nanbo *et al.*, 2002). Different EBV positive BL cell lines were transfected with a flag tagged PKR plasmid. Immunoprecipitation with a flag tag antibody was followed by an RT-PCR using EBER1 or EBER2 primers and the results showed that EBERs co-precipitated with PKR. No signal was observed following transfection of a mutant PKR lacking dsRNA binding activity. The secondary structure of EBER1 was shown to be important to mediate this effect (Clarke *et al.*, 1990, Clarke *et al.*, 1991). Stem loop IV (nucleotides 87-123) of EBER1 was identified as the binding site for PKR (Figure 1.3) (Vuyisich *et al.*, 2002). It was recently determined that PKR and L22 compete for EBER1 binding, suggesting that they bind the same or an overlapping site (Elia *et al.*, 2004), which is in agreement with the observation of Toczyski and Steitz (1993) where two binding sites for L22 were identified, one of which was stem loop IV. Elia *et al.*, (2004) also showed that L22 rescued the inhibitory effect of EBER1 on PKR activation following binding to dsRNA. L22 was also suggested to be a substrate for PKR *in vitro*, as the ribosomal protein was found to be phosphorylated by PKR upon dsRNA treatment.

1.3.4.4. The interferon-inducible 2'5' oligoadenylate synthase

2'5' OAS, like PKR, is involved in the primary response against viral infection and is also activated upon binding of dsRNA. 2'5'OAS is activated by dsRNA and in turn activates endoribonuclease (RNAse L), which leads to mRNA degradation, but its role will be described in more detail in section 1.5.3.2. EBER1 was reported to bind 2'5'OAS *in vitro* (Sharp *et al.*, 1999). Surprisingly, like VAI of Adenovirus, EBER1 was shown to be an activator of 2'5'OAS in a concentration dependent manner. As shown for other proteins, the secondary structure of EBER1 might be critical for this interaction as no binding of 2'5'OAS was observed following digestion with RNase T1. The interaction between EBER1 and 2'5'OAS is of a lower affinity than that of 2'5'OAS with dsRNA.

1.3.4.5. Interaction with the viral protein EBNA1

It had been suggested that EBNA1 binds to RNA through its RGG motifs (Snudden *et al.*, 1994) and more recently was demonstrated that this is the case. Binding was increased when the RNA G U content was increased or when the RNA had extensive secondary structure (Lu *et al.*, 2004). A recombinant EBNA1 protein was also able to bind an *in vitro* transcribed EBER1 probe. The complex was supershifted following the addition of an anti-EBNA1 antibody, suggesting that the interaction was specific between EBNA1 and EBER1. This interaction was also observed in Akata cells using a ribonucleoprotein immunoprecipitation assay (Lu *et al.*, 2004). However, the significance of the interaction between the viral protein and viral RNA in EBV infected cells is not clear.

1.3.5. Role of the EBERs in transformation and growth support

To date the possible contribution of the EBERs to transformation remains unclear. The EBERs are present in the majority of EBV cell lines and EBV positive tumours, with the exception of hepatocellular carcinoma (Sugarawa *et al.*, 1999), which could suggest a possible role in growth transformation. However, this remains controversial. The EBERs are the last latent genes to be expressed following immortalisation of B-cells in culture, 36 hours post-infection, therefore suggesting that they are not required during the early stages

of infection. Moreover, an EBER-deleted EBV recombinant virus was reported to transform primary B lymphocytes into LCLs and was able to replicate like a wild-type EBV (Swaminathan *et al.*, 1991). The recombinant virus was also able to reactivate its lytic cycle and infect other B lymphocytes. However, Yajima *et al.*, (2005) recently revisited these findings and they reported that the previous group failed to produce large quantities of pure EBER-deleted recombinant virus, which they obtained using EBV negative Akata cells. Akata cells were isolated from an EBV positive BL and retained a latency I phenotype (Takada *et al.*, 1991). EBV negative Akata cells spontaneously arose and were also isolated (Shimizu *et al.*, 1994). Yajima *et al.*, (2005) also showed that the EBER-deleted EBV was able to infect B cells but had a much lower transforming ability than that of a wild-type virus. The LCLs harboring the EBER-deleted EBV grew more slowly than wild-type cells with EBV. This recent finding supports the hypothesis that the EBERs contribute to the transforming process of EBV.

The EBERs share similar properties with the VA RNAs of Adenovirus (Rosa *et al.*, 1981). The EBERs can functionally replace the VAs in mutant Adenovirus lacking VA genes (Bhat and Thimmappaya, 1983, Bhat and Thimmappaya, 1985). Therefore it was hypothesised that they have similar functions. For instance, the EBERs can bind and inhibit PKR *in vitro*, like VAI, suggesting that they can rescue protein synthesis. This could be important especially during the later stages of infection to help synthesise growth factors needed to support growth. Moreover, both the VAs and EBERs bind and activate 2'5'OAS, which could lead to the mRNA degradation of anti-viral cellular genes and therefore support growth of the infected cells.

IL10 was shown to support growth of activated B-cells (Rousset *et al.*, 1992). The EBERs have been suggested to support growth by inducing the expression of different autocrine growth factors. For example, IL10 expression was reported to be upregulated in EBV positive Akata and Mutu cells compared to their EBV negative counterparts. Following transfection of EBV negative Akata cells with the different latent genes of EBV it was concluded that the EBERs were responsible for the increased IL10 expression in these cells. This was confirmed using an EBER-deleted EBV. The addition of IL10 to the medium of EBV negative cells enabled their growth under low serum conditions and the growth of EBV positive cells was inhibited following the addition of anti-IL10 antibody to the medium. This suggested that in BL, IL10 acts as an autocrine growth factor, which is

further supported by the finding that in BL biopsies IL10 is also detected (Kitagawa *et al.*, 2000). The same experiments in T cell lymphoma and in NPC have identified IL9 and IGF1 to be acting as autocrine growth factors respectively (Yang *et al.*, 2004, Iwakiri *et al.*, 2005).

The EBV positive BL cell line Akata, when selected for EBV negative subclones, lose the ability to grow under low serum conditions and to form colonies in soft agar and tumours in SCID mice (Shimizu *et al.*, 1994). Several reports have suggested an oncogenic role of the EBERs in BL using this cell line (Takada and Nanbo, 2001, Nanbo and Takada, 2002, for reviews). Studies have reported that high expression of EBERs, following transfection of EBV negative Akata cells, seemed to protect the cells from apoptosis under certains conditions (cycloheximide, glucocorticoid treatment or hypoxic stress) but not under serum deprivation (Komano *et al.*, 1999, Ruf *et al.*, 2000). Both studies showed that the injection of EBV negative Akata cells transfected with EBERs into SCID mice can lead to tumourigenesis. Komano *et al.*, (1999) also reported that EBV negative Akata cells transfected with EBERs were able to form colonies in soft agar and that Bcl2 protein was found upregulated upon introduction of EBERs. Another group has reported that transfection of EBERs into an EBV negative BL cell line, BJAB, rendered the cells more malignant and resistant to apoptosis. It was shown that this transfection caused inhibition of PKR phosphorylation upon polyI polyC (pIC) stimulation (Yamamoto *et al.*, 2000). However, it was not tested whether resistance to apoptosis was due to inhibition of PKR phosphorylation. This was demonstrated using a dominant negative PKR. A catalytically inactivated PKR mutant, which could block phosphorylation of endogenous PKR, was transfected into EBV negative BL. These cells were rendered resistant to IFNα-induced apoptosis compared to untransfected cells. A second PKR mutant, which was catalytically active but lacked dsRNA binding activity, was transfected into EBV positive cells and shown to be able to be phosphorylated. This mutant did not bind the EBERs (Nanbo *et al.*, 2002). These results suggest that in BL, resistance to IFNα-induced apoptosis is conferred by EBERs via binding of PKR and inhibition of its phosphorylation. Taken together, these results suggest that the EBERs are implicated in the disease process of EBV-associated malignant disorders. However, one report showed that expression of EBERs in NIH3T3 (rodent fibroblasts) cells enhanced growth in soft agar but failed to confer a consistent malignant phenotype following injection of the cells into SCID mice, suggesting that the

presence of EBERs only is not sufficient to confer a tumourigenic phenotype in these cells (Laing *et al.*, 2002).

Transfection of EBERs in an NPC cell line did not lead to either formation of colonies on soft agar or a tumourigenic phenotype in SCID mice despite the cells having a higher growth rate compared to cells transfected with the vector control. However, the cells exhibited lower PKR phosphorylation in response to pIC, increased Bcl2 expression and a decreased expression of apoptosis markers (Wong *et al.*, 2005). This suggests that the EBERs lead to resistance to apoptosis in NPC.

1.4. Transgenic mice

1.4.1. Introduction to transgenic mice

In the early 1900s the mouse became one of the mammals of choice for genetic studies due to its small size, ease of reproduction in captivity, large litter size and relatively fast generation time. The use of mice is now widespread and one of the most common uses is to study disease processes *in vivo* and especially to identify if a gene has any oncogenic properties by generating transgenic mice (Palmiter and Brinster, 1986, Jaenisch, 1988 for reviews). The first attempt at pronuclear microinjection was performed in 1966, where bovine gamma globulin protein was injected into mouse pronuclei. The zygotes were reported to have survived the mechanical stress of insertion of a glass needle into their pronuclei (Lin, 1966). It was not until the early 1980s that the generation of transgenic mice following pronuclear microinjection of DNA was described (Gordon *et al.*, 1980, Brinster *et al.*, 1980). Several reports then showed that the gene of interest was expressed and transmitted in the germline (Brinster *et al.*, 1981, Wagner *et al.*, 1981, Gordon and Ruddle, 1981).

1.4.2. Generation of transgenic mice expressing myc genes

The myc family of genes are involved in several cell growth processes including cell proliferation and differentiation (Adhikary and Eilers, 2005, for review). A number of genes from this family have been implicated in the development of malignancies. The myc

family of genes includes *c-myc*, *N-myc*, *L-myc* and *S-myc*. The *myc* genes encode nuclear helix-loop-helix phosphoproteins which dimerise with Max. The Myc-Max dimers bind E box DNA sequences and activate target linked genes (Marinkovic *et al.*, 2004). However, Max also dimerises with other helix-loop-helix proteins, including members of the Mad family and Mnt, which limit supply of Max to heterodimerise with Myc. The Mad-Max and Mad-Mnt dimers act as transcriptional repressors, which antagonize c-Myc functions (Walker *et al.*, 2005, Luscher, 2001, Hurlin and Dezfouli, 2004, for reviews). c-Myc was also shown to be involved in the activation of transcription by RNA polymerase I and III (Grandori *et al.*, 2005, Gomez-Roman *et al.*, 2003), thus suggesting that deregulation of c-Myc could enhance cell growth by increasing the transcriptional activity of both pol I and III complexes and maybe lead to tumourigenesis.

The expression level of c-Myc was shown to be altered in many malignancies including BL. To gain more insight into the oncogenic properties of c-Myc transgenic mice overexpressing c-Myc were generated (Adams *et al.*, 1985). The expression was directed to the lymphoid compartment using the immunoglobulin heavy chain intronic enhancer (Eμ). The mice succumbed to pre-B and B cell lymphoma at an early age. The phenotype was similar in the different lineages generated showing a massive enlargement of the lymph nodes, which was described as a "water wings" phenotype. The spleen also showed signs of enlargement as did the thymus (Harris *et al.*, 1988, for review). The tumours were monoclonal and of B cell origin as indicated by their IgH rearrangement. Several new lines of c-Myc mice have been reported since the publication of the original paper describing the generation of Eμc-myc mice (Butzler *et al.*, 1997, Kovalchuk *et al.*, 2000, Cheung *et al.*, 2004, Park *et al.*, 2005, Wang and Boxer, 2005). These c-Myc mice show a variability in their tumour onset (ranging from several weeks to several months) and pathologies indicating that the generation of transgenic mice with the same gene can lead to slightly different results depending on the construct used. However, the generation of these animals provides a tool to gain more insight into the mechanism of action of c-Myc in the development of lymphomas.

N-myc was discovered as a homologue of *c-myc* in neuroblastoma. EμN-myc mice succumbed to pre-B and B cell lymphoma; however the latency was longer than that of Eμc-myc animals (Dildrop *et al.*, 1989). The phenotype was also similar to that of Eμc-

myc animals with enlargement of the lymph nodes, spleen and sometimes the thymus. The tumours were of B cell origin (15/16) and clonal except for one tumour (1/16) which showed a T cell receptor rearrangement.

L-myc was identified in small cell lung carcinoma. EμL-myc mice in contrast to Eμc-myc and EμN-myc preferentially developed T cell neoplasias and had a much slower onset of tumour development compared to Eμc-myc animals (Moroy *et al.*, 1990). Some animals developed B lymphomas. In both cases the tumours were of clonal origins.

1.4.3. Generation of transgenic mice expressing some of the latent genes of EBV

Transgenic mice have also been used to determine if viral genes have oncogenic properties *in vivo.* For instance SV40 T-antigen transgenic mice develop brain tumours (Brinster *et al.*, 1984). Therefore the use of transgenic mice could be a powerful tool to gain more insight into the function of the different latent genes of EBV (Wilson, 1997, for review).

1.4.3.1. LMP1 transgenic mice

LMP1 is regarded as the primary transforming protein of the virus. EμLMP1 and Polyoma early promoter (Py)LPM1 transgenic mice were generated in the laboratory (Wilson *et al.*, 1990). High expressing EμLMP1 mice died very quickly (post natal lethal for some) and no viable progeny or poor viability for others suggested that widespread expression of the transgene is lethal. However, those with expression in the skin displayed the phenotype of epidermal hyperplasia, seen in the PyLMP1 mice (described below). Those EμLMP1 lines of mice with either low enough or restricted LMP1 expression to survive showed lymphoid pathologies and one line studied over an extended period developed long latency lymphoma (described in Wilson, 1997). Similarly another group also reported the generation of EμLMP1 mice. These mice show very low level expression and succumb to B cell lymphoma with a late onset (mainly after 18 months) (Kulwichit *et al.*, 1998). Directing expression of LMP1 to skin in both PyLPM1 (Wilson *et al.*, 1990) and L2LMP1^{CAO} mice (Stevenson *et al.*, 2005) revealed that this protein induces epithelial

hyperplasia, a first step in carcinogenesis. Moreover, progression of the phenotype to papilloma and carcinoma was observed in mice expressing the NPC derived variant $LMP1^{CAO}$. Taken together these results indicate that LMP1 is oncogenic *in vivo* in both B-cells and epithelial cells. Therefore LMP1 expression is thought to be directly implicated in the development of several EBV associated-malignancies such as HD and NPC.

1.4.3.2. EBNA1 transgenic mice

The use of this technique was of particular interest for EBNA1 as no oncogenic activity had been attributed in tissue culture assays. EμEBNA1 mice were generated and mice expressing the protein succumbed to B cell lymphoma (Wilson and Levine, 1992, Wilson *et al.*, 1996). Two of the lines (lines 26 and 59) developed a phenotype which was characterised by a massive enlargement of the spleen and liver. The lymph nodes were enlarged in some animals. The tumour latency and penetrance was different between lines 26 and 59. The line 26 mice developed lymphomas between 4-12 months whereas the onset of line 59 was much later. The tumours in both lines were characterised and shown to be of B cell origin with IgH rearrangement and not T cell receptor rearrangement. A subline arose spontaneously from line 26, called line 26A, which had lost part of the transgene and was shown not to express EBNA1. Animals carrying this transgene do not develop tumours (Wilson *et al.*, unpublished results). These results suggest that EBNA1 has oncogenic properties *in vivo*. However, one cannot exclude at present that sequences at the site of insertion of the transgene contribute to influence the tumour phenotype. However the insertion has been found to be complex. This is currently under study in the laboratory.

In a recent publication a different series of EμEBNA1 mice have been described. Unlike the mice described above (Wilson and Levine, 1992, Wilson *et al.*, 1996) the Eμ-EBNA1 mice reported in this paper do not succumb to lymphoma even after 26 months (Kang *et al.*, 2005). These mice were generated in the FVB background and importantly were maintained under specific pathogen free (spf) conditions, whereas the mice established in our laboratory are in a C57Bl/6 background and maintained under conventional conditions (ie, not spf). If the reaction of the immune system plays a role in tumour development, as has been hypothesised by our group with respect to T-cell

production of IL2 (Tsimbouri *et al.*, 2002) then the pathogen status of the environment may be all important. The background of strains of mice can play a role in the development of tumours. For instance Eμc-myc mice in a C57Bl/6 background develop B cell lymphoma, whereas in a C3H/HeJ they also develop T cell lymphomas (Yukawa *et al.*, 1989). Mice of line 26 were backcrossed to FVB background in the laboratory and they also developed lymphoma (Drotar and Wilson, unpublished results).

1.4.3.3. EBNA2 and EBNA-LP transgenic mice

EBNA2 is one of the first genes of EBV to be expressed following B-cell infection *in vitro*. SV40 promoter and enhancer (SV)EBNA2 transgenic mice have been generated (Törnell *et al.*, 1996). The animals succumb to kidney adenocarcinoma following a very long latency period. The expression of the transgene was low in kidney, spleen and liver and even lower in other tissues. EμEBNA2 lines of mice were generated (J.B. Wilson, personal communication) but these lines of mice showed no phenotype and it was suspected that expression levels were very low or negative and these studies were not pursued.

EBNA-LP transgenic mice have been reported and showed a phenotype of congestive heart failure (Huen *et al.*, 1993). In these constructs EBNA-LP was under the control of the metallothionein promoter, which would be expected to drive expression in the liver of the animal. To date, no EμEBNA-LP mice have been reported (or generated in this group).

1.4.3.4. LMP2A transgenic mice

LMP2A is a transmembrane protein, which has been shown to inhibit B cell receptor (BCR) induced apoptosis in BL cells (Fuduka and Longnecker, 2005). EμLMP2A transgenic mice were generated and no oncogenic phenotype was detected *in vivo* (Caldwell *et al.*, 1998). However, expression of LMP2A in the B cells abrogates normal B cell development enabling IgM negative cells (cells lacking a BCR) to amass in the peripheral lymphoid organs. This result suggests that LMP2A provides a signal in the absence of the BCR, which supports the survival of the cells.

1.4.4. Cooperation studies in mice

The activation of an oncogene is one of several steps involved in tumour development and progression. However, in order to fully develop a phenotype, the "pre-tumour" cell must undergo secondary events. Therefore to investigate the mechanism of cooperation between two genes in lymphomagenesis, cross-breeding studies have been undertaken with transgenic mice expressing the genes of interest. A cooperation between the two genes in tumourigenesis can be observed by an acceleration of the phenotype or a change of the pathology.

1.4.4.1. Cooperation between cellular genes

Several genes have been shown to cooperate with *c-myc* in tumourigenesis. For instance, a cooperation between *c-myc* and *bcl2* was reported (Strasser *et al.*, 1990). Eμc-myc transgenic mice were crossed with EμBcl2 mice and the bi-transgenics developed tumours somewhat faster than the Eμc-myc mice and with a more immature B-cell phenotype. This suggests a complementary role between c-Myc and Bcl2 where c-Myc activates proliferation and Bcl2 inhibits apoptosis. A cooperation was also demonstrated between between *c-myc* and *pim1*. EμPim1 mice are slightly predisposed to lymphoma developing after a very long latency period; however when crossed with Eμc-myc mice bi-transgenic mice develop pre-B cell lymphoma (Verbeek *et al.*, 1991). A strong synergy between the two genes was observed, as the bi-transgenic mice die in utero or just post-natal. To date this is one of the strongest synergisms observed *in vivo*.

A synergy between *pim1* and *N-myc* and *L-myc* was reported (Moroy *et al.*, 1991). In both cases an acceleration of the tumour onset was demonstrated. EμPim1/EμN-myc bi-transgenic mice succumbed to pre-B cell lymphoma at an average age of 5 weeks compared to the 13 to 16 weeks observed for EμN-myc animals. EμPim1/EμL-myc bi-transgenic mice succumbed to T cell lymphoma at an average age of 3 months compared to 9 months observed for EμL-myc animals.

1.4.4.2. Cooperation between cellular genes and viral latent genes of EBV

Cooperation studies have been described for EBNA1. A synergy between EBNA1 and Myc was reported (Drotar *et al.*, 2003). EμEBNA1 animals were crossed with Eμc-myc or EμN-myc animals. In both cases a cooperation was observed between the two genes due to an acceleration of the tumour onset. However, the cooperation was more pronounced between *EBNA1* and *N-myc*. This is likely due to the fact that EμN-myc animals have a longer latency for tumour development compared to Eμc-myc animals and acceleration is more easily observed rather than any difference in the basis of the cooperation. This cooperation can give further insight into the mechanism of eBL, where both EBNA1 and c-Myc are expressed.

EμEBNA1 animals were also crossed with EμBcl2 animals. No cooperation in lymphomagenesis was observed between the two genes, as the age of tumour onset from the bi-transgenic animals was the same as that of EμEBNA1 animals and no difference in tumour pathology was noted from the EμEBNA1 mice (Tsimbouri *et al.*, 2002). This suggests that the two genes are redundant in lymphomagenesis and provides an insight into the mechanism of EBNA1 in this system, that it may act through anti-apoptotic (or survival) pathways. Evidence in support of this idea was provided by the observation that BCl_{XL} is upregulated in pre-tumour transgenic samples, and subsequently EBNA1 has been shown to have a survival function in BL cells (Kennedy *et al.*, 2003).

Therefore cooperation studies can reveal, in addition to cooperative action, the possible mechanism of action of an oncogene through the redundancy with oncogenes with known functions.

1.5. The interferon response

1.5.1. Introduction on the interferon response

The interferons (IFNs) are part of a large family of secreted proteins, which are involved in different processes such as cellular growth, hematopoiesis, immunoregulation

and antiviral defense (Goodbourn *et al.*, 2000, Samuel, 2001, Malmgaard, 2004, for reviews). There are two types of IFNs termed type I and type II. Type I IFNs are induced directly by a virus and are composed of IFNα and IFNβ. The former is predominantly expressed by leucocytes whereas the latter is synthesised by most cell types but mainly by fibroblasts. Type II IFN (IFNγ) is induced by mitogenic and antigenic stimuli and is produced by natural killer (NK) cells, Th1 $CD4^+$ cells and $CD8^+$ cytotoxic suppressor cells. Therefore, IFNα and β are the main cytokines for the innate immune response whereas IFNγ is a regulator of the adaptive immune response (Schindler and Brutsaert, 1999).

1.5.2. First steps of the IFN response

1.5.2.1. The interferon regulatory factors 3 and 7 and induction of IFNα and IFNβ

The interferon regulatory factor (IRF) 3 and IRF7 are transcription factors located in the cytoplasm of un-stimulated cells (Sato *et al.*, 2000, Zhang and Pagano, 2002, for review, Hiscott and Lin, 2005). IRF3 is constitutively activated whereas the expression of IRF7 is induced by the IFNα and β signalling pathway as it is under the control of IFN-stimulated gene factor 3 (ISGF3) (described in section 1.5.3). Following a virus infection, both factors become phosphorylated by IκB kinase epsilon and TANK-binding kinase 1 (Fitzgerald *et al.*, 2003, Sharma *et al.*, 2003) and translocate to the nucleus (Figure 1.6). Phosphorylated IRF3 forms a complex with CBP/p300 and binds to the promoters of IFNα and IFNβ genes with phosphorylated IRF7. NFκB also binds to the promoter of IFNβ but not of IFNα. IFNα and IFNβ are then secreted from the cells and bind to their receptors in an autocrine and paracrine manner.

In non-stimulated cells a weak constitutive signal of IFNα and β was shown to be present (Taniguchi and Takaoka, 2001, for review). The spontaneous expression of IFNα and β occurs by an unknown mechanism. This weak constitutive signal is thought to allow a stronger response when the cells encounter a viral infection, which could be due to the pre-accumulation of IRF7 in the cytoplasm.

Figure 1.6: Summary of the IFNα and β pathway following a viral infection

Following a viral infection, viral dsRNA is produced and activates 2'5'OAS, which in turns activates RNaseL and leads to mRNA degradation. dsRNA also activates PKR which leads to translational arrest and NFκB release and translocation to the nucleus. A viral infection also leads to phosphorylation of IRF3 and IRF7, which translocate to the nucleus. Phosphorylated IRF3 then interacts with CBP/p300 and activates transcription of the IFNα gene along with phosphorylated IRF7 and of the IFNβ gene with phosphorylated IRF7 and NFκB. IFNα and IFNβ are secreted and bind to the IFN activated receptor on the same cell (autocrine) or on a different cell (paracrine). This activates a signal transduction pathway, which leads to the increased expression of several genes including IRF7, 2'5'OAS and PKR. This figure was adapted from Taniguchi and Takaoka, 2002.

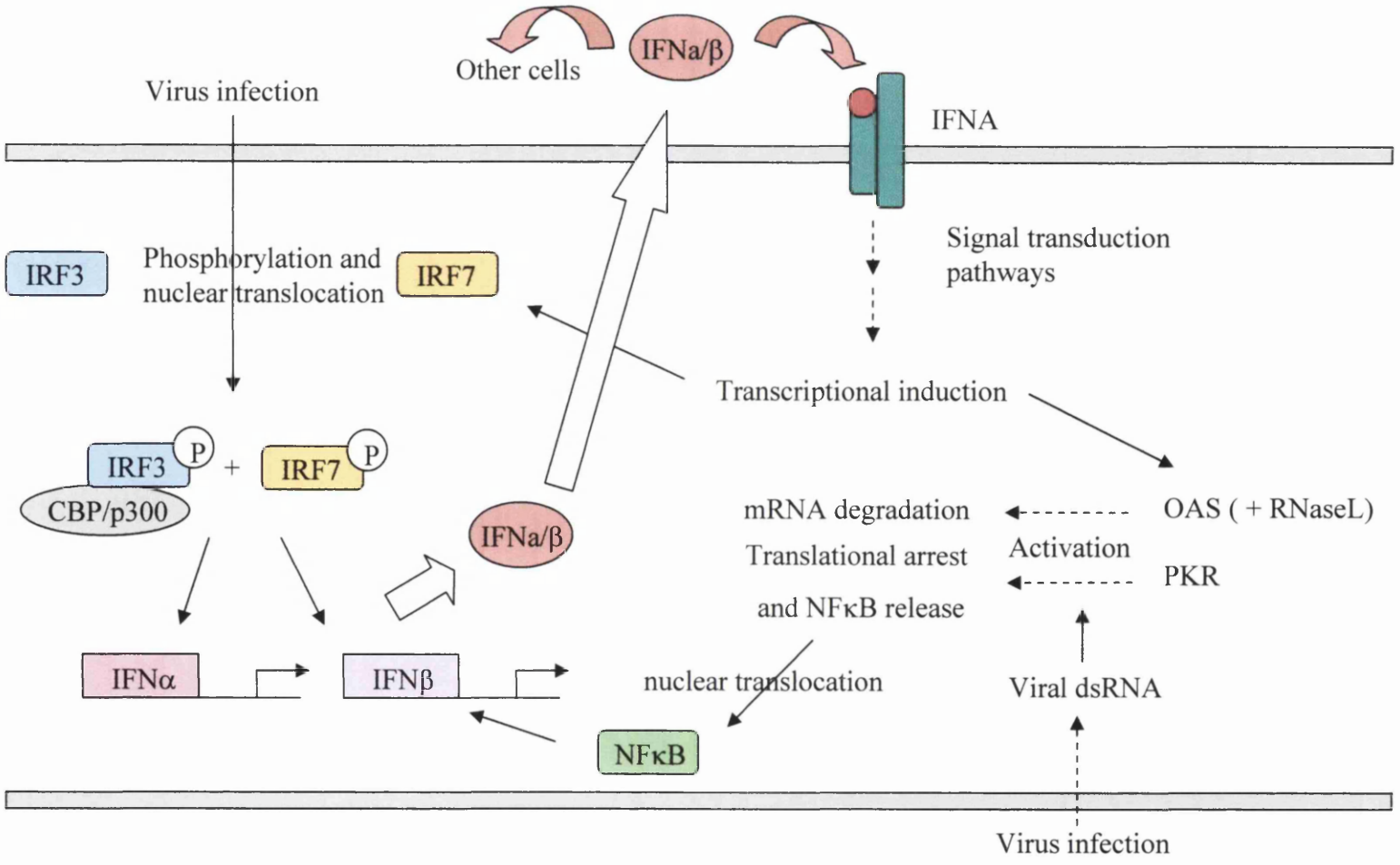
Other cells
IFNa/β
Virus infection
IFNA
IRF3
Phosphorylation and
nuclear translocation
IRF7
Signal transduction
pathways
Transcriptional induction
IRF3
P
+
IRF7
P
CBP/p300
IFNa/β
mRNA degradation
OAS (+ RNaseL)
Translational arrest
Activation
PKR
and NFκB release
IFNα
IFNβ
nuclear translocation
Viral dsRNA
NFκB
Virus infection

1.5.2.2. Induction of IFNγ

IFNγ is not induced following a viral infection but mediates the second wave of cytokines and is induced by early cytokines or antigen stimuli. The main cytokine responsible for induction of IFNγ production is IL12. Several other cytokines can induce IFNγ expression and include IL2, IL18, IL21, IL23, IL27, IFNα and β and TNFα. In NK cells and $CD4^+$ cells induction of IFNγ involves Stat4 activation (Thierfelder *et al.*, 1996, Nguyen *et al.*, 2002). It also involves NFκB and nuclear factor activating transcription (NFAT) following stimulation by IL18 (Tsuji-Takayama *et al.*, 1999).

1.5.2.3. IFNα-inducible genes: PKR and 2'-5'oligoadenylate synthetase

Following a viral infection, dsRNA is produced from the viral replication and protein synthesis. Two IFNα and βinducible genes, PKR (Der and Lau, 1995) and 2'5'OAS (Goodbourn *et al.*, 2000, Samuel, 2001, for reviews) are activated following binding of dsRNA (Figures 1.6 and 1.7). Both PKR and 2'5'OAS are induced by ISGF3.

1.5.2.3.1. Characteristics and functions of dsRNA-activated protein kinase PKR

PKR is a ubiquitously expressed kinase, which is composed of two functional domains (Clemens, 1997, Williams, 1999, for reviews). The N-terminal domain contains the dsRNA binding domain, which is divided into two dsRNA binding sites. The structure of this domain has been determined and a model was proposed for its interaction with dsRNA (Nanduri *et al.*, 1998). The C-terminal domain is composed of the kinase catalytic domain. Following binding of dsRNA, PKR undergoes a conformational change which exposes the catalytic domain of PKR. Homodimerisation of PKR was shown to be important for autophosphorylation. It was suggested that one molecule of PKR would be phosphorylated by the other one (Williams, 1999). A cellular protein, p58, was identified as an inhibitor of PKR (Lee *et al.*, 1994). Using co-immunoprecipitation Polyak *et al.*, (1996) have shown that p58 binds PKR. The binding of p58 to PKR leads to inhibition of its autophosphorylation.

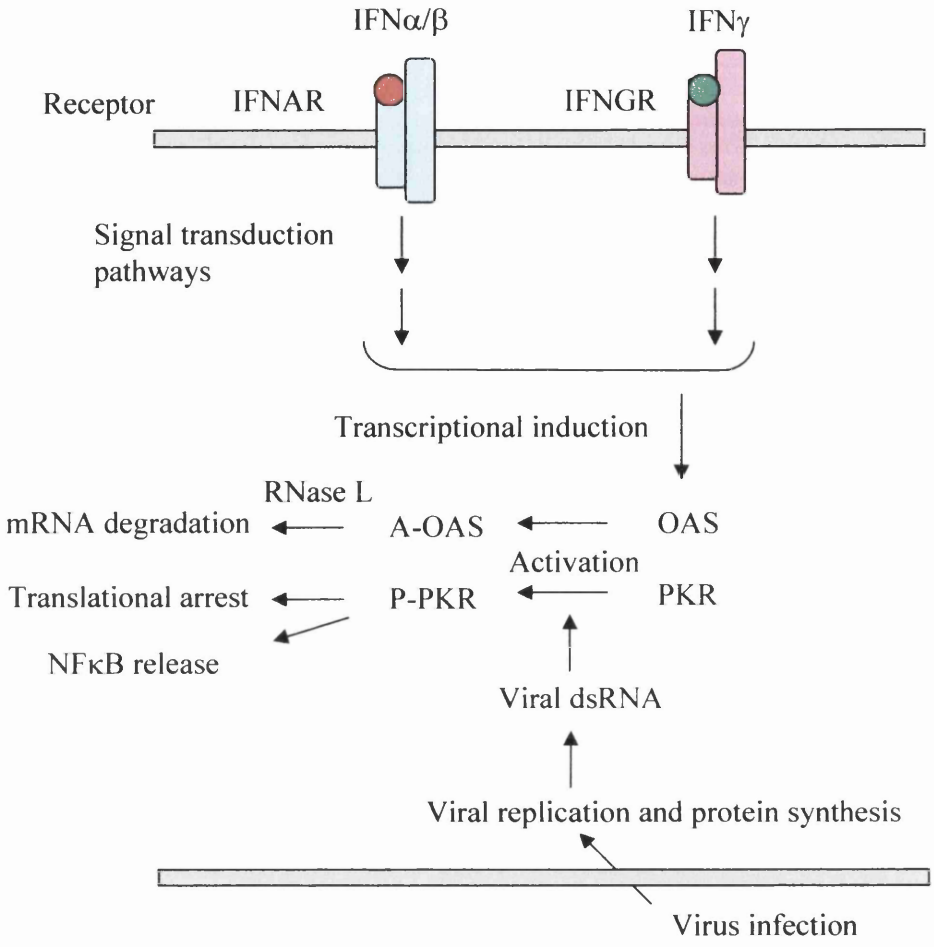

Figure 1.7: PKR and 2'5'OAS signalling following an interferon response

Following binding of IFN to its receptor signal transduction pathways are induced leading to the expression of PKR and 2'5'OAS. Upon viral infection, viral dsRNA is produced. Binding of viral dsRNA leads to the phosphorylation of PKR (P-PKR) and the activation of 2'5'OAS (A-OAS). Activated PKR blocks translation through the phosphorylation of eIF2α and releases NFκB to activate transcription of several target genes. Activated 2'5'OAS generates 2'5' oligoadenylate compounds which bind and activate RNAseL leading to mRNA degradation. This figure was modified from Goodbourn *et al.*, 2000.

To date the best characterised substrate of PKR is the alpha subunit of the initiation factor eIF2 (eIF2α) (Chong *et al.*, 1992) (Figure 1.8 A). Activated PKR phosphorylates eIF2α on serine 51, which results in the sequestration of the recycling factor eIF-2B in an inactive complex with eIF-2GDP. The consequence of blocking eIF2 into its inactive form is inhibition of protein synthesis (both cellular and viral).

Another substrate of PKR is IκB, which is the specific inhibitor of NFκB. In response to dsRNA, PKR phosphorylates IκB (Kumar *et al.*, 1994) by a mechanism involving NFκB inducing kinase (NIK) and IkB kinase (IKK) (Zamanian-Daryoush *et al.*, 2000). This leads to the release of NFκB and thus its translocation to the nucleus to activate the transcription of various genes implicated in mediating the anti-proliferative and survival effects of IFN such as class I major histocompatibility complex (MHCI) and IRF-1, as well as regulating IFNβ transcription (Visvanathan and Goodbourn, 1989) (Figure 1.8 B).

PKR loss of function phenotype in U-937 cells was investigated using two different strategies: a dominant negative mutant and overexpression of an antisense PKR transcript (Der and Lau, 1995). Suppression of PKR resulted in impaired IFN induction at both protein and mRNA levels. Moreover, loss of function of PKR resulted in enhanced replication of EMCV.

Mice devoid of functional PKR ($PKR^{-/-}$) were generated (Kumar *et al.*, 1997). The mice exhibited a reduced antiviral response following IFNγ and pIC treatments. Mouse embryo fibroblasts (MEFs) derived from these mice have been used in transfection assays. An IFN response was stimulated using different inducers and induction was measured using IRF1 reporter gene. Signalling deficiencies in $PKR^{-/-}$ MEFs were observed and the defects were rescued when PKR function was restored. A defect in activation of NFκB and IRF-1 was also observed in response to IFNγ and pIC by electrophoretic mobility shift assays (EMSAs), as well as in the induction of several genes, such as the murine *Gbp* and MHCI (which are dependent on IRF1) shown by northern blots.

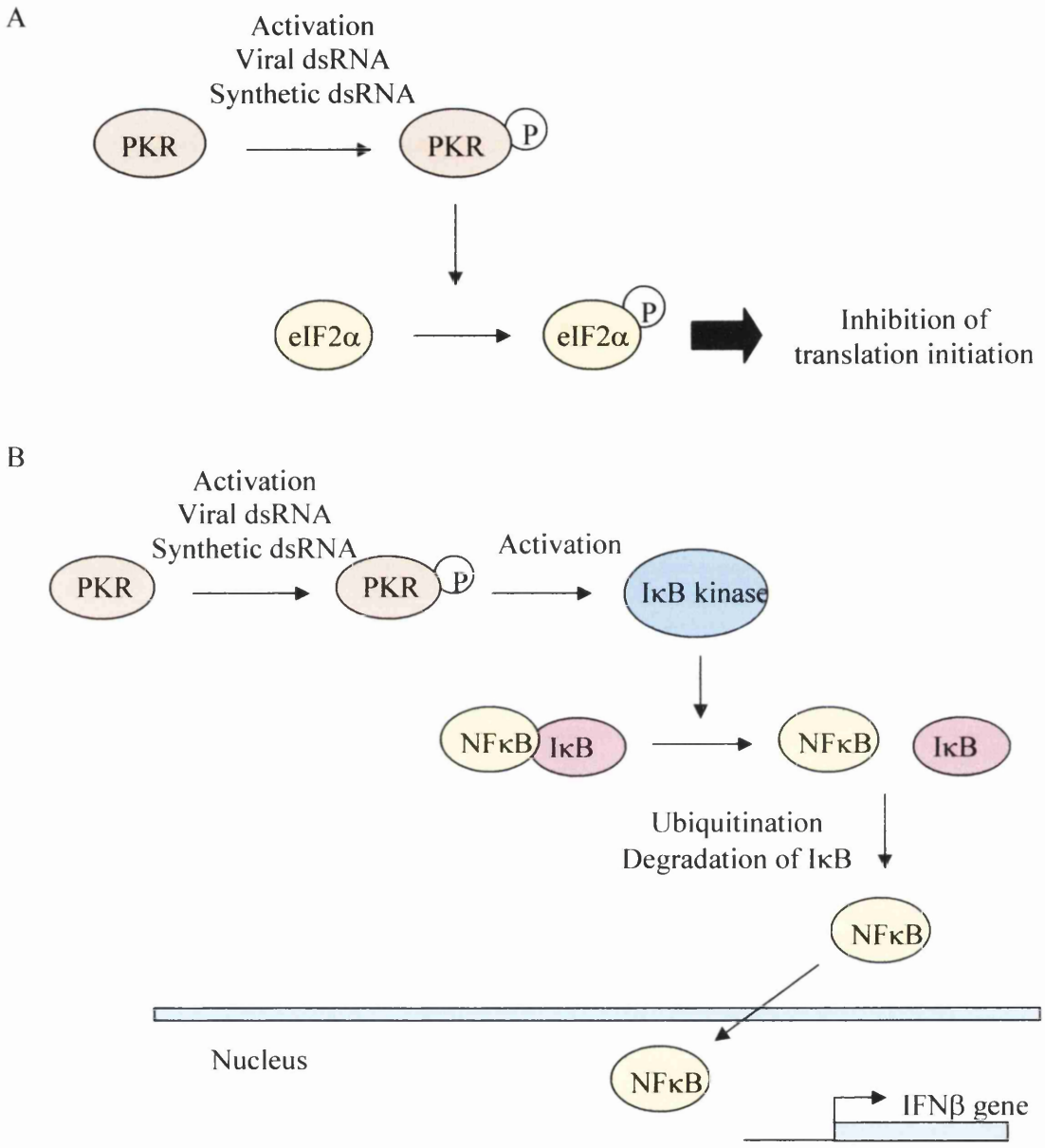

Figure 1.8: Role of PKR on eIF2α and NFκB

Following binding of dsRNA, PKR becomes autophosphorylated. Activated PKR then phosphorylates eIF2α (panel A). This leads to inhibition of initiation of translation. Activated PKR also activates IκB kinase (panel B), which will dissociate NFκB from IκB. IκB then becomes ubiquitinated and degraded by the proteasome, whereas NFκB translocates to the nucleus where it will activate target genes including IFNβ.

1.5.2.3.2. Characteristics and functions of 2'5' oligoadenylate synthetase and endoribonuclease L

2'5' oligoadenylates are small active compounds, which are synthesized from adenosine triphosphate by activated 2'5'OAS (Kerr and Brown, 1978). The enzyme becomes activated upon binding of dsRNA. The newly synthesised 2'5'oligoadenylates bind to the inactive monomeric endoribonuclease (RNase) L, inducing its activation and dimerisation. Once activated, RNAse L degrades single-stranded RNA, including mRNA, which leads to inhibition of protein synthesis (Goodbourn *et al.*, 2000, Samuel, 2001, for reviews). It was also shown that RNase L cleaves 28S ribosomal RNA which inhibits translation (Iordanov *et al.*, 2000).

RNase $L^{-/-}$ transgenic mice have been generated and showed an impaired antiviral effect following IFNα treatment (Zhou *et al.*, 1997). The RNase $L^{-/-}$ thymocytes and fibroblasts exhibited resistance to apoptosis when compared to wild-type thymocytes and fibroblasts following treatment with different apoptotic agents.

1.5.3. The signalling response pathway of IFNα and β

The signalling pathway of IFNα and β is mediated by interferon activated receptor (IFNAR), which has 2 subunits denoted IFNAR1 and IFNAR2 (Kim *et al.*, 1997). IFNAR1 and IFNAR2 are associated with Tyk2 (a member of the Jak family of kinases) and Jak1 respectively in un-stimulated cells (Figure 1.9). IFNAR2 was also shown to be pre-associated with the signal transducer and activator of transcription (Stat) 2 (Li *et al.*, 1997b). Upon ligand binding, IFNAR1 and IFNAR2 form a complex leading to the cross-phosphorylation of Tyk2 and Jak1. The activated Jaks phosphorylate IFNAR1 creating a docking site for Stat2, which is then phosphorylated by Tyk2 on tyrosine 690 (Qureshi *et al.*, 1996). This favours the recruitment of Stat1, which becomes phosphorylated on tyrosine (Tyr) 701 by the activated Jaks. Two isoforms of Stat1 have been described and are generated by alternative splicing and denoted Stat1α and Stat1β. Stat1β lacks an exon encoding the last amino acids of Stat1 (Horvath, 2000, for review) and therefore cannot induce transcriptional activation of target genes. Thus the transcriptional activation domain of Stat1 resides in the 38 amino acids unique to the α isoform. The activated Stats are

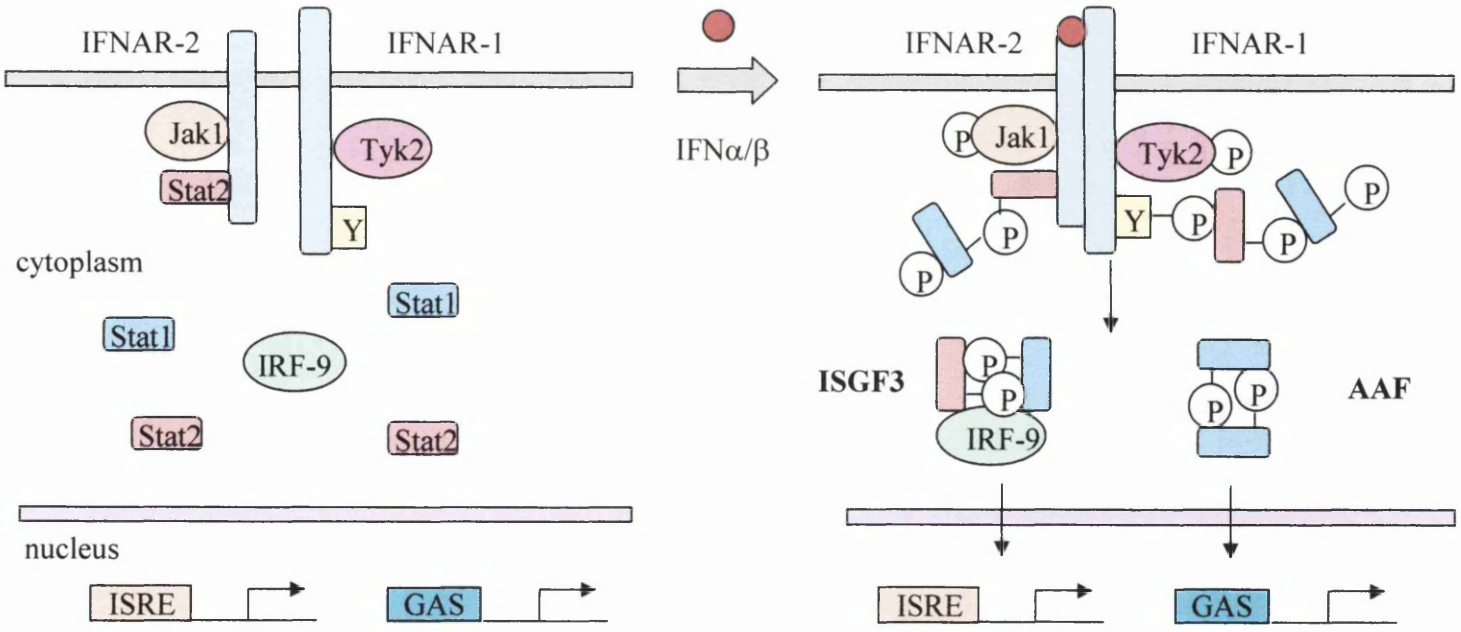

Figure 1.9: The signalling response pathway of interferon α and β

The panel on the left shows an un-stimulated cell. IFNAR1 and IFNAR2 are associated with Tyk2 and Jak1 respectively. Upon binding of IFNα and β to IFNAR2, the subunits form a complex, which leads to the phosphorylation of Jak1 and Tyk2 and then of the receptor. Stat2 binds to the receptor and becomes activated leading to the binding of Stat1. Following activation of Stat1, Stat1 and Stat2 dissociate from the receptor and two different complexes are formed denoted IFNα-associated factor (AAF), composed of Stat1 homodimers and IFN-stimulated gene factor 3 (ISGF3) made of Stat1 and Stat2 heterodimers and IFN regulatory factor (IRF) 9. These complexes translocate to the nucleus and activate the transcription of different target genes implicated in the IFN response, with either an IFN-stimulated response element (ISRE) or an IFNγ-activated site (GAS) element on their promoters. This figure was adapted from Taniguchi and Takaoka, 2001.

released from the receptor and form two complexes termed IFN-α-associated factor (AAF) and IFN-stimulated gene factor 3 (ISGF3). The former is a homodimer complex composed of activated Stat1 whereas the latter is composed of both activated Stat1 and Stat2 and IRF9 (also known as p48) (Figure 1.9) (Horvath *et al.*, 1996). Both Stat1α and β can functionally dimerise with Stat2 in ISGF3 complexes as Stat2 retains its transcriptional activity (Muller *et al.*, 1993). The two complexes are translocated to the nucleus where they bind specific sequences and stimulate transcription. ISGF3 activates the IFN-stimulated response element (ISRE) (Li *et al.*, 1998), which is present on the promoter of genes including IRF7, 2'5'OAS and PKR. AAF binds to the IFNγ-activated site (GAS) element, which is present on the promoter of IRF1.

The phosphorylation of Tyr 701 is important for the dimerisation of Stat1 and also for its translocation and retention in the nucleus. The dephosphorylation of Stat1 on Tyr 701 is required for it to leave the nucleus (Meyer *et al.*, 2003). For maximal induction of IFN-responsive genes the phosphorylation of Stat1 on serine (Ser) 727 is also required (Wen *et al.*, 1995). Several serine kinases are involved in this process including mitogen activated protein kinase (MAPK) p38. This kinase was shown to be activated in HeLa S3 cells following treatment with either IFNα or IFNγ (Goh *et al.*, 1999) The authors also showed that following the pre-treatment of HeLa S3 cells with a p38 inhibitor prior to stimulation with either IFNα or IFNγ Stat1 Ser 727 phosphorylation was reduced and that the antiviral activities of IFNs were diminished.

Balb-c mice with a null mutation in the IFNAR1 gene were generated and showed no sign of abnormal foetal development or morphological changes in adults. Male and female IFNAR1$^{-/-}$ were fertile suggesting that type I IFNs are not important for development and reproduction (Hwang *et al.*, 1995). However, these mice succumb to infection with Semliki Forrest Virus and Encephalomyocarditis Virus very quickly following injection, indicating that type I IFNs are involved in antiviral defence. Stimulation with IFNα or IFNβ failed to induce 2'5'OAS activity, suggesting that IFNAR1 is essential for transducing signals responsible for induction of 2'5'OAS activity in response to IFNα and β stimulation. The mice also showed elevated levels of myeloid lineage abnormalities of hemopoietic cells.

A different group also generated IFNAR1 KO mice. The mice were unresponsive to type I IFNs, and extremely susceptible to viral infection by Vesicular Stomatitis Virus (Muller *et al.*, 1994). Functional inactivation of the receptor was confirmed by analysis of different IFN-inducible genes, including MHC class I gene, 2'5'OAS, IRF1 and Mx-1 (a type I specific response marker in mouse cells).

1.5.4. The signalling response pathway of IFNγ

The IFNγ receptor is composed of 2 subunits: interferon gamma receptor (IFNGR) 1 and IFNGR2, which are dissociated in unstimulated cells (Bach *et al.*, 1996). IFNAGR1 is associated with Janus protein tyrosine kinase (Jak) 1 and IFNAGR2 is associated with Jak2 through their intracellular domains (Figure 1.10). Upon binding of IFNγ, the two subunits associate bringing Jak1 and Jak2 closer. Jak2 becomes phosphorylated and in turn phosphorylates Jak1 (Briscoe *et al.*, 1996). The activated Jaks phosphorylate IFNGR1 on specific tyrosine residues leading to the generation of a Stat docking site. Following its binding to the receptor, Stat1 becomes phosphorylated by the Jaks on Tyr 701. The phosphorylated Stat1 proteins (Horvath, 2000, Shuai and Lui, 2003, for reviews) then dissociate from the receptor and dimerise. The Stat1 homodimers, termed γ-activated factor (GAF), translocate to the nucleus and bind to GAS promoter elements, thus stimulating transcription of IFNγ-inducible genes.

1.6. Aims and approaches of the project

1.6.1. Aims of the project

This project was designed to test hypotheses in relation to the action of the EBERs and more specifically of EBER1. It was decided to study EBER1 and not EBER2 in the first instance due to the fact that EBER1 is more abundant than EBER2 in most EBV-infected cells and because knowledge of the involvement of EBER1 in the inhibition of the IFN response is more detailed. Moreover, both EBER1 and EBER2 have been shown to have similar properties so far and therefore studying only EBER1 may provide an hypothesis from which to test EBER2.

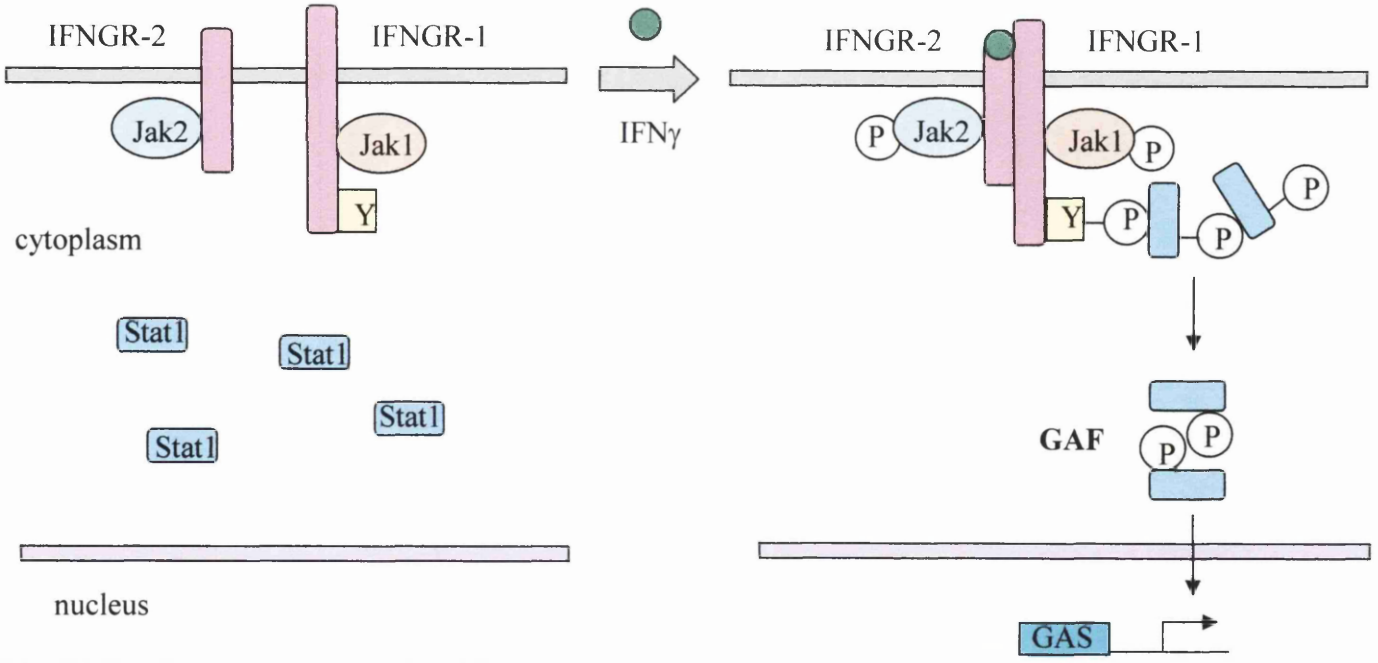

Figure 1.10: The Signalling response pathway of interferon γ

The panel on the left shows an un-stimulated cell. IFNGR1 and IFNGR2 are associated with Jak1 and Jak2 respectively. Upon binding of IFNγ to IFNGR2, the subunits associate, which leads to the phosphorylation of Jak2 and Jak1 and then of the receptor. Stat1 binds to the phosphorylated receptor and becomes activated leading to its dissociation from the receptor. A complex composed of Stat1 homodimers and denoted γ-activated factor (GAF) is generated and translocates to the nucleus to activate the transcription of different target genes implicated in the IFN response, with an IFNγ-activated site (GAS) element on their promoters.

The role of the EBERs in viral pathogenesis remains unclear. Recent evidence has suggested an oncogenic role of the EBERs in BL cells, thus indicating that they may contribute to the disease process of EBV-associated disorders. This led to the hypothesis of this project which was that EBER1 contributes to the pathogenesis of EBV associated disorders either through or in addition to its role in inhibiting the anti-viral effect of IFN. Therefore the aim of this project was to examine and investigate the phenotypic consequences of expression of EBER1 *in vivo* by generating transgenic mice expressing EBER1 in their B cell compartment.

1.6.2. Approaches and summaries of the project

1.6.2.1. Chapter 3 Generation of EBER1 transgenic mice

In order to approach our hypothesis, the first step of this study involved the design of the transgene and the generation of EBER1 transgenic mice. As EBER1 is a pol III transcript, it was decided to construct three different transgenes, which encompassed different sections of the promoter fused to the immunoglobulin heavy chain intronic enhancer (Eμ) to direct expression to the B cells. This was a completely novel approach as no transgenic mice had been reported in the literature with both pol II and pol III elements. As the unusual EBER1 promoter already contained pol II motifs, it was speculated that a tissue specific pol II motif could be functional. The different transgenes were tested for expression in culture using reverse transcriptase- polymerase chain reaction (RT-PCR) and northern blotting and then used for pronuclear microinjection to generate several EBER1 positive founders. The transgenic status of the founders and their offspring was analysed by Southern blotting. Several lines were established (127, 131, 132, 133, 134, 135, 136, 137, 138, 141, 142, 143, 144 and 145) and their inheritance pattern discerned, X-linkage or autosomal integration and transgene copy number were determined.

1.6.2.2. Chapter 4 Expression of EBER1 in the different lines generated

In the generation of transgenic mice, once the lines have been established, the next step is to determine if the transgene is expressed and in which tissue expression is detected. This step is of importance for this study, as expression of the transgene is needed for any

phenotype to develop and it was hoped to achieve tissue specific expression. The expression of the transgene was determined for each line generated using RT-PCR in all the lymphoid tissues and in selected lines (127, 131, 136, 137, 145) in non-lymphoid tissues.

To determine if in this transgenic system EBER1 was transcribed by RNA pol III, as it is in Burkitt's lymphoma cell lines, an RT-PCR assay was developed. This was of importance as the transgene contains both pol II and pol III promoter elements as well as a pol II enhancer, which could lead to a distorted pol II expression. Therefore, RNAs from the highest expressing tissue of lines 127, 131, 134, 136 and 137, were used as template for different RT-PCRs.

In Raji cells, the presence of a minor species of EBER1 was observed with a 5' upstream start (Jat and Arrand, 1982, Arrand and Rymo, 1982). Therefore the possible presence of an upstream start for EBER1 and a minor species was also investigated in the transgenic EBER1 system of lines 127, 131, 134, 136 and 137. This gives further insight into the transcription of EBER1 from the different EBER1 constructs in the transgenic system.

1.6.2.3. Chapter 5 Phenotype analysis of the different expressing lines

The main aim in the generation of transgenic mice is to study their phenotype. For this purpose developmental defects, abnormal behaviour, abnormal immune response, or tumour formation can be analysed. A cohort of animals from the main expressing lines (127, 131, 136, 137, 142 and 145) was placed under a phenotype watch. To determine the origins of the tumour phenotype in animals of line 127, the protein level of different oncogenes and tumour suppressor genes from tumour tissues was analysed by western blotting. The binding activity of Myc was also determined by mobility shift assays.

An *in vivo* assay was developed to determine if EBER1 was able to block a response to dsRNA induced in lines 127 and 137 animals. For this purpose polyIC, which mimics double-stranded RNA, was injected in the tail vein of the animals and tissues were collected and analysed for expression and activation of different proteins involved in the interferon pathway by western blotting.

To further investigate the phenotypic effect of EBER1 expression at the cellular level, FACS analyses were performed on cells isolated from the different lymphoid tissues of mice of lines 127 and 131. The different antibody combinations were designed to test if

expression of EBER1 modified the proportions of B and T cells or their differential status. Similarly, the levels of secreted IgM antibodies and of different cytokines were investigated in serum samples from mice of lines 127, 131 and 137 by enzyme-linked immunosorbent assay (ELISA).

1.6.2.4. Chapter 6 Cooperation study between EBER1 and EBNA1 or Myc

In EBV positive Burkitt's lymphoma cells, EBNA1 and EBER1 are expressed and c-Myc deregulated (Magrath, 1990), suggesting a possible cooperation between these genes. Therefore, the aim of this chapter was to investigate the possible cooperation of EBER1 in lymphomagenesis with EBNA1 and/or Myc (both N-myc and c-Myc were tested) using transgenic mice expressing these genes. This could give further insight into the mechanism leading to the development of eBL. For this purpose, EμEBER1 and EμEBNA1mice were cross-bred and monitored for the development of lymphomas. Similarly, EμEBER1 and EμN-myc or Eμc-myc mice were cross-bred and monitored. To determine the B or T cell origin of the tumour cells immunoglobulin heavy chain and T cell receptor rearrangements were investigated. To understand the cooperative mechanism between EBER1 and Myc, tumour tissues were collected and analysed using western blotting, to monitor changes in the expression levels of different genes, and by EMSA to test the binding activity of Myc.

Chapter 2. Materials and Methods

2.1. Materials

2.1.1. Cell lines

Cell line	Transgene	EBV status	Latency	Reference
39.415	LMP1			Dabbagh and Wilson Unpublished
BJAB		Negative		Menezes *et al.*, 1975
AK31		Negative		Jenkins *et al.*, 2000
AK2003		Positive	I	From Prof Farrell's lab Takada, 1984
Raji		Positive	III	Pulvertaft, 1965
IB4		Positive	III	King *et al.*, 1980

Table 2.1: The different cell lines used

2.1.2. Bacterial strains

All transformations were performed using the *Escherichia coli* (*E. coli*) DH5α–F' bacterial strain.

2.1.3. Mice strains and mouse lines for cross-breeding

The following strains of mice were purchased from HarlanOlac: C57Bl/6, B6D2.F1 (C57Bl/6 x DBA/2), ICR.

Line number	Transgene	Strain	Reference
26	EBNA-1	C57Bl/6	Wilson and Levine, 1992; Wilson *et al.*, 1996
96	N-myc	Balb-c	Dildrop *et al.*, 1989
97	c-myc	C57Bl/6	Adams *et al.*, 1985, Jackson laboratories Stock number: 002728 http://jaxmice.jax.org

Table 2.2: Mouse lines for cross-breeding experiments

2.1.4. pcDNA 3.1 vector for cloning of the different EBER1 constructs

pcDNA3.1 version A (Invitrogen) was used to clone EBER1 PCR products and the Eμ enhancer (appendix 1). It is a 5.5kb vector which contains a CMV promoter, an ampicillin gene for selection in bacteria and a neomycin gene for selection in mammalian cells.

2.1.5. Enzymes and primers

All enzymes were provided by Invitrogen or New England Biolabs (NEB) except for *Pfu* Turbo polymerase (Stratagene), Taq polymerase, T4 DNA ligase, DNAse I (Promega) and the reverse transcriptase MMLV (Invitrogen). All the primers used for PCRs, genotyping, sequencing and EMSA oligos were obtained from Sigma Genosys.

2.1.6. Chemicals, tissue culture and microinjection reagents

All chemicals were provided by Sigma unless otherwise indicated. Tissue culture reagents were purchased from Invitrogen. The hormones and buffers used for microinjections were purchased from Sigma.

2.1.7. Probes used for Southern and northern blotting

Probe fragment	Plasmid number	Expected size of insert	Digest/PCR primers
EBER1	p670	501bp	CR1-CR4
EμEBER1	p670	1995bp	*Xba*I
EBNA1	p114	966bp	*Eco*RI/*Bst*XI
N-myc	p75	800bp	*Pst*I
IgH, J region	p79	900bp	*Xba*I/*Xho*I
TCR, Jβ1	p463	3300bp	*Eco*RI/*Bam*HI
rpL32	p92	1600bp	*Sac*I

Table 2.3: Probe fragments

2.1.8. Antibodies used for FACS analysis, western blots and ELISA

Antibody name	Stage	FITC/PE	Supplier	Catalog number
B220	Pro-B to mature B	FITC PE	eBioscience Caltag	11-0452-85 RM 2604-3
CD43	Immature B	FITC	Pharmigen	553270
sIgs	Mature B	FITC	Caltag	M 30901
CD5.2	Subtype B1 Mature	FITC PE	Caltag eBioscience	MM 3201 12-0051-83
CD2	Pre-B to B	FITC	Caltag	RM 7801
CD23	Mature B	FITC	Caltag	MCD 2301
CD80	B activation	FITC	Pharmigen	553768
CD86	B activation	FITC	Pharmigen	553691
MHCI		FITC	Pharmigen	553579
MHCII		FITC	Pharmigen	553605
RatIgG2a	Isotype control	FITC PE	Serotec	MCA 1212F MCA 1212PE

Table 2.4: B cell FACS antibodies

Antibody name	Stages	FITC/PE	Supplier	Catalog number
CD3	Mature T	FITC PE	Caltag	HM 3401-3 RM 3404
CD90.2	Immature T	PE	Caltag	MM 2004
CD4	Mature T (T helper)	FITC PE	Caltag	RM 2501 RM 2504
CD8a	Mature T (T killer)	PE	Caltag	RM 2204

Table 2.5: T cell FACS antibodies

Antibody	Catalog number	Supplier	Expected size in kDa	Dilution factor used	Species
Id2 (C20) Blocking peptide	sc 489 sc 489P	Santa Cruz Santa Cruz	15	1/1000 5x excess weight	Rabbit
c-Myc (C19)	sc 788	Santa Cruz	67	1/1000	Rabbit
β-tubulin	sc 9104	Santa Cruz	55	1/1000	Rabbit
Nmyc (C19) Blocking peptide	sc 791 sc 791P	Santa Cruz Santa Cruz	67	1/1000 5x excess weight	Rabbit
Stat1	9172	Cell signaling	84, 91	1/1000	Rabbit
P- stat1 (Tyr 701)	9171S	Cell signaling	84, 91	1/1000	Rabbit
P- stat1 (Ser 727)	9177	Cell signaling	91	1/1000	Rabbit

Antibody	Catalog number	Supplier	Expected size in kDa	Dilution factor used	Species
PKR	3072	Cell signaling	74	1/1000	Rabbit
P-PKR (Thr 446)	07532	Upstate	74	1/1000	Rabbit
eIF2α	9722	Cell signaling	40	1/1000	Rabbit
P-eIF2α (Ser 51)	9721S	Cell signaling	40	1/1000	Rabbit
Rb (C15) Blocking peptide	sc 50 sc 50P	Santa Cruz Santa Cruz	110	1/1000	Rabbit
P-Rb (Ser 780)	9307	Cell signaling	110	1/1000	Rabbit
p53 (M19) Blocking peptide	sc 1312 sc 1312P	Santa Cruz Santa Cruz	53	1/1000	Goat

Table 2.6: Primary antibodies used for western blotting

The different antibodies used to detect a phophorylated form are labeled P followed by the antibody name. The phosphorylated residue is indicated.

Antibody	Catalog number	Supplier	Dilution factor used	Species
Goat anti-rabbit IgG-HRP	sc 2030	Santa Cruz	1/4000	Goat
Donkey anti-goat IgG-HRP	sc 2020	Santa Cruz	1/4000	Donkey

Table 2.7: Secondary antibodies used for western blotting

Antibody	Catalog number	Supplier
c-Myc (N262)	sc 764X	Santa Cruz
N-myc	sc 791	Santa Cruz

Table 2.8: Antibodies used for supershifts in mobility shift assays

Antibody type	Antibody name	Catalog number	Company
Coating	Rat anti-mouse IgM heavy chain	MCA 199	Serotec
Detection	Goat anti-mouse IgM-HRP	1021-05	Southern biotechnology associates inc
Standard curve	Mouse IgM kappa chain	M-3795	Sigma
Coating	anti-mouse IL10	14-7101-81	eBioscience
Detection	Biotin conjugated anti-mouse IL10	13-7102-81	eBioscience
Standard curve	Recombinant Mouse IL10	BMS347	Bender MedSystem

Antibody type	Antibody name	Catalog number	Company
Coating	Rat anti-mouse IgG1heavy chain	MCA 336	Serotec
Detection	Goat anti-mouse IgG1-HRP	1070-05	Southern biotechnology associates inc
Standard curve	Rat anti-mouse IgG1 kappa	M-9035	Sigma

Table 2.9: Antibodies used for the ELISA

2.1.9. The different PCR primers used

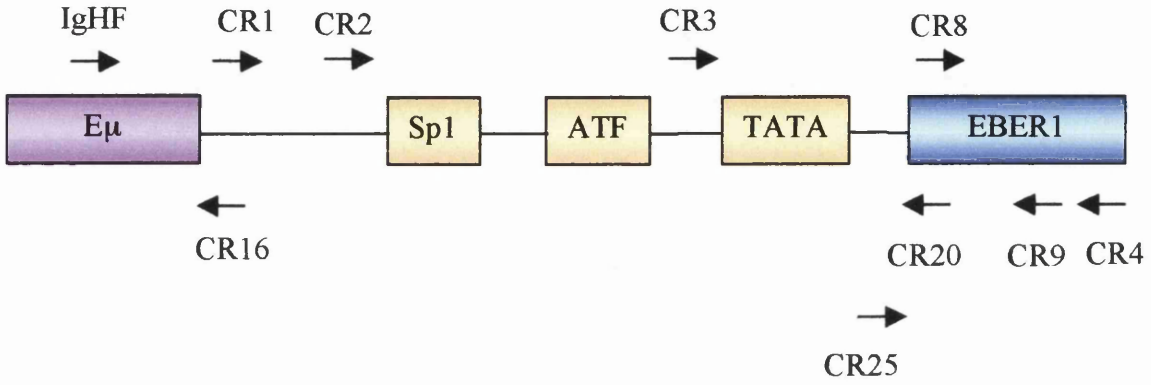

Figure 2.1: Diagram of the different EBER1 primers

Schematic representation of the different primers used for EBER1 PCRs, RT-PCRs and quantitative PCRs. For the primer sequence see table 2.10.

Primer name	5' to 3' primer sequence	Tm °C
CR1	gtgtgtgtgaattcgtcagcctgcaaggtg	78.8
CR2	gtgtgtgtgaattcactataqcaaaccccg	73.1
CR3	gtgtgtgtgaattctcttgaggagatgtag	68.4
CR4	gtgtgtgtctcgagaaaagatgcggaccac	78
CR8	aggacctacgctgc	51.8
CR9	tacttgaccgaagac	44.8
CR16	ctcagaaaacacgccatcc	63.3
CR20	tctagggcagcgtagg	57.4
CR25	gtagacactgcaaaacctc	54.6

Table 2.10: PCR primers for EBER1

Table of the sequence of the different EBER1 primers used for cloning, PCRs, RT-PCRs and QPCRs. The primer sequences (5' to 3') along with the melting temperatures (Tm) are shown. For primers CR1, CR2, CR3 and CR4 the EBER1 specific sequence is underlined.

Primer name	Forward or reverse	5' to 3' primer sequence	Tm °C
Cmyc-F	Forward	cagctggcgtaatagcgaagag	66.9
Cmyc-R	Reverse	ctgtgactggtgagtactcaacc	62.6
G3PDH5'	Forward	tccaccaccctgttgctgta	66.6
G3PDH3'	Reverse	accacagtccatgccatcac	66
IgHF	Forward	cgaggaatgggagtgaggc	67.1
tRNALeu-F	Forward	gaggacaacggggacagtaa	63.8
tRNALeu-R	Reverse	tccaccagaaaaactccagc	64.1

Table 2.11: Other primers used for PCR

For the Cmyc primers the sequence was obtained from the Jax laboratory website. For the tRNALeu primers the sequence was obtained from Gomez-Roman *et al.*, 2003.

Primer name	Forward or reverse	5' to 3' primer sequence
EMSAMycF	Forward	gagcggaagcagac**cacgtg**gtctgcttcc
EMSAMycR	Reverse	gtagggaagcagaccacgtggtctgcttcc
Sp1 F	Forward	gagcattcgatc**ggggcggggc**gagc
Sp1 R	Reverse	gtaggctcgccccgccccgatcgaat
NF-κB F	Forward	gagcagttga**ggggactttccc**aggc
NF-κB R	Reverse	gtaggcctgggaaagtcccctcaact

Table 2.12: Oligonucleotides used for the different electromobility shift assays

The nucleotides in bold in the forward oligonucleotide sequence indicate the consensus binding motifs.

2.1.10. Formulation of frequently used solutions

TE, pH7.5:
10mM Tris HCl, pH 7.5
1mM EDTA pH8

10x loading buffer DNA:
0.42% (w/v) bromophenol blue
50% (v/v) TE
50% (v/v) glycerol
0.42% (w/v) xylene cyanol

10x TBE (1L):
55g Boric acid
40µl 0.5M EDTA pH8
108g Tris base

50x TAE (1L):
57.1ml glacial acetic acid
37.2g $Na_2EDTA.2H2O$
242g Tris base pH 8.5

Church buffer:
1% (w/v) BSA
1mM EDTA
500mM $NaPO_4$
7% (w/v) SDS
pH 7.2

Denaturing solution:
0.6M NaCl
0.4M NaOH

STE:
1mM EDTA
10mM NaCl
10mM Tris HCL pH 7.5

SSC:
150mM NaCl
15mM Sodium citrate
pH 7.5

Tail solution:
100mM EDTA pH8
150mM NaCl
1% (w/v) SDS
10mM Tris-HCl pH7.5

2FC:
49.45% (v/v) chloroform
0.1% (w/v) 8-hydroxyquinoline
1% (v/v) isoamyl alcohol
49.45% (v/v) buffered phenol saturated with 1M Tris pH 8.0
Wrap with foil and keep at 4°C]

Loading buffer RNA:
1x MOPS
17.8% (v/v) formaldehyde
50% (v/v) pure, deionised formamide

Loading dye RNA:
50% (v/v) glycerol
0.1% (w/v) bromophenol blue
0.1% (w/v) xylene cyanol
50% (v/v) TE pH 7.5

10x MOPS buffer:
200mM MOPS
10mM EDTA
50mM NaOAc
pH, NaOH, 7

High salt buffer:
20mM Hepes pH 7.9
0.4M NaCl
1mM EDTA pH8
1mM EGTA pH8
1mM DTT
1mM PMSF

Protein 4x loading dye:
1M Tris pH 6.8
8% (v/v) SDS
30% (v/v) glycerol
10% (v/v) 2β mercaptoethanol
Bromophenol blue trace

Phosphate buffered saline (PBS):
80mM Na_2HPO_4
20mM NaH_2PO_4
100mM NaCl
pH 7.5

Protein blocking buffer:
1xPBS
0.001% (v/v) tween
5% (w/v) non-fat dried milk

Protein wash buffer:
1xPBS
0.001% (v/v) tween

Protein stripping buffer:
100mM βmercaptoethanol
2% SDS
62.5mM Tris HCl pH 6.8

NH_4Cl solution:
9 volumes of NH_4Cl [0.83% (w/v) in H_2O]
1 volume of Tris [2.06% (w/v) in H_2O, pH 7.65]
pH to 7.2 and filter sterilise

5x Tris/glycine buffer (3L):
337.5g glycine
90.6g Tris
30ml 0.5M EDTA
make up to 3L and pH 8.7

2.2. Methods

2.2.2. DNA techniques

2.2.2.1. Small scale plasmid DNA preparation

The procedure was performed using the Sigma miniprep kit and is based on the alkaline lysis of bacterial cells, followed by adsorption of DNA on to a silica membrane (in a column) in the presence of high salt (this protocol was adapted from the method of Birnboim and Doly, 1979). The DNA is then eluted from the column. Single-plasmid transformed bacterial colonies were inoculated in 5ml of L-Broth usually containing 50μg/ml of Amp (unless otherwise stated) and incubated overnight with shaking at 37°C. 1.5ml of the bacterial suspension was transferred into a microfuge tube and centrifuged for 3 minutes at 13000g. Each sample was resuspended in 200μl of suspension buffer and subjected to a modified alkaline-SDS lysis by the addition of 200μl of lysis buffer, mixed and left for 5 minutes at room-temperature. Following lysis, the samples were neutralised by adding 350μl of neutralisation buffer. The cell debris, proteins, lipids, SDS and chromosomal DNA form a white viscous pellet after centrifugation at 13000g for 10 minutes. The clear lysate was transferred to a GenElute miniprep binding column containing a silica membrane, which was centrifuged at 13000g for 1 minute in order to bind the plasmid DNA. The column was washed once with 750μl of wash solution and centrifuged at 13000g for 1 minute. This step removes any traces of contaminants which were introduced during the column load. The flow-through was discarded and the column was centrifuged an additional time to ensure that the excess of ethanol from the wash solution was removed. The elution step was performed with 100μl of elution solution or with 100μl H_2O if the products were to be used for sequencing. The plasmid DNA was then kept at 4°C or -20°C.

2.2.2.2. Large scale plasmid DNA preparation

An endofree plasmid preparation maxi kit (Qiagen) was used for the preparation of plasmid DNA for transfection of mammalian cells or for zygote microinjection. The purity of the plasmid DNA is one of the requirements for these 2 techniques. Bacterial endotoxins, also known as lipopolysaccharides, strongly influence transfections by reducing the transfection efficiency. Moreover, in B cells, the endotoxins can cause non-specific activation of immune responses. The endotoxins are released during lysis of bacterial cells. LPS molecules are lipids and thus can form micellar structures leading to their co-purification with plasmid DNA. During the procedure, an endotoxin removal buffer is used which inhibits the LPS from binding to the resin of the QIAGEN-tips. Two different types of columns are used in this procedure: a QIAfilter maxi cartridge, which is used for clearing the bacterial lysates by filtration instead of centrifugation, and the QIAGEN anion-exchange tip, which is used for the plasmid DNA purification step.

The procedure is based on the same principle as the small scale preparation. A single plasmid-transformed colony was inoculated into 5ml of L-Broth usually supplemented with 50μg/ml of Amp (unless otherwise stated) and incubated with shaking at 37°C for 6 to 8 hours. 200μl of this starter culture was transferred to 200ml L-Broth containing the required antibiotic and incubated overnight with shaking at 37°C. The bacterial cells were harvested by centrifugation at 6000g for 15 minutes at 4°C (in a Beckman JA-17 rotor). The preparation was performed following the manufacturer's instructions using endotoxin-free plastic-ware. The pellet was resuspended in 10ml of P1 buffer [50mM Tris.Cl (pH 8.0), 10mM EDTA, 100μg/ml RNase A], lysed with 10ml of P2 buffer [200mM NaOH, 1% SDS (w/v)] and incubated for 5 minutes at room temperature. During this incubation the syringe format of the QIAfilter maxi cartridge was assembled. 10ml of Pre-chilled neutralisation buffer (P3) [3.0M potassium acetate (pH 5.5)] was added to the sample and mixed. The lysate was poured into the barrel of the QIAfilter maxi cartridge and incubated for 10 minutes at room temperature. The white precipitate containing proteins, genomic DNA (gDNA), cell debris and detergent floats and forms a layer on top of the solution; this avoids clogging of the column. The lysate was filtered through the column by pushing the liquid through the filter with the plunger; 2.5ml of ER buffer [composition not given in the manufacturer's instructions] was added to the

sample and incubated for 30 minutes on ice. This step removes any traces of endotoxins. The QIAGEN anion-exchange tip column was equilibrated using 10ml of QBT buffer [750mM NaCl, 50mM MOPS (pH 7.0), 15% isopropanol (v/v), 0.15% Triton® X-100 (v/v)], which contains a detergent. This column is an anion-exchange resin composed of defined silica beads coupled with positively charged DEAE groups. The negatively charged phosphates of the DNA backbone will interact with the positively charged DEAE group and will only be eluted with the presence of high-salt. The filtered lysate was applied to the column and the flow-through removed. The column was washed twice with 30ml of buffer QC [1.0M NaCl, 50mM MOPS (pH 7.0), 15% isopropanol (v/v)], which will remove the majority of contaminants, such as RNA, protein, carbohydrates and small metabolites. The plasmid DNA was eluted in 15ml of the high salt QN buffer [1.6M NaCl, 50mM MOPS (pH 7.0), 15% isopropanol (v/v)] and precipitated using 10.5ml of isopropanol (0.7 volumes). The sample was centrifuged at 15000g, 4°C for 30 minutes (in a Beckman JA-14 rotor). The supernatant was carefully decanted as the isopropanol pellet is fairly loose. The pellet was washed by adding 5ml of endotoxin-free 70% ethanol and centrifuged at 15000g, 4°C for 10 minutes (in a Beckman JA-14 rotor). The 70% ethanol removes any traces of salt and replaces isopropanol with a more volatile solvent. The pellet was air-dried for 5 to 10 minutes, resuspended in 50µl or 100µl of endotoxin-free H_2O depending on the size of the pellet and transferred to a microfuge tube. The concentration was determined using a spectrophotometer and also by loading an aliquot on a gel. Different digestions were performed to check the profile of the plasmid.

2.2.2.3. Genomic DNA preparation

Genomic DNA (gDNA) extraction was performed on mouse tail fragments and tissues and on cell pellets. The tail tissues were digested with 700µl of tail solution [50mM Tris (pH 8.0), 100mM EDTA (pH 8.0), 100mM NaCl, 1% SDS] plus freshly added 35µl of proteinase K (10mg/ml). Non-tail tissues were first minced with a scalpel blade before the addition of tail solution and proteinase K. For the cell pellets, 300µl of tail solution and 15µl of proteinase K were used. The samples were placed overnight at 55°C with shaking in an Eppendorf thermomixer. The proteins were separated by adding an equal volume (700µl or 300µl) of Tris-HCl buffer-saturated phenol pH 7.5. The samples were thoroughly mixed and microfuged for 5 minutes at 13000g at room-temperature. After the

centrifugation step DNA and RNA are in the upper aqueous phase whereas the proteins and cell debris are in the lower hydrophobic layer. Using cut yellow tips, the upper phase was transferred to a new microfuge tube without disturbing the interphase. An equal volume of 2FC was added to each sample and thoroughly mixed before being microfuged for 5 minutes at 13000g. This step further ensures the purification of the DNA from any residual proteins. The upper aqueous phase containing the DNA and RNA was transferred to a fresh microfuge tube. To preferentially precipitate the gDNA, 100µl of 10M NH4OAc and 750µl ice-cold 100% ethanol (43µl and 321µl respectively for cell pellets) was added to each sample and mixed until a white precipitate was observed. The tubes were microfuged at 8000g for 2 minutes to collect the gDNA. The supernatant was removed and the pellet was washed once with 750µl of 70% ethanol to remove excess salt. The samples were centrifuged at 8000g for 2 minutes. After removing the supernatant, the pellet was air-dried and resuspended in 100µl of TE pH7.5, using 15µl to quantify by optical density (OD). To ensure that the gDNA was resuspended the samples were heated at 55°C for up to one hour and then stored at 4°C indefinitely.

2.2.2.4. Quantification of DNA and RNA

The concentration of a sample was determined by measuring the OD at 260nm. After large scale plasmid DNA preparation 5µl of DNA was added to 295µl of H_2O (dilution factor of 60), whereas after a gDNA preparation 15µl of gDNA was added to 285µl of H_2O (dilution factor of 20). The sample was transferred to a quartz cuvette and the OD read on a spectrophotometer (Molecular Devices, Spectra Max plus). The concentration was determined using the following formula:

DNA concentration of the sample = OD_{260} x 50* x dilution factor x 1/light path (cm)

* For a double stranded DNA an OD_{260} of 1 equals a concentration of 50µg/ml.

* For a single stranded DNA an OD_{260} of 1 equals a concentration of 33µg/ml.

* For a single stranded RNA an OD_{260} of 1 equals a concentration of 40µg/ml.

For large scale plasmid preparation the concentration was subsequently checked by electrophoresing an aliquot on an agarose gel along with a marker of a known concentration.

For plasmid DNA preparation the samples were adjusted to a concentration of 1μg/μl and stored at -20°C. For gDNA the different samples were adjusted to a concentration of 0.33μg/μl or 0.5μg/μl and stored at 4°C.

2.2.2.5. Sequencing DNA fragments

An in house sequencing service was used (MBSU-DNA sequencing, Joseph Black Building, Department of Infection and Immunity). The sequencing primers were used at a concentration of 3.2pmoles. The sequences were analysed using Editview software.

2.2.2.6. DNA agarose gel electrophoresis

Agarose gels were prepared using either Ultrapure agarose (Gibco) for checking digests, PCR products or Southern blots, or low melting agarose (Nusieve) for gel extraction or making probes, in 1x TAE buffer or 1x TBE buffer. The agarose in buffer was melted in a microwave oven for 2 to 3 minutes. After slight cooling, ethidium bromide (EtBr) was added to a final concentration of 0.5μg/ml to the gel prior to casting. Samples were loaded and electrophoresed at 120V for 1 to 5 hours depending on the size of the expected fragments and the gel. The DNA fragments in the gel were visualised using a short wave (280nm) UV transilluminator. However the DNA fragments were visualised using a long wave UV for probe fragments and fragments for collection for construct generation.

2.2.2.7. Restriction digests

Restriction digestion of gDNA was performed according to Wilson *et al.*, (1990). 5 to 10μg of gDNA was digested with a restriction enzyme (usually 3 units/μg of DNA) along with the manufacturer's recommended buffer, in a total volume of 30 to 60μl. The samples were digested overnight at 37°C (or other recommended temperature). The following day, a further 1μl of enzyme was added and the samples were placed at 37°C for 2 to 3 hours. The reactions were then stopped by heating the samples at 65°C for 10 minutes.

Diagnostic digests were performed after each small and large scale plasmid preparation. For this, 1 to 3 μg of DNA was used with 1μl (1unit/μl) of enzyme (up to 3 units) along with the manufacturer's recommended buffer. The samples were usually digested for 2 hours at 37°C (unless otherwise stated by the manufacturer). The reactions were stopped by heating the samples at 65°C for 10 minutes. For preparative digests, more DNA was used (10 to 50μg) with suitably increased enzyme quantities and time.

2.2.2.8. DNA modification by ligation

Ligations were usually performed with a molar ratio of 1:3 to 1:10 (vector: insert). The following formula was used to determine the quantity of insert to add for the reaction (in ng):

$$\frac{\text{ng of vector x kb size of insert}}{\text{kb size of vector}} \times \text{molar ratio of } \frac{\text{insert}}{\text{vector}} = \text{ng of insert}$$

Usually between 50 to 200ng of purified vector DNA was used for the reaction. The reaction was set up in a PCR tube with the appropriate amounts of vector and insert and H_2O and 10x ligase buffer. 1 unit (1μl) of T4 DNA ligase was then added and mixed and the tube was placed in the PCR machine and incubated overnight at 16°C. Self-ligation of the vector was also performed as a control and in that case 50ng of vector was used. The reaction was performed in the same way as above.

Ligations of vector and insert were also performed in low melting agarose. For this purpose, the appropriate gel fragments were extracted from the low melting agarose and the concentration was determined (as described in section 2.2.2.9.1). The molar ratio of 1:3 to 1:10 (vector: insert) was also used for this type of ligation. Both the vector and the insert tubes were heated at 70°C for 5 minutes and the appropriate amounts of vector and insert were added and mixed in a PCR tube which was then cooled down to 37°C before adding the required amount of 10x ligase buffer and 1 unit of T4 DNA ligase. The tube was quickly placed on ice as the buffer contains ATP and both ATP and the T4 DNA ligase are heat labile. The PCR tube was placed in the PCR machine and incubated overnight at 16°C. The following day the PCR tube was heated at 70°C for 5 minutes and the DNA was

diluted in 200µl of TE to dilute the agarose, which could "inhibit" the transformation into bacteria.

2.2.2.9. DNA fragment isolation and purification

2.2.2.9.1. Isolation of DNA fragments in low melting agarose

DNA fragments to be used as a probe, for Southern blots or northern blots, or to be used for cloning were electrophoresed through low melting agarose gels. The DNA fragments in the gel were visualised using a long wave UV transilluminator and the appropriate DNA fragments were collected with a scalpel and placed in a microfuge tube. The quantity of the DNA fragment (in ng) was also estimated visually against a known quantity standard. The tube containing the appropriate DNA fragment was heated at 70°C for 5 minutes and the volume was checked in order to determine the concentration of the sample. The sample was then kept at -20°C until further use.

2.2.2.9.2. Gel extractions

DNA fragments to be used for cloning or as a standard for the quantitative PCR reaction were electrophoresed through 1% agarose gels. The DNA fragments in the gel were visualised using a long wave UV transilluminator and the appropriate DNA fragments were collected with a scalpel and placed in a microfuge tube. The quantity of the DNA fragment (in ng) was also estimated in the gel against a known quantity standard. Qiagen gel extraction kit was used for the procedure. The first step consists of the solubilisation of the gel slice which is followed by the absorption of the DNA fragment to a silica membrane column and an elution step. The tube containing the appropriate DNA fragment was weighed and 3 volumes of QG buffer was added to 1 volume of gel (100mg of DNA/gel fragment to 100µl of the kit's solutions). The sample was heated at 50°C for 10 minutes and mixed every 2 minutes. The QG buffer solubilises the agarose gel slice and also provides appropriate conditions for binding of the DNA to the silica membrane. 1 volume of isopropanol was then added to the sample and mixed. The sample was applied to the QIAquick column and centrifuged for 1 minute at 13000g. The flow-through was discarded and 0.5ml of buffer QG was added to remove all traces of agarose. The column was centrifuged for 1 minute at 13000g and the flow-through was discarded. The bound DNA was washed with 0.75ml of buffer PE, which contains ethanol, and centrifuged for 1

minute at 13000g. The flow-through was discarded and the sample was centrifuged for an additional 1 minute in order to remove any traces of residual ethanol. The DNA was then eluted in an appropriate volume (usually 50µl) of filter sterilised H_2O. The quantity of the DNA fragment recovered after the elution step was estimated by electrophoresing 1µl through a gel against a known quantity standard.

2.2.2.9.3. NA45 isolation and purification of DNA fragments

This procedure was used for the isolation of DNA fragments for use in the microinjection of embryos. 20µg of plasmid DNA was digested with the appropriate restriction enzyme (60 units of enzyme were used). For the different EBER1 transgenes the *Xba*I restriction enzyme was used to generate the linear transgene fragment.

The NA45 paper (Schleicher and Schuell), which is a Diethylaminoethyl (DEAE)-Dextran paper, was cut into strips of the correct size and activated by placing it in a solution of 1mM EDTA (pH 8.0) for 10 minutes at room-temperature. The strips were transferred to a solution of 0.5M NaOH for 5 minutes at room-temperature. The NA45 was then washed several times with sterile water and could be kept at 4°C indefinitely in this state.

The different digested plasmids were electrophoresed through a 1% agarose gel at 100V for 1 hour or longer if further separation was required. A strip of activated NA45 was inserted below the desired fragment into a slot cut into the gel. To prevent contamination from the vector DNA or other larger fragments, the gel above the desired fragment was cut off and discarded. The gel was electrophoresed for a further hour to allow transfer of the fragment on to the paper. The complete transfer was assessed by examination of the gel and paper on a long wave UV light box. Once the transfer was complete, the paper was trimmed into several small pieces and placed in a microfuge tube. The paper was washed with NET solution [0.15M NaCl, 0.1mM EDTA (pH 8.0), 20mM Tris (pH 8.0)] by vortexing and removing all the NET solution. The wash step was repeated. The DNA was then eluted from the paper in 200µl of high salt solution [1M NaCl, 0.1mM EDTA (pH 8.0) and 20mM Tris (pH 8.0)] at 68°C for 15 minutes. The eluate was transferred to a new microfuge tube and a further 200µl of high salt solution was added to the NA45 paper. The second elution was performed at 68°C for 20 minutes or as required to elute all DNA. This can be monitored by examining the NA45 paper under long wave UV light. The eluates were pooled and precipitated overnight at -20°C by adding

50µl of H_2O and 1ml of EtOH. The following day the sample was centrifuged at 13000g, 4°C for 15 minutes and washed once with 70% EtOH. The pellet was air-dried and resuspended in 40µl of H_2O.

The quality of the fragment was checked and quantity estimated by electrophoresis of 1µl and 5µl through an agarose gel against a known quantity standard. The volume of remaining sample was then made up to 360µl with H_2O and the sample was precipitated overnight at -20°C by the addition of 40µl 3M NaOAc (pH 4.5) and 1ml of EtOH. The following day the sample was centrifuged at 13000g, 4°C for 15 minutes and washed once with 70% EtOH. The pellet was air-dried and resuspended in filter sterilised injection buffer [5mM Tris (pH 7.4), 5mM NaCl, 0.1mM EDTA (pH 8.0)] at a concentration of 5µg/ml. A dilution to 2µg/ml was also made. The concentration was checked by running an aliquot on a gel along with an appropriate standard.

Prior to using for microinjection, the DNA solution was centrifuged at 13000g for 15 minutes at room-temperature. The top 2/3 was transferred to a new microfuge tube, leaving behind the lower part with any particulate matter, which could clog the injection needle. The lower part was kept and used as a fragment to generate a probe for Southern blot analysis.

2.2.2.10. Southern blot

The DNA samples used for the Southern blot analysis were electrophoresed through a 0.8 to 1.6% agarose gel in 1x TAE buffer. The gel was electrophoresed for 5 to 7 hours at 120V or overnight at 30V. The EtBr stained DNA was visualised using a short wave UV transilluminator and the gel trimmed of any excess and the ladder track. The gel was placed in denaturing solution shaking for 30 minutes at room-temperature. The gel was washed 3 times 10 minutes in 0.5x TAE buffer. The DNA was transferred onto a Nytran supercharge membrane (Schleicher and Schuell) by electroblotting at 1500mA for 3 hours in 0.5x TAE in a Hoeffer electroblotting tank. The DNA was UV crosslinked to the membrane using a Stratalinker at 1200kJ and either kept at -20°C until used or probed as described by Wilson *et al.* (1990).

2.2.2.11. Slot blot

The slot blots were performed using either gDNA or plasmids as test samples. For each sample 10μg of gDNA was used and the volume was made up to 120μl with H_2O. For plasmid DNA 20, 100 and 500pg were used. The DNA was denatured by the addition of 40μl of 1M NaOH and vortexed for 10 minutes at room-temperature. 160μl of 10x TAE was added to the samples, which were vortexed briefly, microfuged for 1 minute at 13000g and placed on ice. Positively charged Nytran membrane (Schleicher and Schuell) was pre-soaked in 1x TAE and the apparatus was assembled. The samples were then loaded onto the slots and then the vacuum was switched on so that the samples could pass through the membrane. One drop of 5x TAE was loaded onto the slots and the vacuum was stopped when all liquid had passed through the membrane. The apparatus was dismantled and the membrane was UV cross-linked in a Stratalinker at 1200kJ. The blots were then kept at room-temperature until probing. The probing conditions, hybridising and washing conditions of the probe were the same as for Southern blots.

2.2.2.12. Probing of Southern blots, slot blots and northern blots with ^{32}P labelled DNA fragments

The membranes were rolled up in perspex tubes with the DNA loaded side facing the inside of the tube. 10 to 15ml of Church buffer were added and the tubes were placed in a rotary hybridisation oven to pre-hybridise for at least 2 hours at the appropriate temperature. This step was performed to block any non-specific binding sites of the probe on the membrane.

The probes were generated using Stratagene's PrimeIt labelling kit following the manufacturer's instructions. 25ng of the appropriate DNA fragment (Table 2.3) isolated on low melting point agarose gel was added to random primers and the DNA was denatured at 95°C for 5 minutes. 5x buffer lacking dCTP, 40 to 50μCi of ^{32}P αdCTP and 5 units of Klenow enzyme were added to the sample in this order. The reaction was incubated at 37°C for 30 minutes to 4 hours. The probe was purified from unincorporated nucleotides using the NucTrap push columns system (Stratagene) according to the manufacturer's instructions. The radiolabelled sample was applied on to a prewet column and the probe

was eluted from the column by pushing down a syringe. The column was rinsed once with 1x STE and pushed down using a syringe. The liquid from the sample and rinse were combined in the same collection tube. The probe was then denatured at 95°C for 5 minutes and added to the membrane in Church buffer. Hybridisation was carried out overnight at the appropriate temperature (Table 2.13). For Southern blots, the following day the membranes were washed 4 times for 10 minutes in 2x SSC, 0.1% SDS, shaking at room-temperature. A hot wash was also carried out at the appropriate temperature (Table 2.13), shaking for 30 minutes to 1 hour in pre-heated 0.1x SSC, 0.1% SDS. For northern blots, the following day hot washes were carried out at the appropriate temperature, shaking for 15 minutes in pre-heated 2x SSC, 0.1% SDS, for 15 minutes in pre-heated (60°C) 1x SSC, 0.1% SDS and for 15 minutes in pre-heated (60°C) 0.5x SSC, 0.1% SDS. The membranes were then sealed in plastic bags and visualised by autoradiography. The exposure time varied depending on the intensity of the bands.

Probe	Hybridisation temperature	Hot wash temperature
EBER1	60°C	60°C
EμEBER1	65°C	65°C
EBNA1	68°C	68°C
N-myc	65°C	65°C
IgH	65°C	65°C
TCR	65°C	65°C

Table 2.13: Hybridisation and wash stringencies of Southern blot probes

2.2.2.13. Polymerase chain reaction

Polymerase chain reaction (PCR) is a method for selectively and repeatedly replicating defined DNA sequences from a DNA mixture. The technique is based on the annealing of two short oligonucleotides (primers) to the opposite strands of a denatured target DNA molecule, thereby providing free 3'OH ends for DNA polymerase-mediated chain primer elongation. With each cycle (of 20-40 cycles in total) the DNA present after the previous cycle serves as a template; therefore the quantity of DNA is doubled. Cycling was performed in a PCR thermal cycler (MJ Research).

The PCRs were performed using either *Pfu* Turbo DNA polymerase or *Taq* DNA polymerase and plasmid DNA or gDNA as a template. The reactions were carried out in 25 or 50μl final volume with 1ng to 300ng of template DNA as indicated. The figure below shows an outline of the different steps of the reaction:

denaturing step: 95°C for 5 minutes

denaturing step: 95°C for 30 seconds
annealing step: X°C for 30 seconds
elongation step: 72°C for Z minutes
} Y cycles

final elongation step: 72°C for 10 minutes

X, Y and Z are different with the different sets of primers as detailed in figure 2.2.

Reagents	Concentrations
DNA or gDNA	Between 1ng and 300ng
10x buffer, supplied with the enzyme	$1/10^{th}$ of the final volume
$MgCl_2$ if not included in buffer	1.5mM to 2mM
dNTPs (dATP, dCTP, dGTP, dTTP)	0.4mM
Forward primer	0.2µM
Reverse primer	0.2µM
Enzyme (*Taq* or *Pfu*)	2.5 units

Table 2.14: Composition of a PCR

To clone the three EBER1 fragments into pcDNA3.1, three different PCRs were performed using *Pfu* Turbo DNA polymerase and pLEXIII as template for the EBER1 gene (kind gift from Prof M. Clemens). The reaction was performed in 50µl final volume with 1ng of template DNA. The following reagents were used: 5µl of 10x buffer, 1µl of 20mM (stock concentration) dNTPs, 1µl of 10µM (stock concentration) forward and reverse primers (CR1-CR4, CR2-CR4 and CR3-CR4) and 2.5units of *Pfu* Turbo DNA polymerase. The cycling conditions were the following:

denaturing step: 95°C for 5 minutes

denaturing step: 95°C for 30 seconds
annealing step: 60°C for 30 seconds
elongation step: 72°C for 1 minute
} 30 cycles

final elongation step: 72°C for 10 minutes

To check for the presence of the *c-myc* transgene, PCRs were performed using *Taq* DNA polymerase and tail gDNA as template. The reaction was performed in 25µl final volume with 300ng of template gDNA. The following reagents were used: 2.5µl of 10x buffer, 2µl of 25mM (stock concentration) $MgCl_2$, 0.5µl of 20mM (stock concentration)

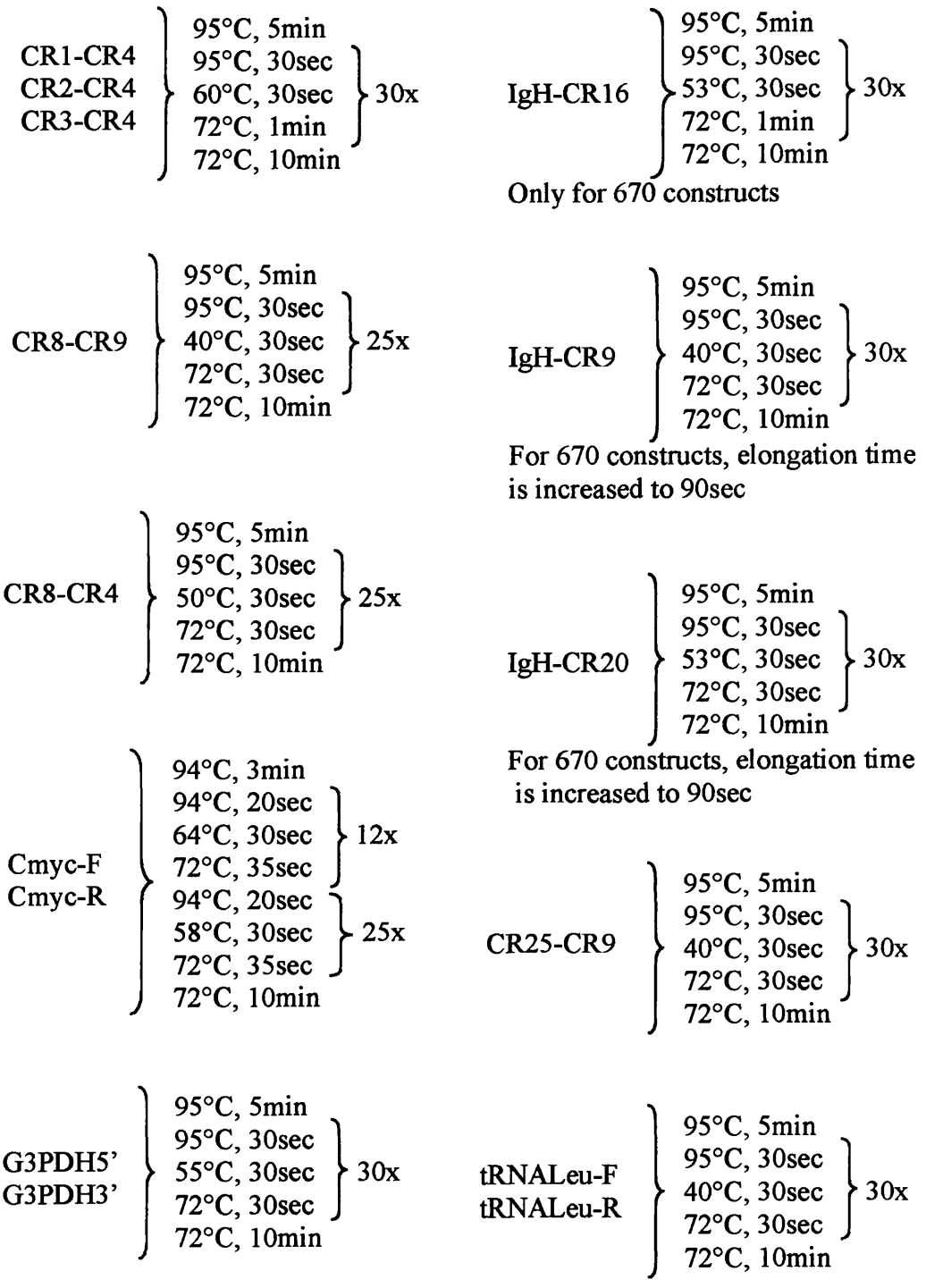

Figure 2.2: Cycling conditions for the different primer pairs

dNTPs, 1.25µl of 10µM (stock concentration) CmycF and CmycR primers and 2.5units of *Taq* Turbo DNA polymerase. The cycling conditions are shown in figure 2.2.

2.2.3. RNA techniques

2.2.3.1. RNA extraction according to Chomczynski and Sacchi

During the procedure, gloves were worn at all times to avoid any ribonuclease degradation via RNases. The bench and the different pieces of equipment were washed or soaked with 1%SDS (w/v) and rinsed with 75% EtOH (v/v). All the solutions were made up with diethyl-pyrocarbonate (DEPC)-H_2O or treated directly with DEPC and autoclaved to destroy RNases. All the chemicals, solvents, solutions, microfuge and PCR tubes were kept in a separate RNA cupboard.

This method is based on the protocol developed by Chomczynski and Sacchi (1987). The tissues were kept either on dry-ice or in liquid nitrogen to avoid thawing until being processed. The frozen tissues were placed in a 5ml RNase-free falcon tube and 1ml of solution D (1ml per 50 to 100mg of tissue) was added [0.36ml of 2β mercaptoethanol, 50ml of 4M GT [250g guanidinium thiocyanate (Sigma), 0.75M Na citrate pH7 with citric acid and 10% sarcosyl, 350ml dissolved at 65°C and 3 months life shelf], 1 months shelf life] and homogenised using a polytron homogeniser. For larger size tissues, they were cut on dry ice using a scalpel blade. The tissues were kept on ice until all the tissues were homogenised. For cell pellets the procedure was the same except that the cells were resuspended in solution D by vortexing. 100µl of 2M NaOAc (equivalent to 0.1 volume of solution D used) was added to the samples and they were mixed thoroughly. 1ml of acid phenol (equivalent to 1 volume of solution D used, catalog number P1037, Sigma) was added to the samples and they were mixed thoroughly. 200µl of $CHCl_3$-isoamylalcohol (49:1 ratio) (equivalent to 0.2 volume of solution D used) was added and the samples were vortexed thoroughly for 10 seconds and placed on ice for 15 minutes. The mixture was then centrifuged at 10000g (6000rpm in a JA-17 Beckman rotor) for 20 minutes at 4°C. This step separates the mixture into three phases: a colourless organic phase containing proteins (bottom phase), an interphase containing DNA, and a colourless aqueous phase containing RNA (the upper phase). For each sample the colourless aqueous phase was transferred to 2 microfuge tubes and 0.5ml of isopropanol was added to each tube

(equivalent to 1 volume of solution D used). The RNA was then precipitated at -20°C for at least 4 hours or longer. The samples were centrifuged in a microfuge at 13000g for 20 minutes at 4°C. The wet pellets were resuspended in 300µl of solution D (for each of the _ samples 150µl of solution D was added and the samples were combined in the same tube), vortexed and 600µl of EtOH was added. The RNA was precipitated at -20°C for 2 hours. The samples were microfuged at 13000g for 20 minutes at 4°C and the pellet was washed twice in 75% EtOH, air-dried and resuspended in 100µl DEPC-H_2O for small tissues and up to 400µl of DEPC-H_2O for larger tissues by heating at 65°C and vortexing. The RNA was then DNAse I treated if used for RT-PCRs or quantitative RT-PCRs.

2.2.3.2. Analysis and quantitation of RNA

Following RNA extraction the quality of the RNA was checked visually on a 1.4% formaldehyde agarose gel. 5µl of RNA was added to 15µl of RNA loading buffer and heated at 68°C for 10 minutes. 2µl of 10x loading buffer was added to each sample and they were loaded on to a 1.4% formaldehyde agarose gel, as described for the northern blot (section 2.2.3.5). The gel was electrophoresed at 100V for 1 hour in 1x MOPS. The RNA was visualised using a short wave UV transilluminator to check for the presence of the three ribosomal RNA bands. Degraded samples were discarded.

To measure the RNA concentration, 5µl of each sample was used. Both the OD at 260 and 280 was measured and the ratio (OD260/OD280) was determined. A good ratio was considered to be between 1.8-1.6 and optimal at 2. This ratio provides an estimate of the protein content in the sample (below 1.6). The RNA samples were then stored at -20°C until further use.

2.2.3.3. DNAse I treatment

Usually 10µg of RNA was treated with 2.5units of DNase I. The volume was made up to 50µl with DEPC-H_2O and buffer. The samples were incubated at 37°C for 1 hour and heated at 75°C for 10 minutes to inactivate the enzyme. To remove any traces of DNA, 200µl of DEPC-H_2O was added to the samples, which were further subjected to an acid phenol extraction (see section 2.2.3.4).

2.2.3.4. Acid phenol extraction

250µl of acid phenol (Sigma, phenol citrate, pH 4.7) was added and mixed. The samples were centrifuged at 13000g for 2 minutes at room-temperature. The aqueous phase was transferred to a microfuge tube and 250µl of chloroform was added and mixed. The samples were centrifuged at 13000g for 2 minutes at room-temperature. The aqueous phase was transferred to a microfuge tube. $1/10^{th}$ volume of 3M NaOAC and 2.5 volume of EtOH were added and the RNA was precipitated overnight at -20°C. The samples were microfuged at 13000g for 20 minutes at 4°C. The pellet was washed in 75% EtOH, air-dried and the RNA resuspended in 20µl of DEPC-H_2O by vortexing and heating the samples at 65°C. The RNA was usually used for RT-PCR.

2.2.3.5. Northern blot

The gel tank, tray and combs were soaked overnight in 1% SDS and rinsed with DEPC-H_2O in order to remove traces of RNases. Between 10 and 20µg of sample RNA was used and usually 1µg of EBV positive cell line (eg Raji) RNA was used for the positive control, unless otherwise stated. The samples were aliquoted in microfuge tubes and precipitated with 3M NaOAc ($1/10^{th}$ aqueous volume) and 100% EtOH (2.5x total aqueous volume) overnight at -20°C. The samples were centrifuged for 30 minutes, 4°C at 13000g and the pellets washed once with 75% EtOH. The RNA pellets were air-dried and resuspended in 4µl of DEPC-H_2O by heating to 65°C and vortexing thoroughly. 16µl of RNA loading buffer was added and the samples heated at 68°C for 10 minutes to denature secondary structures, before being placed on ice and briefly centrifuged to collect the sample. Prior to loading the samples on a 1.4% formaldehyde agarose gel, 2µl of 10x loading dye was added to each sample. 1.4g of agarose was melted in 84.8ml of DEPC-H_2O in a microwave. 10ml of 10x MOPS was added to the gel mix and cooled down before adding 5.2ml of formaldehyde and poured. Electrophoresis was performed in the cold room in 1x MOPS buffer at 80V for 2 to 3 hours. A 1kb ladder was also loaded as a size control after all the RNA samples were loaded and usually a spare well was left between the ladder and the first RNA sample. After running, the gel was washed 3 times 20 minutes in 0.5x TAE buffer and in the third wash EtBr was added to a final

concentration of 0.5μg/ml. The DNA ladder and RNA were visualised using a short wave UV transilluminator and the gel trimmed of any excess and the ladder track. The RNA was transferred onto a Nytran supercharge membrane by electroblotting at 1500mA for 2.5 hours in 0.5x TAE in a Hoeffer electroblotting tank. The RNA was UV crosslinked to the membrane using a Stratalinker at 1200kJ and either kept at -20°C until used or probed as described by Wilson *et al.* (1990).

2.2.3.6. Reverse transcriptase

cDNA synthesis was performed using a gene specific primer for EBER1 (CR4) and Moloney murine leukemia virus (M.MLV) reverse transcriptase (RT). For RNA polymerase II genes, such as GAPDH, the reaction was performed using the cDNA first strand synthesis kit from Abgene and oligodT primers. However, the procedure was performed in the same way.

2μg of total RNA (DNAse I treated or not) was mixed with 1μM of either gene specific primer or oligodT, 0.4mM of dNTP and made up to a final volume of 12μl with DEPC H_2O. The reaction was incubated for 5 minutes at 65°C to denature any secondary structures. The buffer was added to the reaction mix (1x final concentration), plus 0.01M DTT and 200 units of RT enzyme. A negative control was also performed without the RT enzyme; this was used to check for gDNA contamination in the RNA sample. The samples were incubated at 37°C for 1 hour followed by 72°C for 10 minutes to stop the reaction. A PCR, or QPCR was usually performed using $1/5^{th}$ of the RT reaction. The RT samples were stored at 4°C or -20°C for longer storage.

2.2.3.7. Quantitative reverse transcriptase-polymerase chain reaction

Quantitative PCR (QPCR) is a fluorescence-based method, which allows initial quantities of the template to be determined. The bigger the initial template the fewer cycles are required before a significant fluorescence signal is detected. The QPCR machine records the amount of fluorescence emitted after each cycle. Quantitect™ SYBR Green kit (Qiagen) was used along with the DNA engine Opticon™ (MJ research). SYBR Green is a fluorescent double stranded (ds) DNA binding dye thought to bind in the minor groove. The major drawback using this dye is that false positive signals from secondary structures

or primer dimers can interfere with accurate quantification of the fragment under test. To try and minimise this, a water control with primers was always performed along with a -RT control for each sample. A melting curve was also performed at the end of the reaction to analyse product homogeneity and help to distinguish between a primer dimer and a PCR product.

For each QPCR a standard curve was generated so that an accurate comparative quantity of DNA could be determined in the different samples. To generate the standard curve, a PCR was first carried out using the appropriate plasmid DNA as template and the same primers as the ones used for the QPCR. The PCR product was electrophoresed through an agarose gel and the correct DNA fragment was cut out of the gel and gel isolated using the Qiagen kit. The concentration of the sample was determined by measuring the OD at 260nm and subsequently checked by running an aliquot on an agarose gel along with a marker of a known concentration. The standard curve template was adjusted to 1ng/µl and stored at -20°C until used. For the standard curve itself, 6 serial dilutions (1/10) of the standard curve template were performed starting with a concentration of 0.1ng/µl. 1µl of each standard template was then used for the reaction. The standard reactions were always performed in duplicate. The fluorescence emitted by each standard sample was recorded by the machine and as the initial quantity of these samples was known a standard curve could be generated and plotted as log quantity versus threshold cycle (Ct). The Ct is defined as the cycle at which the sample's fluorescence trace crosses the Ct line. A baseline-subtracted graph of the samples and standard sample is displayed as the fluorescence versus the cycle number. It is on this graph that the Ct line is positioned such that it intersects the fluorescence traces at a point where the signal surpasses the background noise and begins to increase. The following equation describing the linear standard curve is presented in the form of:

$$Y = mX + B$$

where m is the slope and B is the intercept of the line

An R^2 value is also given and indicates how well the fit of the standard curve describes the variation of the data. Values closer to 1 indicate a good fit. The initial quantity in a sample can then be determined by replacing the Ct value of the sample in the following equation:

$$Q = 10^{(mX+B)}$$

where Q is the quantity in ng, m the slope and X the Ct value of the sample

The reactions for the cDNA samples were either performed in duplicate or triplicate. The figure below shows an outline of the different steps of the reaction:

denaturing step: 95°C for 15 minutes (hot start enzyme)

denaturing step: 95°C for 30 seconds
annealing step: X°C for 30 seconds
elongation step: 72°C for Z minutes
} Y cycles, plate read after each cycle

final elongation step: 72°C for 10 minutes

plate read

melting curve: 70°C to 90°C, increment: 0.3 and hold time: 1 sec

X, Y and Z values differ with the different sets of primers.

Reagents	Concentrations
cDNA	Xµl
10x buffer	1/10th of the final volume
dNTPs (dATP, dCTP, dGTP, dTTP)	0.4mM
Forward primer	0.2µM
Reverse primer	0.2µM

Table 2.15: Composition of a QPCR

2.2.4. Protein techniques

2.2.4.1. Protein extraction from tissues using a high salt buffer

The proteins were extracted in high salt buffer containing phosphatase inhibitors (Sigma, cat. No. P5726, as recommended by the manufacturer's instructions) and protease inhibitors (Sigma, cat. No. P2714, as recommended by the manufacturer's instructions). The phosphatase inhibitor cocktail contains sodium vanadate, sodium molybdate, sodium tartrate and imidazole; this cocktail can inhibit acid/alkaline and tyrosine protein kinases. The protease inhibitor cocktail contains AEBSF, E-64, bestatin, leupeptin, aprotinin and sodium EDTA; this cocktail can inhibit serine, cysteine, aspartic acid and metalloproteases. For each sample usually 0.5ml of high salt buffer per 0.1-0.2mg of tissue was added to a

5ml Falcon tube. The samples were homogenised using a Kinematica polytron homogeniser. Before and after each sample was processed the polytron was washed with 1% SDS, 3 H_2O washes and 70% (v/v) ethanol. Once homogenised the samples were placed on ice for 10 minutes, transferred to a fresh collection tube and microfuged at 13000g, 4°C for 15 minutes. The supernatant was transferred to a fresh microfuge tube and the protein concentration was determined using a Bradford assay. The samples were then placed at -70°C until used.

2.2.4.2. Quantification of proteins using a Bradford assay

This method is based on the Bradford dye-binding procedure (Bradford, 1976), which is a colourimetric assay. A standard curve was performed with a known concentration of BSA as shown in the table 2.16. 5µl of high salt buffer was added to all the BSA standards. 5µl of sample was added to 795µl of TE in the appropriate cuvette. 200µl of Biorad dye was added to each sample and standard; the samples were inverted a few times and left to stand for 5 minutes for the colour to develop. The optical density of each standard and sample was read at 595nm. Using the values obtained for the BSA standard a standard curve was drawn (X axis = OD and Y axis = concentration) and the protein concentration of each sample was determined.

BSA quantities in µg	BSA (100µg/ml) added in µl	TE in µl
0	0	795
1	10	785
2	20	775
4	40	755
8	80	715
16	160	635

Table 2.16: Standard protein curve for the Bradford assay

2.2.4.3. Western blot

2.2.4.3.1. SDS polyacrylamide gel electrophoresis of protein samples

The polyacrylamide gels were prepared as described in table 2.17. Different percentage gels were performed in order to separate different sizes of proteins. For instance, a higher percentage gel was used to resolve small proteins.

The running gel was poured first and overlaid with a layer of butanol-saturated water. Once set (usually after 30 minutes), the water was removed and the stacking gel was poured on top and the comb was placed. This was allowed to set for approximately 40 minutes and then assembled into the electrophoretic apparatus. One litre of running buffer was added and the samples were loaded as described in section 2.2.4.3.2.

Reagents	5% stacking gel (for 2 gels)	7.5% running gel (for 1 gel)	10% running gel (for 1 gel)	12.5% running gel (for 1 gel)
40% Bis-Acrylamide	3.75ml	9.375ml	12.5ml	15.63ml
1M Tris pH 6.8	3.75ml	-----	-----	-----
1.5M Tris pH 8.8	-----	12.5ml	12.5ml	12.5ml
20% SDS	150µl	250µl	250µl	250µl
0.5M EDTA	60µl	100µl	100µl	100µl
H_2O	22ml	27.175ml	24.05ml	20.97ml
TEMED	30µl	50µl	50µl	50µl
20% APS	300µl	500µl	500µl	500µl

Table 2.17: Running and stacking gels for western blots

2.2.4.3.2. Western blotting

Usually between 50 to 100µg of protein extract was loaded on the gel. The samples were added to 4x loading buffer and placed at 65°C for 5 minutes. 10µl of either high or low molecular weight ladder (catalogue number 756 or 755, respectively, Amersham) was also loaded on to the gel. The samples were electrophoresed at 200V (0.1 A) for 3 hours until the dye reached the bottom. Prior to setting up the western transfer, the membrane (Immobilon P, Millipore, cat No. IPVH 00010) was pre-wetted in methanol for 15 seconds, then in H_2O for 2 minutes and finally left to equilibrate in transfer buffer for 10 minutes. The gels were also left to equilibrate in transfer buffer for 10 minutes. The transfer was performed in the cold room at 1200mA for 2 hours and 20 minutes. After transfer, the membranes were placed for at least 1 hour in blocking buffer. The membrane was then incubated overnight with the appropriate primary antibody at the required dilution (Table 2.6) in blocking buffer. The following day, the membrane was washed for 3 times 15 minutes in wash buffer. The appropriate secondary antibody fused to horseradish peroxidase (HRP) was added at the required dilution (Table 2.7) in blocking buffer and usually incubated for 1 hour at room-temperature. The membrane was washed for 3 times 15 minutes in wash buffer. Amersham's ECL™+ kit (Amersham) was used for the

detection of antibody binding. The process converts acridan into acridinium ester intermediates with the use of peroxide and HRP. These intermediates react with peroxide under slight alkaline conditions to produce a high intensity chemoluminescence, which can be detected using autoradiography film. The solution was left for 5 minutes and then the excess of solution was drained and the membrane was placed in a plastic bag and sealed. The membrane was then exposed to X-AR Kodak film for various exposure times depending on the intensity of the signal and the film was developed using an X-Omat developer. To determine if the proteins were loaded equally, a ponceau (Sigma) stain was sometimes performed, which stains all the proteins. 100ml to 200ml of ponceau was added to the membrane and placed on a rocking platform for 10 minutes at room-temperature. Several washes with 100ml of distilled water were then performed to "destain" the membrane and visualise the proteins. The membrane was placed in a plastic bag and scanned.

2.2.4.4. Stripping and reprobing western blots

The membrane was stripped of antibody using stripping buffer by shaking at 50°C for 1 hour. The membrane was then washed twice for 10 minutes at room-temperature in wash buffer. Following the washing steps, the membrane was placed in blocking buffer for at least 1 hour at room-temperature and probed as described above. After use, the membranes were stored at 4°C in a sealed plastic bag to keep them from drying out and allow re-use.

2.2.4.5. Electrophoretic mobility shift assay

2.2.4.5.1. Annealing of the probe

Both the forward and reverse oligonucleotides (Table 2.12) were separately resuspended to 100μM. To anneal the two oligonucleotides 2μl of each oligonucleotide was added to 10μl of 5M NaCl and 186μl TE. The sample was mixed and placed at 80°C for 10 minutes in a heat block. Once the incubation was finished the tube was allowed to cool slowly in the block to 23°C. Aliquots were prepared and stored at -20°C. The final concentration of the annealed oligonucleotide was 1pmol/μl. In this way, double-stranded

DNA sequences were generated, incorporating the required protein recognition sequence and showing 4 nucleotides 5' overhang.

2.2.4.5.2. Generation and purification of the EMSA probe

To generate the Electrophoretic mobility shift assay (EMSA) probe, 1µl of the required annealed oligonucleotide (1pmol per probe) was added to 33µl of H_2O, 10µl of dCTP 5x buffer (Prime it labelling kit, Stratagene) 5µl of ^{32}P αdCTP (50µCi) and 1µl of Klenow to fill in the overhang. The sample was mixed and incubated at 37°C for 20-30 minutes. Following the incubation, the probe was purified away from unincorporated nucleotides using NICK™ columns (Amersham), which contain Sephadex® G-50. The column was equilibrated with 3ml of TE buffer, which was allowed to run through the column. The labelled mix was placed on to the column and after a few seconds 400µl of TE was added to the column. At this point all the unincorporated nucleotides should be eluted. The radiolabelled oligonucleotide was then eluted using a further 400µl of TE and collected in a fresh tube. The probe was either used directly or stored at -20°C in a lead container until use.

2.2.4.5.3. Preparation of the samples

5 to 10µg of protein extract (the extraction was performed using the high salt extraction protocol, section 2.2.4.1) were aliquoted into microfuge tubes. Usually duplicate samples were analysed, unless a supershift assay was performed in which case three replicate samples were aliquoted. To each sample 1µl of polydIdC (1µg/µl, Sigma), 25µl of GR2 buffer [1ml 1M Tris pH 7.5, 3ml 5M NaCl, 10µl 50mM $ZnCl_2$, 0.25ml $MgCl_2$, 0.025ml 1M DTT, 1.25ml glycerol (final 25%), make up to 25ml with H_2O] and 9µl of H_2O were added. A tube with no protein extract was also prepared as a free probe control. The samples were incubated on ice for 10 minutes. 4µl of labelled probe was added to all samples and to the duplicate of each sample between 100 to 200x (1pmol to 2pmol final) of cold competitor (unlabelled double-stranded oligo compared to labelled oligo) was added. The samples were incubated on ice for 20 minutes.

If a supershift assay was performed, 4µg of the appropriate antibody was added to the third replicate sample, which was incubated at room-temperature for 15 to 20 minutes. 4µl of labelled probe was then added to the third replicate sample and incubated on ice for 20 minutes.

2.2.4.5.4. Non-denaturing acrylamide gel preparation

A 6% non-denaturing acrylamide gel was used to electrophorese the samples using the following reagents:

Reagent	Volume in ml
5x Tris/glycine buffer	10
40% acrylamide	8.3
H_2O	30
20% (v/v) APS	0.5
TEMED	0.15

Table 2.18: 6% non-denaturing acrylamide gel composition

The gel was left to polymerise for 1 hour and then pre-run for at least 30 minutes in the cold room in 1x Tris-glycine buffer. The samples were then loaded on to the gel. In the first lane, loading dye was usually loaded alone so that the running of the samples (without dye) could be monitored. The samples were electrophoresed at 150V for 3 hours or until the dye was about 3cm from the bottom. The gel was then transferred on to 2 sheets of 3MM paper, covered with saran wrap and dried at 80°C for 2 hours. The dried gel was exposed to X-AR Kodak film for various exposure times depending on the intensity of the signal and the film was developed using an X-Omat developer.

2.2.5. Enzyme-linked immunosorbent assay

Enzyme-linked immunosorbent assay (ELISA) can be used to quantify levels of circulating antibodies or cytokines in the serum or cell supernatant. To quantify serum IgM a flat-bottom 96 well plate was coated with 100µl of rat anti-mouse IgM (coating) antibody (1/200 dilution to a final concentration of 5µg/ml) and placed overnight at 37°C. The following day, the surplus coating antibody was removed and to each well was added 200µl of blocking buffer [1xPBS, 0.05% (v/v) Tween 20, 0.5% BSA (w/v)] and placed at 37°C for 30 minutes. The wells were then washed three times quickly with washing buffer [1xPBS, 0.1% (v/v) Tween 20] and three times for three minutes each with washing buffer. All liquid was removed by tapping the plates on to blotting paper before adding 100µl of serum sample to each well (1/800 dilution, for IgM only, in PBS-0.05% Tween 20) and incubating at room-temperature for 90 minutes. The unbound serum sample was removed

and the wells washed and dried as described above. 100µl of horseradish peroxidase (HRP)-conjugated goat anti-mouse IgM antibody (1/4000 dilution in PBS-0.05% Tween 20) was then added to each well and incubated at room-temperature for one hour. The wells were washed and dried as described above and then 100µl per well of tetramethylbenzidine (TMB) substrate (Sigma) was added and incubated until a colour change was observed in the samples (usually between 5 and 20 minutes). A dark blue colour indicated a high level of IgM, whereas a light blue colour indicated a low level. The optical density of each sample was then read at 620nm and the concentration of secreted IgM determined using a standard curve. To obtain the IgM standard curve, 1/250 dilution of 1mg/ml mouse IgM antibody was added in the first well. For the following wells, serial 1/2 dilutions were performed until 1/512000 dilution factor. The assay was performed as described for the samples. The same protocol was followed to determine the levels of IgG1 and IL10, except that for IL10 the serum sample was diluted 1/2 instead of 1/800. An extra step was also performed for the detection of IL10. Following the incubation with the detection antibody, 100µl of 1/1000 dilution of streptavidin peroxidase (Diagnostics Scotland, catalog number T245, as recommended by the Manufacturer) was added to each well and incubated for one hour at room-temperature. The wells were washed and dried as described above and then 100µl per well of TMB substrate was added and incubated until a colour change was observed in the samples.

2.2.6. Proteoplex 16 well murine cytokine array kit

A cytokine array kit was supplied by Novagen, catalog number 71454, and the reaction performed according to the manufacturer's instructions. The kit allows for testing the levels of 10 different cytokines (IL1α, IL1β, IL2, IL4, IL6, IL10, IL12p70, GM-CSF, IFNγ and TNFα) in 10 test samples. Briefly, the pre-coated wells were washed [PBS-Tween, provided by the kit] and then 100µl of 1/3 diluted serum samples and 100µl of each of the five point standard curve samples (which contain different purified cytokines and cover a range between 15pg/ml and 800pg/ml) was added to the wells. The samples were incubated for one hour at room-temperature with orbital rotation. The wells were then washed with PBS-Tween and 80µl of murine detection antibody cocktail was added and incubated for one hour at room-temperature with orbital rotation. The wells were washed with PBS-Tween and then 100µl of PBXL-3 fluorophore detection mix was added to each

and covered with foil before being incubated for 90 minutes at room-temperature. The array apparatus was disassembled, the slide was rinsed and dried by centrifugation at 200g for 1 minute before being kept 4°C and mailed to the company for analysis. The slide was scanned and the data was extracted as pixel density values. The background signal was subtracted from both the standard signal and the experimental signal. The mean average of the four spots was also determined and used to generate the standard curve and to determine the cytokine concentration of each experimental sample. A standard curve was generated for each cytokine tested by plotting the signal from each cytokine standard against the known cytokine concentration. The signal value of each experimental sample along with the different standard curves was used to determine the cytokine concentration in the samples. The data was sent as an Excel file and included in a spot data table, a well data table and a summary table with the final calculated concentrations for each cytokine for all the experimental samples (this is the data presented in table 5.10).

2.2.7. Bacterial techniques

2.2.7.1. Generating competent DH5 *E. coli* cells

A single colony of DH5 cells was grown in 5ml of Luria Bertani (LB) medium at 37°C for approximately 2 hours to an absorbance at 550 nm of 0.3 and then transferred to 100ml of warmed LB medium. The cells were incubated with shaking at 37°C until they reached a maximum OD at 550nm of 0.48. The cells were immediately cooled down on ice and pelleted at 4°C, 4000g for 5 minutes. The cell pellet was gently resuspended in 40ml of ice-cold filter sterilised transforming buffer I (TfbI) [30mM potassium acetate, 100mM $RbCl_2$, 10mM $CaCl_2$, 50mM $MnCl_2$, glycerol to 15% v/v and pH adjusted to 5.8 with 0.2M glacial acetic acid]. The cells were incubated on ice for 5 minutes and centrifuged at 4°C, 4000g for 5 minutes. The pellet was resuspended in 4ml ice-cold filter sterilised TfbII [10mM MOPS, 10mM $RbCl_2$, 75mM $CaCl_2$, glycerol to 15% v/v and pH adjusted to 6.5 with KOH]. 200µl of cells were aliquoted in microfuge tubes, snap frozen on dry ice and stored at -70°C for up to 3 months.

2.2.7.2. Transformation of competent DH5 *Escherichia coli* cells with plasmid DNA

An aliquot of competent DH5 *Escherichia coli* (*E. coli*) cells was thawed on ice for 10 minutes. The appropriate amount of DNA (usually 100ng) was added to the cells and incubated on ice for 15 minutes. The cells were then heat shocked at 42°C for 90 seconds and returned on ice for 2 minutes. 800µl of LB medium was added to the cells and incubated for 50 minutes at 37°C, not shaking. The bacteria were plated out on 1.1% agar plates supplemented with the appropriate antibiotic (usually ampicillin at 50µg/ml).

2.2.8. Cell culture techniques

2.2.8.1. Tissue culture and propagation

The cells were cultured in RPMI 1640 supplemented with 10% FCS, 2mM glutamine and 100 units/ml of penicillin/streptomycin in a 37°C and 5% CO_2 incubator. The cells were grown in $25cm^2$ or $75cm^2$ vented flasks. The medium was changed every 2 to 3 days by diluting the cells 1/2 with fresh medium. Occasionally the cells were centrifuged at 194g for 5 minutes and the pellet resuspended fresh medium.

2.2.8.2. Trypan blue exclusion detection of viable cells

The cells were diluted (1/2 to 1/10) in 0.4% trypan blue/PBS and incubated for a few minutes at room temperature to allow the dye to penetrate dead cells. Trypan blue is a polar dye that cannot cross intact cell membranes but crosses the membranes of necrotic cells and apoptotic cells. 10µl of this cell suspension was placed on the haemocytometer chamber and the cells were counted under the microscope, where blue stained cells are non viable and unstained cells are viable. The number of viable cells counted are expressed as a multiple of 10^4 cells/ml.

2.2.8.3. DNA transfection of mammalian cells by electroporation

5 to 20µg of either supercoiled or linear DNA was diluted into 50µl of serum free medium (SFM) and placed in a 0.4 cm cuvette on ice. $1x10^7$ cells were resuspended in

250µl of SFM, mixed with the DNA and incubated on ice for 5 minutes. The cells were electroporated at 250V, 960µF (Kilger *et al.*, 1998). After electroporation, the cells were incubated at 37°C for 10 minutes. The electroporated cells were added to 10ml of pre-warmed RPMI supplemented medium and incubated until being harvested.

2.2.8.4. Liquid nitrogen storage of viable cells

For storage in liquid nitrogen, $2x10^6$ cells were frozen in 1ml of freezing medium [90% FBS and 10% DMSO (v/v)] in a cryotube placed in an insulating styrofoam box and placed overnight in the -70°C freezer to allow slow cooling. The vials were transferred to liquid nitrogen for long-term storage.

2.2.8.5. Revival of frozen stocks

The liquid nitrogen vials were thawed quickly in a 37°C water bath and added to 6ml of fresh pre-warmed RPMI supplemented medium. The cells were centrifuged at 194g for 5 minutes and the pellet resuspended in 5ml of pre-warmed RPMI supplemented medium, transferred to a flask and placed in the incubator.

2.2.9. Animal procedures

All procedures were performed at the biological services animal house under the home office regulations and with a home office license.

2.2.9.1. Breeding of transgenic mice

The general housing requirements such as food, water and changing the bedding was carried out by the animal house staff. They also set up breeding pairs, monitored litters and weaned the pups. Weaning was generally performed at 3 weeks of age and the males and females were placed in separate cages.

2.2.9.2. Numbering of transgenic mice

Each new litter born from the microinjection procedure was given an alphabetical letter as a provisional batch number until a transgenic founder was identified following genotyping. Once a new transgenic animal was identified it was given a consecutive line number.

Animals were given an ID number at tail biopsy (for genotyping, see section 2.2.9.4) under halothane anaesthesia. Mice in each line were numbered by ear punching with consecutive numbers. The tail biopsy and ear punching of the animals was usually carried out by Donald Campbell (of our lab).

2.2.9.3. Animal monitoring

The health of the mice (discomfort, behaviour, coat appearance or lymphoma-tumour development) was monitored at least twice-weekly. If an animal appeared to suffer it was euthanised by a schedule 1 method.

2.2.9.4. Monitoring the status of the transgenic founders and lines generated

Tail gDNA was extracted as described in section 2.2.2.3 and digested with the appropriate restriction enzyme. The digested gDNAs were electrophoresed through an agarose gel and this was followed by Southern blotting. The presence of a partial or intact EBER1 transgene was also determined by PCR. The PCR reactions were performed with 300ng of gDNA. For the Eμcmyc mice the presence of the transgene was determined by PCR.

2.2.9.5. Animal tissue collection

Once the animals for tissue collection were identified they were euthanised by a schedule 1 method. The animal was wiped with 70% ethanol and a small incision in the dorsal skin was performed. To check for expression profile all organs and different tissues

were collected. The organs, such as spleen, liver, peripheral lymph nodes, were routinely collected and snap frozen in liquid nitrogen before being stored in a -70°C freezer.

2.2.9.6. Production of transgenic mice

2.2.9.6.1. Strain of superovulated females and superovulation

B6D2.F1 give a large number of embryos, and are usually more resistant to the mechanical insults of microinjection. The mice were bought at 4 to 5 weeks and were left for at least one week to acclimatise to the animal house and the light-dark cycle. Superovulation was performed when the mice were older than 6 weeks.

This procedure was usually performed by animal house staff. As microinjections require a large number of zygotes, the females are administered gonadotropins prior to mating in order to increase the number of oocytes released. This procedure also minimises the number of mice used; for instance 5 superovulated females generally produce about 150-200 embryos instead of 50-70 if they are not superovulated. Two different hormones were used: pregnant mare's serum gonadotropin (PMS) and human chorionic gonadotropin (hCG) (Sigma), dissolved in H_2O and filter sterilised. The times of administration of each hormone depend on the light-dark cycle of the mouse room. 5 to 10 IU of PMS was administered between 12 and 2pm, on day 1 to mimic the oocyte maturation effect of endogenous follicule-stimulating hormone (FSH). hCG was administered 45 to 47 hours later, day 3 (11am to 1pm) at 5IU and was used to mimic the ovulation induction effect of luteinizing hormone (LH). It is important to administer hCG prior to the release of endogenous LH in order to control the time of ovulation, which usually takes place 10 to 13 hours after injection of hCG. After the administration of hCG a female was placed in a cage with one stud male. The next day (day 4) the female was checked for a plug, which signifies that mating has occured. The embryos were then harvested from the plugged B6D2.F1 females. Usually between 5 and 10 females were superovulated for each microinjection round.

2.2.9.6.2. Harvesting zygotes

This procedure was usually performed by animal house staff. Superovulated B6D2.F1 female mice were sacrificed and the ovary and oviduct collected as described in

Nagy *et al.*, 2003b. The fragment of oviduct and uterus from all the mice was transferred to a 5cm petri dish containing PBS. The zygotes are found in the enlarged ampulla surrounded by cumulus cells. Each oviduct was transferred separately to a dish containing M2 medium and hyaluronidase (5µl of 10mg/ml stock, from Sigma). Using watchmaker's forceps the oviduct was torn near the ampulla to release the embryos and cumulus cells. Hyaluronidase digests the cumulus cells releasing the zygotes. After 5 minutes in the hyaluronidase solution, the zygotes were transferred to fresh drops of M2 medium to rinse them from hyaluronidase solution and debris. The embryos were then transferred to a drop of M16 medium in a 5cm dish covered with mineral oil to prevent evaporation (Sigma) and placed at 37°C, 5% CO_2 until used for microinjection.

2.2.9.6.3. Pronuclear microinjections of mouse embryos

The harvested embryos with a normal morphology were chosen for microinjections and were transferred to a drop of M2 medium, which was covered with mineral oil, in a depression slide using an embryo transfer pipette. Usually between 40 and 60 embryos were transferred to the slide at a time; the others were kept in the incubator.

Prior to setting up the microinjection microscope, holding and injection needles were made. The holding needles were made using a microburner and a microforge and 10µl calibrated pipettes (catalog number P0674) (Nagy *et al.*, 2003a) and usually kept and reused until broken or clogged. The injection needles were made using pipettes from Harvard Apparatus (catalog number GC100F-10) and pulled using a mechanical pipette puller (Nagy *et al.*, 2003a) with the following settings: heat 570, pull 150, velocity 100 and time 100. These settings were already optimized when I started doing microinjections. However, they need to be re-optimised when a new filament is needed. The injection needles were usually made on the day of microinjection, or a few days before, to avoid any accumulation of dust. The injection needles were changed if the pipette touched a nucleolus, the pipette was clogged or the opening of the pipette was too wide. After each set of microinjections, needles containing DNA solution were disposed of.

The depression slide containing the embryos to be injected was placed on an inverted microscope platform (Nagy *et al.*, 2003a), which is on an antivibration table. The microscope is flanked by 2 micromanipulators: one for the holding needle and one for the injection needle. The holding needle was then assembled into the instrument holder of the left-hand micromanipulator and filled from the tip with 0.5cm of M2 medium. It was

inserted in the depression slide so that the curved end lay horizontally on the bottom of the depression and entered the drop of medium at an angle of about 45°. At that time, the low power, 60x (15x eye piece and 4x objective) of the microscope was used so that all the embryos could be seen. The focus and the field of the microscope were then set up. An embryo was picked up with the holding needle and the magnification was increased to 600x (15x eye piece and 40x objective). The focusing ring on the lens and the microscope condenser were adjusted until one could clearly distinguish the membrane surrounding the pronucleus. These settings were not touched again during a microinjection session, only the level of the micromanipulators was used to bring the embryos into the plane of focus. If the zygote appeared abnormal at any time during the microinjection procedure or non-fertilised, it was discarded. The magnification was decreased to 40x and an injection needle was placed in the DNA solution loaded from the rear end, at either 2 or 5μg/ml, allowing the DNA solution to enter by capillary action. The injection needle was assembled into the instrument holder of the right-hand micromanipulator and inserted in the depression slide parallel to the holding needle and at a low angle (5 to 20°). The magnification was then increased to 400x. If the pronucleus was not in a good position to be injected, the embryo was released from the holding needle and re-loaded. The pronucleus to be injected was brought into alignment with the focal plane, using the micromanipulator, and the tip of the injection needle was brought in the same focal plane. The injection needle was then pushed through the zona pellucida, then the cytoplasm and into the pronucleus avoiding the nucleoli as they are very sticky and adhere to the pipette. The pipette was then pulled in the center of the pronucleus and pressure was applied to the injection needle so that the DNA solution was delivered. If the pronucleus swelled, it was successfully injected and the pipette was pulled quickly out of the zygote. If swelling of the cytoplasm was observed or movement of the pronucleus, the pronucleus was not penetrated and re-injection with the needle was attempted until there was clear swelling of the pronucleus. If the pronucleus did not swell, it could mean that the pipette was clogged, in which case another needle was filled with DNA and assembled into the micromanipulator and the procedure was repeated. The non-swelling of the pronucleus could also be due to the fact that the pipette did not puncture the oocyte's plasma or nuclear membranes (which are very elastic), which is apparent when a small liquid "bubble" is formed around the tip of the pipette. In that case the focus on both the pronucleus and the tip of the injection pipette was changed and the procedure was repeated

until the pronucleus was visibly seen to swell. The injection chamber was nominally divided into 3 parts: non-injected embryos at the bottom of the slide, injected embryos at the top right-hand corner and abnormal and non-fertilised embryos at the top left-hand corner. Once an embryo was successfully injected, the magnification was taken to low power and it was released into its group and a non-injected embryo was picked up for injection. When all the zygotes were injected they were transferred to M16 medium (apart from the abnormal ones which were discarded) and placed in the incubator until implanted. A new group of non-injected embryos were transferred to the depression slide to be injected. The injection procedure was continued until all zygotes collected were injected.

Some of the injected zygotes lyse due to mechanical damage caused by the microinjection procedure and will appear translucent and fill their zona pellucida. The lysis usually takes place between 5 and 60 minutes after injection. Only the healthy zygotes were implanted and can be distinguished by their space between the zona pellucida and the plasma membrane. Moreover the cytoplasm appears compact and evenly shaped. Between 40 and 75% of the embryos should survive the injection procedure. The embryos were usually implanted on the day of microinjection; however, when there were not enough pseudopregnant females, the embryos were left overnight in the incubator and implanted the following day at the 2 cell stage.

2.2.9.6.4. Pseudopregnant recipient and embryo transfer

This procedure was usually performed by animal house staff. ICR strain mice were selected as embryo transfer recipients. The day before the microinjections were performed, the female ICR mice were set up for mating with vasectomized males. Vasectomies on ICR male mice were conducted by animal house staff. Only the plugged females (evidence of mating) were used for the implant procedure, as they would be "hormonally" in a state of pseudopregnancy. The females were usually 6 weeks to 6 months of age.

The ICR strain was chosen as these mice have a different colour coat (albino), compared to the donor strain B6D2 (black, brown) and also because they are relatively out bred and fit.

The embryo transfer procedure was usually performed by animal house staff. The embryos were either transferred at the one cell stage (approximately 16 hours old) or at a two cells stage (approximately 34 hours old). The method used was the oviduct transfer, which was first reported on rats by Tarkowski (1959). Whittingham (1968) developed a

method for the mouse, which provides the basis for this protocol. The method used was performed as described in Nagy *et al.*, 2003c. The embryos are transferred to pseudopregnant females of like mating timing.

The embryos were transfered using a transfer pipette connected to a mouth-piece. In order to reduce the capillary action, the pipette was loaded with air bubbles before picking up the embryos. The embryos were loaded between 2 air bubbles and with a minimum of medium (M2).

The surgical instruments were sterilised by autoclaving and during procedure rinsed in 70% ethanol. The anaesthetic (hypnorm (Janseen Animal Health): hypnovel (Roche) 1:1 ratio) was used at 0.1ml per g of body weight and injected intraperitoneally (IP). The back of the mouse was wiped with 70% ethanol and a small incision in the dorsal skin at the level of the last rib was performed with fine scissors either central to access both sides, or on one side at a time. An incision was made in the body wall above the ovary. Using blunt forceps the ovarian fat pad was picked up and the ovary, oviduct and uterus isolated. The mouse was transfered to a stereomicroscope where the oviduct opening (infundibulum) and the ampulla could be identified. With watchmakers forceps, the bursa was torn to expose the infundibulum. The embryos were transfered into the oviduct, monitored visually by following the air-bubbles to the ampulla, which indicates successful transfer. The body wall was sewn up with one or two stitches and the dorsal skin was closed with wound clips. Embryo transfer to one or both sides was conducted depending on the number of embryos. At the end of the procedure the mouse was placed on a warm heated pad until recovery.

2.2.9.7. Isolation of primary cells from tissues

Different lymphoid tissues were collected in 1xPBS in bijous and placed on ice until the isolation was performed. The isolation was performed in a tissue culture hood. Once all the tissues were collected, they were transferred to a Petri dish and 3ml of 1xPBS was added. They were then squeezed between 2 frosted glass microscope slides to release the cells. Depending on the size of the tissue more PBS was added to isolate the cells. The isolated cells along with the debris were transferred to a 15ml Falcon tube and placed on ice. To isolate cells from BM, a 21 $^{1/2}$ G needle and a 1ml syringe was used. The femur was held with tweezers above a 15ml Falcon tube and the needle was placed inside the bone. The BM was then flushed with1x PBS. The cells were centrifuged at 1000rpm

(194g) for 5 minutes. For red blood cell-free tissues, such as PP, PLNs and MLNs, the cells were resuspended in 10ml of 1xPBS, left to stand for 1 minute and filtered through a MACs filter to remove any traces of debris. However, for tissues such as spleen, liver, thymus and BM an erythrocyte exclusion was performed as they contain large numbers of red blood cells. After centrifugation, the cells were resuspended in 3ml of NH_4Cl and incubated at room-temperature for 10 minutes, which leads to red blood cell lysis. 12ml of 1xPBS was added and the cells were centrifuged at 1000rpm (194g) for 5 minutes and resuspended in 10ml of 1xPBS. The washing step was repeated twice and the cells were resuspended in 10ml of 1xPBS. They were then filtered on MACs filters to remove any traces of debris. The live cells for each tissue were counted using trypan blue exclusion as described in section 2.2.8.2. The cells could then be used for *in vivo* passage, culture or FACS.

2.2.9.8. *In vivo* passage of tumour cells

This is a procedure which is used to accelerate the development of a tumour phenotype. *In vivo* passages were performed with cells isolated from tumour tissues (see section 2.2.9.7). Usually 10^6 cells in 100µl of 1xPBS were injected into the tail vein of each recipient B6D2.F1 animal or negative matched sibling. Female recipients were only used with injections of tumour cells collected from females. A male recipient was used when tumour cells from either female or male were injected. Males express antigens from the Y chromosome recognised as non-self by females whereas X antigens are expressed by both males and female.

2.2.9.9. Explantation of tumour cells

The tumour tissue was collected from the mouse and externally cleaned with ethanol and then cut into smaller pieces. One piece was placed in sterile 1xPBS on ice, one was placed in formaldehyde for pathology and the rest was snap frozen in liquid nitrogen and stored at -70°C until use.

The cells were isolated from the tumour tissue placed in 1xPBS as described in section 2.2.9.7. The cells were centrifuged at 194g for 5 minutes and resuspended in 5ml of RPMI supplemented with 20% FCS, 2mM glutamine and 100 units/ml of

penicillin/streptomycin, fungizone (2ml of 250μg/ml stock solution) and 50μM of β–mercaptoethanol. The resuspended cells were transferred to a 25cm^2 flask and placed at 37°C and 5% CO_2. The medium was changed the following day. The cells were monitored and cultured in complete tissue culture medium until they expanded. They were then grown in 10% FBS medium. Aliquots of the cells were frozen down as liquid nitrogen stocks as described in section 2.2.8.4.

2.2.10. Fluorescence activated cell sorting

Fluorescence activating cell sorter (FACS) analysis was performed on cells isolated from tissues. 10^6 cells were transferred into a FACSCan tube in a final volume of 500μl 1xPBS. The cells were then stained with the appropriate antiserum, usually with approximately 1μg and incubated for at least 45 minutes in the dark at 4°C. Two different dyes, which are conjugated to the different antibodies were used (Tables 2.3 and 2.4): phycoerythrin (PE) and fluorescein isothiocyanate (FITC). Two washes with 1xPBS were performed to remove the excess of antibody. The cells were either resuspended in 500μl 1xPBS and followed by FACS analysis or resuspended in 500μl 1xPBS, 0.1% formaldehyde, and placed in the dark at 4°C to fix them overnight. The analysis was then performed the following day.

Several staining controls were used including a negative staining control (unstained cells) for each cell type, which establishes the background fluorescence of the cells as the degree of autofluorescence varies between cell types and the instrument used, and an isotype control, which determines non-specific interactions. Single stain controls were also used and establish the non-specific staining of the primary or secondary antibodies (FITC or PE conjugated), and a few double stain controls (usually CD43FITC/B220PE and B220FITC/CD5PE) were also used to calibrate the flow cytometer. The cells were analysed using a FACScalibur flow cytometer (Becton Dickinson). Data were collected and analysed using CellQuest software (Becton Dickinson). Dead cells and debris were excluded from the analysis using the forward and side scatter light distribution gate.

2.2.11. B and T cell enrichment using Dynabeads

This method enriches B or T cells from mixed populations by antibody affinity using either anti-B220 conjugated magnetic beads (Dynal) or anti-Thy1.2 conjugated magnetic beads (Dynal).

When both selections were to be done the T cell selection was performed first. Cells were isolated from the appropriate tissue. After counting the cells, an estimation of the target cell number was performed in order to determine the number of beads required to isolate the cells (number of beads used = 4x number of target cells). Before using the beads for the selection, they were thoroughly resuspended and the appropriate amount of beads was transferred to a collection tube. The tube was placed on the magnetic device (Dynal) and left to stand for 2 minutes. The buffer was removed, the tube was dismantled from the magnetic device and the beads were resuspended in 1ml of washing buffer [1xPBS, 1% FBS (v/v)]. The wash step was repeated and the beads were resuspended in the original volume of washing buffer. Once the beads were washed, the cells were added and the tube was incubated for 20 minutes at 4°C with gentle rotation. The tube was placed on the magnetic device and left to stand for 2 minutes. The supernatant was transferred to a new collection tube and was used for the subsequent B cell selection. The cells/beads were washed twice in washing buffer and stored at -70°C until used. The B cell selection was performed as described for the T cell selection. After incubation, the tube was placed on the magnetic device, the supernatant was transferred to a new collection tube and was called the "left over" fraction. This tube was centrifuged and the pellet was placed at -70°C.

For some assays such as FACS, detachment of the beads was required. This was performed by incubating the cells overnight at 37°C in 2ml of supplemented medium. The following day the medium was transferred to a collection tube and placed on the magnetic device. The supernatant was transferred to a new tube and contained the cells. These could then be used for FACS analysis (see section 2.2.10).

Chapter 3. Generation of EBER1 transgenic mice

3.1. Introduction

In order to explore the role of EBER1 *in vivo*, transgenic mice designed to express EBER1 in lymphoid cells were generated. This chapter comprises the design of the different transgenes, the generation of founder transgenic mice and their establishment to transgenic lines.

3.2. Design of the transgenes

One of the critical steps in the generation of transgenic mice is the design of the transgene. This is of particular importance for EBER1 as the transcript is abundantly expressed in cells and may well be lethal if expressed globally from the viral polymerase III (pol III) promoter in the entire organism. Therefore, the immunoglobulin heavy chain (IgH) intronic enhancer (Eμ) was used in order to direct expression of EBER1 in a spatial specific manner to the lymphoid compartment. This enhancer has been previously used in the laboratory to direct the expression of pol II transcripts encoding EBNA1 to the B-cell compartment (Wilson *et al.*, 1996), LMP1 to the lymphoid compartment (Wilson *et al.*, 1990) and LMP2A to B cells (Caldwell *et al.*, 1998). However, in the case described here the approach was to attempt using Eμ (a pol II enhancer) to restrict expression of the pol III EBER transcript. The rationale for this novel approach was based on the presence of pol II motifs (Sp1 and ATF sites) within the natural EBER1 promoter suggesting that pol II factors can influence the expression of pol III transcripts.

As this is a novel approach and there are no such transgenic models in the literature, three different EBER1 constructs were designed. This was done to test if Sp1 and ATF sites are essential or dispensable for efficient expression of EBER1 *in vivo* in addition to Eμ and to test if spacing between the elements is critical. The first EBER1 gene construct maintains upstream sequences of EBER1 to -322, incorporating the TGTA box (-23), ATF (-46), Sp1 (-60) sites and the putative Myc binding region at -122. The second construct is shorter (-78) incorporating only the Sp1, ATF sites and the TATA-like box and

the third construct only maintains the TGTA box of EBER1. The TGTA box was maintained in all constructs as it has been shown that this element is important for EBER2 transcription by RNA pol III (Howe and Shu, 1993) and therefore may also be critical for EBER1 expression. Each of the three constructs includes the transcription unit of EBER1 from +1 to +167 while the Eμ enhancer was linked 5' to the promoter of each (Figure 3.1).

3.3. Generation of the three different EBER1 constructs

The murine sequence incorporating the Eμ enhancer (Figure 3.1, pink box) was isolated on a 1594bp *Hin*dIII and *Eco*RI fragment (Banerji *et al.*, 1983) from lab stock plasmid p79. This was inserted into the *Hin*dIII-*Eco*RI site of the multiple cloning site of vector pcDNA3.1A. The vector backbone pcDNA3.1A incorporates the CMV promoter upstream of the multiple cloning sites and a neomycin resistance gene driven by the SV40 promoter (Appendix 1). This Eμ vector was denoted lab stock p669 and used as "empty" vector control in several assays. Plasmid pLEXIII (lab stock number p661) was a kind gift from Prof M. Clemens (Laing *et al.*, 2002) and was used as a template for EBER1 sequences. The forward primers CR1, CR2 and CR3 incorporating a 5' *Eco*RI restriction site and reverse primer CR4 incorporating a 3' *Xho*I restriction site (Figure 3.2) were used to amplify the three EBER1 gene fragments from p661. The three PCR products were digested with *Eco*RI and *Xho*I, isolated and ligated into *Eco*RI-*Xho*I linearised p669 vector. Plasmids clones containing the different EBER1 constructs were sequenced and only correct clones were used for subsequent analysis. The resulting plasmids containing the long, middle and short constructs were denoted p670, p671 and p672 respectively. The plasmids were prepared using endotoxin free preparations so as not to trigger an immune response in tissue culture assays or cause toxicity as transgenes *in vivo*, which could obscure any effect due to EBER1 expression.

3.4. Assaying expression of the different constructs in tissue culture

Once the different constructs were generated, the efficacy of expression of each construct was tested in culture. This is an important step prior to use of the constructs as transgenes for microinjection of mouse embryos. If the designed transgene does not express in tissue culture assays it would be unwise to go through the lengthy process of

A. p670

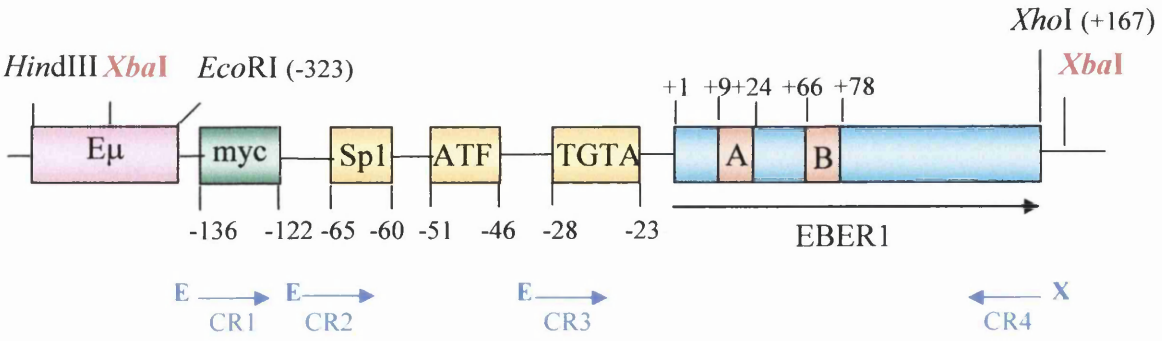

B. p671

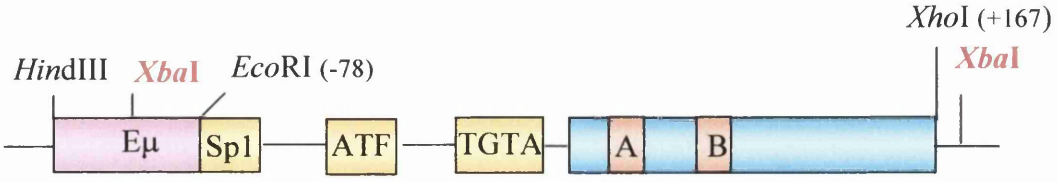

C. p672

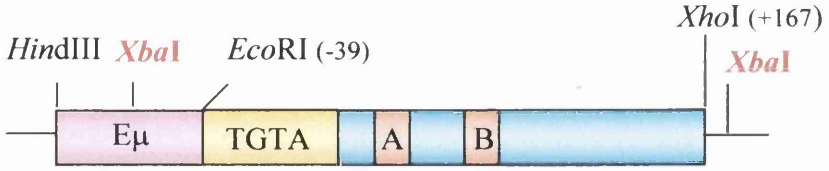

Figure 3.1: Schematic diagram of the three different transgenes used for microinjection

The three different constructs are presented in this figure and called p670 (long construct, A), p671 (middle construct, B) and p672 (short construct, C). The different EBER1 inserts were generated using *Eco*RI and *Xho*I restriction sites and linked to the Eμ via the *Eco*RI site (pink). The EBER promoter is composed of pol II/pol III motifs (Sp1 and ATF - yellow) and pol III motifs (TGTA - yellow, and "A" and "B" boxes - orange). The Myc binding site is also shown in green on construct A. The transgenes used for microinjection were the *Xba*I (shown in red and bold) restriction fragments. The nucleotide position of each element is shown. The PCR primers used to generate the three fragments are shown with blue arrows for construct A (E = *Eco*RI and X = *Xho*I). The black arrow indicates the transcription orientation.

EBER1 sequence 1: CR1-CR4 primers (501 nt), p670 insert

-323

gaattcgtcagcctgcaaggtggatggcgtgttttctgaggttatccccgctacgtgcatg

ctgggtgatagagaccctagaatgtgtcgaaatgaccaagcgtccccgcagcggggctccc

aacacgggttcccagagagggtaaaagagggggccataaagcccagggtgtaaaacaccga

ccgcgccaccagatggcacacgtgggggaaatgagggttagcataggcaacccccgcctac

acaccaactatagcaaacccgcccgtcacggtgacgtagtctgtcttgaggagatgtag

acttgtagacactgcaaaacctcaggacctacgctgccctagaggtttgctagggaggag

acgtgtgtggctgtagccacccgtcccgggtacaagtcccgggtggtgaggacggtgtctg

tggttgtcttcccagactctgctttctgccgtcttcggtcaagtaccagctggtggtccgc

atgttttgagctc

EBER1 sequence 2: CR2-CR4 primers (256 nt), p671 insert

-78

gaattcactatagcaaacccgcccgtcacggtgacgtagtctgtcttgaggagatgtag

acttgtagacactgcaaaacctcaggacctacgctgccctagaggtttgctagggaggag

acgtgtgtggctgtagccacccgtcccgggtacaagtcccgggtggtgaggacggtgtctt

ggttgtcttcccagactctgctttctgccgtcttcggtcaagtaccagctggtggtccgca

tgttttgagctc

EBER1 sequence 3: CR3-CR4 primers (217 nt), p672 insert

-39

gaattctcttgaggagatgtagacttgtagacactgcaaaacctcaggacctacgctgccc

tagaggtttgctagggaggagacgtgtgtggctgtagccacccgtcccgggtacaagtcc

cgggtggtgaggacggtgtcttggttgtcttcccagactctgctttctgccgtcttcggtc

aagtaccagctggtggtccgcatgttttgagctc

Figure 3.2: Sequences of the different EBER1 inserts

The sequences of the different EBER1 inserts incorporated into p669 (pcDNA 3.1 containing the Eμ enhancer) using *Eco*RI (5' end) and *Xho*I (3' end) restriction sites (in green and bold) are shown. The EBER1 transcription unit is underlined. The different upstream elements (ATF, Sp1 and TGTA box) are shown in bold and red. The A and B boxes are shown in bold and blue.

generating transgenic mice, especially in this case with the trial pol II/pol III hybrid promoters. The different supercoil or linear (*Xba*I fragments) fragments were transiently transfected into 39.415 cells, a murine B cell line derived from an LMP1 transgene positive lymphoma (Dabbagh and Wilson, unpublished). A mock (no DNA) transfection and a transfection of p669 were performed as negative controls. The supercoiled parental EBER1 plasmid (p661) was transfected as a positive control for EBER1 expression. 24 hours post-transfection, the cells were harvested followed by RNA extraction. An RT reaction was performed on total RNA using an EBER1 gene specific reverse primer (CR4). For each sample a no RT control was performed in order to check for possible genomic DNA (gDNA) contamination in the RNA sample. The RT product was used as template for a quantitative PCR using EBER1 primers (CR8 and CR9, Figure 2.1) (Figure 3.3). BJAB was used as negative control and Raji and IB4 were used as positive controls. As expected, no signal was observed for BJAB as it is a BL cell line negative for EBER1 expression. Raji expressed EBER1 at a higher level than IB4. For the supercoil samples, EBER1 expression level from p670 was similar to that of IB4, p671 and p661, whereas expression from p672 was lower (Figure 3.3 A). For the *Xba*I linear fragments, EBER1 expression from p670X is low compared to that of p661, but higher than p671X and p672X (Figure 3.3 B). It was noticed that expression was higher from the supercoil constructs compared to the linear fragments (if the expression level of p661 is used as a reference). This suggests that the transfection efficiency could be higher for the supercoil constructs or that the presence of the CMV promoter (upstream of the Eμ) increases expression levels. However, as the samples were not normalised against an internal control, no conclusions can be drawn to fully compare the expression level of the different constructs.

This experiment was repeated with only the linear *Xba*I fragments (as they are the same as the transgene) and two RT reactions were performed one with an EBER1 specific reverse primer (CR4) and one with an oligodT primer. The RT products of these reactions were used as template for a quantitative PCR using either EBER1 primers (CR8 and CR9, for the EBER1 RT) or GAPDH primers (G3PDH5' and G3PDH3', for the oligodT RT) to be used as internal controls. The supercoil EBER1 parental plasmid, p661, was used as positive control for EBER1 expression (Figure 3.4). Following normalisation EBER1 expression from p661 is 9 times higher than that of p670X which is nearly equal to p671X. The expression from p672X is the lowest (15 times) compared to p670X and p671X. Therefore these results suggest that the Sp1 and ATF sites in constructs p670 and p671 (both supercoiled and linear fragments) still contribute to EBER1 expression. It has been

A

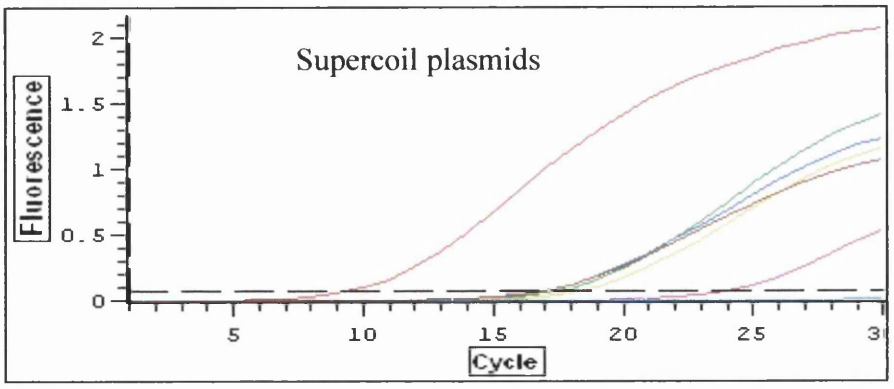

Raji

IB4
p670
p661
p671
p672X

BJAB

B

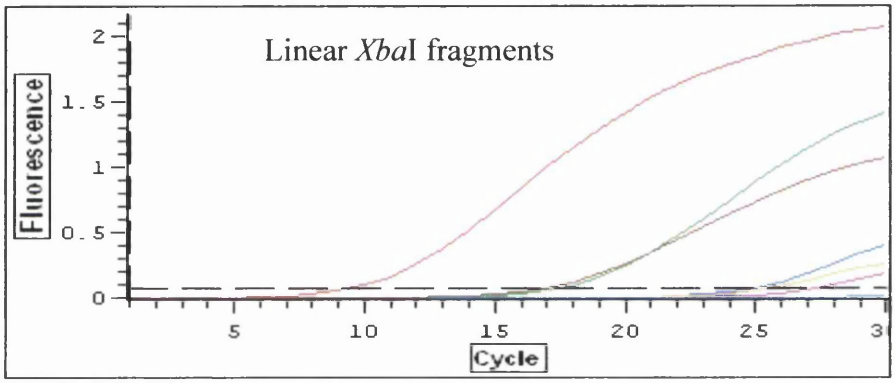

Raji

IB4
p661

p670X
p671X
p672X
BJAB

Figure 3.3: Quantitative PCR for EBER1 expression from the different constructs in culture

39.415 cells were transiently transfected with either supercoiled plasmids p661, p670, p671, p672 and p669, and linear *Xba*I fragments p670X (linear *Xba*I fragment of p670), p671X, p672X and p669X (vector only sequence). A mock transfection with no DNA was also performed as negative control (39.415 sample). 24 hours post-transfection the cells were harvested and followed by an RNA extraction. BJAB (EBV negative human BL cell line) was used as negative control and Raji (EBV positive 50 copies human BL cell line) and IB4 (EBV positive human cell line) were used as positive controls for EBER1 expression. Total RNA was subjected to DNAse I treatment followed by an acid phenol extraction. The RT reaction was performed with an EBER1 specific primer (CR4, for the EBER1 Q-RT-PCR) and 5μg of total RNA. An RT plus and minus reaction was performed for each sample. The Q-RT-PCR reaction was performed with $1/4^{th}$ of the RT reaction using CR8 and CR9 primers Panel A shows the results from the supercoil plasmid transfections and panel B shows the results from the linear *Xba*I fragment transfections.

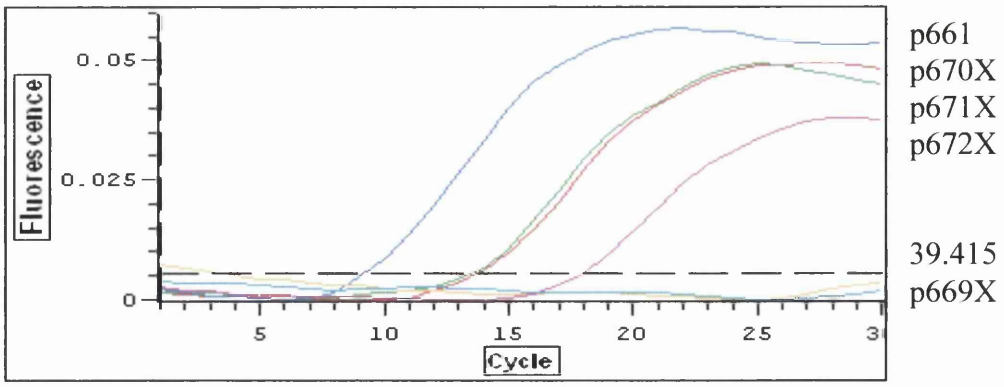

661	0.48
670X	0.052
671X	0.031
672X	0.002

9.2 x

1.6 x

15.5 x

Figure 3.4: Normalised data of EBER1 expression from the linear *Xba*I fragments

39.415 cells were transiently transfected with p661, p670X (linear *Xba*I fragment of p670), p671X, p672X and p669X (vector only sequence). A mock transfection with no DNA was also performed as negative control (39.415 sample). 24 hours post-transfection the cells were harvested and followed by an RNA extraction. Total RNA was subjected to DNAse I treatment followed by an acid phenol extraction. The RT reaction was performed with an EBER1 specific primer (CR4, for the EBER1 Q-RT-PCR) or an oligodT primer (for the GAPDH Q-RT-PCR) and 5μg of total RNA. An RT plus and minus reaction was performed for each sample. The Q-RT-PCR was performed with 1/4th of the RT reaction using either CR8 and CR9 primers (for EBER1) or the G3PDH5'and G3PDH3'primers (for GAPDH). The results for the QPCR with the EBER1 primers are shown and the normalised data is tabulated below. The fold differences are also presented.

shown for both EBER1 and EBER2 using deletion mutants in transfection assays, that the deletion of the two upstream pol II elements, Sp1 and ATF, greatly reduces transcription of the EBERs (Wensing *et al.*, 2001, Howe and Shu, 1989). This assay also demonstrates that all three linear constructs express EBER1 in culture following transient transfections.

A northern blot was performed on the RNA of the cells transiently transfected with both supercoil and *Xba*I linear fragments. The blot was probed with radiolabelled EBER1 sequence and subsequently with rpL32 to control for loading (Figure 3.5). EBER1 expression from Raji and IB4 was observed and no expression was detected for BJAB (Figure 3.5 A). For the three human B-cell lines no expression of rpL32 internal control was detected, which was expected as it is a mouse specific gene (Figure 3.5 B). EBER1 expression was observed following transfection of the three linear fragments at low level and at a relatively even intensity between the three constructs as observed with the normalised data (Figures 3.5 A and C). This result is different from the quantitative PCR data as EBER1 from p672X was expressed at a lower level compared to p671X and p670X. EBER1 expression was also detected from the supercoiled plasmids and at a relatively higher level (Figures 3.5 A and C). In this assay p661 expressed EBER1 at a lower level compared to p670 and p671 supercoiled plasmids (Figure 3.5 C). As observed with the quantitative PCR assay, the expression from the supercoiled constructs was higher than that of the linear fragments. The higher expression of supercoil versus linear fragment could be due to higher transfection efficiency of supercoiled DNA compared to linear DNA, or due to the fact that in the supercoil construct a CMV promoter is present upstream of the Eμ (see appendix) and could therefore increase the rate of transcription. It could also be a combination of both as p661 (the parental EBER1 plasmid), which does not have a CMV promoter or the Eμ enhancer, was transfected as a supercoiled fragment and the expression of EBER1 from that plasmid is lower than that of p670, p671 and p672. It was also noted on figure 3.5 that the size of EBER1 from the supercoiled fragments was higher than that of Raji and IB4. This could be due to the presence of transcripts with a polyA tail as the constructs contain two additional pol II elements (a CMV promoter and the Eμ enhancer) compared to EBER1 in Raji. However, pol II or pol III transcription specificity was not analysed for these samples.

Figure 3.5: Northern blot for EBER1 expression of the different constructs in culture

A transient transfection of *Xba*I linear constructs (669*Xba*I, 670*Xba*I, 671*Xba*I and 672*Xba*I) or supercoil plasmids (669 (Eμ only plasmid), 661 (parental EBER1 plasmid), 670, 671 and 672) was performed into 39.415 cells. A mock (no DNA) transfection control was also performed. The cells were harvested 72 hours post-transfection, which was followed by an RNA extraction. 12μg of total RNA sample derived from the transiently transfected cells was electrophoresed through a 1.4% agarose-formaldehyde gel and electroblotted. The membrane was first hybridised overnight at 60°C with an EBER1 probe. Cold washes were followed by a 30 minutes hot wash at 60°C (panel A). The membrane was then stripped and re-probed overnight at 65°C with rpL32, a mouse specific probe (internal loading control). Cold washes were followed by a 30 minutes hot wash at 65°C (panel B). Raji and IB4 were used as positive human B-cell line controls along with a negative human B cell line control BJAB. For both blots, the membrane was exposed to a phosphorimager intensifying screen for the required amount of time, before being scanned. In panel C a table with the signal intensities of each sample from the EBER1 and rpL32 probes is presented as determined by the phosphorimager software. The background value was subtracted to the "determined value" of each sample. The relative expression (EBER1/rpL32) for each sample is also presented. For p672 supercoil no RNA was loaded on the gel (panel B). It was subsequently shown that supercoil p672 does express in culture.

A

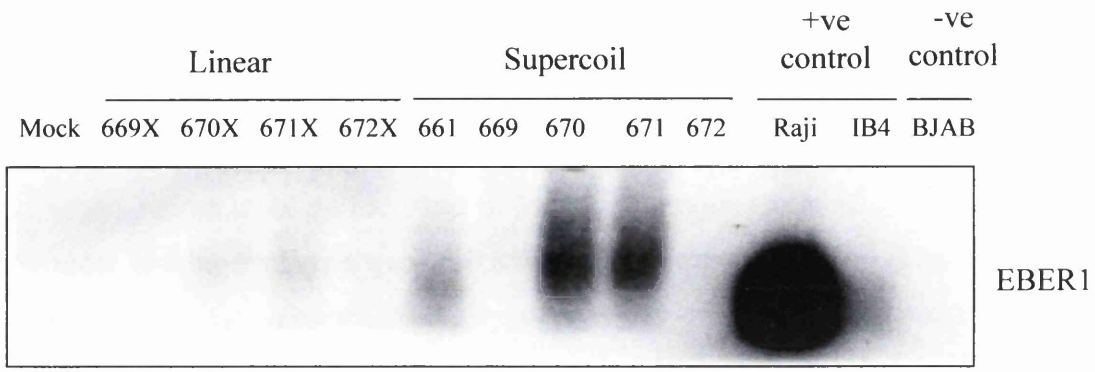

B

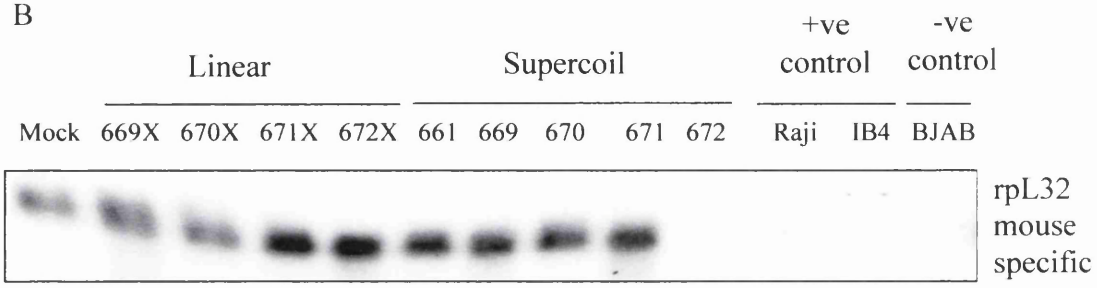

C

Sample name	rpL32 value	EBER1 value	Normalised value
39.145 no DNA	7042		
669 *Xba*I	10690		
670 *Xba*I	8318	974	0.1
671 *Xba*I	9599	1344	0.14
672 *Xba*I	10110	898	0.09
661	7574	3053	0.4
669	8311		
670	7156	7775	1.04
671	9069	7529	0.83
672	Not measured		
Raji	Not measured	170800	
IB4	Not measured	4096	
BJAB	Not measured	114	

3.5. Microinjection into mouse embryos

As the three constructs all expressed in tissue culture assays, they were prepared for microinjection of zygotes. For the generation of transgenic mice, B6D2.F2 zygotes were harvested and selected on the basis of having 2 visible pronuclei. Any non-fertilised or abnormal looking embryos were discarded prior to microinjection. The three transgenes were microinjected in turns into the zygotes as shown in figure 3.6. Successfully injected embryos were then implanted into pseudopregnant ICR recipient mice.

3.6. Generation of transgenic mice

3.6.1. Screening of the pups

Between 19 and 21 days following implant of the microinjected embryos, pups were born. These pups were tail-tipped at 3-4 weeks of age so that their genotype could be determined. gDNA was extracted from digested tails and then an aliquot subjected to digestion with *Eco*RI. The digested gDNA was electrophoresed through a 1% agarose gel, Southern blotted and hybridised with an appropriate radiolabelled EBER1 sequence probe. A summary of the pups born following injection of the three constructs and of the number of transgenic positive founders is presented in table 3.1. The status of the transgene was also assessed by PCR to evaluate if the transgene was either an intact or a partial copy. Different PCR reactions were performed with either IgHF-CR20 (for p670 constructs), IgHF-CR16 (for all constructs) or CR3-CR4 (for all constructs) pairs of primers and gDNA as template (Figure 3.7). For each line two different PCRs were performed. The first one was to check for the presence of the Eμ and part of the EBER1 promoter and the second one was to check for the presence of the EBER1 gene. Figure 3.8 shows a representative example of the IgHF-CR16 PCR. A DNA fragment of the expected size was observed in sample 136.30 but not in sample 129.2. When the EBER1 part of the transgene was analysed a DNA fragment of the expected size was observed for both samples (Figure 3.9) indicating that the transgene was an intact copy for animal 136.30 but a partial copy for animal 129.2. Figure 3.10 shows a representative example of the IgHF-CR20 PCR for a sample with a p671 construct. A DNA fragment of the expected size was observed in

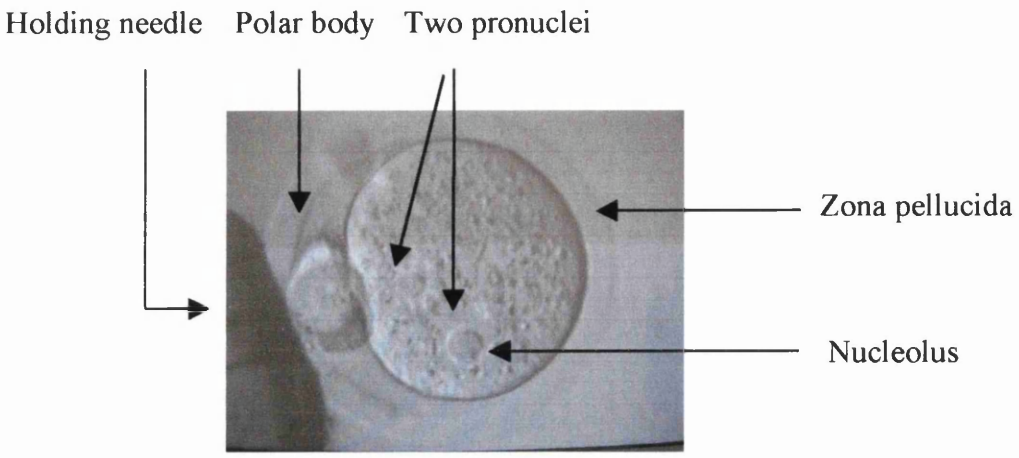

Before injection of the DNA solution

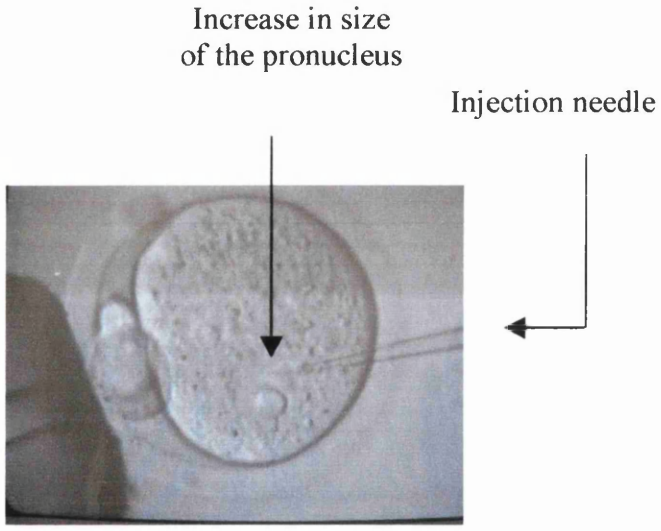

After injection of the DNA solution

Figure 3.6: Pronuclear microinjection of mouse embryo

B6D2.F2 embryos were harvested and microinjection was performed into either of the pronuclei of the embryo with the transgene sequences. If the injection was successful, the pronucleus membrane was seen to increase in size without rupture of the embryo, as shown in the bottom picture.

Construct	Number of pups born	Number of founders
p670 *Xba*I	68	6
p671 *Xba*I	58	3
p672 *Xba*I	104	10

Table 3.1: Summary of the number of pups and founders born from the different microinjections performed

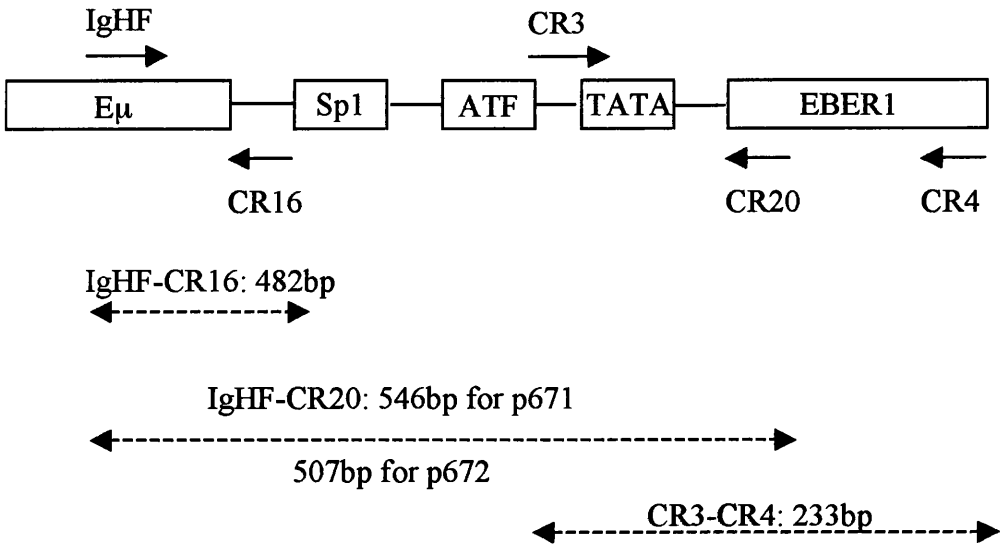

Figure 3.7: Schematic diagram of the different PCR primers used to determine if the transgene was an intact or a partial copy in the different lines generated

The different primers used are shown with an arrow along with their orientation, location on the construct and their name. A bi-directional arrow shows the expected size of the PCR product for each primer pair.

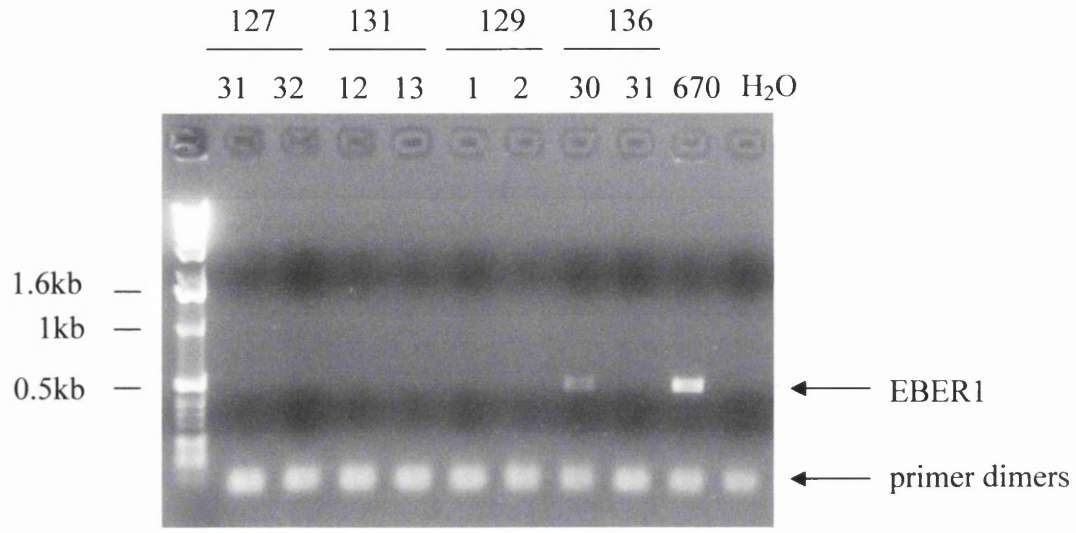

Figure 3.8: PCR of line 136 gDNA with IgHF and CR16 primers

A PCR was performed using IgHF and CR16 primers and 300ng of gDNA. Two controls were performed for the reaction: a no DNA control (H_2O) and a positive plasmid DNA control (670). The PCR products were electrophoresed through a 1.5% agarose gel. The expected size product for the PCR is 482bp. Arrows indicate the EBER1 DNA fragment and the primer dimers. The sizes of a DNA ladder are shown in kb on the left hand side. The transgenic status of the animals was first determined by Southern blotting. For line 127 samples 31 and 32 are transgenic positive, samples 131.12 and 13 are transgenic positive, sample 129.1 is negative and 129.2 is transgenic positive. For line 136, sample 30 is transgenic positive and sample 31 is transgenic negative. Note that with this primer pair only transgenic positive samples with a p670 construct (lines 129 and 136) will show a DNA fragment by PCR.

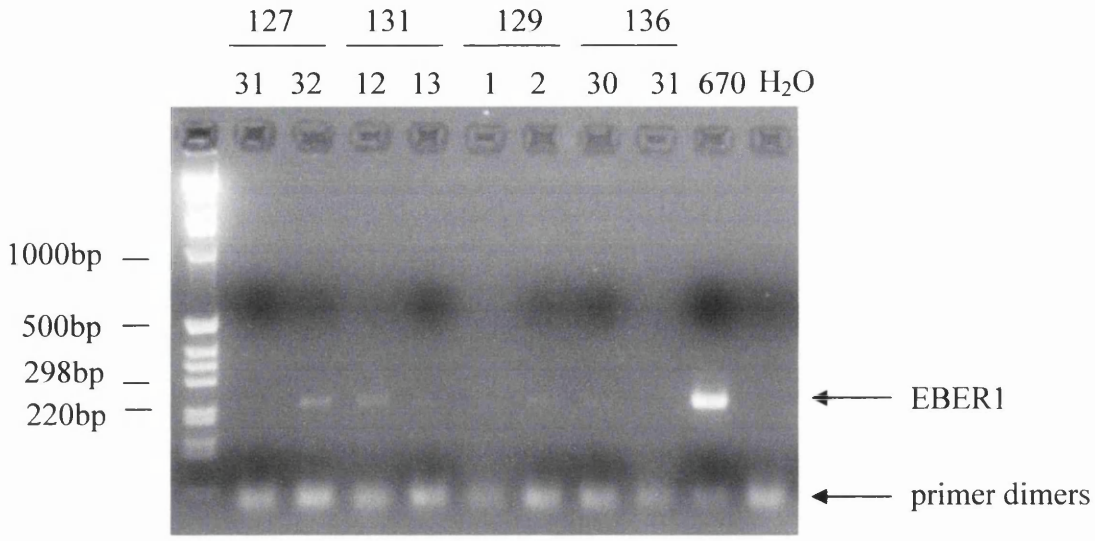

Figure 3.9: PCR on gDNA from lines of each construct using CR3 and CR4 primers

A PCR was performed using CR3 and CR4 primers and 300ng of gDNA. Two controls were performed for the reaction: a no DNA control (H_2O) and a positive plasmid DNA control (670). The PCR products were electrophoresed through a 1.5% agarose gel. The expected size product for the PCR is 233bp. Arrows indicate the EBER1 DNA fragment and the primer dimers. The sizes of a DNA ladder are shown in bp on the left hand side. The transgenic status of the animals was first determined by Southern blotting. For line 127 samples 31 and 32 are transgenic positive, samples 131.12 and 13 are transgenic positive, sample 129.1 is negative and 129.2 is transgenic positive. For line 136, sample 30 is transgenic positive and sample 31 is transgenic negative.

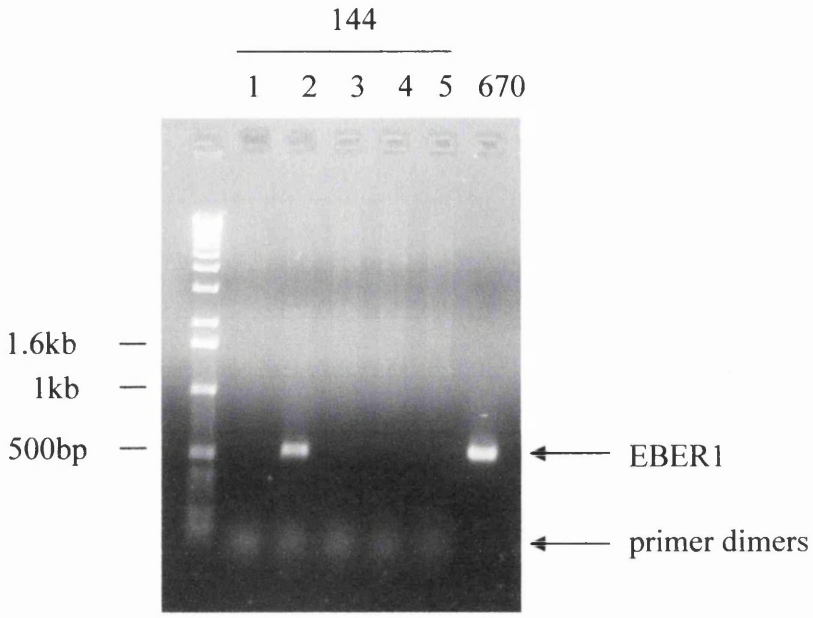

Figure 3.10: PCR of line 144 gDNA with IgHF and CR20 primers

A PCR was performed using IgHF and CR20 primers and 300ng of gDNA. A positive plasmid DNA control (670) was also performed for the reaction. The PCR products were electrophoresed through a 1% agarose gel. The expected size product for the PCR is 546bp. Arrows indicate the EBER1 DNA fragment and the primer dimers. The sizes of a DNA ladder are shown in kb on the left hand side. The transgenic status of the animals was first determined by Southern blotting and sample 144.2 was shown to be transgenic positive and is the founder of line 144 and the other offspring are negative siblings.

sample 144.2, indicating that this part of the transgene was intact. A similar example is also presented for lines with a p672 construct (figure 3.11) and samples 131.7, 133.8, 134.9 and 135.11 all showed a DNA fragment of the expected size. For line 131 the transgene was an intact copy as the EBER1 part also showed a DNA fragment of the correct size (figure 3.9). A summary of the intact or partial copy of the transgene is presented for each founder in tables 3.2, 3.3 and 3.4.

3.6.2. Establishment of lines from the founders

The next step in the generation of transgenic mice is to establish lines from the founders. For this purpose, the different founders were bred to C57B1/6 strain stock mice. The genotype of all offspring born was determined by Southern blotting. From the six founders generated for construct p670 three lines were established (lines 136, 141 and 142, table 3.2). From the three founders generated for construct p671 two lines were established (lines 127 and 145, table 3.3) and from the ten founders generated for construct p672 eight lines were established (lines 131, 132, 133, 134, 135, 137, 138 and 143, table 3.4). However, six founders did not give rise to a new line (126.1, 128.1, 129.2, 130.1, 140.2 and 144.2). For five of these founders (126.1, 128.1, 129.2, 130.1, 140.2) no transgenic positive offspring were born indicating that they might be mosaic. A mosaic arises when the transgene integrates after fusion of the two pronuclei. Therefore some cells in the animal will be transgenic whereas some others will not. For founder 144 no offspring were born despite several pairings, indicating that it was sterile. All the founders along with a matched negative sibling were kept and monitored regularly and tissues were collected when the mouse showed signs of ill health or at the end of the 2-year study period.

3.6.3. Inheritance patterns of the different lines established

3.6.3.1. Integration

For line 127, it was noticed that only the female offspring of the male founder were transgene positive. This lead to the hypothesis that the transgene might be X-linked. To test this hypothesis, two positive females were crossed with C57Bl/6 negative males and as would be expected for either autosomal or X-linkage both male and female positive

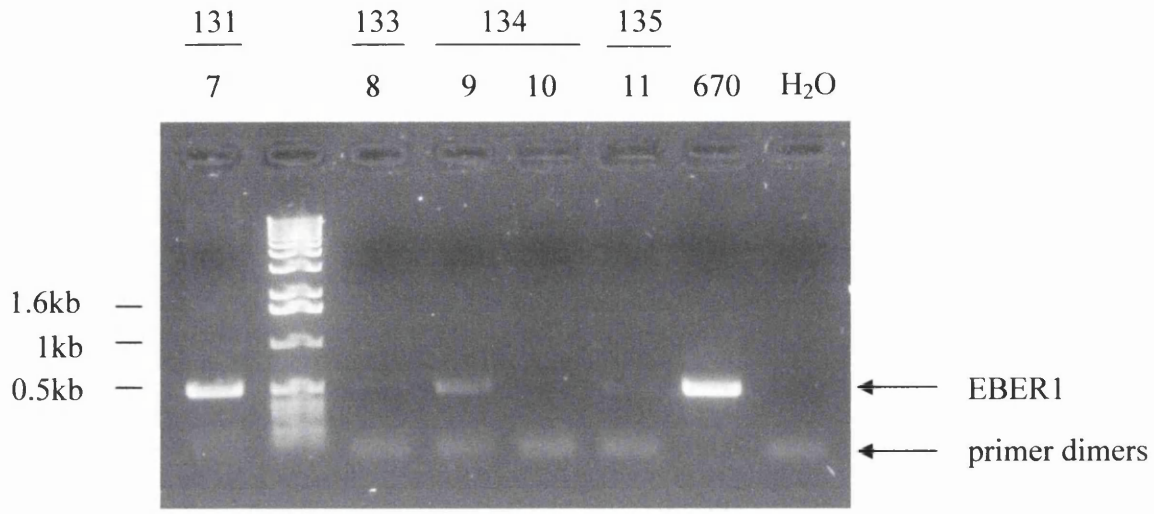

Figure 3.11: PCR on gDNA of lines of construct p672 using IgHF and CR20 primers

A PCR was performed using IgHF and CR20 primers and 300ng of gDNA. Two controls were performed for the reaction: a no DNA control (H_2O) and a positive plasmid DNA control (670). The PCR products were electrophoresed through a 1% agarose gel. The expected size product for the PCR is 507bp. Arrows indicate the EBER1 DNA fragment and the primer dimers. The sizes of a DNA ladder are shown in kb on the left hand side. The transgenic status of the animals was first determined by Southern blotting. Sample 131.7 is transgenic positive, sample 133.8 is transgenic positive, sample 134.9 is transgenic positive and 134.10 is negative. Finally sample 135.11 is transgenic positive.

Line/founder number	M/F founder	Partial or intact transgene	Founder or line
126	M	Partial	Founder
129	F	Partial	Founder
136	M	Intact	Line
140	M	Intact	Founder
141	M	Intact	Line
142	M	Intact	Line

Table 3.2: Summary of the partial or intact transgene, line established and copy number for the different p670 founders

Line number	M/F founder	Partial or intact transgene	Founder or line
127	M	Intact	Line
144	M	Intact	Founder
145	M	Intact	Line

Table 3.3: Summary of the partial or intact transgene, line established and copy number for the different p671 founders

Line number	M/F founder	Partial or intact transgene	Founder or line
128	F	Partial	Founder
130	M	Partial	Founder
131	F	Intact	Line
132	M	Intact	Line
133	F	Intact	Line
134	F	Intact	Line
135	F	Intact	Line
137	M	Intact	Line
138	F	Intact	Line
143	F	Intact	Line

Table 3.4: Summary of the partial or intact transgene, line established and copy number for the different p672 founders

offspring were born. Two positive males from this cross were then bred with C57Bl/6 negative females and only the female offspring from both crosses were positive for the EBER1 transgene confirming that the transgene in this line is integrated into the X-chromosome (Figure 3.12). The other lines show autosomal inheritance patterns.

3.6.3.2. Transgene copy number

The transgene copy number of each line was estimated once the lines were established as the founder can be a mosaic. Two approaches were used for this purpose. For the first one, a partial digest of gDNA from two offspring of each line was performed using an enzyme which only cuts the transgene once, in this case *Eco*RI, and followed by a Southern blot (Figures 3.13 and 3.14). For line 143, only one offspring was present when the assay was performed. The number of transgene length multimers (for example 900 bp, 1800bp, 2700bp etc...) will reflect the copy number in a head to tail tandem configuration (excluding the junction fragments) (Figure 3.13). Thus, the number of bands observed in each track plus one reflects the total copy number. With this method the estimated copy number from each line was determined. The number of copies is variable from one line to the other, ranging from 1 to 11 with the majority of the lines having 8 or 9 copies (145, 131, 134, 142 and 127) (Table 3.5). With this method the line with the highest estimated copy number is line 132 and the one with the lowest is line 141. For the second approach, a slot blot was performed with undigested gDNA from two offspring for each line (except for line 143 where only one offspring was present) and known quantities of plasmid control (*Xba*I fragment of plasmid 672). The intensity of each sample was determined using a phosphorimager (Figure 3.15 and table 3.5). With this approach a relative copy number for each line can be determined with respect to the quantity of DNA in plasmid controls. For instance, with a transgene of approximately 900bp and a haploid genome of $3x10^9$bp, a single copy transgene per haploid genome equals $3x10^{-7}$. Therefore, 5μg of gDNA will have 1.67pg of transgene. Hence 1 copy of a 900bp transgene equals 1.67pg of DNA. The copy number of plasmid control used for this assay and the copy number of the different samples are shown in tables 3.6 and 3.5 respectively. In this assay the upper limit of copy number is greatly increased compared to the first assay (with a maximum of 208). However, the lines with the highest and lowest copy numbers are the same with both approaches. Lines 136, 141, 133 and 137 have a similar copy number with the two

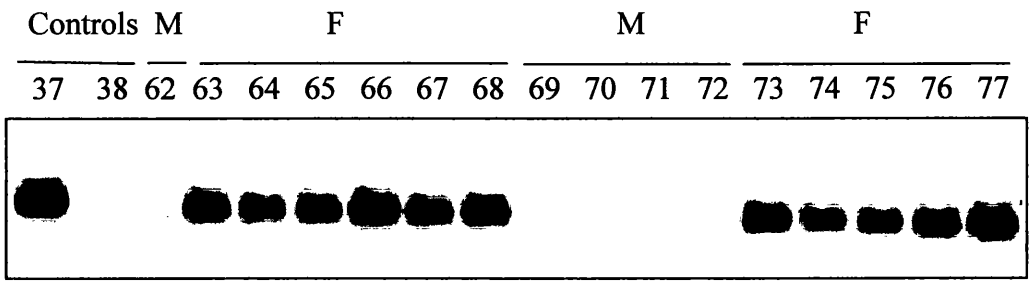

Figure 3.12: Southern blot of generation 3 pups of line 127

Two generation two transgenic positive males (line 127) were bred with C57Bl/6 females. 5μg of gDNA from the offspring were digested with *Eco*RI overnight. The digested products were electrophoresed through a 1% agarose gel and Southern blotted with a radiolabelled EBER1 probe overnight at 60°C. A final hot wash was performed at 60°C. Animal numbers are indicated along with their male or female status for the offspring. Animal 127.38 was used as negative control and animal 127.37 was used as positive control. The expected size of the transgene was 0.9kb.

A

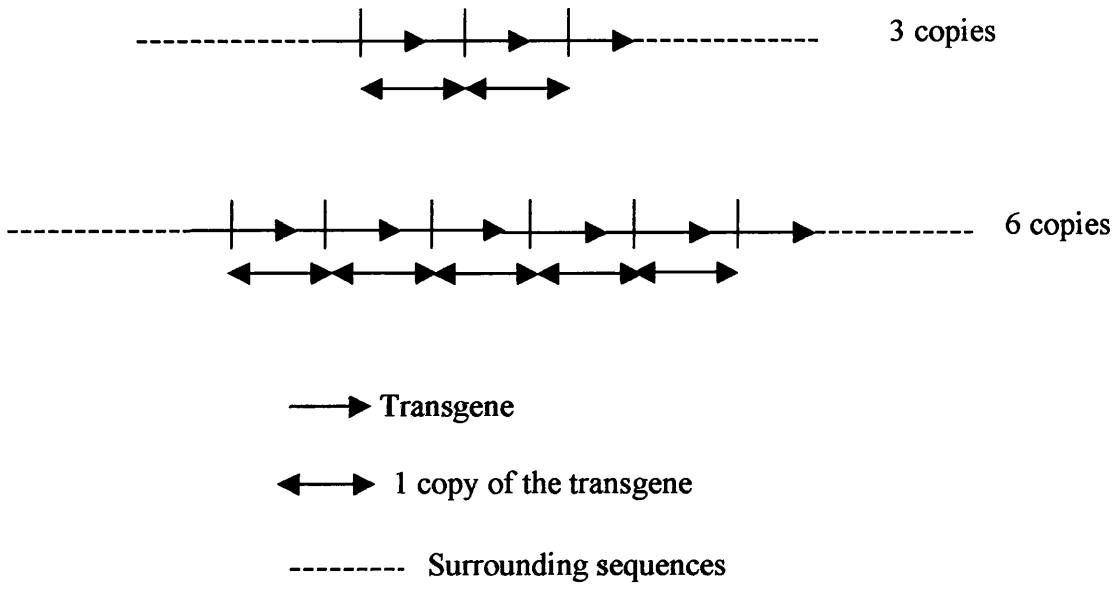

B

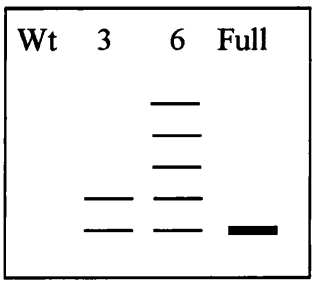

Figure 3.13: Schematic diagram of the estimated copy number following a partial digest with a single cutter

Panel A represents a schematic diagram of two different lines, one with 3 copies of the transgene, the second one with 6. The restriction enzyme used is represented by a vertical line and cuts only once in the transgene. Therefore, following partial digestion of gDNA and Southern blotting, the line with 3 copies of the transgene will have two bands visible on the autoradiograph, whereas the line with 6 copies will have five bands on the autoradiograph, as represented on panel B. The total copy number in a line is determined as the number of bands observed +1. A full digest of the line with 6 copies of the transgene is also presented on panel B (full).

Figure 3.14: Southern blot of the different 670, 671 and 672 lines generated

5μg of gDNA from two different samples of each 670, 671 (panel A) and 672 (panel B) lines generated was partially digested with *Eco*RI for 1 hour at 37°C. Then the enzyme was inactivated by incubating the samples at 70°C for 10 minutes. The partially digested gDNAs were electrophoresed through a 1% agarose gel and Southern blotted with a radiolabelled EBER1 probe overnight at 60°C. A final hot wash was performed at 65°C. The line number and animal numbers are indicated. Animal 127.28 was used as negative control for 670 and 671 lines and animal 131.9 was used as a negative control for 672 lines. The molecular weight markers are shown according to their size on the left hand side.

A

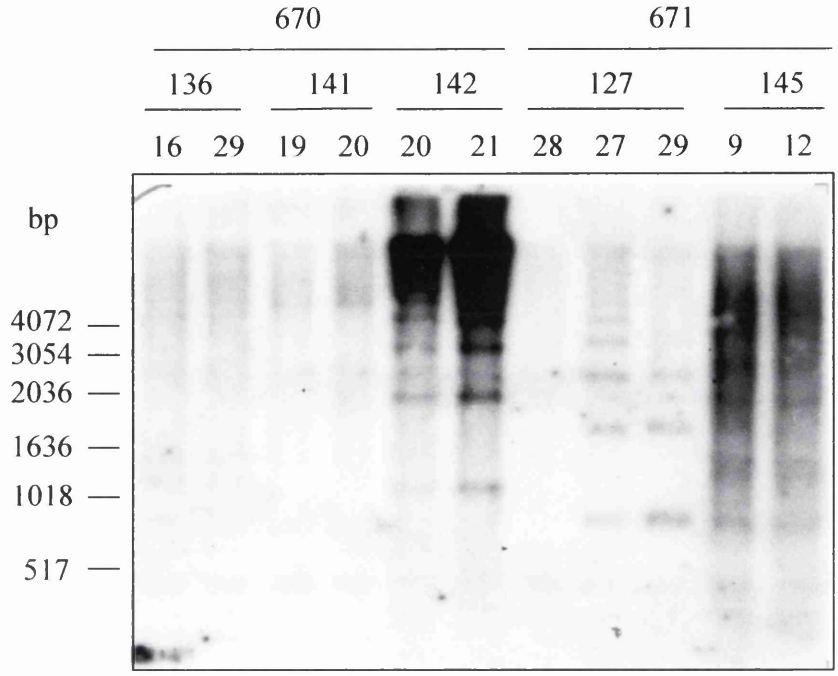
670
671
136
141
142
127
145
16 29 19 20 20 21 28 27 29 9 12
bp
4072
3054
2036
1636
1018
517

B

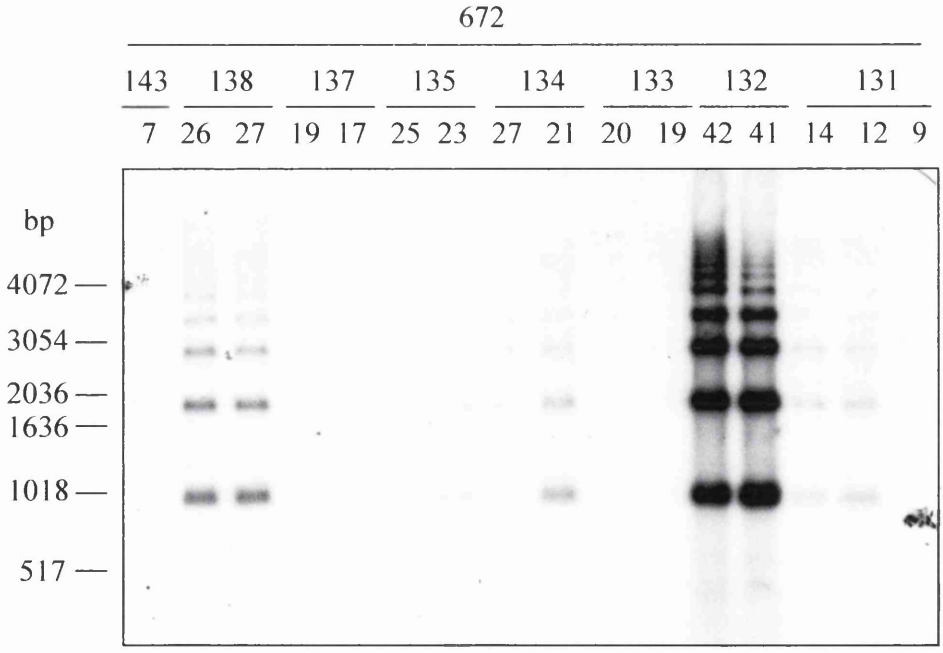
672
143
138
137
135
134
133
132
131
7 26 27 19 17 25 23 27 21 20 19 42 41 14 12 9
bp
4072
3054
2036
1636
1018
517

Table 3.5: Relative and estimated copy number of the different EBER1 lines generated

The intensity value is presented as the intensity observed minus the background value as determined using the phosphorimager software. The average intensity is presented as the average of two samples. The relative quantitative copy number shows the copy number determined following the slot blot approach. The minimum copy number indicates the copy number determined using the partial digest method. The final estimate copy numbers are the values determined using the relative copy number, except for lines 141, 127 and 143 where the values determined using the minimum copy number were chosen. The sign * indicates lines with similar relative and estimated copy numbers.

Line number	Animal number	Intensity value	Average intensity	Relative quantitative copy number	Minimum copy number	Final estimate
136 *	16	-	117.6	2.1	2	2
	29	235.2				
141 *	19	68.1	34.05	0.6	1	1
	20	-				
142	20	2747.4	2876.1	51.2	9	51
	21	3004.8				
127	27	150.7	355.9	6.3	9	9
	29	561.5				
145	9	1283.6	1418	25.2	8	25
	12	1552.4				
131	12	865.4	830.4	14.8	8	15
	14	795.4				
132	41	9353.4	11699.5	208.2	11	208
	42	14045.5				
133 *	19	375.2	233.6	4.2	4	4
	20	92				
134	21	1666.4	1074.2	19.1	8	19
	27	481.9				
135	25	645.4	652.4	11.6	7	12
	23	659.4				
137 *	17	380.6	389.1	6.9	5	7
	19	397.6				
138	27	2291.4	2351.4	41.8	10	42
	26	2411.4				
143	7	369.9	369.9	6.6	2	2

A

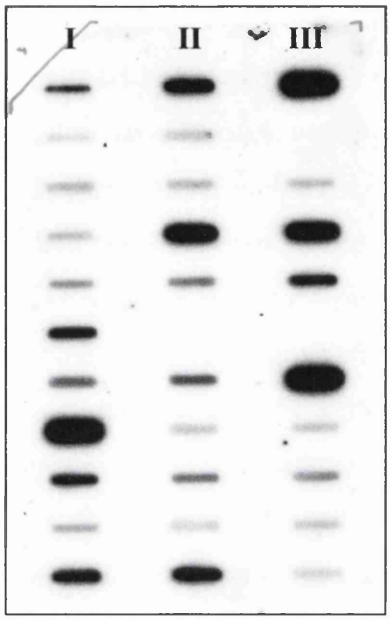

B

I	II	III
2pg	10pg	50pg
127.28 (-ve)	131.9 (-ve)	
136.16	136.29	141.19
141.20	142.20	142.21
127.27	127.29	145.9
145.12		
131.12	131.14	132.41
132.42	133.19	133.20
134.21	134.27	135.23
135.25	137.17	137.19
138.27	138.26	143.7

Figure 3.15: Slot blot of the different lines generated

Panel A shows a slot blot of 5µg of gDNA from each sample which hybridise with EBER1. The samples in the top line of the slot blot were from different quantities of linear plasmid DNA. The samples were loaded onto a pre-soaked membrane. The slot blot membrane was hybridised overnight at 60°C with an EBER1 specific probe. Cold washes were followed by a 30 minutes hot wash at 65°C. Panel B shows the ID of the samples in the order they appear on the slot blot. For each line two samples were used except for line 143. Two wild-type mice were also used as negative controls (127.28 and 131.9) in lanes I and II.

Plasmid amount	Copy number	Phosphorimager intensity	Intensity 1 copy
20pg	11.9	699.1	58.7
100pg	59.9	2918	48.7
500pg	299.4	18330	61.2

Table 3.6: Phosphorimager intensities of the plasmid controls

The intensity of each control is presented as the intensity observed minus the background value. From this table, the average intensity of one copy is 56.2.

approaches and are the lowest. For the other lines the copy number is different when the two methods are compared; however, it follows the same trend. For instance, a line with a high copy number with one approach also has a high copy number with the other approach. For example, line 145 was determined to have 25 copies when using the relative copy number method and 8 with the estimated copy number method, whereas line 135 was determined to have 12 copies when using the relative copy number method and 7 with the estimated copy number method. Lines 132, 142, 145, 138 and 134 have a high (very high for lines 132 and 142) relative copy number compared to the estimated copy number. One has to bear in mind that the first approach does not provide an accurate copy number because the highest bands are hard to distinguish as they all run together; therefore a line which was estimated to have approximately 9 copies of the transgene with this method could have more than this. Moreover, this method relies on a partial digestion. It is possible that under the conditions used a line with 100 copies only gives a maximum of 9 transgenes uncut in a row (thus giving the value of 10). Therefore it is likely that this partial approach depending on the conditions has an upper limit that vastly underestimates the copy number. Due to time constraint this aspect was not explored further. In the case of line 134, the intensity values obtained from the two samples are very different, suggesting that one of the samples was either over or underloaded compared to the other one which would lead to an inaccurate copy number. It is possible that sample 21 was overloaded compared to sample 27. For instance, when the value of sample 27 is used the copy number equals 8.6 which is very close to that obtained with the other approach (8 copies). For line 143, the presence of a second sample could bring the copy number values from both approaches closer together. Line 127 is the only line where the estimated copy number is higher than that of the relative copy number. In this case, with 8 actual bands, the copy number cannot be 6, suggesting that the estimate approach shows a definite minimum but under estimates the maximum. As observed for line 134, the intensity values of the two samples used are very different. If the value of sample 29 only is used to calculate the copy number of the transgene for this line it would equal 9.9, which is similar to that observed from the other approach. A summary of the final copy number estimate is also presented in table 3.5. For lines 136, 141, 133 and 137 the values of both methods were used to determine the final copy number estimate. For line 127, the final estimate is 9 as determined using the partial digestion method. In the case of lines 142, 145, 131, 132, 134 and 138 the copy number determined using the slot blot approach was chosen as the final estimate as it is more likely that these lines have more copies than the ones

determined using the partial digestion method, which could under estimate copy number. However in the case of line 132 208 copies might not be a very reliable estimate. For instance, if the minimum value determined using the partial digest method is 10 fold out compared to that of the relative quantitative value, the final copy number should have been 110. The intensity values of both samples are different and it could be that one sample was overloaded compared to the other. If the value of sample 41 only is used to calculate the copy number of the transgene for this line it would be equal to 166.5, which is closer to 110 than 208. For line 143 a difference in copy number was also observed between the two methods. Therefore for the final estimate the minimum value was chosen as it was shown this approach shows a definite minimum (see line 127 copy number). However more conclusions could be drawn with a second sample.

3.7. Line 127 homozygous breeding

As described in section 3.6.3.1 the transgene of line 127 is X-linked, whereas it is autosomal for all the other lines. Due to the phenomena of X inactivation in females (Heard, 2004) a different transgene amount is likely to be expressed in the tissues of heterozygous females of this line and most likely never with a maximum transgene expression. Males have only one X chromosome and therefore EBER1 is expressed at the same level in these animals. In order to determine if a phenotype could arise faster with maximum expression in females, homozygous line 127 was established. A positive male was crossed with a positive female. The genotype of the offspring was characterised by Southern blot using an EμEBER1 probe (Figure 3.16). The endogenous Eμ band was used as internal loading control and allows the comparison between animals if this band is equal in intensity. From the Southern blot both the endogenous and transgenic Eμ bands can be observed. Two females, numbers 109 and 111 were identified as possible homozygous. The intensity of the Eμ endogenous band in these two animals is similar to that of male 106 whereas the intensity of the EBER1 band is stronger for 109 and 111 compared to 106. The genotype of female 108 was undetermined due to partial digestion of the DNA. To confirm that female 109 was homozygous, it was bred with a negative C57Bl/6 male. All the offspring (eight in total) from this cross were transgenic positive (both males and females) leading to the conclusion that this female was homozygous (had this female been heterozygous, 50% of the offspring would be expected to be wild-type). Therefore female

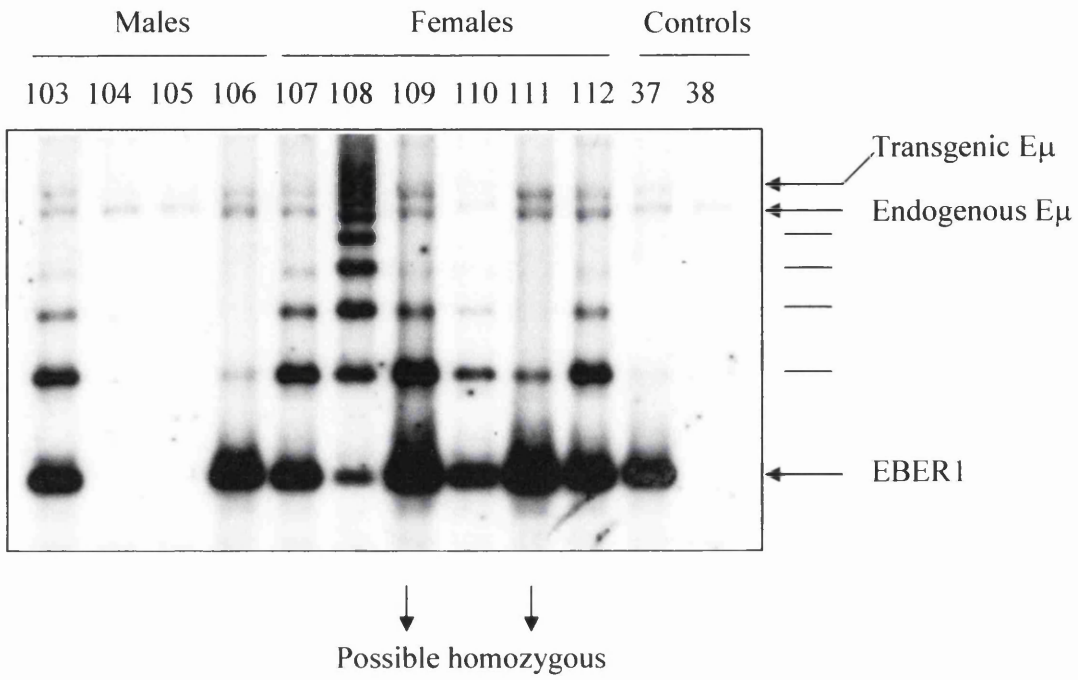

Figure 3.16: Line 127 homozygous breeding

Line 127 positive females and males were bred together in order to generate homozygous females. gDNA of the offspring tails was extracted and 5μg was digested with *Eco*RI. The digested gDNAs were electrophoresed through a 1% TAE gel and Southern blotted. The membrane was hybridised overnight at 60°C with an Eμ-EBER1 radiolabelled probe. Cold washes were followed by a hot wash at 60°C. The numbers shown are the animal numbers. Number 37 was used as positive control and number 38 was used as negative control for the blot. The transgenic and endogenous bands of Eμ are indicated as well as the EBER1 specific monomer band. Note that partial digestion leads to an EBER1 ladder of transgene multimers (indicated with bars).

109 was bred with a positive male in order to fully establish the homozygous line. The animals from this line were not genotyped further as they should all be positive. The homozygous females were monitored for any sign of phenotype.

3.8. Summary

The aim of this chapter was to generate transgenic mice expressing EBER1. As pol III transcripts are highly expressed in cells, we decided to direct the expression of the transgene to the B cell compartment of the animal using the immunoglobulin heavy chain intronic enhancer. Three different EBER1 constructs were generated to explore which factor binding sites would be essential to achieve tissue specific transgene expression.

Expression in culture from the three different constructs was confirmed and pronuclear microinjections were performed into mouse embryos. In total 19 founders were generated, 6 for p670, 3 for p671 and 10 for p672. To date this is the first report of a transgenic model in which the transgene combines both tissue specific pol II and pol III elements. 13 lines have been successfully established. The intact or partial copy of the transgene was analysed for the different founders and lines. In line 127 the transgene was also shown to have integrated on the X chromosome, whereas the other lines showed autosomal inheritance patterns. In line 127 homozygous breeding was also established. For all the established lines the transgene copy number was determined using two different approaches and mice of line 132 were shown to have the highest copy number, whereas mice of line 141 have the lowest. It was also observed that the copy number is variable between the lines.

The next step of this study is to test the expression status of each line established and to verify if it is directed to the lymphoid compartment.

Chapter 4. Expression of EBER1 in the different lines generated

4.1. Introduction

The generation of EBER1 transgenic mice was described in the previous chapter. Nineteen founders were generated and thirteen lines were established from these. The aim of the work presented in this chapter was to study the expression pattern of the EBER1 transgene in the different lines. This is an important step for the phenotype study. For instance, if a phenotype occurs in one (or more than one) of the lines it needs to be correlated with the transgene expression.

The Eμ enhancer was cloned upstream of EBER1 in order to direct expression to the lymphoid compartment. Therefore the expression analysis has mainly been focused on the lymphoid tissues for each line. As the EBERs are pol III transcripts the expression analysis was only performed at the RNA level.

4.2. Mice with 670 transgene: lines 136 and 142

The transgene for these lines incorporates all the defined upstream elements of the EBER1 promoter. RNA was extracted from tissues collected from positive offspring usually between two to four months of age and from a transgene negative control (line 127 control, section 4.3). For small tissues, such as Peyer's patches, peripheral lymph nodes, mesenteric lymph nodes and bone marrow, tissues from two animals from the same line were pooled. Total RNA was DNase I treated followed by an acid phenol extraction to minimise DNA contamination of the samples. The RNA was reverse transcribed (RT) using an EBER1 specific 3' primer (CR4, Figure 2.1) followed by PCR using a nested 3' reverse primer (CR9) and a 5' forward primer (CR8) (Figure 2.1). A minus RT reaction was performed as control to check for possible gDNA contamination. Two PCR controls were performed: a positive control using an EBER1 plasmid as template and a negative water control. The RT-PCR products were electrophoresed through an agarose gel

followed by a Southern blot as the expression was usually too low for the products to be visualised under UV light. The Southern blot was probed with an EBER1 probe. The expression has been tested in the two 670 lines, line 136 and line 142 (Figures 4.1, 4.2 and summary table 4.1). Line 141 had only produced two offspring and therefore expression analysis has not been performed on this line. Both lines express EBER1 in the lymphoid tissues and in both cases the highest expressing tissue is the thymus. While this assay is not precisely quantitative (explored later in section 4.6) relative expression levels between tissues can be estimated. For line 136 expression was strongest in thymus followed by peripheral lymph nodes, mesenteric lymph nodes, bone marrow and Peyer's patches. EBER1 expression level was relatively low in the spleen and liver (Table 4.1). For line 142 expression was strongest in the thymus followed by bone marrow, spleen and liver. EBER1 expression level in this line was lowest in peripheral lymph nodes, mesenteric lymph nodes and Peyer's patches (Table 4.1). For line 136 the expression of EBER1 has also been checked in several non-lymphoid tissues (Figure 4.2 and table 4.1). Expression was detected in most of the tissues tested at a relatively even level except for ovaries, kidney and trachea where the expression level of EBER1 is slightly higher.

The expression analysis was also performed on a transgenic negative sibling to ensure that the expression was specific to the transgene itself and not a result of a non-specific binding of the primers to a different gene. The analysis was performed on line 127 negative siblings and the results are shown in figure 4.3. No signal was detected in any of the lymphoid tissues, suggesting that the signal detected in the plus RT samples of lines 136 and 142 is specific to EBER1.

4.3. Mice with 671 transgene: lines 127 and 145

The transgene for this construct contains the Eμ enhancer as well as the three upstream elements of the EBER1 promoter: Sp1, ATF and TATA like box. The expression analysis was performed for both 671 lines (127 and 145) and the results are presented in figures 4.3, 4.4 and summary table 4.2. For line 127 the expression analysis was also performed on tissues from transgenic negative siblings, and in all the cases no signal or background signal was detected (Figure 4.3). Mice of both lines express the transgene in all the lymphoid tissues; however the pattern of expression is slightly different. For line

Line 136

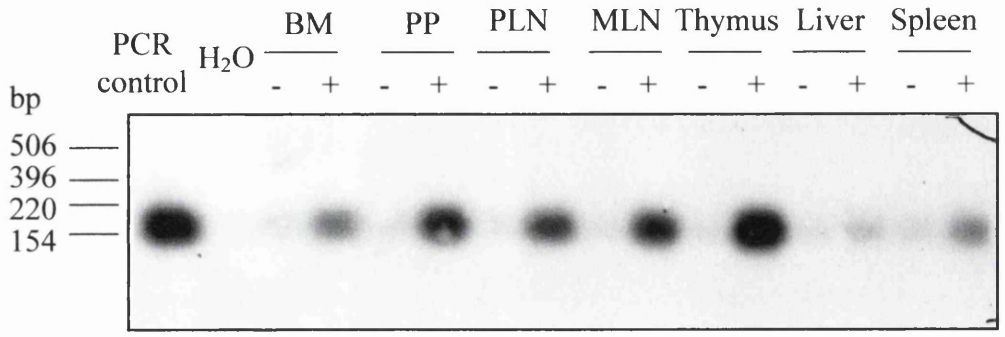

Line 142

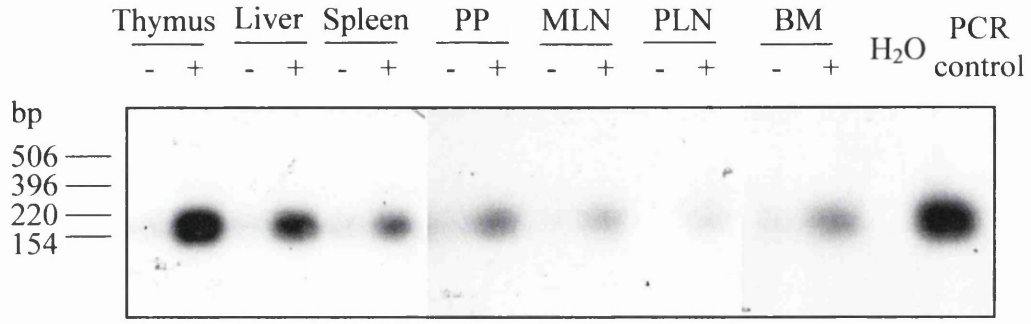

Figure 4.1: Expression analysis in the different lymphoid tissues of 670 transgenic lines

The lymphoid tissues from lines 136 and 142 were collected from transgenic positive animals. RNA extraction was performed, followed by DNAse I treatment, acid phenol extraction and RT-PCR. The RT reaction was performed with an EBER1 specific primer (CR4) and 5μg of total RNA. For each sample a minus RT (-) control was performed. The PCR was performed with $1/4^{th}$ of the RT reaction using CR8 and CR9 primers. A no DNA control (H_2O) and a positive plasmid DNA control (PCR control) were also performed for the PCR as indicated. The RT-PCR products were electrophoresed through a 1% agarose gel followed by Southern blotting and probing using an EBER1 probe. The expected product size is 144 bp. Line 136 is presented in the top panel and line 142 in the bottom panel. The sizes of a DNA ladder are shown in bp on the left hand side.

BM: bone marrow, PP: Peyer's patches, PLN: peripheral lymph nodes, MLN: mesenteric lymph nodes.

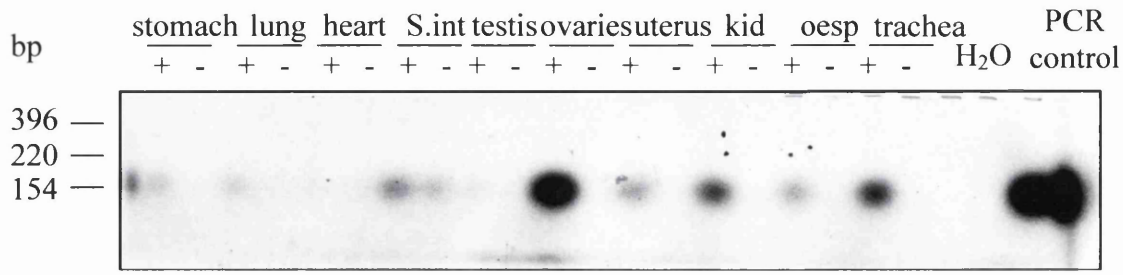

Figure 4.2: EBER1 expression in different tissues of line 136

The different tissues were collected from positive transgenic animals of line 136. RNA extraction was performed, followed by DNAse I treatment, acid phenol extraction and RT-PCR. The RT reaction was performed with an EBER1 specific primer (CR4) and 5μg of total RNA. For each sample a minus RT control (-) was performed. The PCR was performed with $1/4^{th}$ of the RT reaction using CR8 and CR9 primers. Controls were also performed for the PCR, a no DNA control (H_2O) and a positive plasmid DNA control (PCR control). The RT-PCR products were electrophoresed through a 1% agarose gel followed by Southern blotting and probing with an EBER1 probe. The expected product size is 144 bp. The sizes of a DNA ladder are shown in bp on the left hand side. Note a slight DNA contamination is suggested by the signal in the -RT tracks of the small intestine. S.int: small intestine, kid: kidney, oesp: oesophagus.

Tissues collected	136	142
PLNs	++	+
MLNs	++	+
BM	++	++
Spleen	+	++
Liver	+	++
Thymus	+++	+++
Peyer's patches	++	+
Ovaries	++	Not tested
Testis	-	Not tested
Uterus	+	Not tested
Kidneys	+	Not tested
Small intestine	+	Not tested
Stomach	+	Not tested
Heart	-	Not tested
Lungs	+	Not tested
Trachea	+	Not tested
Oesophagus	+	Not tested

Table 4.1: Summary of the expression in the different lines of construct 670

+++: highly expressed (relative to other lines)

++: medium expression level

+: low expression level

Line 127

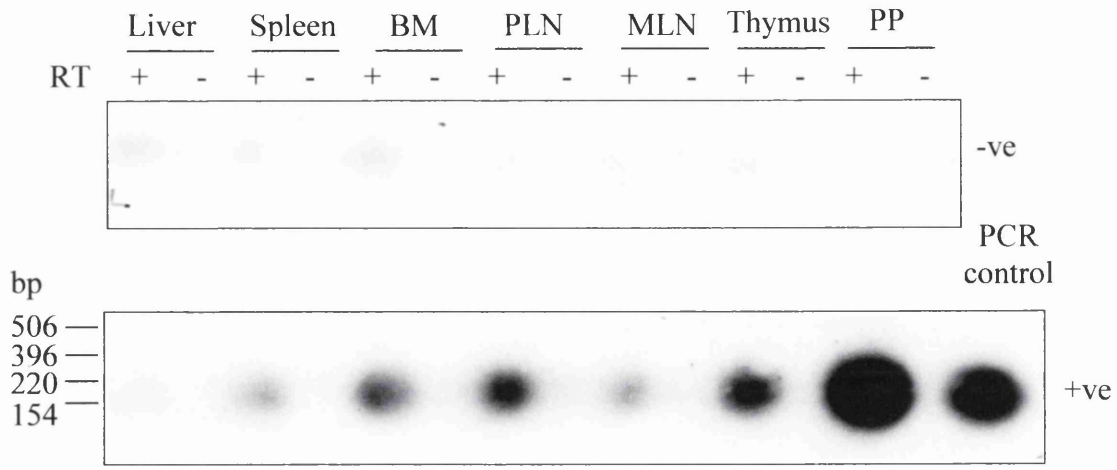

Line 145

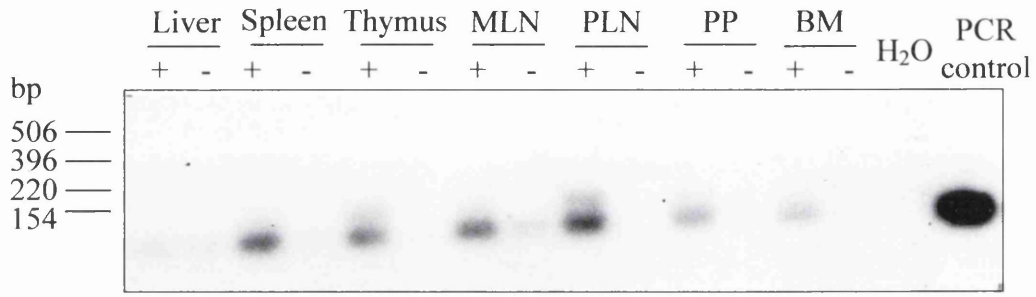

Figure 4.3: Expression analysis in the different lymphoid tissues of 671 transgenic lines

The lymphoid tissues from lines 127 negative and positive siblings were collected and for line 145 the lymphoid tissues were collected from transgenic positive animals. RNA extraction was performed on the collected tissues, followed by DNAse I treatment, acid phenol extraction and RT-PCR. The RT reaction was performed with an EBER1 specific primer (CR4) and 5µg of total RNA. For each sample a minus RT control (-) was performed. The PCR was performed with $1/4^{th}$ of the RT reaction using CR8 and CR9 primers. Controls were also performed for the PCR, a no DNA control (H_2O) and a positive plasmid DNA control (PCR control). The RT-PCR products were electrophoresed through a 1% agarose gel followed by Southern blotting and probing with an EBER1 probe. The expected product size is 144 bp. Line 127 is presented in the top panel with negative (-ve) and positive (+ve) siblings and line 145 in the bottom panel. The sizes of a DNA ladder are shown in bp on the left hand side. BM: bone marrow, PP: Peyer's patches, PLN: peripheral lymph nodes, MLN: mesenteric lymph nodes.

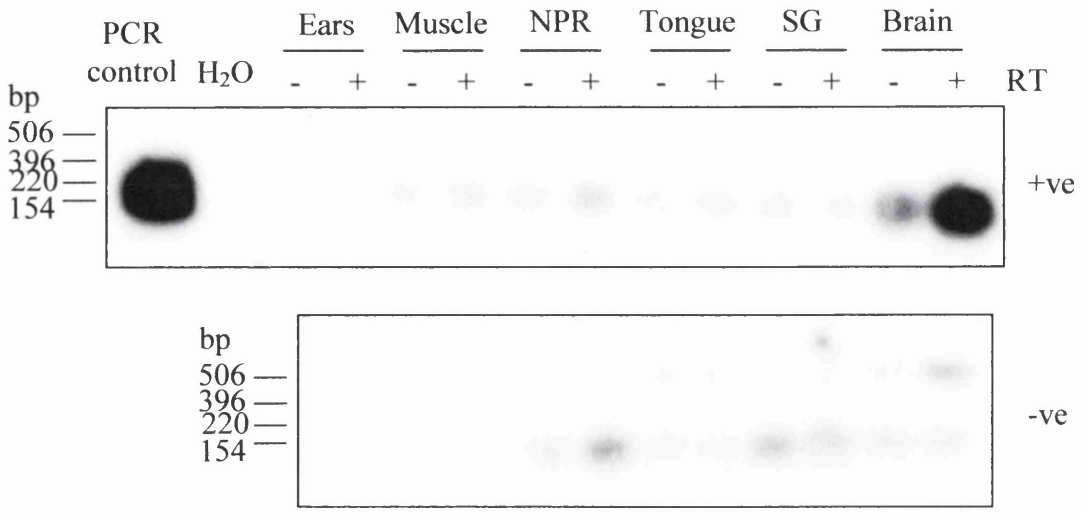

Figure 4.4: EBER1 expression detected in the brain of line 127 transgenic positive mice

Tissues were collected from both positive (+ve) and negative (-ve) line 127 siblings. RNA extraction was performed, followed by DNAse I treatment, acid phenol extraction and RT-PCR. The RT reaction was performed with an EBER1 specific primer (CR4) and 5µg of total RNA. For each sample a minus RT control (-) was performed. The PCR was performed with $1/4^{th}$ of the RT reaction using CR8 and CR9 primers. Controls were also performed for the PCR, a no DNA control (H_2O) and a positive plasmid DNA control (PCR control). The RT-PCR products were electrophoresed through a 1% agarose gel followed by Southern blotting and probing with an EBER1 probe. The expected product size is 144 bp. The sizes of a DNA ladder are shown in bp on the left hand side. Note a slight DNA contamination is suggested by the signal in the -RT tracks and in the +RT tracks of the -ve tissues. NPR: nasopharyngeal region, SG: salivary gland.

Tissues collected	127	145
PLNs	++	+++
MLNs	+	++
BM	++	+
Spleen	+	++
Liver	-	-
Thymus	++	++
Peyer's patches	++++	+
Muscle	-	Not tested
Ovaries	-	Not tested
Testis	-	Not tested
Uterus	-	Not tested
Kidneys	-	Not tested
Small intestine	-	Not tested
Stomach	-	Not tested
Heart	-	Not tested
Lungs	-	Not tested
Trachea	-	Not tested
Oesophagus	-	Not tested
Tongue	-	Not tested
NP region	-	Not tested
Dorsal skin	-	Not tested
Ears	-	Not tested
Brain	+	Not tested
Salivary glands	-	Not tested

Table 4.2: Summary of the expression in the different lines of construct 671

++++: particularly high expression level

+++: highly expressed (relative to other lines)

++: medium expression level

+: low expression level

127 EBER1 expression is highest in Peyer's patches, followed by peripheral lymph nodes, bone marrow and thymus. The lowest expressing lymphoid tissues for this line are mesenteric lymph nodes and spleen. No expression was detected in the liver and in the other tissues tested except for the brain (Figure 4.4 and table 4.2). It is not unusual to observe expression in the brain from a variety of tissue specific promoters/enhancers. However in our case as both Sp1 and ATF are present on 671 it could be that the Eμ is not selective enough to prevent non-lymphoid expression for this particular construct. High expression was detected in the peripheral lymph nodes of line 145 and moderate expression was observed in mesenteric lymph nodes, spleen and thymus. EBER1 expression was low in bone marrow and Peyer's patches and no expression was detected in the liver (Figure 4.3 and table 4.2).

4.4. Mice with 672 transgene: lines 131, 132, 133, 134, 135, 137 and 138

This transgene contains the Eμ enhancer and the TATA-like box of the EBER1 promoter as well as the EBER1 gene but Sp1 and ATF sites are deleted. Line 143 had only produced one offspring at the time of writing and therefore expression analysis has not been performed. The results for the expression of the different lines from construct 672 are presented in figures 4.5, 4.6, 4.7, 4.8 and summary table 4.3. All the different lines tested express EBER1 in lymphoid tissues with different patterns except line 133 where no expression was detected (Figure 4.5). For line 133, DNA contamination was observed in the water control and in several samples tested despite repeated DNaseI treatement. Despite this problem, there was no evidence of expression as the RT+ samples did not reveal a stronger band than in the RT- samples. Therefore analysis of this line was not pursued further and the line was discontinued. However, the founder as well as the three transgenic positive offspring were kept and monitored for any phenotype.

For the other lines, lines 131 and 132 show expression in all the lymphoid tissues; however the intensity of the signal is stronger for line 131 compared to line 132 (Figure 4.6). For line 131 the highest expressing tissues are peripheral lymph nodes and mesenteric lymph nodes, followed by bone marrow, spleen, thymus and Peyer's patches. The lowest expression was observed in the liver (Figure 4.6 and table 4.3). For line 132, the highest expressing tissue was the thymus and low expression was observed in all the other lymphoid tissues (peripheral lymph nodes, mesenteric lymph nodes, bone marrow, spleen,

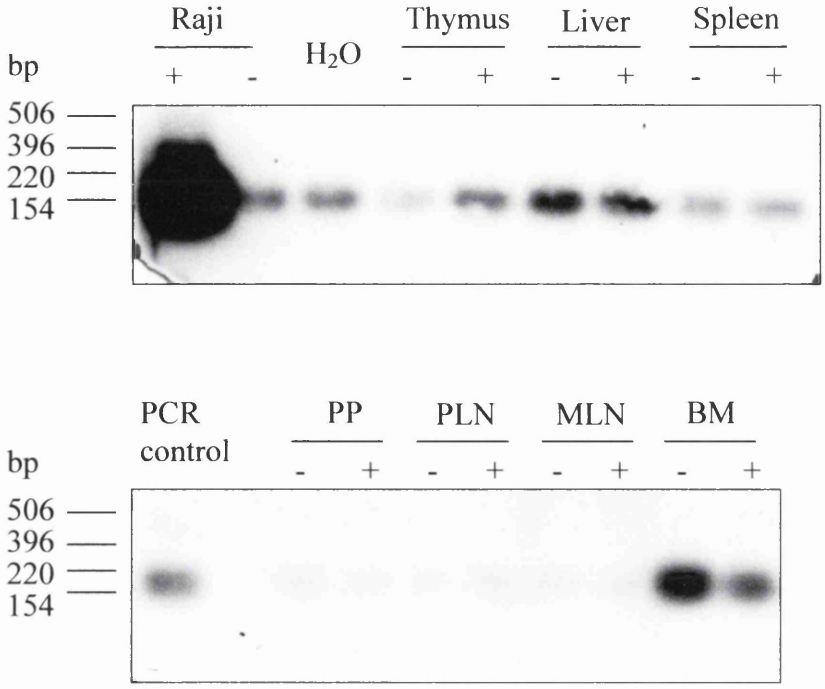

Figure 4.5: Expression analysis in line 133

The lymphoid tissues from line 133 were collected from transgenic positive animals. RNA extraction was performed, followed by DNAse I treatment, acid phenol extraction and RT-PCR. The RT reaction was performed with an EBER1 specific primer (CR4) and 5μg of total RNA. For each sample a minus RT control (-) was performed. The PCR was performed with $1/4^{th}$ of the RT reaction using CR8 and CR9 primers. An RT-PCR was also performed with Raji RNA and used as positive control for the detection of EBER1. A no DNA control (H_2O) was performed for the PCR. The RT-PCR products were electrophoresed through a 1% agarose gel followed by Southern blotting and probing with an EBER1 probe. The expected product size is 144 bp. The sizes of a DNA ladder are shown in bp on the left hand side. Note a DNA contamination is suggested by the signal in the -RT tracks and in the H_2O control. PP: Peyer's patches, PLN: peripheral lymph nodes, MLN: mesenteric lymph nodes and BM: bone marrow.

Line 135

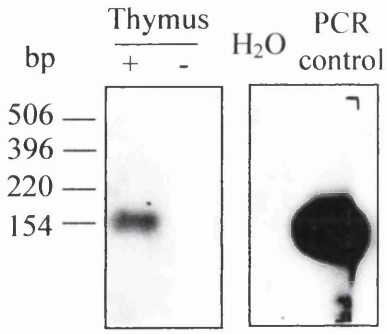

Line 138

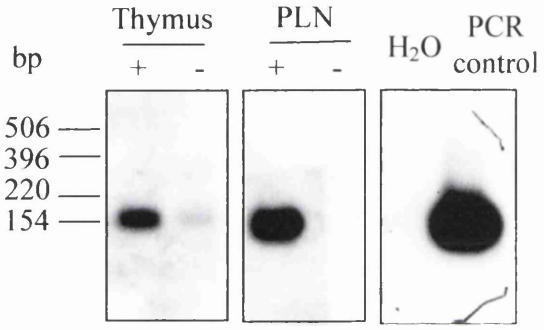

Figure 4.6: Expression analysis in the different lymphoid tissues of 672 transgenic lines

The lymphoid tissues from lines 131, 137, 132, 134, 135 and 138 were collected from positive transgenic animals. RNA extraction was performed, followed by DNAse I treatment, acid phenol extraction and RT-PCR. The RT reaction was performed with an EBER1 specific primer (CR4) and 5µg of total RNA. For each sample a minus RT control (-) was performed. The PCR was performed with $1/4^{th}$ of the RT reaction using CR8 and CR9 primers. Controls were also performed for the PCR, a no DNA control (H_2O) and a positive plasmid DNA control (PCR control). The RT-PCR products were electrophoresed through a 1% agarose gel followed by Southern blotting and probe with an EBER1 probe. For lines 135 and 138 only the expressing tissues are shown. The expected product size is 144 bp. The sizes of a DNA ladder are shown in bp on the left hand side. Note a slight DNA contamination is suggested by the signal in the -RT tracks of line 132 PP and BM, line 134 spleen and line 138 thymus. PP: Peyer's patches, PLN: peripheral lymph nodes, MLN: mesenteric lymph nodes and BM: bone marrow.

Line 131

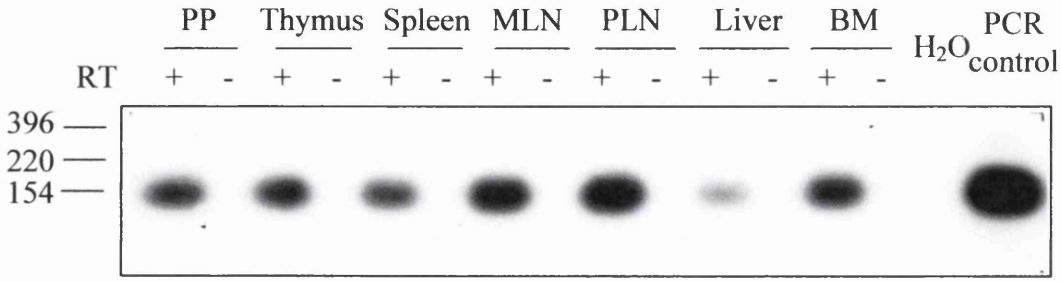

Line 137

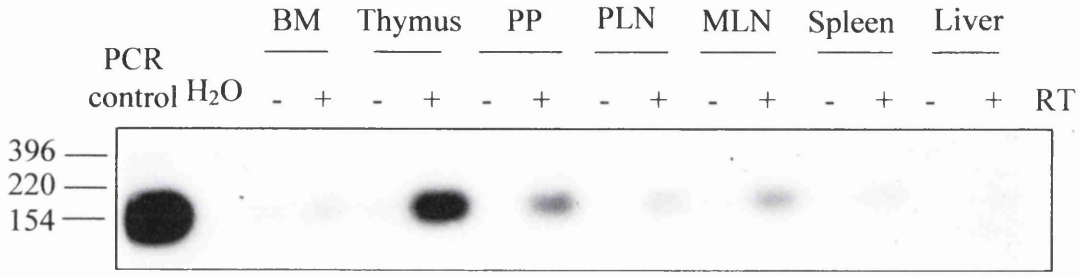

Line 132

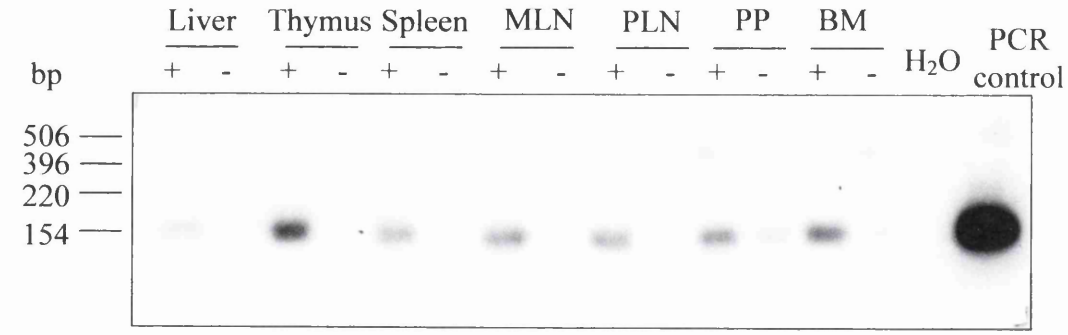

Line 134

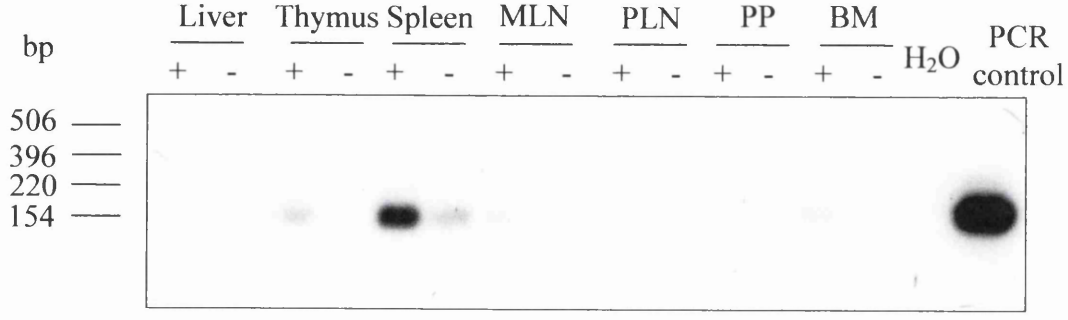

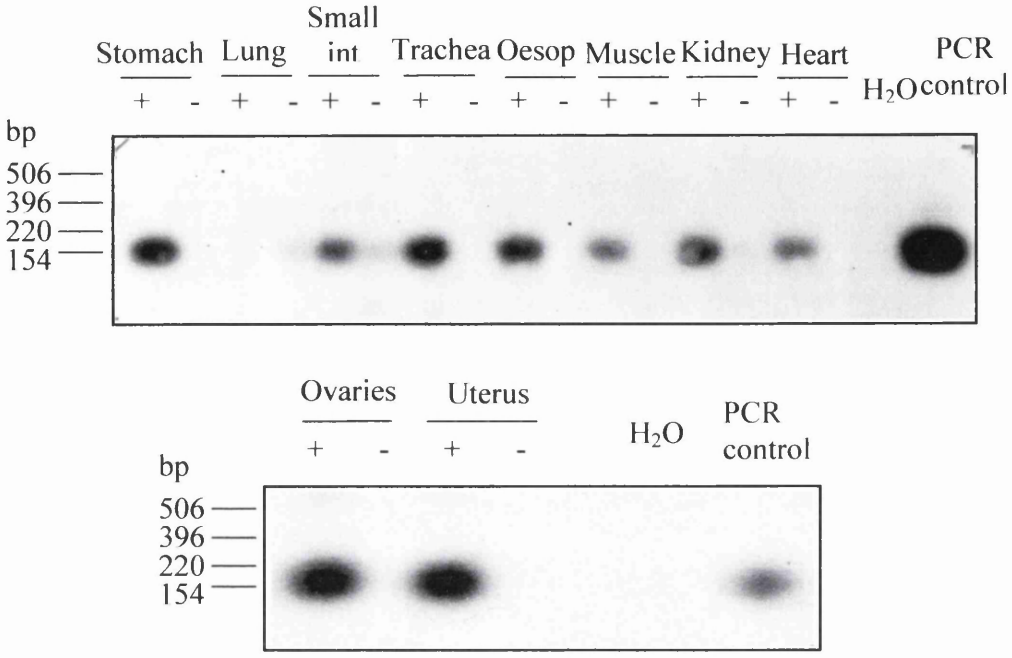

Figure 4.7: EBER1 expression in different tissues of line 131

The different tissues were collected from positive transgenic animals. RNA extraction was performed, followed by DNAse I treatment, acid phenol extraction and RT-PCR. The RT reaction was performed with an EBER1 specific primer (CR4) and 5μg of total RNA. For each sample a minus RT control (-) was performed. The PCR was performed with $1/4^{th}$ of the RT reaction using CR8 and CR9 primers. Controls were also performed for the PCR, a no DNA control (H_2O) and a positive plasmid DNA control (PCR control). The RT-PCR products were electrophoresed through a 1% agarose gel followed by Southern blotting and probing with an EBER1 probe. The expected product size is 144 bp. The sizes of a DNA ladder are shown in bp on the left hand side. Note a slight DNA contamination is suggested by the signal in the -RT tracks of the lung and small intestine. Small int: small intestine, Oesp: oesophagus.

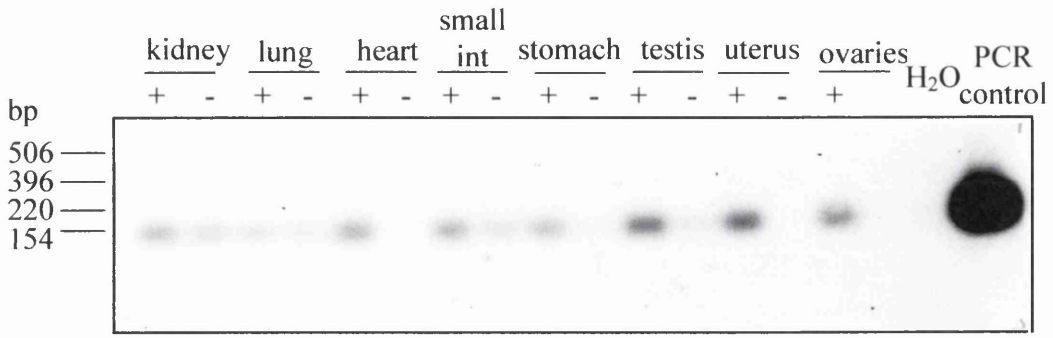

Figure 4.8: EBER1 expression in different tissues of line 137

The different tissues were collected from positive transgenic animals. RNA extraction was performed, followed by DNAse I treatment, acid phenol extraction and RT-PCR. The RT reaction was performed with an EBER1 specific primer (CR4) and 5μg of total RNA. For each sample a minus RT control (-) was performed. The PCR was performed with $1/4^{th}$ of the RT reaction and CR8 and CR9 primers. Controls were also performed for the PCR, a no DNA control (H_2O) and a positive plasmid DNA control (PCR control). The RT-PCR products were electrophoresed through a 1% agarose gel followed by Southern blotting and probing with an EBER1 probe. The expected product size is 144 bp. The sizes of a DNA ladder are shown in bp on the left hand side. Note a DNA contamination is suggested by the signal in the -RT tracks of kidney, lung, small intestine and testis. Small int: small intestine.

Tissues collected	131	132	133	134	135	137	138
PLNs	+++	+	-	-	-	+	+++
MLNs	+++	+	-	+	-	+	-
BM	++	+	-	-	-	+	-
Spleen	++	+	-	+++	-	+	-
Liver	+	+	-	-	-	-	-
Thymus	++	++	-	+	++	+++	++
Peyer's patches	++	+	-	-	-	+	-
Muscle	+	nt	nt	nt	nt	nt	nt
Ovaries	++	nt	nt	nt	nt	+	nt
Testis	nt	nt	nt	nt	nt	++	nt
Uterus	++	nt	nt	nt	nt	++	nt
Kidneys	+	nt	nt	nt	nt	+	nt
Small intestine	+	nt	nt	nt	nt	+	nt
Stomach	++	nt	nt	nt	nt	+	nt
Heart	+	nt	nt	nt	nt	+	nt
Lungs	-	nt	nt	nt	nt	-	nt
Trachea	++	nt	nt	nt	nt	nt	nt
Oesophagus	++	nt	nt	nt	nt	nt	nt

Table 4.3: Summary of the expression in the different lines of construct 672

nt: not tested

+++: highly expressed (relative to other lines)

++: medium expression level

+: low expression level

liver and Peyer's patches) (Figure 4.6 and table 4.3). Several non-lymphoid tissues were also analysed for EBER1 expression in line 131 (Figure 4.7 and summary table 4.3). Expression was detected in most of the tissues tested, except for lung, at a relatively even level.

For lines 134, 137 and 138, expression of EBER1 was observed in one of few lymphoid tissues but not others. For line 134 expression was almost exclusive to the spleen, while for lines 135 and 137 it was predominant in thymus and for line 138 in both thymus and peripheral lymph nodes (Figure 4.6 and table 4.3). For line 137, the expression has also been tested for different non-lymphoid tissues (Figure 4.8 and summary table 4.3). Similarly to line 131, line 137 expresses EBER1 in several non-lymphoid tissues such as testis, uterus, ovaries, heart, small intestine, kidney and stomach but at a very low level. The expression of EBER1 in lines 132, 134, 135 and 138 appears to be lower than that of lines 131 and 137. Therefore these two lines have been selected for further investigation. In the meantime, the other lines have been discontinued by freezing embryos where possible or terminating the lines. All the founders for the lines and their positive offspring were monitored for any signs of phenotype.

4.5. B and T cell expression

4.5.1. Line 127

In line 127 EBER1 is expressed in the thymus (mainly composed of T cells) as well as the spleen (both B and T cells) and other lymphoid tissues of B and T cell composition. Therefore the expression in this line was studied in more detail to determine if it is directed to the B cells, the T cells or both. For this purpose, spleen and Peyer's patches were collected from 3 transgenic positive animals and each tissue type pooled. The lymphocytes were isolated and subjected to positive T cell selection using Thy1.2 dynabeads. The flow through was subjected to positive B cell selection using B220 dynabeads. For the splenocytes only, an aliquot of each fraction collected was used for FACS analysis with B220FITC/CD3PE antibody stain to determine the proportion of B and T cells in each fraction (figure 4.9 A). After T cell selection 91% of the cells were T cells and 1.3% were B cells and after B cell selection 4% of the cells were B cells and 17% of the cells were T cells. Not many B cells were observed following B cell selection because most of the cells

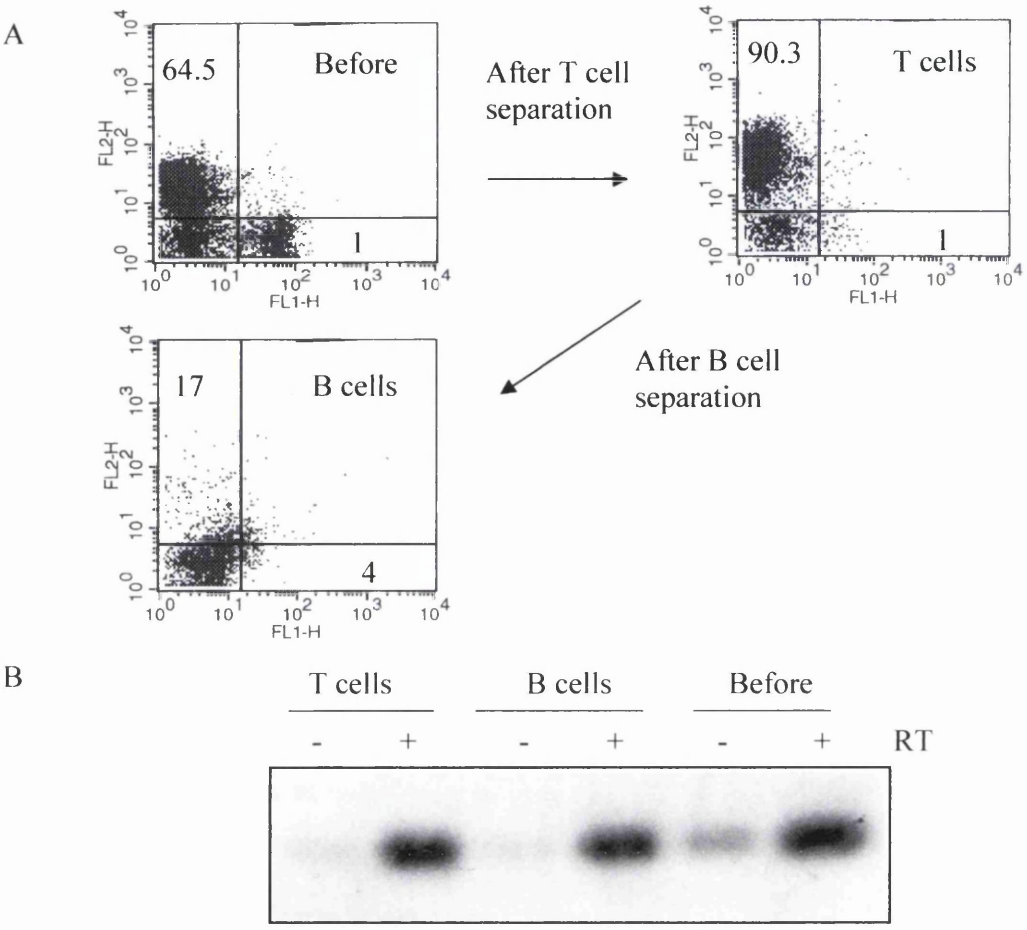

Figure 4.9: Expression in the B and T cells of Peyer's patches in line 127 animals

Cells were extracted from Spleen and PP collected from 3 transgenic positive siblings. A fraction of cells were pelleted prior to the B and T cell selection and was collected "before". T cells were then separated using Thy1.2 dynabeads (the fraction was called T cells) and the flow through was subjected to B cell selection with B220 dynabeads (the fraction was called B cells). Panel A shows the FACS analysis for the splenocytes. An aliquot was collected from each fraction and subjected to B220 FITC (FL1 channel) and CD3 PE (FL2 channel) staining. The percentage of each cell population is also presented. Panel B shows the expression analysis for the PP. RNA was extracted from the different fractions, DNAse I treated followed by acid phenol extraction. An RT-PCR was performed using EBER1 primers. A -RT control was included for each sample. The RT-PCR products were electrophoresed through a 1% agarose gel followed by Southern blotting using an EBER1 probe.

were dead (observation from the forward and side scatter). This could be due to the fact that the cells were left overnight in an incubator to separate them from the beads, and most of the remaining cells died. The thymus was also collected from these animals but not subjected to B and T cell selection as it predominantly consists of T cells. As the B and T cells were enriched in these fractions, RNA was extracted from the cells and the expression of EBER1 was then determined. The results are presented for the Peyer's patches in figure 4.9 B. EBER1 expression was detected in both the B and the T cell enriched fractions of Peyer's patches to similar degree without bias towards one enriched fraction or another. The expression in the spleen is not presented as the gDNA contamination in the minus RT was too extensive to be able to draw any conclusions. These results suggest that in line 127 mice the transgene is expressed in both the B and T cells in the lymphoid tissues.

4.5.2. Other lines

The B and T cells were not separated from different tissues from the other EBER1 lines. However, if a transgene is expressed in several lymphoid tissues including the spleen and the thymus it is possible that expression of this transgene is directed to both the B and T cells. If the transgene is predominantly expressed in the thymus, it is most likely that the expression is directed to the T cells, while expression in spleen but not thymus would be suggestive of B-cell expression. Therefore it was hypothesised that EBER1 is expressed in both the B and T cells in lines 131, 132 and 145.

For line 134 the expression of EBER1 is very high in the spleen and very low in the thymus and mesenteric lymph nodes suggesting that the transgene might be expressed only in B cells in this line.

For lines 135, 137 and 138 the expression of EBER1 is mainly detected in the thymus suggesting that the transgene might be expressed only in the T cells. For lines 136 and 142 the expression in spleen is low and high in thymus suggesting that EBER1 might only be expressed in T cells.

4.6. Quantification between lines 127, 131, 136, 137 and 142

The different lines generated express EBER1 at a low level as an RT-PCR followed by a Southern blot has been usually needed to be able to detect the product. A comparison

of the levels of expression in Peyer's patches and thymus from different lines was undertaken to determine which of these lines expresses the transgene at the highest level. These tissues were chosen for this study because EBER1 expression was most readily detected in these tissues in most of the lines and Peyer's patches was the highest expressing tissue for line 127. For this purpose, a Q-RT-PCR was performed using cDNA from Peyer's patches and thymus from mice of lines 127 (671 construct), 131 and 137 (672 construct) using both EBER1 and GAPDH specific primers (Figure 4.10 A and B). For both thymus and Peyer's patches mice of line 127 express EBER1 at a higher level than line 131 followed by line 137.

A similar study was performed to compare mice of line 127 with lines 136 and 142 (670 construct) (Figure 4.10 C and D). In this case EBER1 expression in the Peyer's patches of mice of line 127 was higher than line 142 and 136. However EBER1 expression in the thymus of mice of line 142 was higher than line 127, followed by line 136. In this figure (panels C and D) AK2003 was included to compare the relative level of expression of the transgene in these three lines to that of an EBV positive BL cell line. The level of EBER1 expression in the thymus of mice of line 142 (Figure 4.10 D) is 100 fold lower than that of AK2003 even when the template for the cell line was used at $1/50^{th}$ dilution. Therefore the level of expression of the transgene is lower than that of an EBV positive BL cell line. In summary, mice of line 127 express EBER1 at a high level in Peyer's patches, followed by lines 131 and 142, then 137. The Peyer's patches of mice of line 136 express EBER1 at the lowest level. For the thymus, EBER1 expression is the highest in mice of line 142, closely followed by line 127, then line 131, line 137 and finally line 136.

4.7. Is the transgene in the different lines transcribed by RNA polymerase II?

It was demonstrated by *in vitro* transcription with the absence and presence of α-amanitin that the EBERs are transcribed by RNA polymerase III (pol III) (Rosa *et al.*, 1981, Howe and Shu, 1989) despite the presence of pol II elements in the promoters: Sp1, ATF and a TATA- like box (Howe and Shu, 1989). In the different transgenic mice described here, an additional pol II element has been included, the Eμ enhancer, which could influence the control of transcription by pol II and pol III. In order to test if EBER1

D

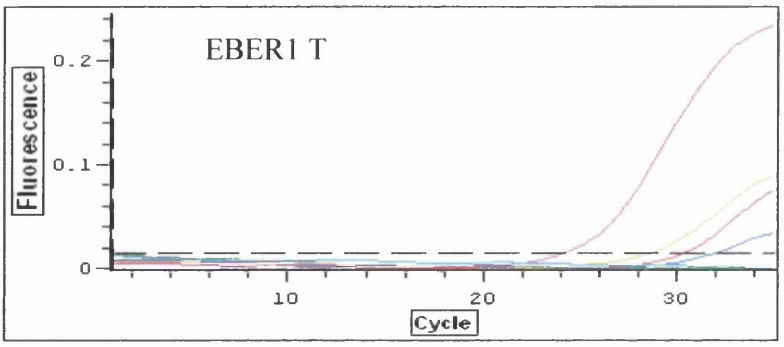

Line	Normalised data T
142 T	$1\ 10^{-8}$
127 T	$1.1\ 10^{-9}$
136 T	$1.5\ 10^{-12}$

9 x

733 x

Figure 4.10: Comparison of the levels of expression of EBER1 in mice of lines 127, 131, 137, 136 and 142 in both thymus and Peyer's patches

RNA was extracted from PP and thymus of transgenic positive animals. Total RNA was subjected to DNAse I treatment followed by an acid phenol extraction. The RT reaction was performed with an EBER1 specific primer (CR4, for the EBER1 Q-RT-PCR) or an oligodT primer (for the GAPDH Q-RT-PCR) and 5μg of total RNA. An RT plus and minus reaction was performed for each sample. The Q-RT-PCR was performed with $1/4^{th}$ of the RT reaction using either CR8 and CR9 primers (for EBER1) or the G3PDH5'and G3PDH3'primers (for GAPDH). AK31 was used as negative control and AK2003 (panels C and D) was used as positive control for EBER1 Q-RT-PCR. The results for the QPCR with the EBER1 primers are shown and the normalised data is tabulated below. The fold differences are also presented. Panel A shows the comparison in Peyer's patches (PP) of lines 127, 131 and 137, whereas panel B shows the comparison in the thymus (T). Panels C and D show the comparison between lines 127, 136 and 142 in Peyer's patches (PP, panel C) and in the thymus (T, panel D).

A

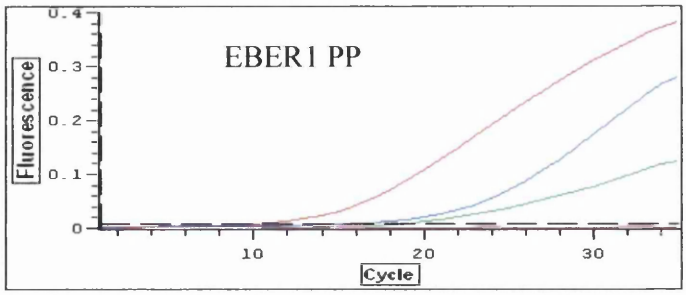

127PP
131 PP
137 PP
AK31

Line	Normalised data PP
127 PP	2453
131 PP	1036
137 PP	318

2.4 x
3.3 x

B

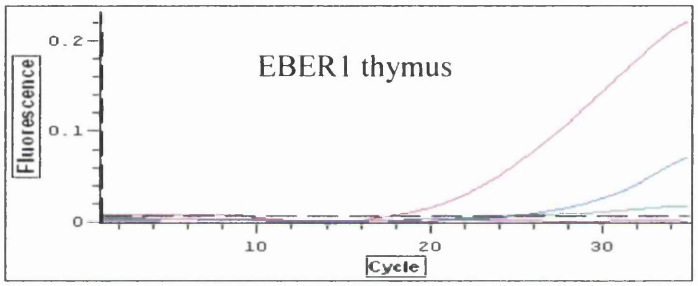

127 T
131 T
137 T
AK31

Line	Normalised data T
127 T	107
131 T	96
137 T	22

1.1 x
4.4 x

C

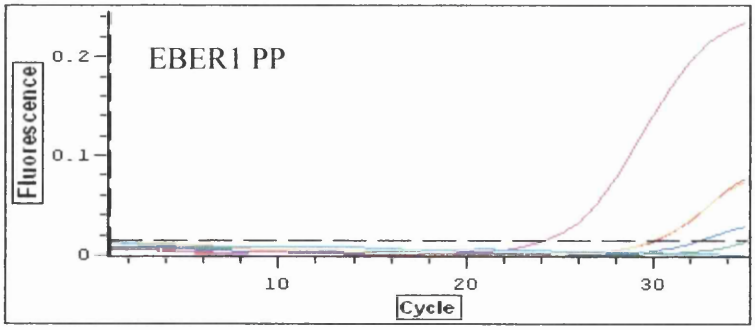

1/50 AK2003
127
142
136
AK31

Line	Normalised data PP
127 PP	$7.8\ 10^{-10}$
142 PP	$3.5\ 10^{-10}$
136 PP	$6.5\ 10^{-12}$

2.2 x
53 x

in this transgenic system is transcribed by pol II or by pol III, two sets of reverse transcriptase reactions were performed, one using an EBER1 specific reverse primer and the second one using an oligodT primer, which recognises mRNA sequences due to the presence of the poly A tail. Then on the RT products several PCR reactions were performed using different sets of primer pairs (Figure 4.11). GAPDH specific primers were used as a control for a pol II gene, therefore no amplification should be expected when these primers are used with a template from the EBER1 specific RT. Similarly, tRNA specific primers were used as a control for a pol III gene and no amplification should be expected when these primers are used with a template from the oligodT RT. The test PCR was performed using EBER1 specific internal primers CR8 and CR9 (Figure 2.1). The GAPDH PCRs showed amplification from the different samples using the oligodT RT primer (Figure 4.12). The fragment intensity from the different samples was similar, except for line 127 which was more intense. However, for this sample a DNA contamination of the RNA sample is likely as observed by the product in the no RT track, which could account for the increased signal in the +RT track. A product was also faintly observed using the EBER1 specific primer for the RT reaction. No signal should have been detected from this PCR; a possible explanation for this is a miss-priming of the EBER1 specific primer CR4, which could have hybridised to similar sequences in several RNAs and allowed amplification of GAPDH. For the tRNA PCR, no signal was detected in any of the tracks except for the PCR control, suggesting that the PCR was working and that the oligodT primer is specific to pol II transcripts (Figure 4.13). The EBER1 PCR showed a signal from the different samples when the EBER1 specific primer was used for the RT reaction, as previously observed in sections 4.2, 4.3 and 4.4 (Figure 4.14 A), indicating that primer CR4 does primarily recognise the EBER1 sequence. However this PCR does not distinguish if the transcript is of pol II or pol III origin. A very faint signal was detected in the EBER1 PCR products following an oligodT RT reaction (Figure 4.14 B). As the signal is only detected after long exposure of the Southern blot gel to the film, it could be due to a miss-priming from the oligodT primer as it was previously observed with GAPDH PCR and EBER1 specific RT primer. These results strongly suggest that in the transgenic mice tested in this assay, EBER1 is not transcribed by RNA Pol II.

A run on assay with untreated AK2003 nuclei or treated AK2003 nuclei with α-amanitin was attempted to further determine if EBER1 is transcribed by RNA pol II or pol III. However, the results were not conclusive and this assay should be repeated.

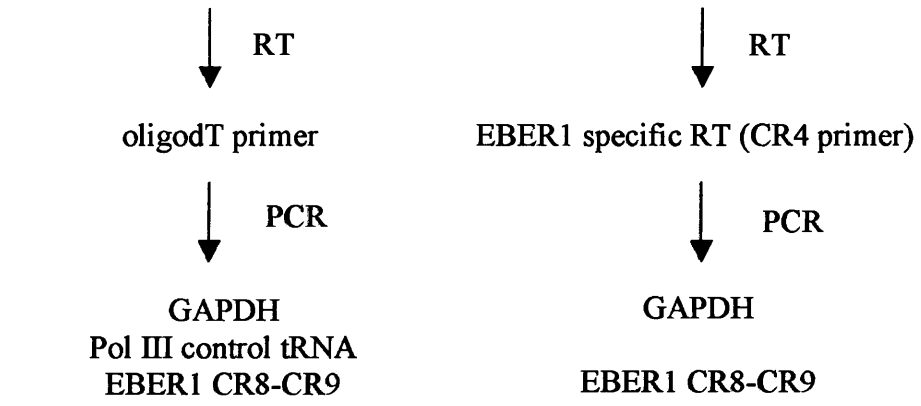

Figure 4.11: Experimental design of pol II/pol III analysis using RT-PCR

Total RNAs from the highest expressing tissue of lines 127, 131, 137, 136 and 134 were either used for a reverse transcriptase reaction using oligodT primer or using an EBER1 gene specific reverse primer. The RT products were then used for different PCRs as indicated in the figure.

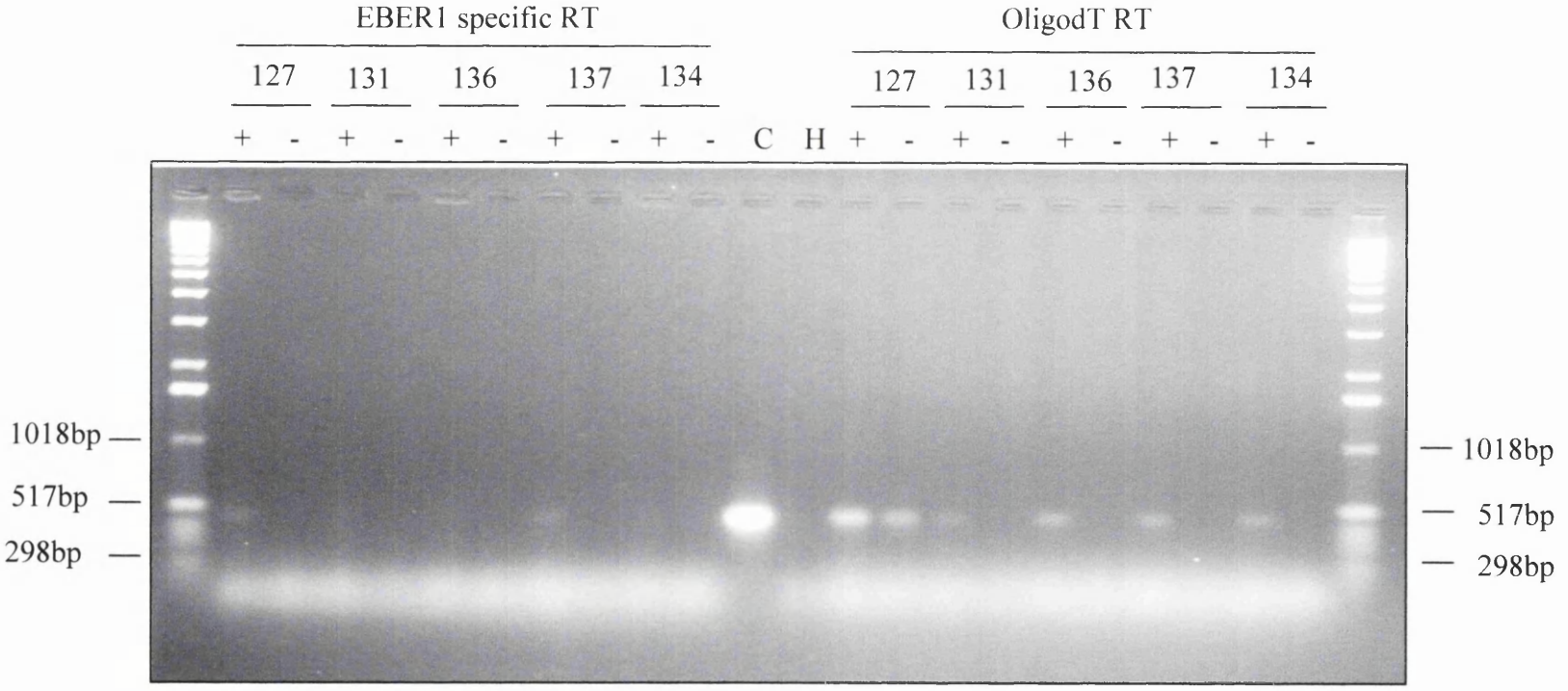

Figure 4.12: OligodT and EBER1 specific reverse transcriptase followed by PCR using GAPDH primers

Total RNA (5µg) from Peyer's patches of line 127, peripheral lymph nodes of line 131, thymus of lines 136 and 137 and spleen of line 134 was subjected to an RT reaction using an EBER1 specific primer (CR4) or an oligodT primer (as indicated). For each sample a minus RT control (-) was performed to reveal any contaminating DNA in the RNA samples. A PCR was performed with $1/4^{th}$ of the RT reaction using GAPDH primers. Controls were also performed for the PCR, a no DNA control (H) and a positive plasmid GAPDH DNA control (C). The expected size product for the GAPDH PCR is 496bp. The RT-PCR products were electrophoresed through a 1% agarose gel.

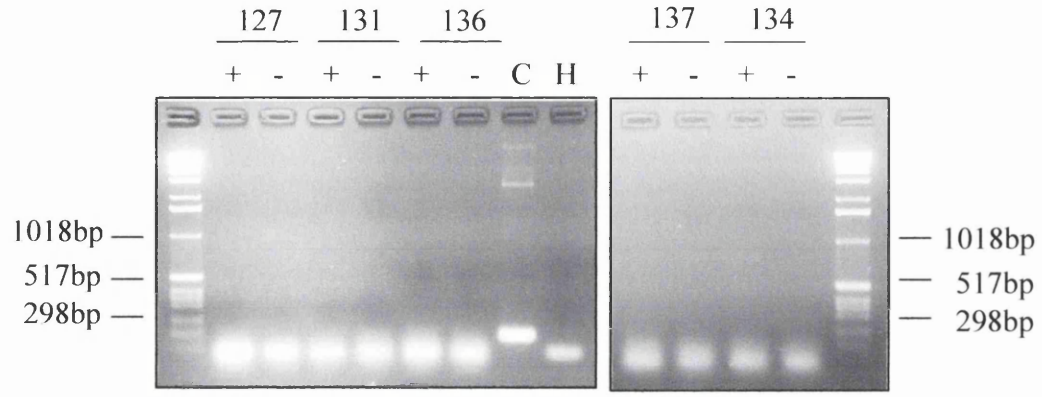

Figure 4.13: OligodT reverse transcriptase followed by PCR using tRNA primers

Total RNA (5µg) from Peyer's patches of line 127, peripheral lymph nodes of line 131, thymus of lines 136 and 137 and spleen of line 134 was subjected to an RT reaction using an oligodT primer. For each sample a minus RT control (-) was performed. A PCR was performed with 1/4th of the RT reaction using tRNA primers. Controls were also performed for the PCR, a no DNA control (H) and a positive plasmid tRNA control (C) showing a DNA fragment of the expected size of 217bp. The RT-PCR products were electrophoresed through a 1% agarose gel. The tRNA plasmid was a kind gift from Prof R.J. White, Gomez-Roman *et al.*, 2003.

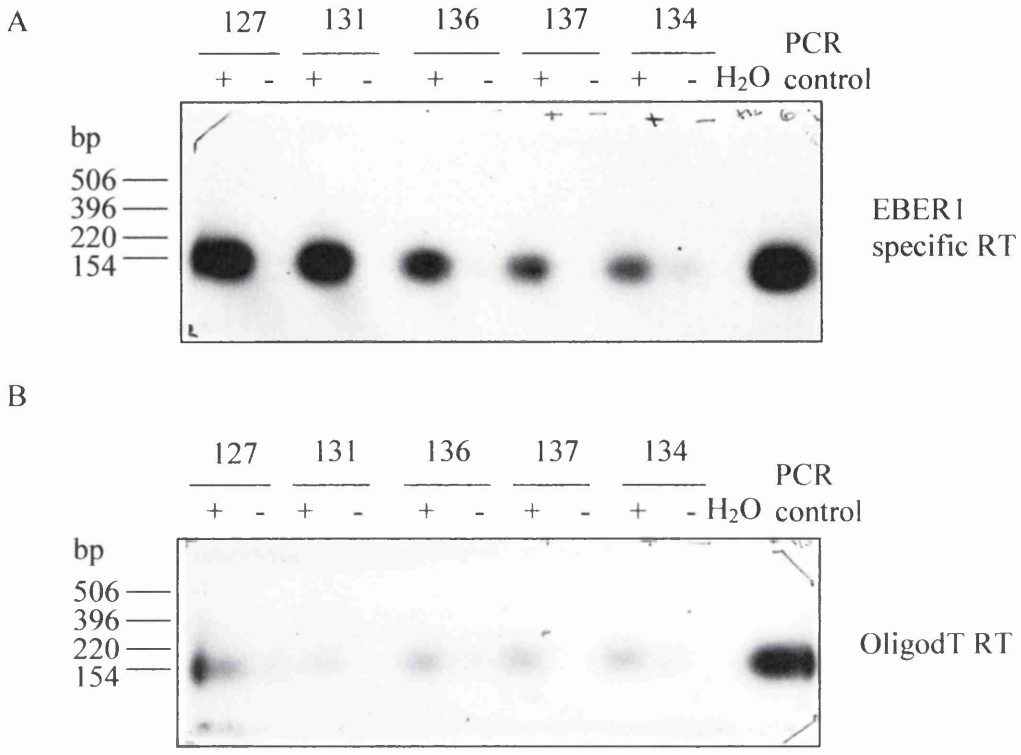

Figure 4.14: Reverse transcriptase either using an EBER1 specific primer or an oligodT primer followed by a PCR using EBER1 primers

Total RNA (5µg) from Peyer's patches of line 127, peripheral lymph nodes of line 131, thymus of lines 136 and 137 and spleen of line 134 was subjected to an RT reaction using an EBER1 specific primer (CR4) (panel A) or an oligodT primer (panel B). For each sample a minus RT control (-) was performed. A PCR was performed with $1/4^{th}$ of the RT reaction using CR8 and CR9 primers. Controls were also performed for the PCR, a no DNA control (H_2O) and a positive plasmid DNA control showing a DNA fragment of the expected size (144bp). The RT-PCR products were electrophoresed through a 1% agarose gel followed by a Southern blot using an EBER1 probe. For panel A the blot was exposed to film overnight whereas for panel B it was exposed for 3 days prior to being developed. Note a slight contamination is suggested by the signals in the -RT tracks of 134 in panel A and in 127, 136 and 134 in panel B.

4.8. The EBER1 gene has an upstream start

4.8.1. A minor species of EBER1 is observed in Raji cell extracts

Two reports have previously described the presence of a minor, slower migrating EBER1 species following S1 nuclease mapping of the 5' start. This minor EBER1 product was estimated to represent 1% of the major species. A similar species was not observed for EBER2 (Jat and Arrand, 1982, Arrand and Rymo, 1982). This suggested the minor use of an upstream start site for EBER1 transcription. In order to confirm if an upstream start site of EBER1 is used in Raji cells, an RT-PCR approach was undertaken. An EBER1 specific RT was performed using primer CR4 followed by two different sets of PCRs using different primer pairs, one being CR8 and CR9 and the second using CR25 and CR9 where CR25 anneals upstream of the recognised start of EBER1 (Figure 4.15 A). The PCR performed using CR8 and CR9 showed an amplification from Raji RNA but not from BJAB RNA as expected (Figure 4.15 B). The PCR performed using CR25 and CR9 primers also showed a signal for Raji, of a lower intensity compared to the previous one (Figure 4.15 C). This indicates that there is a second upstream start for the EBER1 gene, which confirms the previous observations from Arrand and colleagues.

4.8.2. The minor species of EBER1 is observed in lines 127 Peyer's patches and line 131 peripheral lymph nodes

In Chapter 3 northern blotting was used to assess the expression in culture of the different transgenes generated. On this blot, the EBER1 signal appears very smeary which either reflects poor resolution or could suggest the presence of different sizes of EBER1 transcripts. In order to test if a minor upstream start species of EBER1 is also expressed in the transgenic lines as it is in Raji cells, an RT-PCR using CR25 and CR9 primers was performed (Figure 4.16). A signal from line 127 Peyer's patches and line 131 peripheral lymph nodes was observed at lower intensity compared to using the internal CR8/CR9 primers (compare to figure 4.14 A). No signal was detected from the other samples tested following one day exposure, although there is a hint in 137. This result suggests that in the

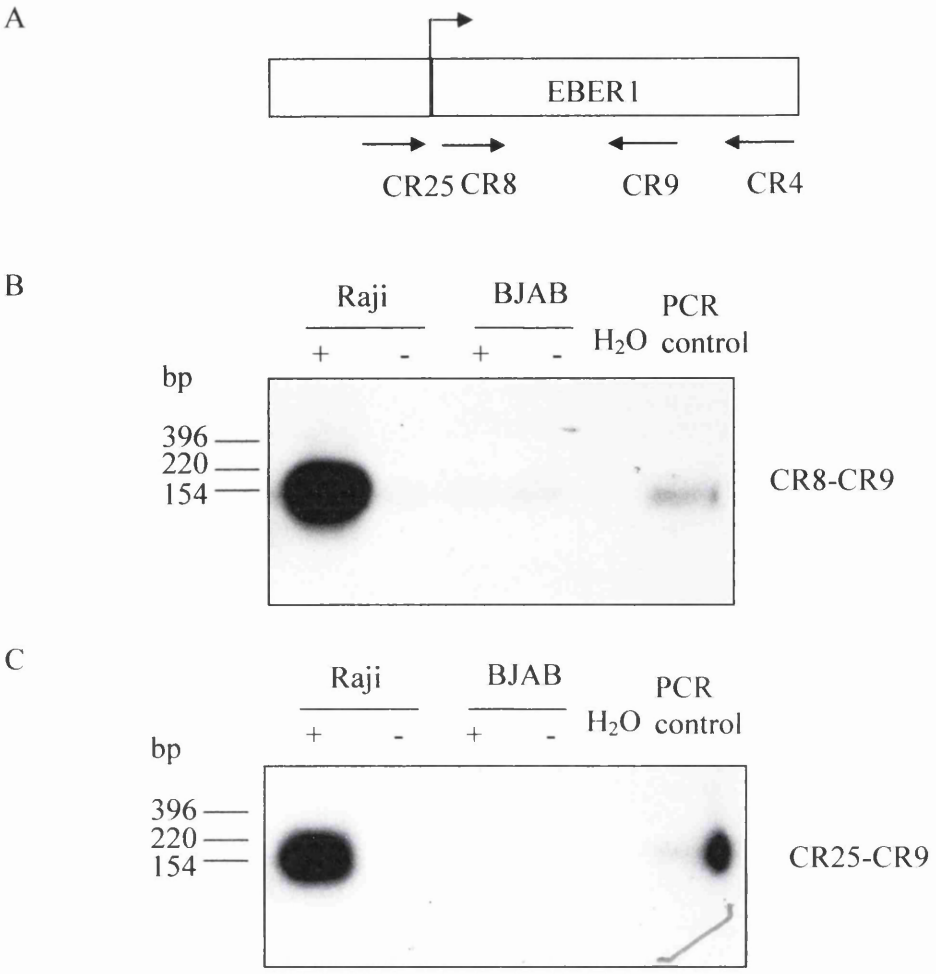

Figure 4.15: Reverse transcriptase using an EBER1 specific primer followed by PCR using different EBER1 primer pairs

Panel A shows the relative position of the different primers used in this assay (not to scale). Total RNA (5μg) from Raji and BJAB cells was subjected to an RT reaction using an EBER1 specific primer (CR4). For each sample a minus RT control (-) was performed. Two PCR were performed with $1/4^{th}$ of the RT reaction using either CR8 and CR9 primers (panel B) or CR25 and CR9 primers (panel C). Controls were also performed for the PCR, a no DNA control (H_2O) and a positive plasmid DNA control. The RT-PCR products were electrophoresed through a 1% agarose gel and followed by Southern blotting using an EBER1 probe. The expected size products are 144bp and 163bp for CR8/CR9 and CR25/CR9 amplifications respectively.

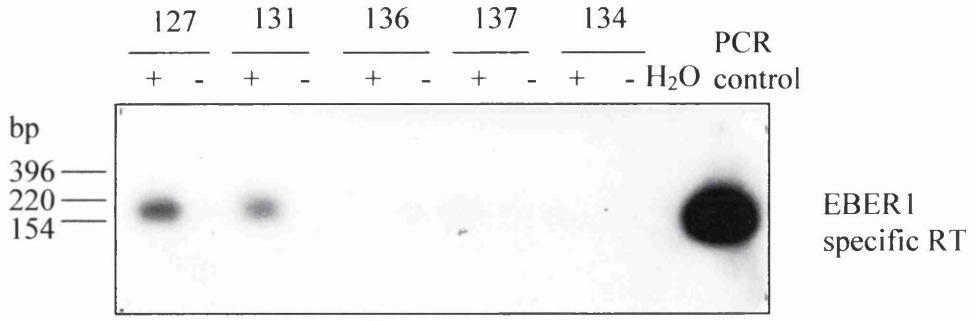

Figure 4.16: EBER1 specific reverse transcriptase followed by PCR primers CR25 and CR9

Total RNA (5μg) from Peyer's patches of line 127, peripheral lymph nodes of line 131, thymus of lines 136 and 137 and spleen of line 134 was subjected to an RT reaction using an EBER1 specific primer. For each sample a minus RT control (-) was performed. A PCR was performed with $1/4^{th}$ of the RT reaction using CR25 and CR9 primers. Controls were also performed for the PCR, a no DNA control (H_2O) and a positive plasmid DNA control showing a DNA fragment of the expected size (163bp). The RT-PCR products were electrophoresed through a 1% agarose gel and followed by Southern blotting using an EBER1 probe. The autoradiographs of the southern blots are presented in this figure. The blot was exposed to film overnight before being developed.

transgenic EBER1 mice, at least from lines 127 and 131, an upstream start site is used to a minor extent.

4.9. Summary

19 EBER1 transgenic positive founders were generated and 13 lines have been established from these. The expression analysis was performed on the lymphoid tissues of all the lines and on other tissues for lines 127, 131, 136 and 137. For construct 670, mice of lines 136 and 142 express EBER1 in the lymphoid tissues. The expression profile has not yet been determined for line 141. For construct 671, mice of the two lines express EBER1 in the lymphoid tissues. For line 127 the expression was also detected in the brain but not in any of the other tissues tested. The expression was also shown to be directed to both the B and T cells. For construct 672, mice of all the lines express EBER1 in the lymphoid tissues with different patterns of expression except line 133 where no expression was detected. Both lines 131 and 137 also express the transgene in non-lymphoid tissues, which could suggest that the transgene has integrated near a cellular gene which could influence the expression pattern or that the transgene was not sufficiently lymphoid specific. This was not investigated further. The expression profile has not yet been determined for line 143.

The expression level has been compared between different lines in both the thymus and Peyer's patches. In summary, mice of line 142 have the highest expression of EBER1 in the thymus, followed by line 127, whereas in the Peyer's patches, mice of line 127 have the highest expression of EBER1 followed by line 131. It was also noted that the expression in the transgenic tissues is much lower than that of an established EBV positive BL cell line in culture.

An RT-PCR approach was used to determine if in the transgenic positive mice EBER1 is an RNA pol II or RNA pol III transcript. The results showed that the EBER1 transcripts in the different tissues tested do not have a poly A tail as no product was detected when a PCR using EBER1 primers was performed following an oligodT RT. This suggests that EBER1, in the tissues tested, is an RNA pol III transcript.

The presence of a second upstream start for EBER1 was confirmed in Raji cell extracts and in tissues of different EBER1 transgenic positive lines using an RT-PCR approach.

For the next chapters the phenotypes of lines 136, 142 (construct 670), lines 127, 145 (construct 671) and lines 131, 137 (construct 672) will be further analysed.

Chapter 5. Phenotype analysis of the different expressing lines

5.1. Introduction

In the previous chapter the generation of transgenic mice expressing EBER1 was described. For each of the three constructs two lines have been selected (lines 136, 140 for construct 670, lines 127 and 145 for construct 671 and lines 131 and 137 for construct 672) and studied in more detail. This chapter describes the phenotype of the different lines selected. Data is also presented on the expression of c-Myc and Id2 in different EBER1 positive tissues. The effect of expression of EBER1 on the proportions of the B and T cells as well as on cytokine secretion is presented. Finally, the activity of PKR and other IFN related genes in response to dsRNA treatment of the mice is described. As line 127 was the first line where EBER1 expression was detected its analysis was taken further than the other lines.

5.2. Tumour phenotype of the different EBER1 lines

5.2.1. Phenotype of the lines

The main aim of this project was to determine if the expression of EBER1 *in vivo* could lead to the development of a phenotype, particularly malignancy. Where possible a cohort of 10-16 mice (of both positive and negative siblings) was set aside for a phenotype watch (Table 5.1) and each group was monitored weekly for any external signs of phenotype. To date, 9 out of 17 animals (53%) have developed lymphoma in line 127 aged between 14 and 22 months old and for the wild-type 2 animals out of 16 have developed lymphoma (12.5%) (one at 18 months and one at 24 months) (Table 5.1). The phenotype observed in the transgenic positive animals was expansion of the spleen (10-15x the normal size), expansion of the thymus (3-5x the normal size, not shown in the figure), enlarged mesenteric lymph nodes (to a pea size) and sometimes a slight expansion of

	136	127		145	131	137	
Tg status	+	+	-	+	+	+	-
Number of mice	11	17	16	13	10	12	11
Number of tumour	0	9	2	0	1	0	0

Table 5.1: Phenotype watch of the different lines selected

For lines 136, 127, 145, 131 and 137, a cohort of animals was monitored in a phenotype watch. The number of animals used is presented as well as their transgenic status (Tg status), + being a transgenic positive animal and - a transgenic negative. The number of animals with tumours to date is indicated.

peripheral lymph nodes and Peyer's patches (Figure 5.1). Some of the lymphoid tissues were sent for pathological analysis.

A Kaplan Meier graph is shown in figure 5.2, which displays incidence of lymphoma in these animals. 53% of the transgenic positive animals (EBER1) developed lymphoma with an average age of onset of 18 months. The P value between the two curves is 0.0258, indicating that the difference between the onset of lymphoma in the transgenic positive mice and wild-type is statistically significant. 12.5% of the wild-type animals developed lymphoma (with expansion of mesenteric lymph nodes, peripheral lymph nodes as well as the spleen for the 18 months old animal and expansion of mesenteric lymph nodes and spleen for the 24 months old animal) which can happen in old C57Bl/6 mice but is observed at low frequency in our colony.

It was also observed whilst dissecting animals for various assays that 20 out of 39 mice between 3 and 11 months old showed signs of expansion of lymphoid tissues (spleen, thymus, peripheral lymph nodes, mesenteric lymph nodes or Peyer's patches) (Tables 5.2 and 5.3) and none of the negative mice of matched age analysed showed a phenotype. This was not observed in younger transgenic animals between 2 and 6 months old, suggesting that the phenotype in this line arises later than 6 months. Therefore our results from line 127 older animals suggest that EBER1 acts as an oncogene. However to be able to conclude that this is exclusively due to the action of EBER1 and not any cellular gene disruption in this line, similar supporting data from other lines are required.

For the other lines, most of the animals are younger than mice of line 127 as the founders were generated afterwards and they are still under study. Line 127 was the first line generated and characterised to express EBER1. However, one transgenic positive animal from line 131 developed a lymphoma at 13.5 months of age and had a similar phenotype compared to line 127 (Figure 5.3 and tables 5.4 and 5.5). It can be noted that the expansion of the spleen was smaller than that observed for line 127 but the animal was also younger. This animal also had an infection and tissues were sent for pathology analysis. In younger mice of line 131 no signs of lymphoid expansion were observed when compared to age matched negative siblings. For line 136, it was observed that 6 out of 10, 2 to 10 months old animals showed signs of lymphoid expansion (Tables 5.4 and 5.5). For line 137 it was observed that 11 out of 14, 4.5 to 8 months old animals showed signs of expansion

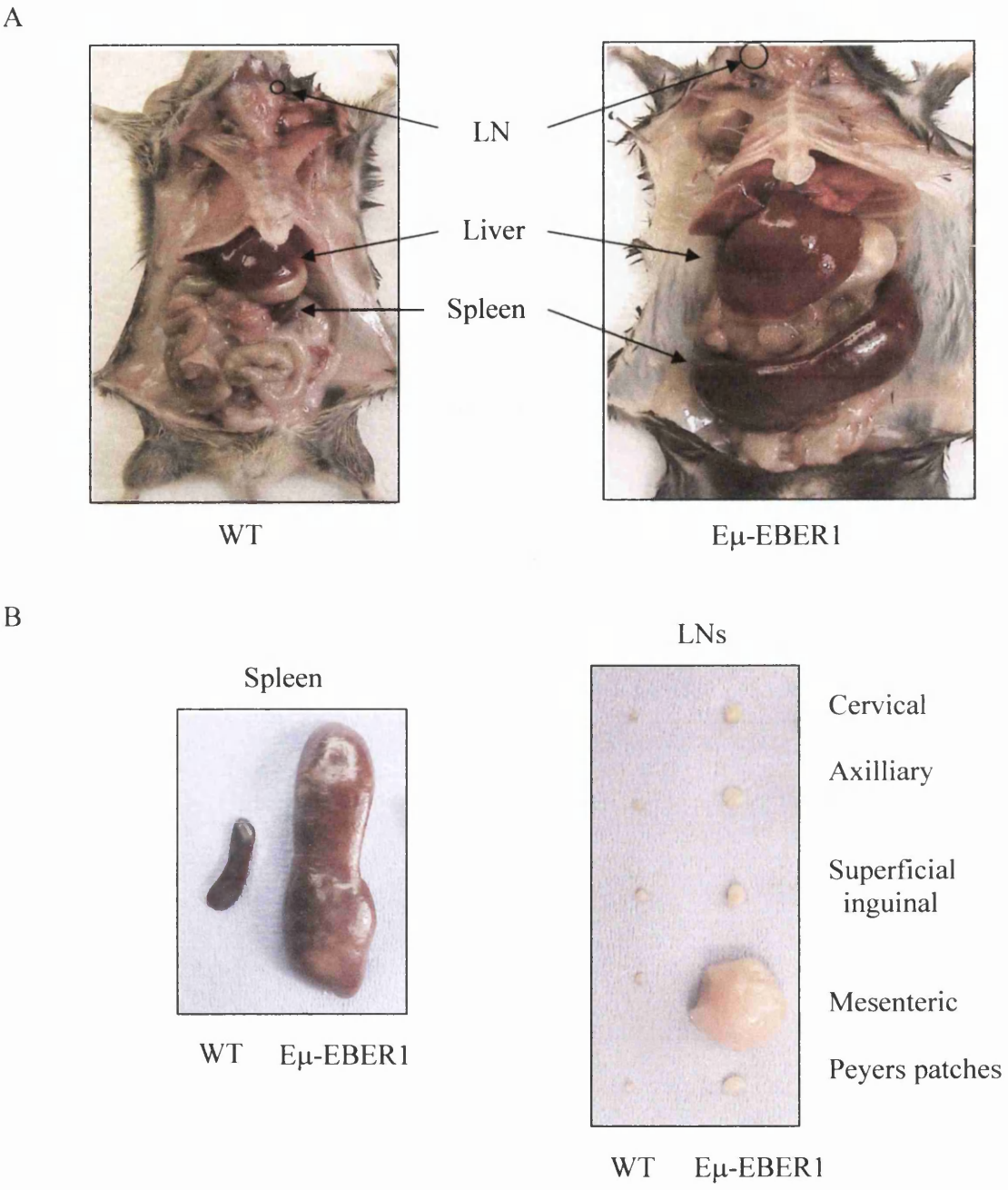

Figure 5.1: Tumour phenotype in line 127

Panel A shows the tumour phenotype observed in a transgenic positive 18 months old animal compared to an aged matched negative sibling (WT). A cervical lymph node (LN), the spleen and the liver are shown by an arrow. Panel B shows the dissected spleen and the different lymph nodes (LNs) alongside their negative aged matched control (WT). The infiltration from the white pulp can be noticed in the transgenic spleen. Note that the transgenic mesenteric lymph node was a portion of a large interconnected series of nodes.

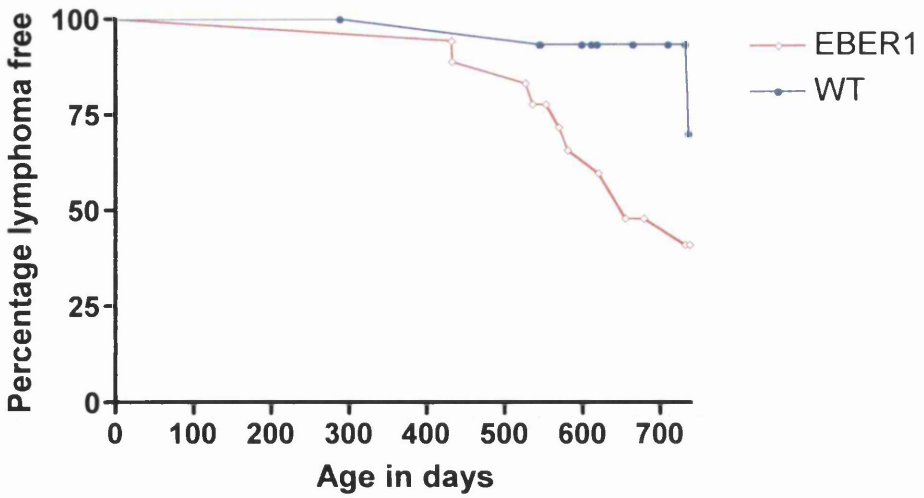

Figure 5.2: Kaplan Meier plot of lymphoma incidence in line 127 animals

This curve shows the percentage of lymphoma free against age (days). The red curve represents the transgenic positive animals of line 127 (EBER1) and the blue curve the negative siblings (WT). The graph was generated and the data analysed for statistical significance with a log rank test using Graphpad Prism 4 software. The study end point was 2 years.

Animal number	Tg status	Age in months	Phenotype observed
127.111	+ (homozygous)	9	T 1x, PLNs 3x, MLNs 5x, 1PP was very large 10x others OK
127.123	+	11	np
127.69, 70, 71, 83, 84 and 85	-	3	np
127.92, 93 and 94	-	3.5	np
127.9, 10, 39 and 40	-	4	np
127.120 and 121	-	7	np
127.113 and 114	-	8	np
127.104 and 105	-	9	np

Table 5.2: Phenotype in younger line 127 animals

In this table the animal ID, transgenic status (Tg status), age and the phenotype observed are presented. np indicates that no phenotype was observed. MLNs: mesenteric lymph nodes, PLNs: peripheral lymph nodes, CLNs: cervical lymph nodes, PP: Peyer's patches, SILNs: superficial inguinal lymph nodes, LN: lymph node, ALN: axillary lymph nodes, T: thymus.

Tg / Age months	+	-
$> 6 - 11 \leq$	14/19	0/6
$> 3 - 6 \leq$	2/14	0/7
≤ 3	4/6	0/6
P χ^2	<0.001	

Table 5.3: Summary of the lymphoid pathology in younger mice of line 127

This table presents the number of animals which have developed signs of lymphoid expansion on the total number of animals for different age categories for mice of line 127. Both the transgenic positive (+) and negative (-) siblings are shown. For full details for the negatives see summary table 7.1. The data was analysed for statistical significance using a Chi squared (χ^2) test and is presented as P χ^2.

Animal number	Tg status	Age in months	Phenotype observed
127.73	+	3	ALN 3x
127.75 and 76	+	3	np
127.86	+	3	CLN 2x
127.87 and 88	+	3	PLNs 2x, MLNs 2x
127.95		3.5	Thymus 2x
127.96, 97, 106 and 110	+	3.5	np
127.108	+	3.5	MLNs 2x, PLNs 2x
127.11. 12, 41, 42, 103 and 107	+	4	np
127.101 and 102	+	5	np
127.119 and 122	+	7	np
127.134	+	7	PLNs 2x and PP2x LN around spine 3x
127.135	+	7	PLNs 2x and PP2x
127.136	+	7	Spleen 2x
127.137	+	7	Spleen 2x, thymus 2x and PP 2x
127.139 and 141	+	7.5	np
127.140	+	7.5	Thymus 2x, PP 2x
127.142	+	7.5	Thymus 2x
127.143	+	7.5	Thymus 2x, PP 2x
127.144	+	7.5	Spleen 2x
127.115	+	8	Spleen 2x, thymus1x
127.116	+	8	Spleen 2x
127.117	+	8	Spleen 6x,
127.128	+	8 1/2	np
127.129	+	8 1/2	Spleen 1x, thymus 2x

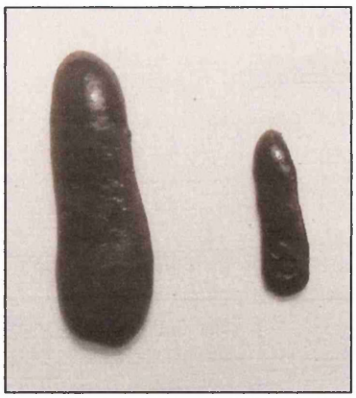

Spleen

131.18
Eμ-EBER1

131.20
Wt control

Figure 5.3: Tumour phenotype in line 131

This figure shows the expanded spleen of a transgenic positive 13.5 months old animal (line 131) alongside its aged matched negative sibling (Wt) control.

Tg / Age months	131 +	131 -	136	145
> 10 – 14 ≤	1/1	0/1		
> 6 – 10 ≤			4/8	2/3
> 3 – 6 ≤				0/1
≤ 3	0/5	0/5	2/2	2/2
P χ^2				
P Fisher's exact	0.18		<0.001	0.00007

Table 5.5: Summary of the lymphoid pathology in younger mice of lines 131, 136 and 145

This table presents the number of animals which have developed signs of lymphoid expansion on the total number of animals for different age categories for mice of lines 131, 136 and 145. Both the transgenic positive (131 +) and negative (131 -) siblings are shown for line 131. For full details for the negatives see summary table 7.1. The data was analysed for statistical significance either using a Chi squared (χ^2) test or a Fisher's exact test and is presented as P χ^2 or P Fisher's exact respectively.

Animal number	Tg status	Age in months	Phenotype observed
131.12, 15, 22, 23 and 25	+	3	np
131.11, 16, 54, 26 and 27	-	3	np
131.18	+	13.5	Tumour: Spleen 4x, MLNs 5x
131.20	-	13.5	np
136. 29	+	2	MLNs 2x, PLNs 4x
136.30	+	2	MLNs 2x
136.47 and 48	+	9	np
136.51	+	9	Thymus 2x
136.38	+	10	Spleen 1/2 size, PP 3-4x
136.42	+	10	Thymus 2x
136.43	+	10	Thymus 2x, PP 2-3x
136.39 and 40	+	10	np
145.9	+	2	SILNs more than 1 LN each side, ALNs and CLNs 2x, MLNs 2x, PP 3x
145.13	+	2	SILNs more than 1 LN each side, ALNs and CLNs 2x, MLNs 4x, PP3x
145.45	+	4	np
145.29 and 31	+	8	2 SILNs each side, thymus 2x, PP 3x
145.30	+	8	np

Table 5.4: Pathology of mice of lines 131, 136 and 145

In this table the animal ID, transgenic status (Tg status), age and the phenotype observed are presented. The line number is indicated first followed by the animal number. np indicates that no phenotype was observed. MLNs: mesenteric lymph nodes, PLNs: peripheral lymph nodes, CLNs: cervical lymph nodes, PP: Peyer's patches, SILNs: superficial inguinal lymph nodes, LN: lymph node, ALN: axillary lymph nodes.

of lymphoid tissues, mainly peripheral lymph nodes, mesenteric lymph nodes and thymus (Tables 5.6 and 5.7). The three without phenotype were young animals (4, 4 and 5 months). None of the age matched negative siblings analysed showed a phenotype. And finally 4 out of 6 line 145 animals (2 to 8 months old) showed an unusual phenotype as well as signs of lymphoid expansion (Tables 5.4 and 5.5). This phenotype has not been seen in other lines, where the superficial inguinal lymph nodes are not markedly expanded, but instead of one at each site, several small individual nodes were detected.

5.2.2. The tumours arising in line 127 are of B cell origin

In order to determine if the tumours arising in line 127 were of B cell or T cell origin, tumour sample gDNA was examined for clonal IgH and T cell receptor (TCR) rearrangements. The IgH rearrangement was analysed by Southern blot using tissues from two animals that developed tumours (Figure 5.4). A wild-type sample was used as negative control to identify the endogenous band and two transgenic Eμ*N*-myc tumour tissues were used as positive controls for IgH rearrangement (Dildrop *et al.*, 1989). IgH rearrangements were observed from two different EBER1 mice with tumours (two tissue samples each) due to the presence of extra bands when compared to the negative control. Moreover the rearrangements were clonal within an animal, the same bands being detected in both tissues analysed. No TCR rearrangements were observed for either of the EBER1 tumour samples (Data not shown). These results indicate that the tumours arising in line 127 animals are of B cell origin. Moreover, FACS analysis performed on a third EBER1 tumour sample (127.51) with B220FITC and CD3PE staining showed an extensive B cell population (B220 positive) compared to the T cell population (CD3 positive) (Figure 5.5).

5.2.3. EBER1 expression in the tumour tissues of line 127

In order to assess if EBER1 expression is altered in the tumour samples an RT-PCR was performed on RNA extracted from two tumour samples and followed by a Southern blot (Figure 5.6 A). A control experiment was performed with different pre-tumour line 127 tissues (Figure 5.6 B). For both the spleen and the mesenteric lymph node sample, no difference in EBER1 expression levels were observed between the pre-tumour and tumour stage, indicating that EBER1 expression does not increase in the tumours. However, this

Tg / Age months	+	-
> 6 – 10 ≤	6/6	0/6
> 3 – 6 ≤	5/8	0/6
P χ^2	<0.001	

Table 5.7: Summary of the lymphoid pathology in younger mice of line 137

This table presents the number of animals which have developed signs of lymphoid expansion on the total number of animals for different age categories for mice of line 137. Both the transgenic positive (+) and negative (-) siblings are shown for line 137. For full details for the negatives see summary table 7.1. The data was analysed for statistical significance using a Chi squared (χ^2) test and is presented as P χ^2.

Animal number	Tg status	Age in months	Phenotype observed
137.24	+	4.5	PLNs 3x, MLNs 2x
137.28	+	4.5	PLNs 3x, MLNs 3x, thymus 3x
137.69	+	4.5	MLNs 2x, CLNs 2x
137.70 and 72	+	4.5	np
137.52	+	5	np
137.57	+	5	MLNs 2x
137.58	+	5	Thymus 2x
137.71	+	6.5	Thymus 2x, spleen 1.5x
137.55	+	7	Thymus 1.5x, spleen 2x
137. 43	+	8	Thymus 2x
137.46	+	8	Thymus 2x
137.50	+	8	Thymus 2x, spleen 1.5x
137.51	+	8	Thymus 2x
137.63, 66, 67 and 68	-	4.5	np
137.56 and 59	-	5	np
137.53 and 54	-	7	np
137.44, 45, 48 and 49	-	8	np

Table 5.6: Pathology of mice of line 137

In this table the animal ID, transgenic status (Tg status), age and the phenotype observed are presented. The line number is indicated first followed by the animal number. np indicates that no phenotype was observed. MLNs: mesenteric lymph nodes, PLNs: peripheral lymph nodes, CLNs: cervical lymph nodes, PP: Peyer's patches.

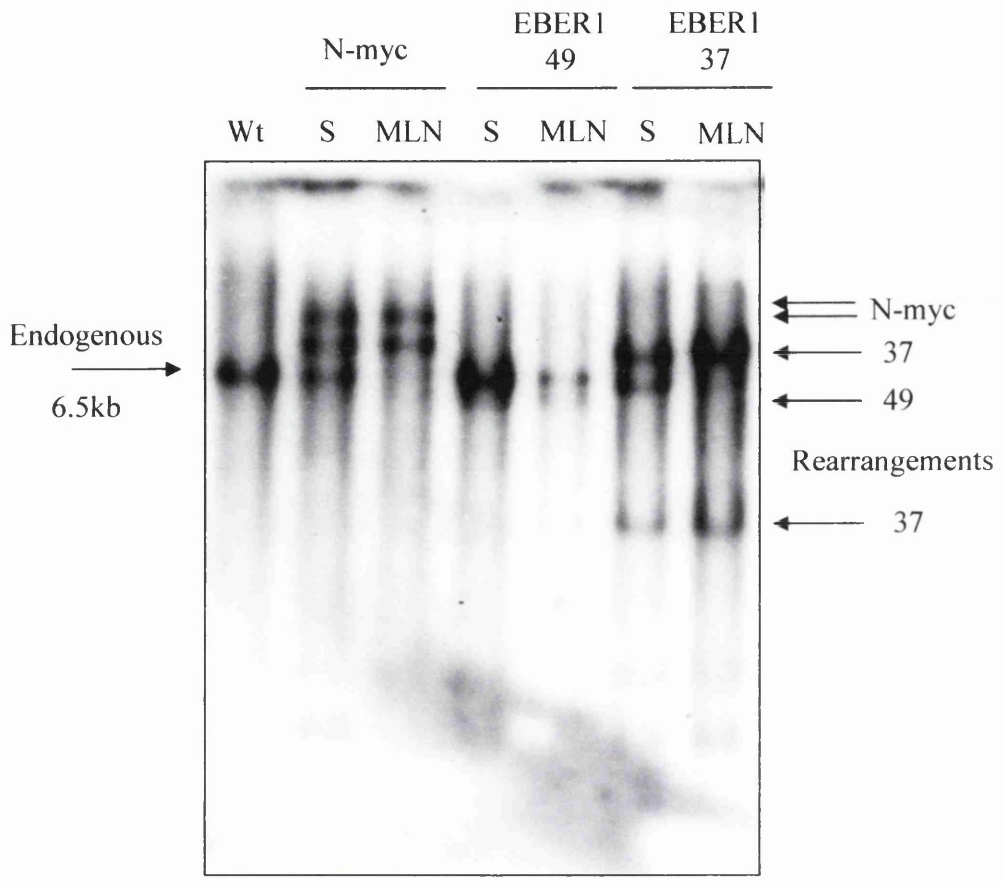

Figure 5.4: IgH rearrangements in line 127 tumour samples

gDNA was extracted from different tissues (spleen: S, and mesenteric lymph node: MLN) and 5μg was digested with *Eco*RI. The digested gDNAs were electrophoresed through a 0.8% TAE gel and Southern blotted. The membrane was hybridised overnight with an IgH radiolabelled probe at 65°C. The washes were performed the following day with a high stringency wash at 65°C and the membrane was exposed to film. A wild-type (Wt) sample was used as negative control. Two N-myc tumour tissues were used as positive controls for IgH rearrangement. The endogenous band is indicated by an arrow on the left hand side and the rearranged bands are shown by arrows on the right hand side.

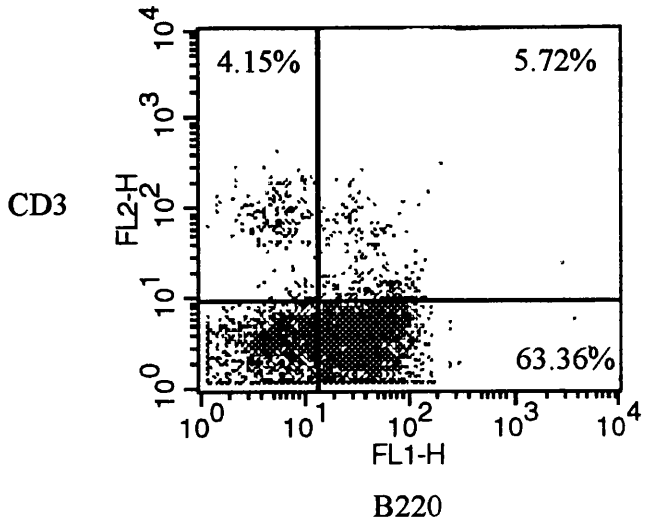

Figure 5.5: The splenocytes from line 127 tumours are of B-cell origin

The spleen was collected from a line 127 mouse with a tumour. Primary cells were isolated and 10^6 cells were stained with B220FITC and CD3PE. The percentage of the cells in each quadrant is indicated. A B cell population with this stain should be in the lower right quadrant, whereas a T cell population should be in the upper left quadrant.

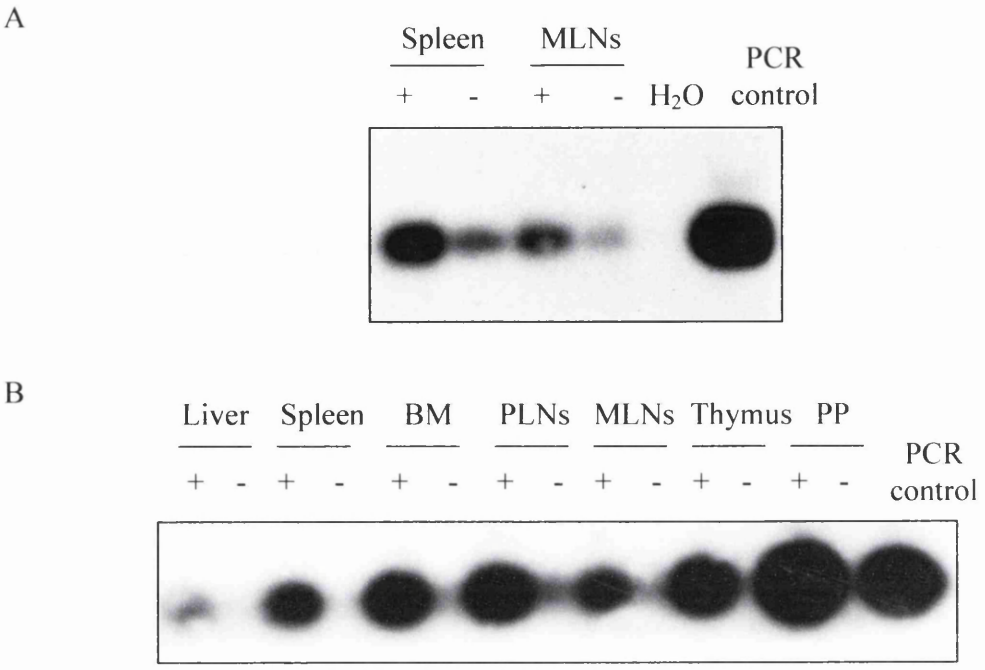

Figure 5.6: EBER1 expression in line 127 tumour samples

The spleen and mesenteric lymph nodes (MLNs) from a line 127 tumour animal were collected. RNA extraction was performed followed by DNAse I treatment, acid phenol extraction and RT-PCR. The RT reaction was performed with an EBER1 specific primer (CR4) and 5µg of total RNA. For each sample a minus RT control was performed. The PCR was performed with $1/4^{th}$ of the RT reaction and CR8 and CR9 primers. A no DNA control (H_2O) and a positive plasmid DNA control were also performed for the PCR. The RT-PCR products were electrophoresed through a 1% agarose gel followed by Southern blotting and probing using an EBER1 probe (panel A). A gDNA contamination can be observed in the Spleen and MLN samples. A similar experiment was performed with different pre-tumour tissues of line 127 (panel B). BM: bone marrow, PLNs: peripheral lymph nodes, MLNs: mesenteric lymph nodes, PP: Peyer's patches.

PCR and blot approach is not strictly quantitative. Nevertheless the higher expression in the Peyer's patches (as seen by quantitative PCR) can be discerned by this method and it is therefore semi-quantitative.

5.2.4. Preliminary protein analysis of line 127 tumour samples

5.2.4.1. c-Myc expression analysis of line 127 tumour samples

In order to assess what secondary events may have occurred in the development of line 127 tumours, the expression of various proteins was examined by western blot. The first protein analysed was c-Myc, due to its involvement in BL (Lindstrom and Wiman, 2002). A western blot was performed with 5 different samples from EμEBER1 mice and controls from a wild-type C57Bl/6 mouse, an Eμcmyc mouse tumour (line 97, Adams *et al.*, 1985) and an EμEBNA1 mouse tumour (line 26, Wilson *et al.*, 1996) and probed with an anti c-Myc antibody (Figure 5.7). Two bands at approximately 66kDa (the expected size for c-Myc) were observed in all the samples. In order to correctly identify the c-Myc band the western was stripped and re-probed using a blocking peptide for this primary antibody. No signal was detected from this blot indicating that the blocking peptide is not an effective means to identify c-Myc in this case. However, the two bands indicated by an arrow are both stronger in the two line 97 samples (as is a band at approximately 130kDa) which are overexpressing c-Myc and were used as positive controls to identify c-Myc, suggesting that either or both could be c-Myc products. Therefore, if the two bands are c-Myc, no increase in c-Myc was detected in the different EBER1 samples (pre-tumours or tumours) compared to wild-type. The signal appears of a similar intensity to that of the wild-type control. This is supported by the normalisation data, as the value obtained is similar in the wild-type (wt), the young line 127 mouse (N), the pre-tumour (P) and the 127.49 tumour samples (49T) (Table 5.8), whereas the value obtained from the c-Myc positive controls (line 97) is clearly higher. However, it should be noted that the signal obtained from the βtubulin blot may be distorted as this blot was stripped several times before being re-probed with an antibody to βtubulin. This could lead to a non-uniform decrease in protein levels and therefore this blot might not be very accurate as a loading control. Moreover, the software comparing pixel number of images is not likely to reflect a true linear quantitation of the protein sample and therefore just represents a rough guide of

	Wt	N	P	49T	49T	37T	37T	97S	97CLN	26	12726
Norm data	0.27	0.15	0.22	0.23	0.73	20.5 *		2.45	5.09	0.85	2.99
Norm data to Wt	1	0.56	0.81	0.85	2.7	76		9.1	18.9	3.1	11.1

Table 5.8: Normalisation of the c-Myc western blot

The intensity of the bands on the c-Myc western blot and the βtubulin western blot were determined using the ID image analysis software. The intensity values of the c-Myc bands 1 and 2 were added and then divided by the βtubulin intensity value to give the normalised data (Norm data). The normalised values were then divided by 0.27 to relate to a wild-type value of 1 (Norm data to Wt) to be able to compare the samples to the wild-type. The order of the samples is the same as on the western. It should be noted that the value with the * sign appears too high for the signal observed on the blot, which may be due to some track distortion for this sample.

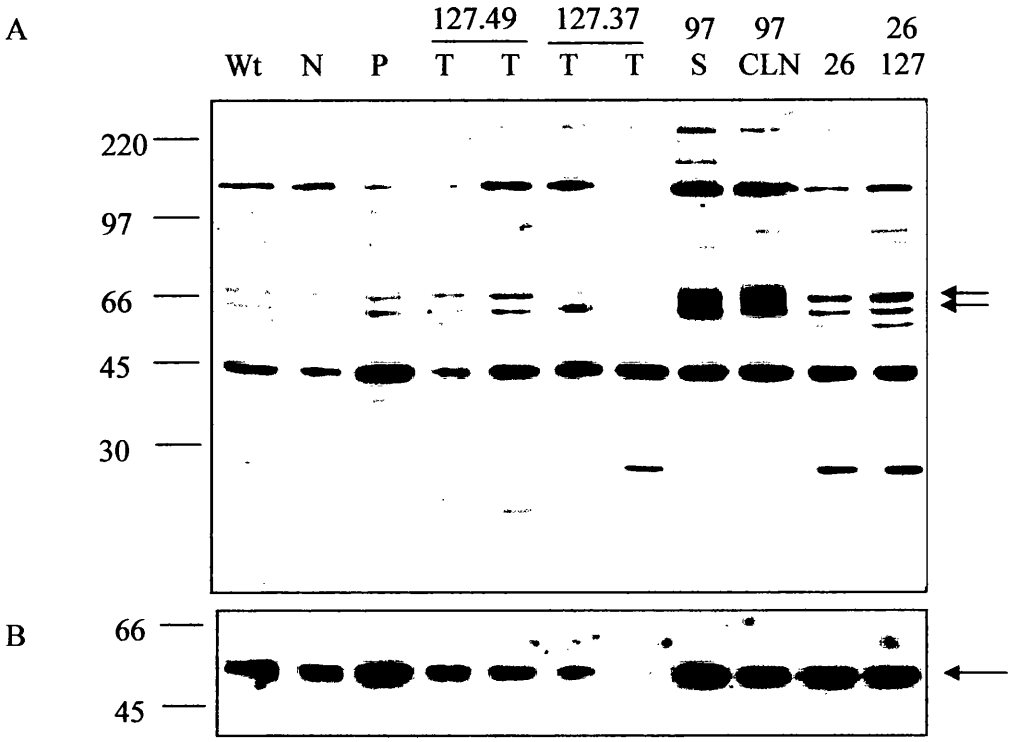

Figure 5.7: c-Myc western blot of line 127 tumour samples

Proteins from tissues of different animals were extracted using the high salt nuclear extraction method. 100μg protein extracts were separated by a 7.5% SDS-PAGE and the gel was western blotted. The membrane was probed with a rabbit anti-c-Myc antibody followed by a goat anti-rabbit IgG-HRP secondary antibody and visualised using ECL+ (panel A). Several controls were used, a wild-type (Wt) spleen control, two c-Myc tumour tissues (S: spleen, CLN: cervical lymph nodes) (97), an EBNA1 spleen tumour tissue (26), an EBNA1/EBER1 bi-transgenic spleen tumour tissue (26127). For the EBER1 line 127 samples, a spleen from a young animal was used (N), a spleen where signs of lymphoid expansion were observed (P) and four tumour tissues (spleen and mesenteric lymph nodes) (T) from two animals (127.37 and 127.49) were used. c-Myc is 67kDa and the most likely c-Myc bands are indicated by two arrows. The membrane was stripped and reprobed with a rabbit anti-βtubulin antibody and a goat anti-rabbit IgG-HRP secondary antibody and visualised using ECL+ (panel B). It should be noted that no c-Myc protein was observed for the second track of animal 127.37; however this sample was shown to be degraded. The molecular weights according to the marker lane (in kDa) are shown.

comparative levels. A slight difference in intensity (3.5 fold) was also observed between the EBNA1 tumour sample (26) and the EBNA1/EBER1 bi-transgenic tumour sample (26 127).

This western blot was stripped several times and re-probed with the following antibodies: anti-p53, since p53 is frequently mutated in BL (Farrell *et al.*, 1991), anti-phospho Rb and anti-total Rb. The results were not very conclusive as for both p53 and pRB several bands were detected at around the expected size. However, for all the different bands the pattern was similar showing no obvious differences in p53 or pRB levels in both EBER1 pre-tumour and tumour stages.

5.2.4.2. c-Myc DNA binding activity of line 127 tumour samples

The DNA binding activity of Myc was addressed by EMSA using a myc binding site oligo for Myc/Max (Figures 5.8 and 5.9). The positive control used for both EMSAs was from a line 97 tumour tissue protein extract. The specific c-Myc band was competed out from each sample using 200x competitor unlabelled oligo. A non-specific band, which was not competed out, was observed in all the tracks. The attempted supershift with a c-Myc antibody showed no shift, suggesting that it either did not work or the band observed is not c-Myc. The same protein extracts were used for an Sp1 EMSA, which reveals the quality of the extracts and also allows monitoring of the loading of the samples, as Sp1 is a ubiquitously expressed protein (Figure 5.10). The wild-type, 127.37 and 127.49 samples appear degraded compared to sample 97 where the three Sp1 expected bands are observed. The Sp1 EMSA was performed after multiple freezing and thawing of the samples and this could lead to protein degradation. Due to time limitations, this assay was not repeated. Unfortunately this limits the interpretation of the c-Myc binding reactions as comparative quality and quantity of the samples loaded is not certain. However, it should be noted that tumours 127.37 and 127.49 show a different banding profile. Two additional bands (B and C in figure 5.9) were observed for sample 127.49, suggesting that in this tumour additional protein complexes binding to this oligo have been activated. Moreover, although the subsequent Sp1 analysis of the extracts after freeze/thaw was not informative, the binding of a non-specific band (see * in figures 5.8 and 5.9) suggests that the extracts are of relatively equal loading. If so, binding to the Myc oligo in both EBER1 tumours (37 and

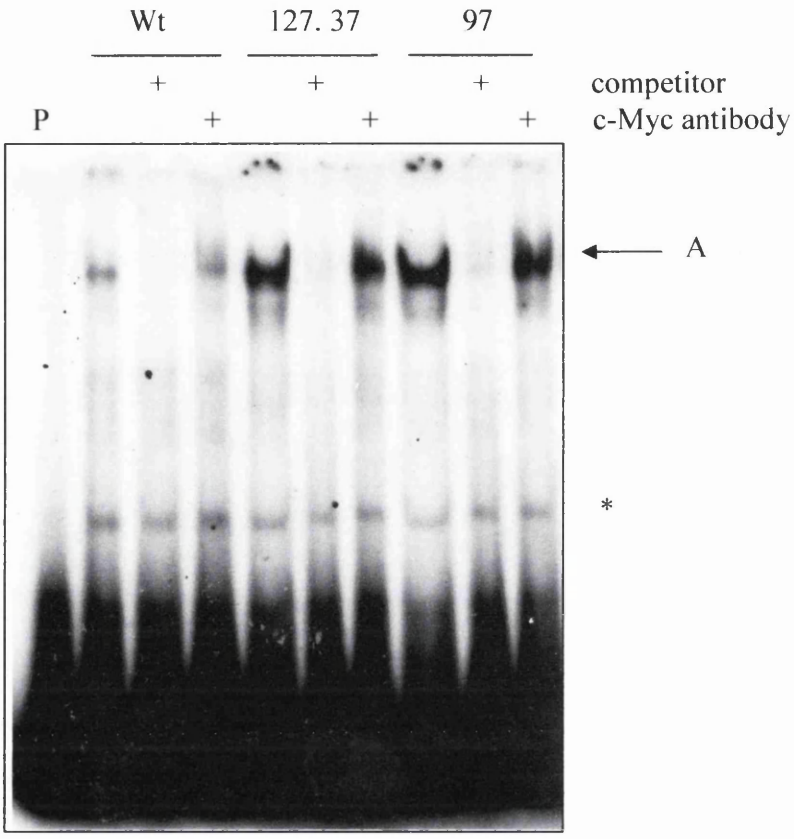

Figure 5.8: EMSA showing the DNA binding activity of Myc in extracts from line 127.37 tumour and a line 97 tumour

Protein was extracted from different samples using the high salt nuclear extraction buffer. 10μg of protein extract was used for each sample. Line 97 (c-Myc) extract was used as positive control and a wild-type splenic extract was used as negative control (Wt). The EBER1 sample was extracted from animal number 37. Three reactions were prepared for each sample: one without and one with 200x unlabelled competitor and a third one with 4μg of c-Myc antibody (as indicated). Labelled myc oligo was added to each sample and incubated for 20 minutes on ice before loading the samples on to a 6% polyacrylamide gel. A labelled oligo without extract was also used as control (P). The gel was electrophoresed for 3 hours before being dried and exposed to film for the required amount of time. The arrow indicates the specific binding band of c-Myc and the * shows a non-specific band.

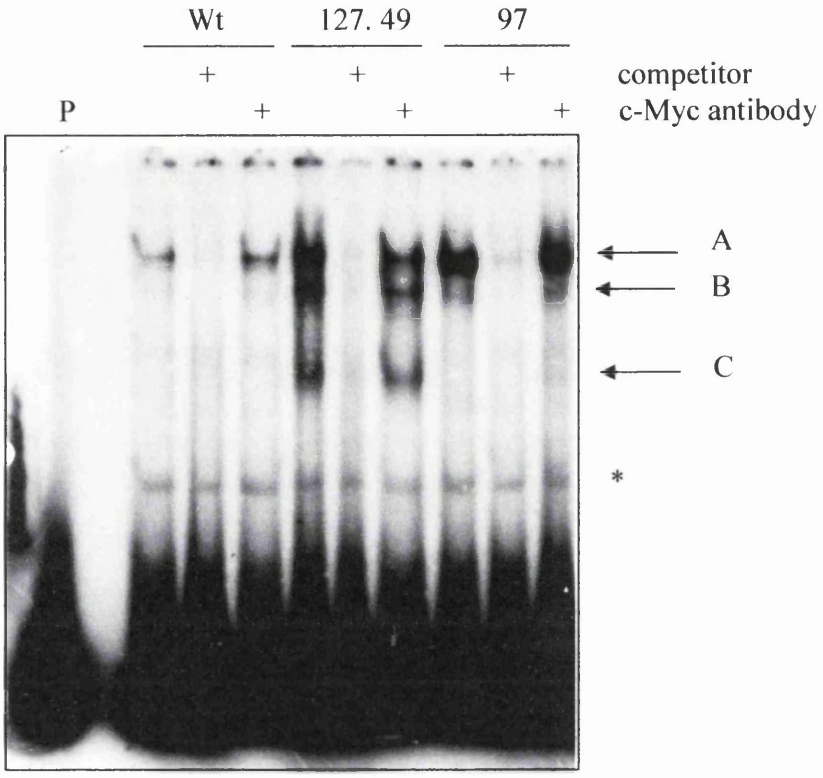

Figure 5.9: EMSA showing the DNA binding activity of Myc in extracts from line 127.49 tumour and a line 97 tumour

Protein was extracted from different samples using the high salt nuclear extraction buffer. 10μg of protein extract was used for each sample. Line 97 (c-Myc) extract was used as positive control and a wild-type splenic extract was used as negative control (Wt). The EBER1 sample was extracted from animal number 49. Three reactions were prepared for each sample: one without and one with 200x unlabelled competitor and a third one with 4μg of c-Myc antibody (as indicated). Labelled myc oligo was added to each sample and incubated for 20 minutes on ice before loading the samples on to a 6% polyacrylamide gel. A labelled oligo without extract was also used as control (P). The gel was electrophoresed for 3 hours before being dried and exposed to film for the required amount of time. The arrow A indicates the specific binding band of c-Myc and the B and C arrows indicate specific bands for animal 49. The * sign shows a non-specific band.

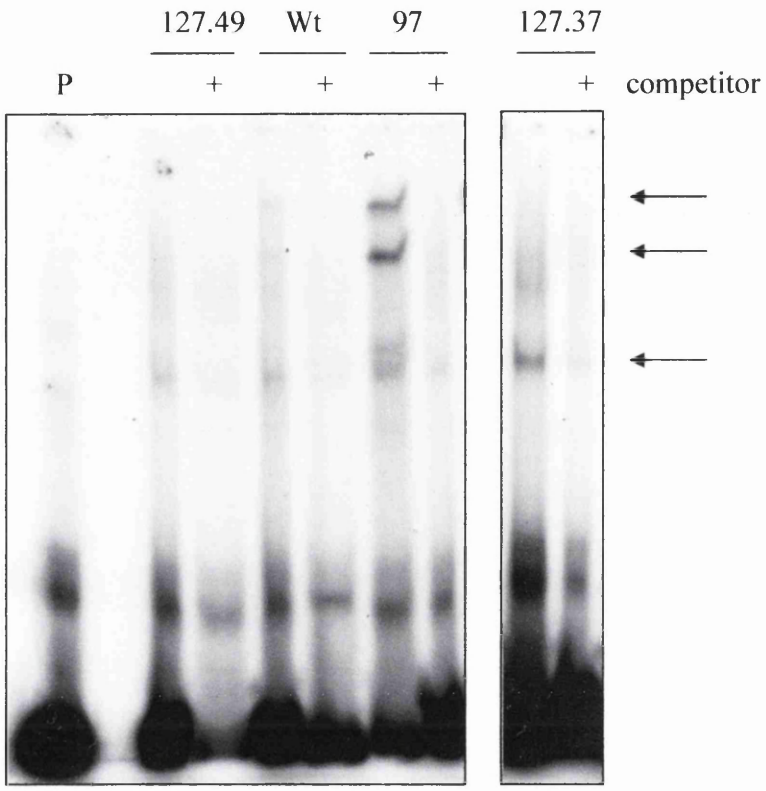

Figure 5.10: EMSA showing the DNA binding activity of Sp1 in extracts from tumour samples of mice of lines 127 and 97

Protein was extracted from different samples using the high salt nuclear extraction buffer. 10μg of protein extract was used for each sample. Two EBER1 tumour extracts (127.49 and 37), a line 97 (c-Myc) extract and a wild-type extract (Wt) were used. Two reactions were prepared for each sample: one without and one with 200x unlabelled competitor. Labelled Sp1 oligo was added to each sample and incubated for 20 minutes on ice before loading the samples on to a 6% polyacrylamide gel. A labelled oligo without extract was also used as control (P). The gel was electrophoresed for 3 hours before being dried and exposed to film for the required amount of time. The arrows indicate the specific binding bands of Sp1.

49) is stronger than the wild-type sample and almost equivalent to the 97 sample, despite overexpression of c-Myc not being apparent by western.

In order to explore this further a Southern blot designed to identify possible rearrangements at the c-Myc locus was performed. This experiment was designed to assess if any rearrangements in close proximity to the c-Myc locus had occurred in the EBER1 tumours. No rearrangements were observed in the different EBER1 samples tested.

5.2.4.3. Id2 expression analysis of line 127 tumour samples

The protein level of Id2, a downstream transcriptional activation target of c-Myc (Lasorella *et al.*, 2000), was analysed in the EBER1 tumour samples by western blot (Figure 5.11). The samples were the same as the ones used for the c-Myc western blot. This blot was probed with an anti-Id2 antibody and a band at approximately 17kDa was observed in the pre-tumour track, the 127.37 tumour samples, the c-Myc and the c-Myc/EBER1 bi-transgenic tumour samples. A faint Id2 band was observed in one of the 127.49 tumour samples. These results suggest that Id2 could be upregulated in the 127.37 EBER1 tumour sample where the banding pattern in the Myc EMSA was similar to that of the c-Myc positive control. Interestingly the sample (127.49) that either shows faint or no Id2 expression is the one that had a different c-Myc binding pattern in the Myc EMSA. It is also interesting to note that the pre-tumour sample showed upregulation of Id2 whereas the sample from a younger line 127 animal did not, nor was expression detected in wild-type. Therefore upregulation of Id2 may occur in tumourigenesis in the EBER1 mice.

5.3. FACS analysis of the different lymphoid tissues in lines 127 and 131

In order to determine if EBER1 expression affects B and T cell proportions in the different lymphoid tissues, the tissues were analysed by FACS. The lymphoid tissues (spleen, thymus, peripheral lymph nodes, mesenteric lymph nodes, Peyer's patches and bone marrow) from young mice of the lines 127 and 131 were collected from both positive and negative siblings and cells isolated. For each line three positive and three negative 3 months old mice were used and separately pooled. FACS analysis was performed with B220FITC and either CD3PE or Thy1.2PE. B220 (or CD45R) is a B cell marker which is

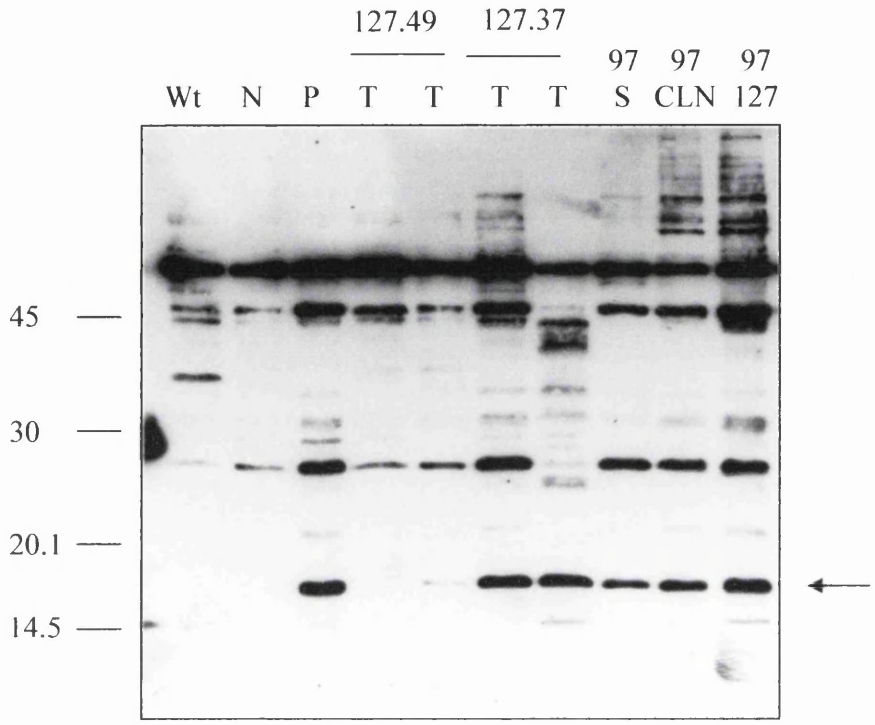

Figure 5.11: Id2 western blot of line 127 tumour samples

Proteins from tissues of different animals were extracted using the high salt nuclear extraction method. 100µg of proteins were separated by 12.5% SDS-PAGE and the gel was western blotted. The membrane was probed with a rabbit anti-Id2 antibody followed by a goat anti-rabbit IgG-HRP secondary antibody and visualised using ECL+. Several controls were used, a wild-type (Wt) spleen control, two c-Myc tumour tissues from the same mouse (S: spleen and CLN: cervical lymph nodes) (97) and a c-Myc/EBER1 bi-transgenic tumour tissue (cervical lymph nodes) (97127). For the EBER1 samples, a spleen from a young animal was used (N), a spleen where signs of lymphoid expansion were observed (P) and four tumour tissues (spleen and mesenteric lymph nodes) from two animals (127.37 and 127.49) (T) were used. The molecular weights according to the marker lane (in kDa) are shown. Id2 is 15kDa and the most likely Id2 band is indicated by an arrow.

expressed from the pro-B cells stage to mature B cells. Thy1.2 (or CD90), is a T cell marker mainly present on immature T cells, whereas CD3 is a T cell marker detected on mature T cells. No differences were observed between mice of the two transgenic positive lines and their negative siblings for the different tissues tested. Figure 5.12 shows a representative example of the results obtained, with the spleen of mice of line 127 stained with B220FITC and CD3PE and the bone marrow with B220FITC and Thy1.2PE. Therefore the transgene does not appear to affect the proportion of the B and T cells in young mice of lines 127 and 131.

In order to determine if EBER1 expression affects the differential status of the B and T cells in the different lymphoid tissues (spleen, thymus, peripheral lymph nodes, mesenteric lymph nodes, Peyer's patches and bone marrow) FACS analysis was performed. The different stains used for the FACS analysis are presented in table 5.9. For this experiment, no differences were observed for line 131 transgenic positive animals compared to negative siblings for any of the lymphoid tissues and strains tested, suggesting that for this line the status of the B and T cells (with respect to the stains used) is not modified by the presence of the transgene. For line 127 no differences were observed for the different stains with all the lymphoid tissues tested except for one tissue and one stain. An increase of the $CD5^{high}$, $B220^{neg/low}$ cell population was observed in the Peyer's Patches of transgenic positive animals compared to the negative animals (figure 5.13 A). This population could be a B1 population as B1 cells are characterised by $CD5^{high}$, $B220^{neg\ or\ low}$ and are also bigger and more granular than normal B cells, which was also observed using the FSC-H and SSC-H channels (figure 5.13 B). As was shown in Chapter 4, Peyer's patches is the highest expressing tissue in this line. This could explain the fact that this is the only affected tissue.

5.4. ELISA analysis of lines 127, 131 and 137 sera

In order to assess if the presence of EBER1 in the lines interferes with the secretion level of different cytokines or antibodies, serum samples were collected whenever possible.

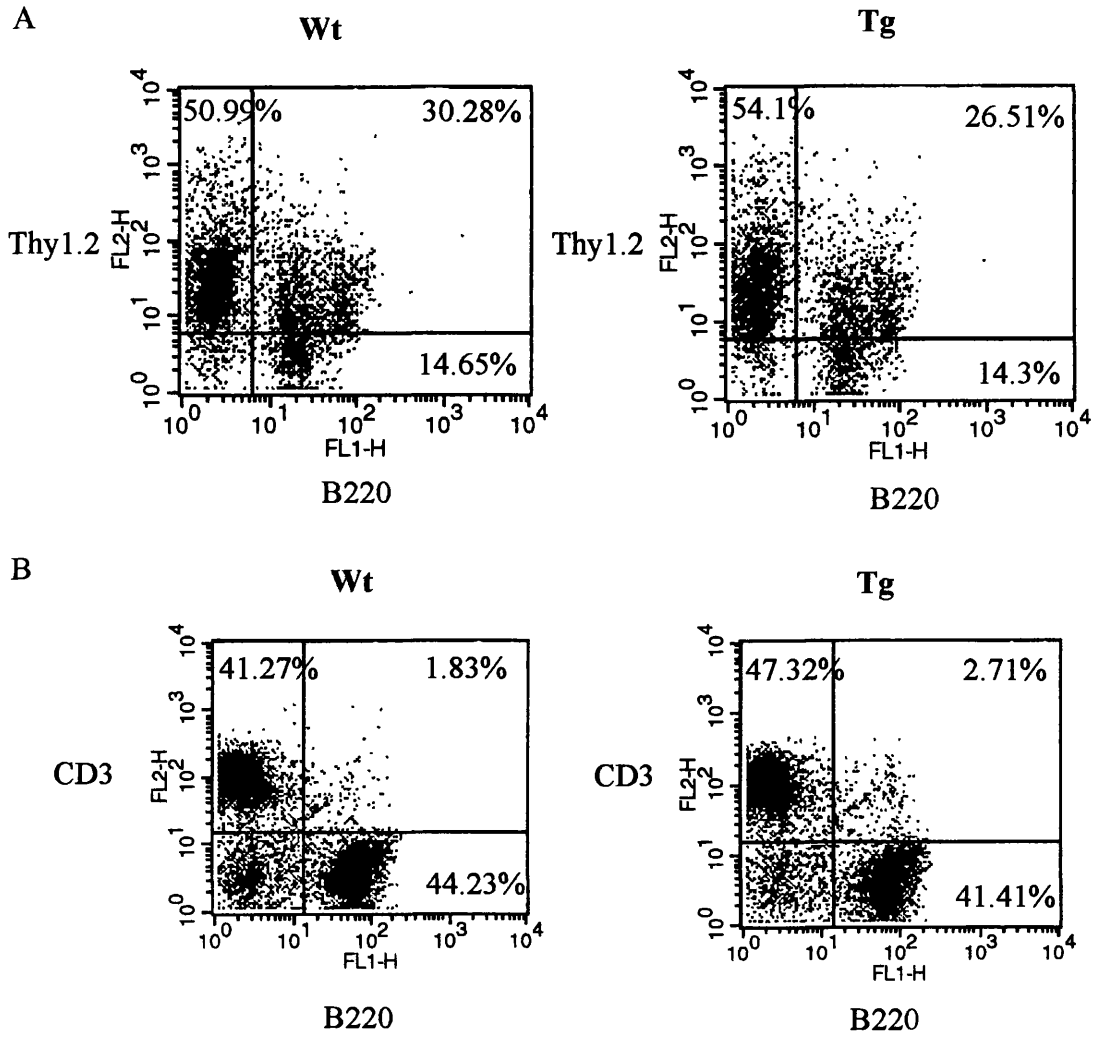

Figure 5.12: B and T cell proportions of line 127 animals

The spleen and bone marrow were collected from 3 positive and 3 negative siblings and separately pooled. Primary cells were isolated and 10^6 cells were stained with B220FITC and Thy1.2PE for the bone marrow cells (panel A) or with B220FITC and CD3PE for the splenocytes (panel B). For both panels, the results for the negative siblings (Wt) are shown on the left whereas the results for the transgenic positive animals (Tg) are presented on the right. The percentage of the cells in each quadrant is indicated.

Antibody name	Stage	In combination with	References
B220 (FITC or PE)	Pro-B to mature B and activated B	All the stains below	Coffman *et al.*, 1982 Hathcock *et al.*, 1992
CD3 (FITC or PE)	Mature T cells	B220, CD5, CD8 and CD4	Miescher *et al.*, 1989
CD5 (FITC or PE)	Subtype B1, Mature B	B220, CD3, CD23 and CD43	Luo *et al.*, 1992
CD43 (FITC)	Immature B also on B1 subtype	B220 and CD5	Gulley *et al.*, 1988 Wells *et al.*, 1994
CD23 (FITC)	Mature and activated B not on B1 subtype	B220 and CD5	Rao et al., 1987 Waldschmidt *et al.*, 1988 Waldschmidt *et al.*, 1992
sIgs (FITC) combination of IgA, IgM and IgG	Mature B	B220	
CD2 (FITC)	Pre-B to mature B and T	B220, CD3	Yagita *et al.*, 1989
Thy1.2 (PE)	Immature T	B220	Ledbetter *et al.*, 1979 Ledbetter *et al.*, 1980
CD4 (FITC or PE)	Mature T helper	CD3 and CD8	Dialynas *et al.*, 1983
CD8 (FITC)	Mature T killer	CD3 and CD4	Ledbetter *et al.*, 1980

Table 5.9: The different FACS antibodies used to determine the status of the B and T cells in animals from lines 127 and 131

This table presents the different FACS antibodies used along with their B or T cell expression pattern. The antibody used for co-staining is also given (in combination with).

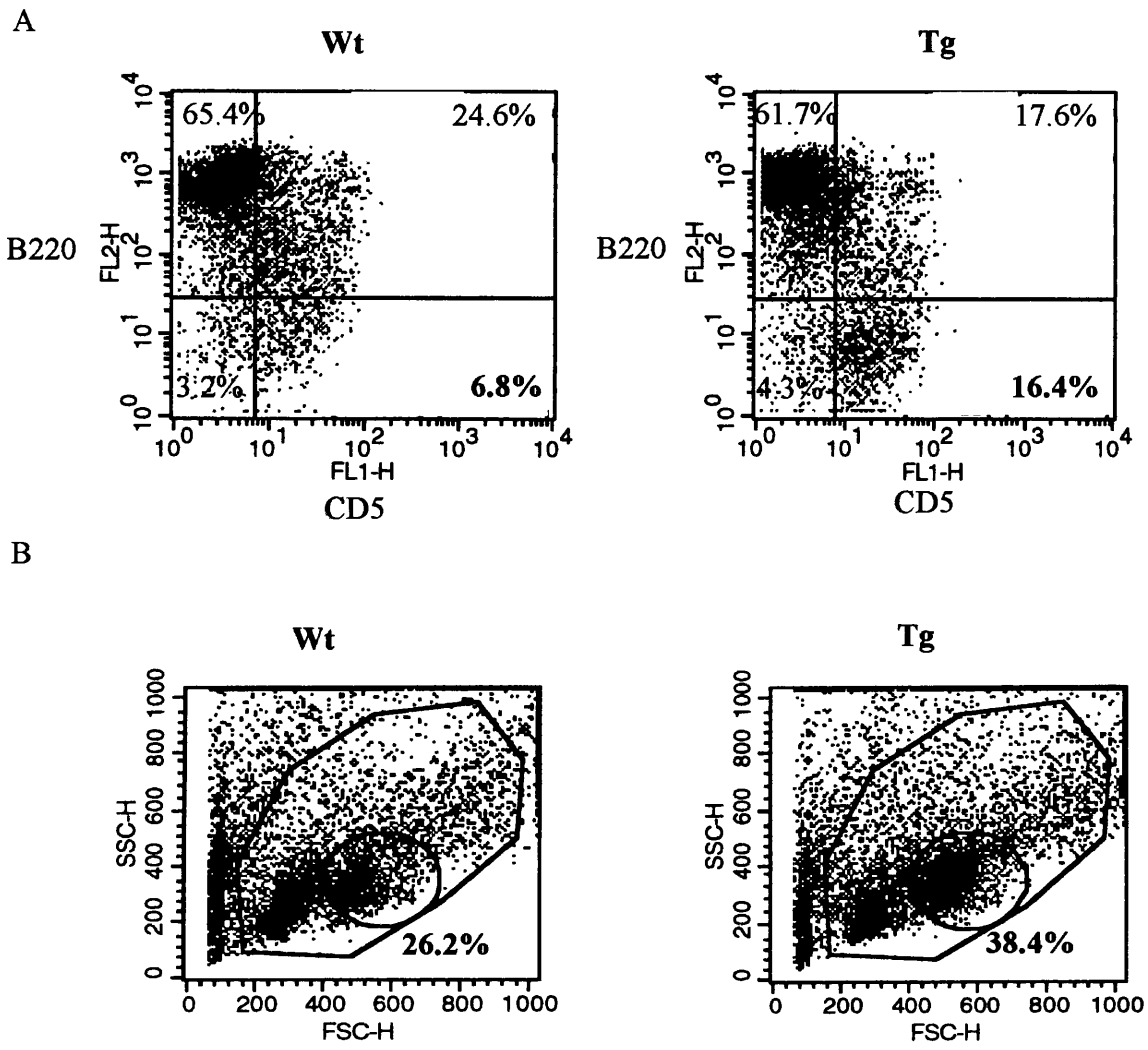

Figure 5.13: CD5FITC and B220PE stain of Peyer's patches from both positive and negative siblings of line 127

Peyer's patches were collected from 3 positive and 3 negative siblings and separately pooled. Primary cells were isolated and 10^6 cells were stained with CD5FITC and B220PE. Panel A shows the FL1 and FL2 channels, which is the repartition of the cells according to the stain. Panel B represents the forward and side scatter, which shows the size (forward scatter, FSC-H) and the granularity (side scatter SSC-H) of the cells. For both panels, the results for the negative siblings (Wt) are shown on the left whereas the results for the transgenic positive animals (Tg) are presented on the right.

5.4.1. Anti-IgM ELISA with serum from lines 127 and 131

The soluble form of IgM is secreted by mature activated B cells; therefore in order to determine if EBER1 modifies the activated status of the B cells or the secretion of soluble IgM, an ELISA was performed using an anti-IgM antibody on the serum of both positive and negative siblings from mice of lines 127 and 131 (Figure 5.14). For line 127 no differences were observed for the production of secreted IgM (P value = 0.91, two sample T test, Minitab software), suggesting that the presence of the transgene does not affect the secretion of this soluble antibody (Figure 5.14 A). For line 131, a lower average was observed for the transgenic positive sample compared to the wild-type sample; however this reduction is not statistically significant (P value = 0.41, two sample T test, Minitab software) (Figure 5.14 B). Moreover, it should be noted that for this line, only 5 serum samples have been used in each group. These data indicate that transgenic EBER1 expression does not affect IgM secretion. A similar assay was performed to monitor levels of soluble IgG1; however no results were obtained even for the standard curve. Due to time limitations this assay was not repeated.

5.4.2. Proteoplex murine cytokine array with serum from lines 127, 131 and 137

It has been reported that in BL cells the presence of EBER1 leads to an increase in IL10 expression and secretion (Kitagawa *et al.*, 2000). To determine if an increase in IL10 serum level is induced in EμEBER1 mice, an ELISA was performed using an anti-IL10 antibody on serum samples from mice of lines 127 and 131. However, several ELISA trials have been performed without success even using recombinant IL10 for the standard curve, suggesting that the antibody may not be sufficiently effective. Therefore the "Proteoplex" 16 well murine cytokine array kit from Novagen was used. It is a chip array, which allows comparison of the level of 10 murine cytokines including IL1α, IL1β, IL2, IL4, IL6, IL10, IL12, GMCSF, IFNγ and TNFα. The chip is composed of 16 wells and each well is spotted with four spots with the different antibodies and four spots of positive and negative controls (which are supplied with the kit). Eight alignment spots are also present and are used for the spot-finding software. The experiment was performed using 5 wells for a

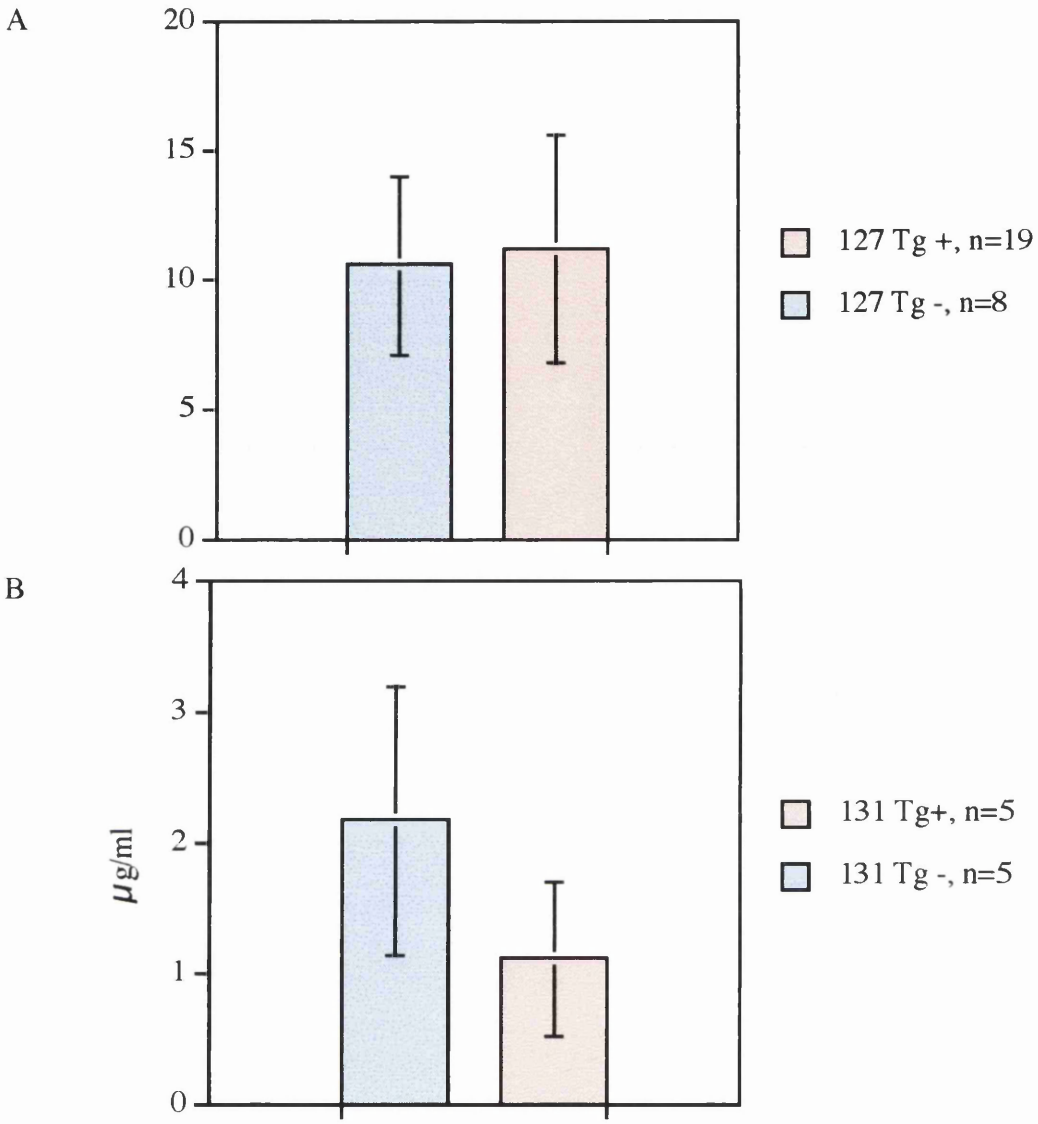

Figure 5.14: Results of the IgM ELISA for lines 127 and 131

Serum samples (diluted 1/800) from mice of lines 127 and 131 (positive and negative controls) were subjected to an ELISA using an anti-IgM antibody. Each sample was analysed in duplicate. Panel A shows the results for line 127 with 19 transgenic positive samples and 8 negative samples analysed and panel B shows the results for line 131 with 5 samples for both the transgenic positive and negative siblings. For both graphs the Y axis represents the cytokine concentration in µg/ml as determined using an IgM standard curve. The error bars show the standard error of the mean. The analysis was performed using Minitab and Cricket graph software. n represents the number of samples.

standard curve in order to obtain an estimate of the cytokine concentration for each serum sample. One well was left blank to measure the background signal for each cytokine. The remaining wells were used for the different serum samples, which were diluted 4 fold. A detection antibody cocktail was then added to each well and was followed by a fluorophore detection reagent (both supplied with the kit). The slide was rinsed and dried before being sent for scanning to Novagen. The experiment was performed once and in total 2 samples from line 127 young animals, 2 samples from line 131, 2 samples from line 137, 2 wild-type controls and 2 samples from line 127 tumour animals were used for the array (Table 5.10). The results show that no cytokines were dectected for the negative controls used, except for a low level of TNFα in sample 131.27. Similarly none of the cytokines present on the chip were detected in the serum of the transgenic positive samples of mice of line 131. However for mice of both lines 127 and 137, several cytokines were detectable in the sera tested. For line 127, IL4, IL6, IL10, IL12 and IFNγ levels were detected in both pre-tumour samples tested. It should be noted that the concentration of cytokines determined are very different between the two samples ranging from 5 to 10 fold difference. Moreover two additional cytokines were detected (IL1α and GMCSF) for sample 127.137 and not 127.136. Furthermore in the two 127 tumour serum samples two cytokines were detected, IL10 and the stress-induced cytokine TNFα. For each sample an additional cytokine was also detected, IL1α for sample 127.31 and IL6 for sample 127.37. For line 137, two cytokines were detected in both samples tested, IL6 and IFNγ and the concentrations detected were relatively similar. In sample 137.58, IL12 and TNFα were also detected. As only two samples were used from each line tested, this assay should be repeated with more samples in order to be able to draw any conclusions. Also, since for mice of line 131 (transgenic positive and negative) young animals were used, it is possible that more cytokines are secreted when the animals are older.

5.5. *In vivo* experiments using mice of lines 127 and 137

5.5.1. Does EBER1 block PKR action *in vivo*?

PKR is implicated in the IFN response following a viral infection and is activated by dsRNA (Goodbourn *et al.*, 2000). EBER1 was shown to block the IFN response in cultured cells by binding PKR and inhibiting its autophosphorylation (Nanbo *et al.*, 2002).

Line	131	131	131	131	127	127	137	137	127	127
ID	26	27	22	23	136	137	58	69	31	37
Age months	3	3	3	3	7	7	5	4	19	17
Tg status	-	-	+	+	+	+	+	+	+	+
Lymphoma	-	-	-	-	-	-	-	-	+	+
IL1α									14.9	
IL1β						22.6				
IL2										
IL4					124.6	899.6				
IL6					55.5	351.3	44.9	19		49.3
IL10					55.6	283			187.2	304
IL12					20.7	205.5	145.3			
GMCSF						14				
IFNγ					259.8	948.7	44.8	35.3		
TNFα		13.8					23		86	46.7

Table 5.10: Cytokine chip array summary table

The concentration of cytokine (in pg/ml) in the serum is presented in the table. No concentration value indicates that the data point was below the limit of detection. The animal number (ID), the age in months as well as the transgenic status (Tg status) is presented. Two of the serum samples were from mice that succumbed to lymphoma (as indicated).

Polyinosinic-polycytidylic acid (pIC) is a chemical which mimics dsRNA and is therefore often used in assays to induce an IFN response. In order to test if EBER1 can functionally block an IFN response *in vivo*, 200μg of pIC was injected in the tail vein of both positive and negative siblings of line 127 and line 137 (7 to 9 months old mice). Both positive and negative mice in the control groups were injected also with PBS as control. Each group was composed of three mice. For each animal, spleen, thymus and Peyer's patches were collected 18 hours post-injection; other tissues were collected if an abnormal phenotype was observed. Serum was collected one week before the injection and at the time of tissue collection. Proteins were extracted from spleen of both pIC and PBS injected mice of line 127 and the expression of several proteins involved in the IFN response was assessed by western blot. The first protein examined was PKR (line 127 spleen samples), due to its involvement in the primary phase of the IFN response. In response to dsRNA PKR becomes phosphorylated. Therefore both the level of total PKR and phospho-PKR was assessed by western blot (Figure 5.15). BJAB cells stimulated with IFNα for 24 hours were used as positive control for the induction of an IFN response. A strong band at 66kDa (the predicted size for PKR) was observed for BJAB on both the anti-phospho PKR blot (Figure 5.15 A) and also on the anti-total PKR blot (Figure 5.15 B). From the figure both the level of total PKR and activated PKR appear similar in mice treated with PBS or pIC for both the wild-type and the transgenic mice. The intensity of each band was normalised against the intensity of β-tubulin (Table 5.11). For the wild-type mice a slight increase in the average of both total PKR and phosphorylated PKR was observed following pIC treatment. For the transgenic positive mice, the level of total PKR remained the same and a very slight increase in the average phosphorylated PKR occurred following pIC treatment, which could be considered as negligible. For both the wild-type and the transgenic positive this assay needs to be repeated with an increased number of samples to determine if the results obtained are consistent and to be able to draw conclusions from them. Problems were previously encountered in the laboratory when using these antibodies with known controls; no signal was detected which suggested the use of these two antibodies was not very reproductible. Therefore, the western blot was stripped and reprobed with both anti-phospho eIF2α and anti-total eIF2α antibodies(Figure 5.16), which is a downstream target of PKR. eIF2α becomes phosphorylated upon PKR activation. A 40kDa band was expected for eIF2α and a single band at approximately 35-40kDa was observed using the anti-phospho eIF2α antibody (Figure 5.16 A) whereas several bands were observed using

	PBS/wt			pIC/wt			PBS/tg			pIC/tg			BJAB
P PKR	0.36	0.31	0.38	0.51	0.57	0.52	0.55	0.44	0.43	0.46	0.46	0.66	0.89
Av		0.35			0.53			0.47			0.53		
T PKR	0.58	0.46	0.47	0.74	0.6	0.67	0.57	0.61	0.72	0.47	0.53	0.83	1.92
Av		0.5			0.67			0.63			0.61		
Ratio	0.62	0.68	0.81	0.69	0.93	0.77	0.97	0.72	0.6	0.99	0.88	0.8	0.46
Av ratio		0.7			0.8			0.8			0.89		

Table 5.11: Normalisation data from the PKR western blots

The intensity of the bands on the PKR and phospho-PKR western blots and the βtubulin western blot were determined. The intensity values of either the PKR (T PKR) or phospho-PKR (P PKR) bands were divided by the βtubulin intensity value to give the normalised data. The ratio of phosphorylated PKR to total PKR was also calculated and shown. The average of the phospho-PKR and total PKR is shown in the row labelled Av. The average of the proportion is shown in the row labelled Av prop. The order of the samples is the same as on the westerns.

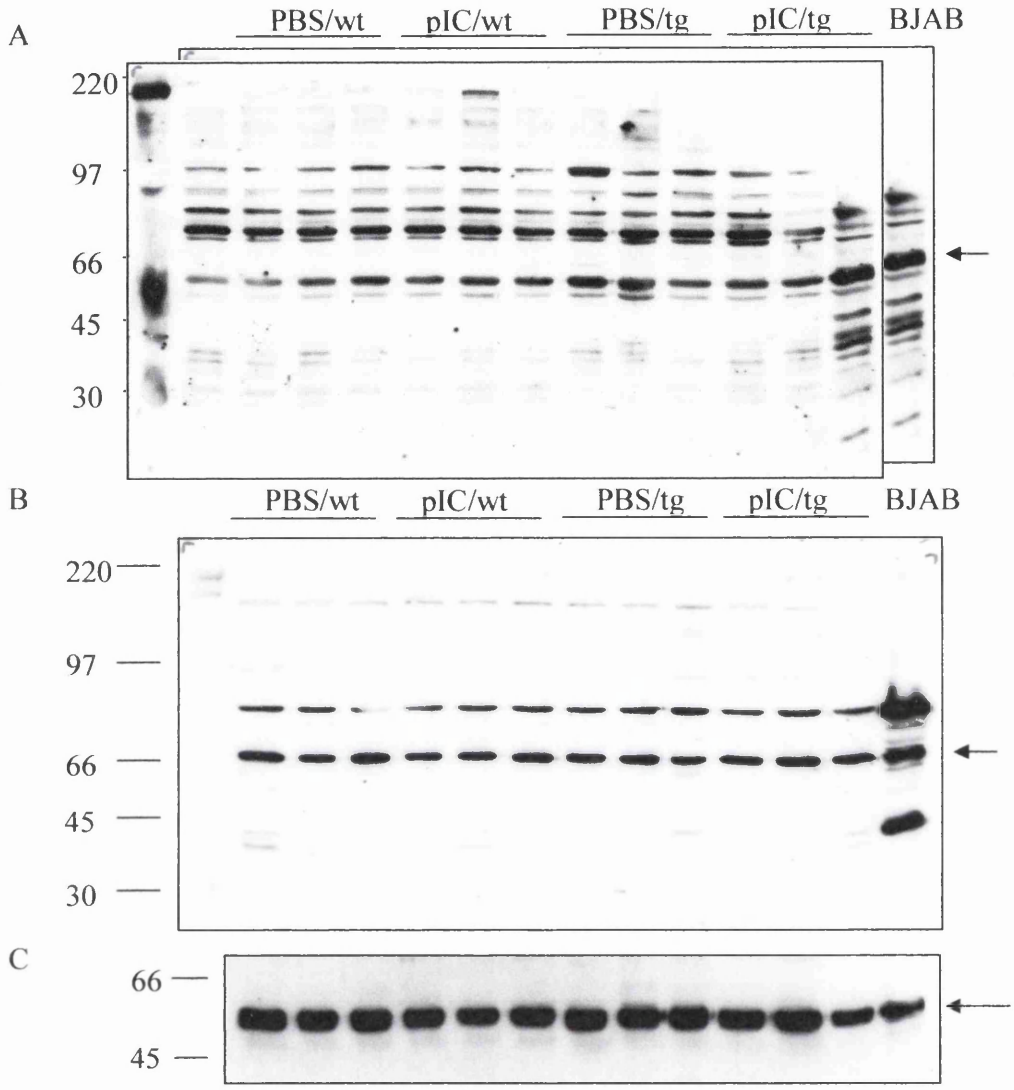

Figure 5.15: PKR expression and activation following pIC treatment in line 127 spleen

Protein from spleens of PBS or pIC injected transgene-positive (tg) or negative (wt) animals was extracted using the high salt nuclear extraction method. 100μg of protein per track was separated by 7.5% SDS-PAGE and the gel was western blotted. The membrane was probed with a rabbit anti-phospho PKR (panel A) antibody, followed by a goat anti-rabbit IgG-HRP secondary antibody and visualised using ECL+. The blot was then stripped and reprobed with a rabbit anti-total PKR (panel B) antibody and then with a rabbit anti-βtubulin (panel C) antibody. For both antibodies a goat anti-rabbit IgG-HRP secondary antibody was used and visualised using ECL+. The molecular weights (in kDa) according to the marker lane are shown. Both PKR and phospho PKR are 66kDa.

	PBS/wt			pIC/wt			PBS/tg			pIC/tg			BJAB
PeIF2α	0.25	0.34	0.38	0.4	0.59	0.51	0.19	0.31	0.35	0.44	0.41	0.49	0.98
Av		0.32			0.5			0.28			0.45		
TeIF2α	0.48	0.49	0.45	0.42	0.46	0.56	0.12	0.63	0.63	0.26	0.52	0.25	0.59
Av		0.47			0.48			0.46			0.34		
Ratio	0.52	0.7	0.83	0.96	1.3 *	0.91	1.57 *	0.49	0.55	1.72 *	0.78	1.95 *	1.64 *
Av ratio		0.68			1.06			0.87			1.5		

Table 5.12: Normalisation data from the eIF2α western blots

The intensity of the bands on the eIF2α and phospho-eIF2α western blots and the βtubulin western blot were determined. The intensity values of either the eIF2α (TeIF2α) or phospho-eIF2α (PeIF2α) bands were divided by the βtubulin intensity value to give the normalised data. The ratio of phospho-eIF2α to total eIF2α was also calculated and shown. The average of the phospho-eIF2α and total eIF2α is shown in the row labelled Av. The average of the proportion is shown in the row labelled Av prop. The order of the samples is the same as on the westerns. It should be noted that for the samples shown with an * the intensity value of phospho-eIF2α was much higher than that of eIF2α.

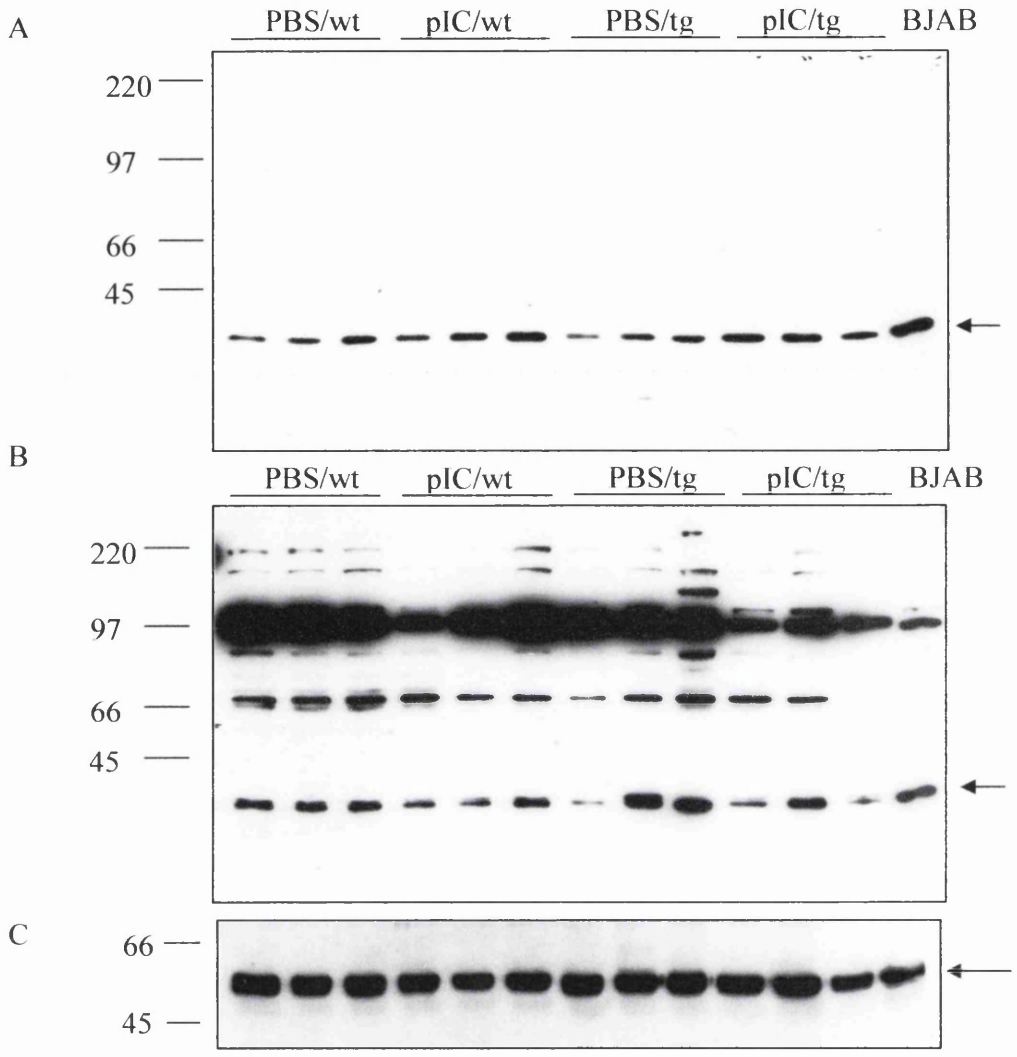

Figure 5.16: eIF2α expression and activation following pIC treatment in line 127 spleen

Protein from spleens of PBS or pIC injected positive (tg) or negative (wt) animals was extracted using the high salt nuclear extraction method. 100μg of protein per track was separated by 7.5% SDS-PAGE and the gel was western blotted. The membrane was probed with a rabbit anti-phospho eIF2α (panel A) antibody, followed by a goat anti-rabbit IgG-HRP secondary antibody and visualised using ECL+. The blot was then stripped and reprobed with a rabbit anti-total eIF2α (panel B) antibody and then with a rabbit anti-βtubulin (panel C) antibody. For both antibodies a goat anti-rabbit IgG-HRP secondary antibody was used and visualised using ECL+. The molecular weights (in kDa) according to the marker lane are shown. Both eIF2α and phospho eIF2α are 40kDa.

the anti- total eIF2α antibody (Figure 5.16 B). When the two blots were superimposed, phospho eIF2α migrated slightly more slowly than total eIF2α. The intensities of both total eIF2α and phospho eIF2α were determined and normalised against the intensity of β-tubulin (Table 5.12). An apparent increase in the level of phospho eIF2α was observed following pIC injection in the wild-type mice. However the amount of total eIF2α remained the same with and without pIC. Similarly for the transgenic positive mice an increase in phospho eIF2α level was noticed upon pIC injection, whereas a slight decrease in total eIF2α level was observed. Therefore eIF2α appears to be phosphorylated in both wild-type and transgenic positive mice following pIC injection. These results indicate that in the spleen of line 127 mice eIF2α was modified in both positive and negative pIC injected mice and therefore EBER1 does not appear to block this activation.

Stat1 is a protein which becomes activated following an IFN response and translocated in a complex into the nucleus to activate several genes (section 1.5.3). Therefore, the previous western blot was stripped and reprobed with an anti-total Stat1 antibody, and an anti-phospho Stat1 antibody (Figure 5.17). Two bands were observed for Stat1 and represent the two isoforms, Stat1α and Stat1β. For both the total Stat1 and the phospho Stat1 blots an increase was observed following pIC injection in both wild-type and transgenic positive mice. The intensity of the band from both isoforms was determined and normalised against the intensity of β-tubulin (Table 5.13). For the wild-type mice, a clear increase in both total Stat1α and β was observed as well as an increase in activated Stat1β following pIC injection. A very slight activation was observed for Stat1α when using the anti-phospho Stat1 tyr701 antibody whereas no increase was observed with the anti-phospho Stat1 ser 727 antibody. For the transgenic positive mice upon pIC injection, again a clear increase in both total Stat1α and β was observed as well as an increase in both activated Stat1α and β. These results first indicate that Stat1 induction and activation can be detected in the spleen samples following intravenous pIC injection and secondly suggest that EBER1 does not block Stat1 induction or activation. Thus no impact upon these branches of the IFN pathway by EBER1 was noted in the spleen of transgenic positive mice of line 127.

Another substrate of PKR is the specific inhibitor of NFκB, IκB. When PKR becomes phosphorylated it phosphorylates IκB by a mechanism involving NFκB inducing

	PBS/wt			pIC/wt			PBS/tg			pIC/tg			BJAB
P stat1α Ser 727	0.22	0.35	0.8	0.32	0.67	0.42	0.53	0.4	0.34	0.51	0.56		
Av		0.46			0.47			0.42			0.54		
Pstat1α tyr 701	0.41	0.37	0.56	0.53	0.54	0.51	0.33	0.37	0.31	0.6	0.67	6.48 *	
Av		0.45			0.53			0.34			0.64		
Pstat1β tyr 701	0.24	0.16	0.12	0.5	0.52	0.45	0.01	0.29	0.28	0.51	0.65	5.21 *	
Av		0.17			0.49			0.19			0.58		
Tstat1 α	0.43	0.33	0.58	0.89	0.94	0.97	0.42	0.2	0.23	1	0.54	5.3 *	
Av		0.45			0.93			0.28			0.77		
Tstat1β	0.18	0.1	0.24	0.96	1.14	0.88	0.19	0.46	0.2	0.82	0.44	0.73	
Av		0.17			0.99			0.28			0.66		

Table 5.13: Normalisation data from the Stat1 western blots

The intensity of the bands on the total Stat1, the two phospho-Stat1 and the βtubulin western blots were determined. The intensity values of the phospho Stat1α ser 727 (Pstat1α, ser 727), the phospho Stat1α tyr 701 (Pstat1α, tyr 701), the phospho Stat1β tyr 701 (Pstat1β, tyr 701), the total Stat1α isoform (Tstat1α) and the total Stat1β isoform (Tstat1β) bands were divided by the βtubulin intensity value to give the normalised data. The average for the different categories are shown in the rows labelled Av. The order of the samples is the same as on the westerns. It should be noted that no intensities were determined for the last two lanes of the western for some of the antibodies used. The values with a * sign were not taken into account to calculate the average.

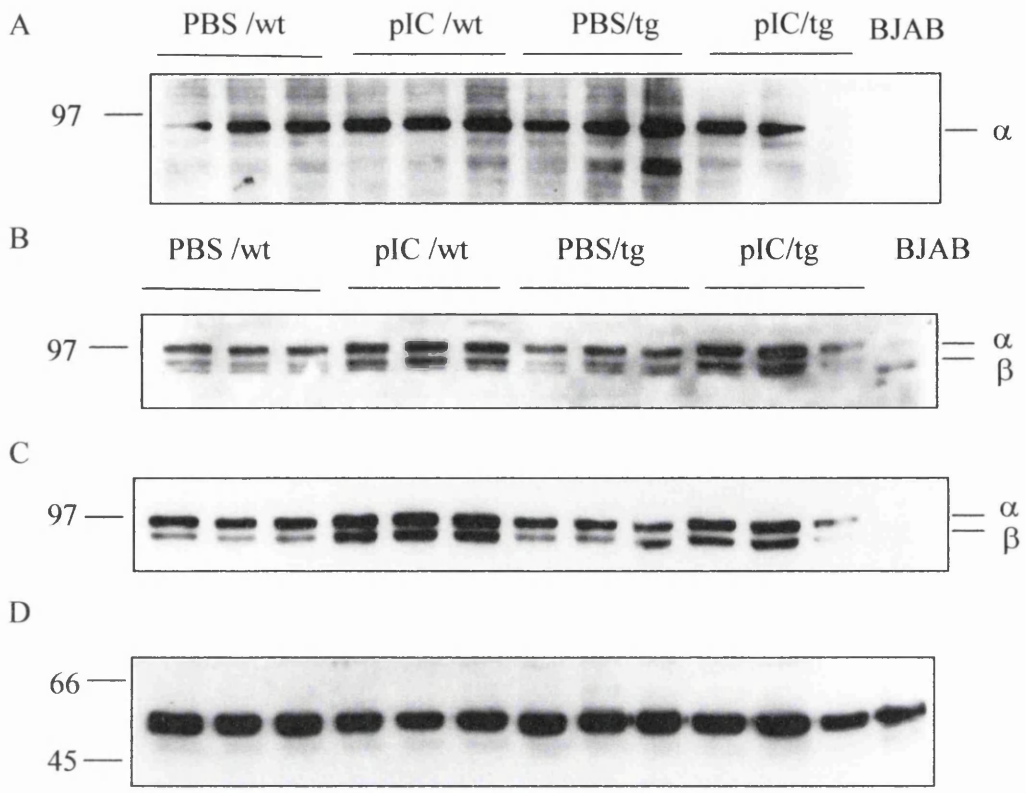

Figure 5.17: Stat1 expression and activation following pIC treatment in the spleen of line 127 mice

Protein from spleens of PBS or pIC injected positive (tg) or negative (wt) animals was extracted using the high salt nuclear extraction buffer. 100μg of protein per track was separated by 7.5% SDS-PAGE and the gel was western blotted. The membrane was probed with a rabbit anti-phospho Stat1 ser 727 (panel A) antibody, followed by a goat anti-rabbit IgG-HRP secondary antibody and visualised using ECL+. The blot was then stripped and reprobed with a rabbit anti-phospho Stat1 tyr 701 (panel B) antibody, followed by a goat anti-rabbit IgG-HRP secondary antibody. The blot was stripped and reprobed with a rabbit anti-total Stat1 (panel C) antibody and then with a rabbit anti-βtubulin (panel D) antibody. For both antibodies a goat anti-rabbit IgG-HRP secondary antibody was used and visualised using ECL+. The molecular weights (in kDa) according to the marker lane are shown. There are 2 isoforms of Stat1 α and β and their sizes are 97 and 84kDa. Anti-phospho Stat1 ser 727 antibody only recognises the Stat1α isoform whereas the anti-phospho Stat1 tyr 701 and the anti-total Stat1 antibodies recognise both isoforms.

kinase (NIK) and IκB kinase (IKK) (Zamanian-Daryoush *et al.*, 2000) which releases NFκB from IκB, leading to an increase in NFκB translocation to the nucleus and DNA binding. In order to examine this, an EMSA was performed using the spleen protein extracts and an NFκB nucleotide recognition oligo (Figure 5.18). The positive control used was an epithelial extract from a transgenic positive mouse line expressing LMP1 (line 117) which was previously shown to have an NFκB DNA binding activity (Charalambous, 2005 thesis). Two specific binding bands were observed for NFκB and were competed out when the 200x competitor was added. When comparing the intensities of the two specific bands, no differences were noticed between PBS and pIC injected animals in either the positive or the negative siblings. An Sp1 EMSA was performed using the same extracts to check the quality of the samples and the loading (Figure 5.19). Sample 117 may be of lower quantity or quality as no shift was observed using this extract. All the extracts appeared equally loaded on the first gel and of equal quality (Figure 5.19 A), whereas for the second gel the pIC/wt and the pIC/tg samples appeared underloaded. However, these extracts were used after multiple freeze-thaw cycles and therefore the samples could have been partially degraded by this process. This assay should be repeated to be able to draw any conclusions on the DNA binding activity of NFκB with these extracts. These preliminary results show no apparent increase in NFκB DNA binding activit, although with samples in gel B, if the Sp1 is lower, there may be an increase in NFκB. These results show that no increase in NFκB DNA binding activity upon pIC treatment was observed. Despite lack of induction by pIC an increase of phospho eIF2α and Stat1 was observed with pIC injection. This indicates that the pIC reached the spleen collected. However, eIF2α and Stat1 were also activated in transgenic positive mice upon pIC injection suggesting that EBER1 in this assay did not block the induction of this arm of the IFN response. This could be due to the low expression of EBER1 in the spleen in these mice.

Therefore as both mice of lines 127 and 137 express EBER1 at a higher level in the thymus, proteins were then extracted from this tissue of both pIC and PBS injected mice and the expression of total Stat1 and phosphorylated Stat1 was analysed at the time of writing (Figures 5.20 and 5.21). For line 127, if the non-specific band indicated is used to reflect the sample loading, an increase was observed in total Stat1 in the wild-type samples following pIC treatment, as well as for Stat1α activation. For the transgenic positive animals, there was no increase in either Stat1 expression (both isoforms) or activation

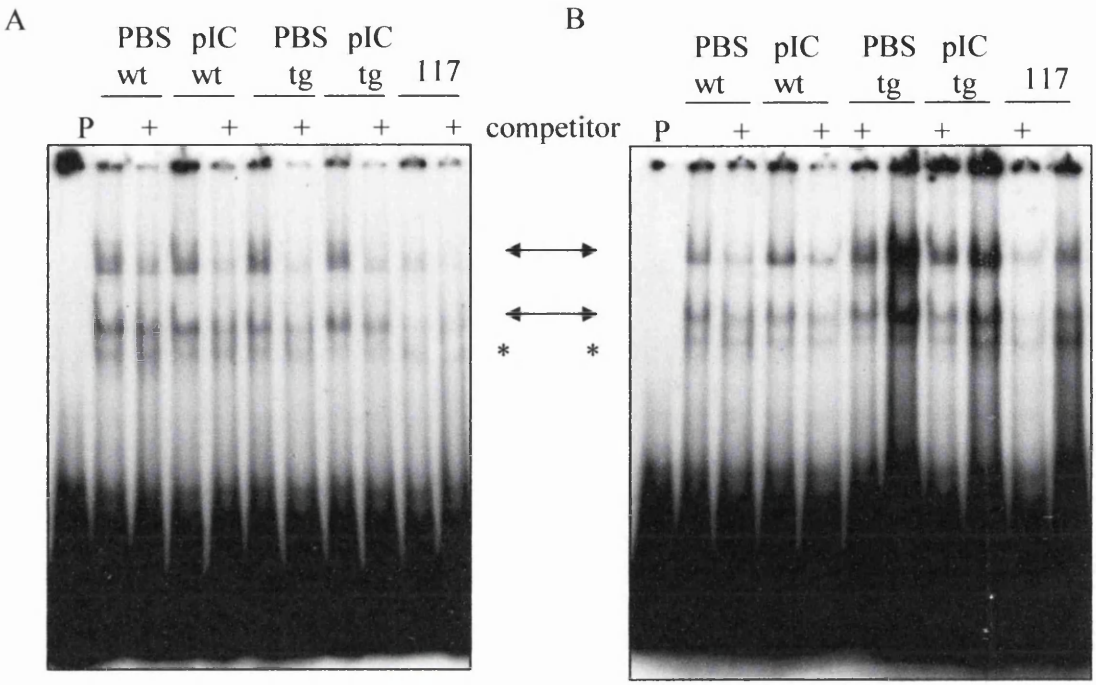

Figure 5.18: EMSA showing binding activity of NFκB in extracts from pIC or PBS treated positive or negative line 127 mice

Proteins were extracted from spleens of PBS or pIC injected positive (tg) or negative (wt) animals using the high salt nuclear extraction buffer. 10μg of protein extract was used for each sample. A hyperplastic epithelial tissue extract was used as positive control (117). Two reactions were prepared for each sample: one without and one with 200x unlabelled competitor. Labelled NFκB oligo was added to each sample and incubated for 20 minutes on ice before loading the samples on to a 6% polyacrylamide gel. A labelled oligo without extract was also used as control (P). The gel was electrophoresed for 3 hours before being dried and exposed to film for the required amount of time. Panels A and B are gels with different samples except for the 117 control. The double arrows indicate the specific binding bands. The * indicates a non-specific band.

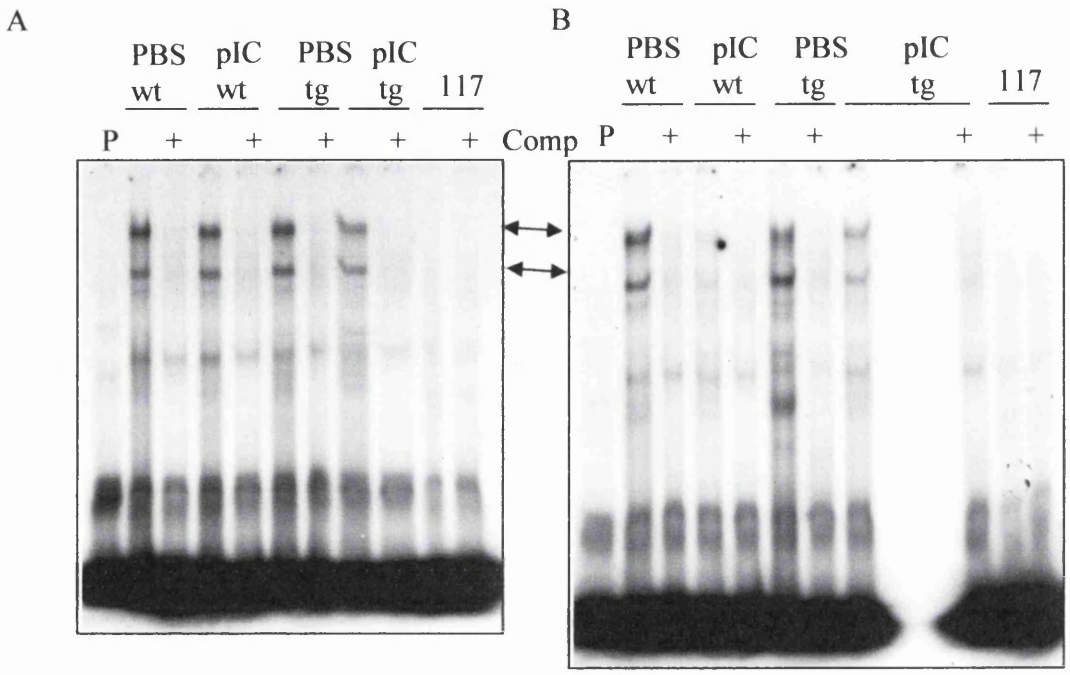

Figure 5.19: EMSA showing binding activity of Sp1 in extracts from pIC or PBS treated positive or negative line 127 mice

Proteins were extracted from spleens of PBS or pIC injected positive (tg) or negative (wt) animals using the high salt nuclear extraction buffer. 10μg of protein extract was used for each sample. A hyperplastic epithelial tissue extract was used as positive control (117). Two reactions were prepared for each sample: one without and one with 200x unlabelled competitor (Comp). Labelled Sp1 oligo was added to each sample and incubated for 20 minutes on ice before loading the samples on to a 6% polyacrylamide gel. A labelled oligo without extract was also used as control (P). The gel was electrophoresed for 3 hours before being dried and exposed to film for the required amount of time. Panels A and B are gels with different samples except for the 117 control. The samples on panel A are the same as the samples on panel A from figure 5.18 and the samples from panel B are the same as the samples on panel B from figure 5.18. The double arrows indicate the specific binding bands.

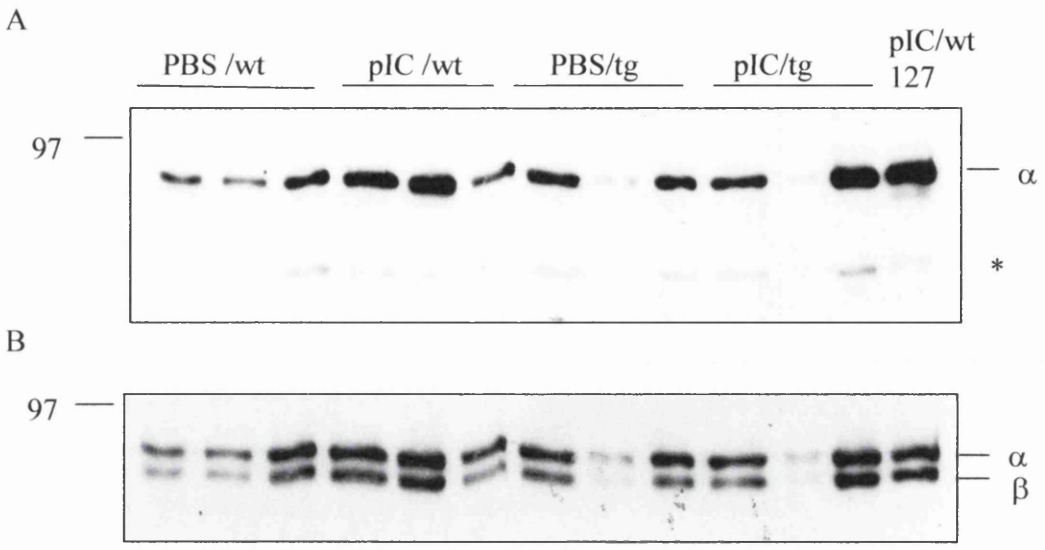

Figure 5.20: Stat1 expression and activation following pIC treatment in the thymus of line 127 mice

Protein from thymuses of PBS or pIC injected positive (tg) or negative (wt) animals was extracted using the high salt nuclear extraction buffer. 100μg of protein per track was separated by 7.5% SDS-PAGE and the gel was western blotted. Extract pIC/wt from the spleen of mice of line 127 was used as a positive control. The membrane was probed with a rabbit anti-phospho Stat1 Ser 727 (panel A) antibody, followed by a goat anti-rabbit IgG-HRP secondary antibody and visualised using ECL+. The blot was stripped and reprobed with a rabbit anti-total Stat1 (panel B) antibody followed by a goat anti-rabbit IgG-HRP secondary antibody and visualised using ECL+ The molecular weights (in kDa) according to the marker lane are shown. There are 2 isoforms of stat1 α and β and their sizes are 97 and 84kDa. Anti-phospho Stat1 Ser 727 antibody only recognises the Stat1α isoform whereas the anti-total Stat1 antibody recognises both isoforms. The * sign indicates a non-specific band which could reflect the loading of the samples.

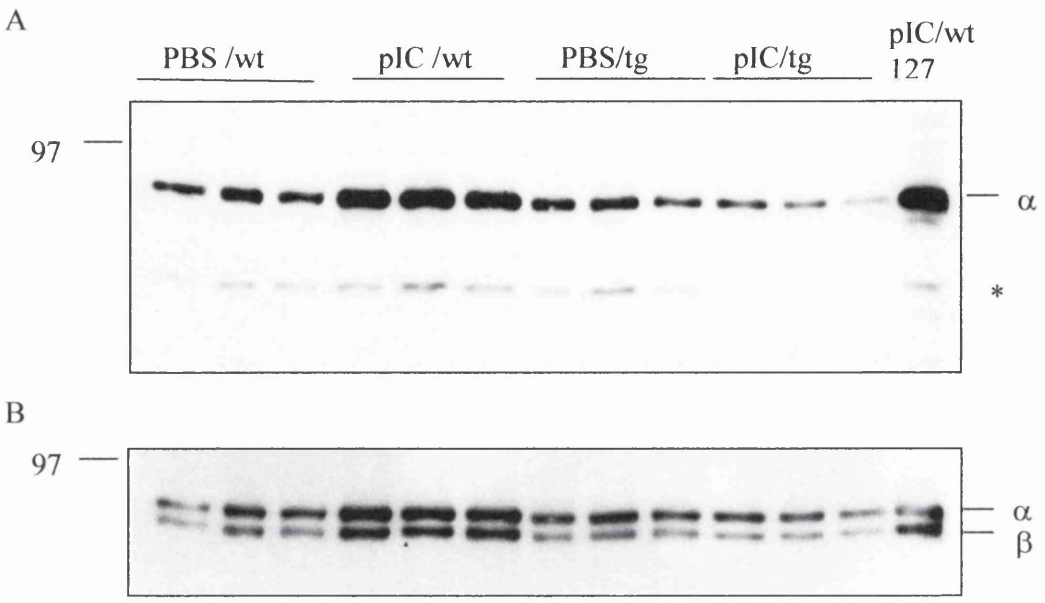

Figure 5.21: Stat1 expression and activation following pIC treatment in the thymus of line 137 mice

Protein from thymuses of PBS or pIC injected positive (tg) or negative (wt) animals was extracted using the high salt nuclear extraction buffer. 100μg of protein per track was separated by 7.5% SDS-PAGE and the gel was western blotted. Extract pIC/wt from the spleen of mice of line 127 was used as a positive control. The membrane was probed with a rabbit anti-phospho Stat1 Ser 727 (panel A) antibody, followed by a goat anti-rabbit IgG-HRP secondary antibody and visualised using ECL+. The blot was stripped and reprobed with a rabbit anti-total stat1 (panel B) antibody followed by a goat anti-rabbit IgG-HRP secondary antibody and visualised using ECL+ The molecular weights (in kDa) according to the marker lane are shown. There are 2 isoforms of Stat1 α and β and their sizes are 97 and 84kDa. Anti-phospho Stat1 Ser 727 antibody only recognises the Stat1α isoform whereas the anti-total Stat1 antibody recognises both isoforms. The * sign indicates a non-specific band which could reflect the loading of the samples.

following pIC injection, again if the non-specific band is used as loading control (the third pIC/tg sample appears overloaded compared to the first one). This blot should be re-probed with anti-β-tubulin to check the loading more accurately and tested for anti-phospho Stat1 (tyr 701). For line 137, a similar pattern was observed. An increase in total Stat1 (both isoforms) and in Stat1α activation following pIC treatment was observed in wild-type mice, suggesting that the pIC reached the thymus. For the transgenic positive samples, no increase in expression of Stat1 or activation of Stat1α was observed. However these samples appear to be underloaded, as judged by the non-specific band, and therefore it is important to confirm this finding. If confirmed these results would suggest that in the thymus of mice of lines 127 and 137 treated with pIC, EBER1 blocks the induction of Stat1 expression and its activation (of at least the α isoform), which might reflect the higher level of EBER1 expression in the thymus compared to the spleen.

5.5.2. Treatment of lines 127 and 137 splenocyte and thymocyte explants with pIC and IFNα

In order to stimulate the cells directly with pIC and IFNα, an explant of splenocytes and thymocytes was performed. It was hypothesised that this assay might show a more pronounced IFN response by treating the cells directly and possibly reveal any EBER1 effect. Spleen and thymus were chosen as they are larger tissues and therefore have more cells than lymph nodes or Peyer's patches. In addition the thymus was expressing EBER1 at a comparatively high level in lines 127 and 137. Spleen and thymus were collected from six transgenic positive mice of each line, 127 (7-10 months of age) and 137 (4 months of age) and from six wild-type controls. The phenotypes of these mice were described in tables 5.2 and 5.3. Other tissues were collected if a phenotype was observed. This was followed by primary cell isolation. In figure 5.22 a schematic diagram of the experiment is presented. Each group of six animals was divided into three independent subgroups as two tissues were pooled together in each subgroup to provide sufficient cells for the assay. The cells were then counted and from each subgroup $1x10^7$ cells were plated into each of three wells of a 24 well plate in 1ml of medium. Each well was subjected to a different treatment. To the first of the three wells PBS was added and used as a negative control, 200μg of pIC was added to the second well and 1000U of IFNα was added to the third well. The cells were incubated for 18 hours at 37°C before being harvested. At the time of

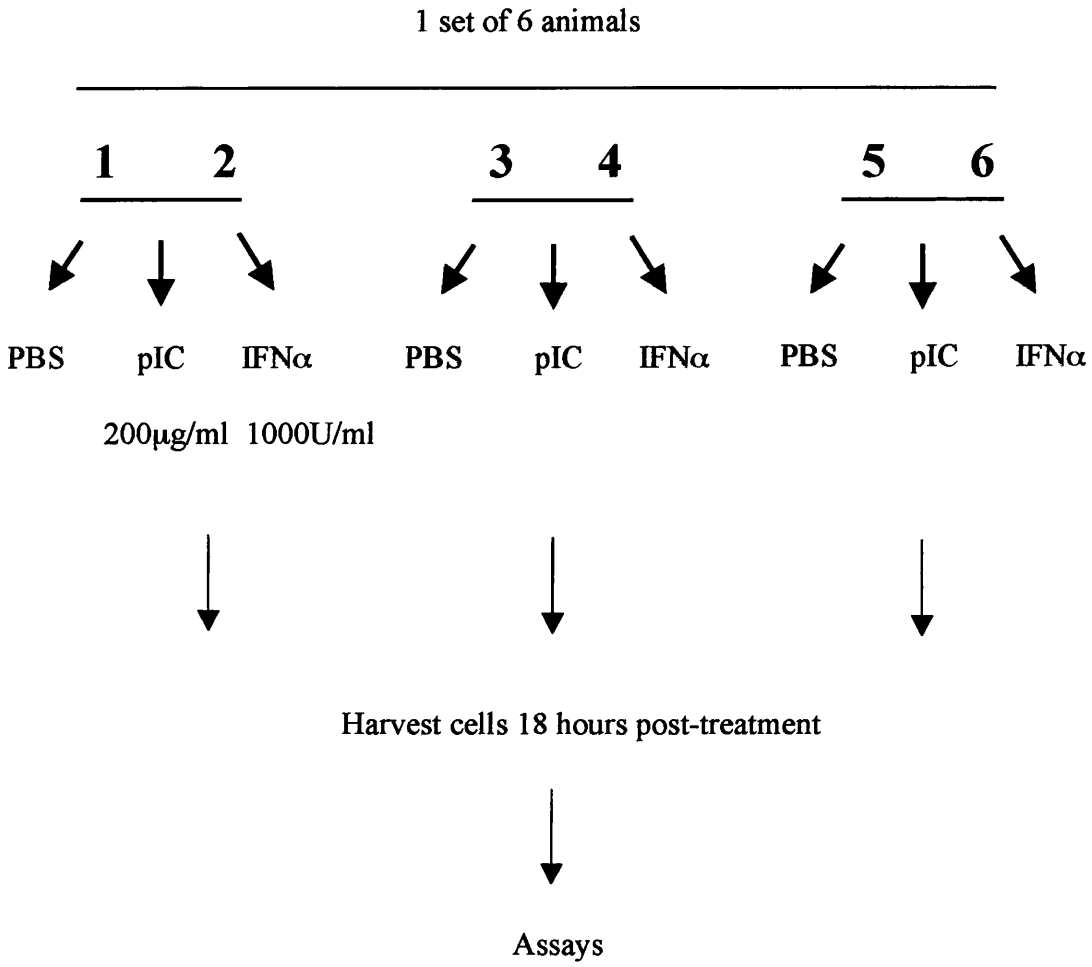

Figure 5.22: Schematic diagram of the design of the splenocytes and thymocytes explant of lines 127 and 137

Only 1 set of six animals is represented and the animals are numbered 1 to 6. Two animals from each set were pooled together leaving three independent groups. For each group cells were plated on a 24 well plate and PBS (control), pIC or IFNα was added. The cells were placed at 37°C and 5% CO_2. The cells were harvested after 18 hours. This assay was performed with splenocytes and thymocytes.

writing the extractions had not been performed and therefore no results can be presented on this part.

5.6. Summary

In this chapter the phenotype of the different lines and particularly of line 127 was presented. Several mice of line 127 developed a lymphoma phenotype and early signs of lymphoid expansion were also observed in younger mice of this line. One animal from line 131 also developed a lymphoma. Several mice of lines 136, 137 and 145 have shown early signs of lymphoid expansion and pathology.

Analysis of several tumour tissues from mice of line 127 has revealed that the tumours were of B cell origin. No increase in EBER1 expression was detected in the EBER1 tumours. No increase or loss of c-Myc, p53 or Rb expression was observed in the tumour samples. No rearrangements of the c-Myc locus were observed in the line 127 tumours. However, this will not reveal if a translocation or trisomy has occurred. The Myc DNA binding activity was also analysed by EMSA in two tumour samples and appeared stronger. Furthermore, two additional bands were observed in one of the tumour sample (number 49) tested. This suggested that in this tumour sample other protein complexes have been activated and bind the Myc oligo. In addition, tumour 127.49 did not show an upregulation of Id2 whereas the tumour sample 127.37 did. The mechanism of tumour formation in line 127 is unknown.

For both lines 131 and 127, no differences were observed in the B and T cell proportions between transgenic and wild-type mice. For line 131, no differences were observed in the status of the B and T cells. A similar result was seen for line 127, except for an increased CD5+ cell population, possibly a B1 population, in the Peyer's patches of transgenic positive mice. No differences were observed in the serum of lines 127 or 131 for IgM secretion. None of the cytokines tested in the Proteoplex chip array were upregulated in the serum of line 131. For lines 127 and 137 several cytokines were present at higher levels including IL4, IL6, IL10, IL12 and IFNγ. Whether this represents a consistent induction is yet to be confirmed.

In vivo experiments to monitor the response to dsRNA were performed in lines 127 and 137 with pIC injection. In the spleen from line 127 mice eIF2α and Stat1 and possibly PKR were activated following pIC injection, whereas NFκB binding activity was unchanged. This suggests that EBER1 in this tissue does not block this part of the IFN response following pIC treatment. However for Stat1 an observation was made using the thymus of mice of lines 127 and 137. An upregulation of total Stat1 and activation was observed in wild-type animals following treatment with pIC, whereas no increase in Stat1 expression or activation was observed in the transgenic positive samples. Therefore in the thymus of these mice, EBER1 may be blocking Stat1 expression/induction and activation following pIC treatment, by as yet unknown mechanism and yet to be confirmed.

Chapter 6. Cooperation study between EBER1 and EBNA1 or Myc

6.1. Introduction

Burkitt's lymphoma (BL) is one of the malignancies associated with EBV (Magrath, 1990, for review). In BL, EBNA1 and the EBERs are the only latent genes to be consistently expressed. BL is also characterised by a *c-myc* translocation to an immunoglobulin locus (usually IgH) leading to de-regulated expression of c-Myc in the B cells. In order to examine if EBER1 cooperates with either Myc or EBNA1 in lymphomagenesis, crosses were undertaken between EμEBER1 and Eμ-EBNA1, EμN-myc or Eμc-myc mice. If cooperation occurs, the phenotype may arise faster or be altered in some way in the bi-transgenic mice. The generation of the different bi-transgenic mice and the bi-transgenic data are presented in this chapter.

6.2. Does EBER1 cooperate with EBNA1 in lymphomagenesis?

A cross-breeding programme was started by breeding mice of EμEBER1 line 127 with mice of EμEBNA1 line 26 (Wilson *et al.*, 1996). The genetic status of the offspring was determined by Southern blotting, probing with both EBNA1 and EBER1 at the same time as they show a distinguishable pattern (representative examples shown in figure 6.1). From this blot, mice numbered 26127.3, 6, 8, 9 and 10 were negative, mice numbered 26127.4, 7 and 13 were EBNA1 positive, mouse number 26127.12 was EBER1 positive and mice numbered 26127.5 and 11 were bi-transgenic. A summary of the number of animals used in this study and their genetic status is presented in table 6.1. The animals were monitored weekly for any sign of phenotype. Once the appearance of lymphoma (mainly observed by an enlargement of the abdomen for the EBNA1 animals) was detected, the mice were euthanised and tissues were collected. The observed phenotype was the same in both the EBNA1 mice and the bi-transgenic EBER1/EBNA1 mice and was described previously (Wilson *et al.*, 1996). A Kaplan Meier plot to explore a possible cooperation between EBER1 and EBNA1 is shown in figure 6.2. In the time frame of this study only one EBER1.127 mouse developed a lymphoma at 310 days, whereas none of

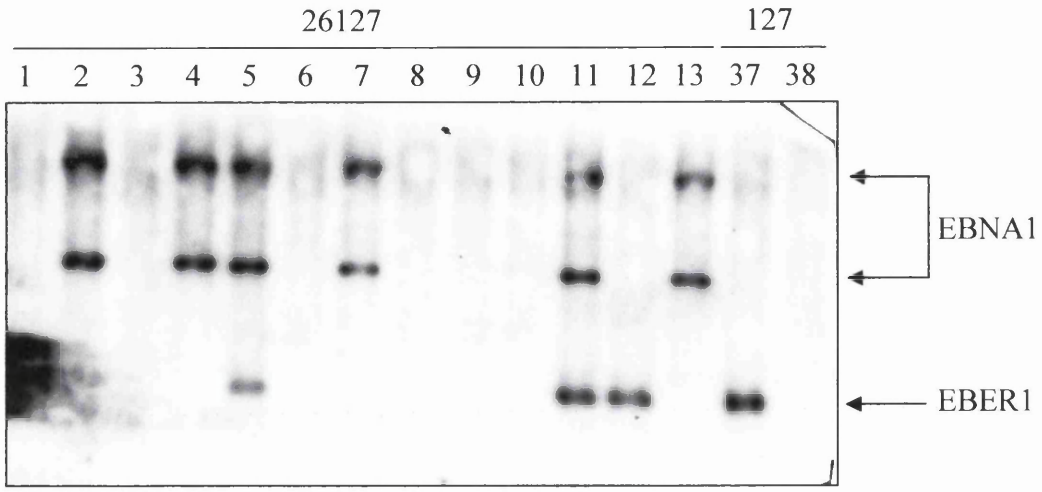

Figure 6.1: Southern blot from EBNA1 (line 26) and EBER1 (line 127) cross-breeding programme

Line 127 transgenic positive mice were crossed with line 26 transgenic positive mice. The offspring were genotyped as described in the materials and methods section. 5µg of gDNA was digested with *Eco*RI and the products electrophoresed through a 0.8% agarose gel and Southern blotted. The Southern blot was hybridised with both EBER1 and EBNA1 radiolabelled probes at 60°C in Church buffer. A final hot wash was performed at 60°C. The numbers shown above the tracks are the animal numbers either from line 127 or from the 26x127 cross. Number 127.37 was used as positive control and number 127.38 was used as negative control for EBER1. Numbers 26127.1 and 26127.2 were used as negative and positive controls for EBNA1 respectively. The EBNA1 and EBER1 bands are indicated with arrows. Note that the strong signal in lane 26127.1 is not EBER1 as this mouse is negative for EBER1, but is a blot artifact.

Transgene	Number of animals
EBNA1	9
EBER1	6
EBNA1 and EBER1	8
Negative	7

Table 6.1: Summary of the 26127 cross-breed

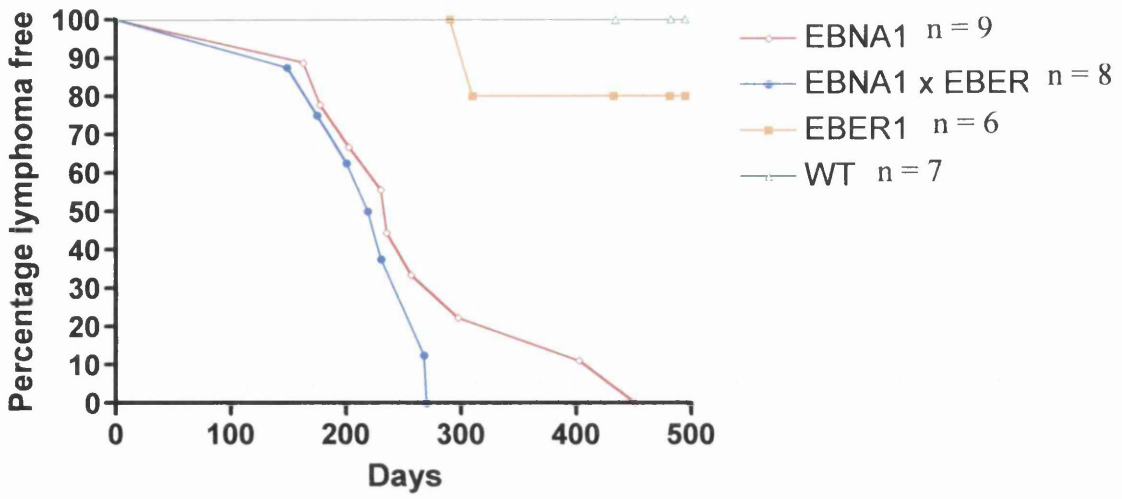

Figure 6.2: Kaplan Meier survival curve of line 26127 mice

The graph shows the proportion of mice succumbing to lymphoma (Y axis) over time (X axis). The graph was generated and the data analysed for statistical significance with a log rank test using Graphpad Prism 4 software.

the negative control mice developed lymphoma. While the EBNA1.26 mice and the bi-transgenic.26127 mice developed lymphoma at a similar rate initially, all bi-transgenic mice had succumbed to lymphoma by the age of 270 days, while a tail of EBNA1.26 showed a longer survival period up to 452 days. The median age is similar between the EBNA1.26 and the bi-transgenic.26127 animals with 236 days and 225 days respectively. The P value between the bi-transgenic.26127 and the EBNA1.26 curves is 0.2627, which demonstrates that the difference between the two curves is not statistically significant. These results suggest that EBER1 and EBNA1 do not cooperate in lymphomagenesis *in vivo* in our transgenic system. However, the absence of a tail in the curve of the bi-transgenic mice compared to that of the EBNA1.26 mice may suggest an additive effect between the effects of the two genes. The tail might also suggest that if a larger study was conducted a difference could be revealed between EBNA1.26 mice and bi-transgenic.26127 mice.

6.3. Does EBER1 cooperate with N-myc in lymphomagenesis?

6.3.1. Generation of EμEBER1 and EμN-myc bi-transgenic mice

At the start of this study the Eμc-myc mice were no longer available in the laboratory and had to be imported from the Jackson laboratory. However, the EμN-myc animals were present in the laboratory colony and it is published that N-myc can replace most of c-Myc's functions (Malynn *et al.*, 2000). Moreover, when N-myc is overexpressed in B cells in transgenic mice, the phenotype is similar to that of Eμc-myc animals with the only difference being the delayed tumour onset (Dildrop *et al.*, 1989, Adams *et al.*, 1985). Therefore a cross-breeding study was undertaken between EμEBER1 lines 127 and 137 and EμN-myc line 96 (Dildrop *et al.*, 1989) mice. It should be noted that for this study the parental mice were from different strains, the EBER1 mice were in a C57Bl/6 background (as described in Chapter 3) whereas the N-myc mice were in a Balb/c background. However, all the offspring issuing from the crosses were identical in their genetic background as they were all F1 of C57Bl/6 and Balb/c strains and therefore the offspring could be directly compared to each other. The genetic status of the offspring from these crosses was determined by Southern blotting (a representative example is shown in figure 6.3). From this blot, mice numbered 96127.3, 4, 6, 10 and 15 were N-myc positive, mice

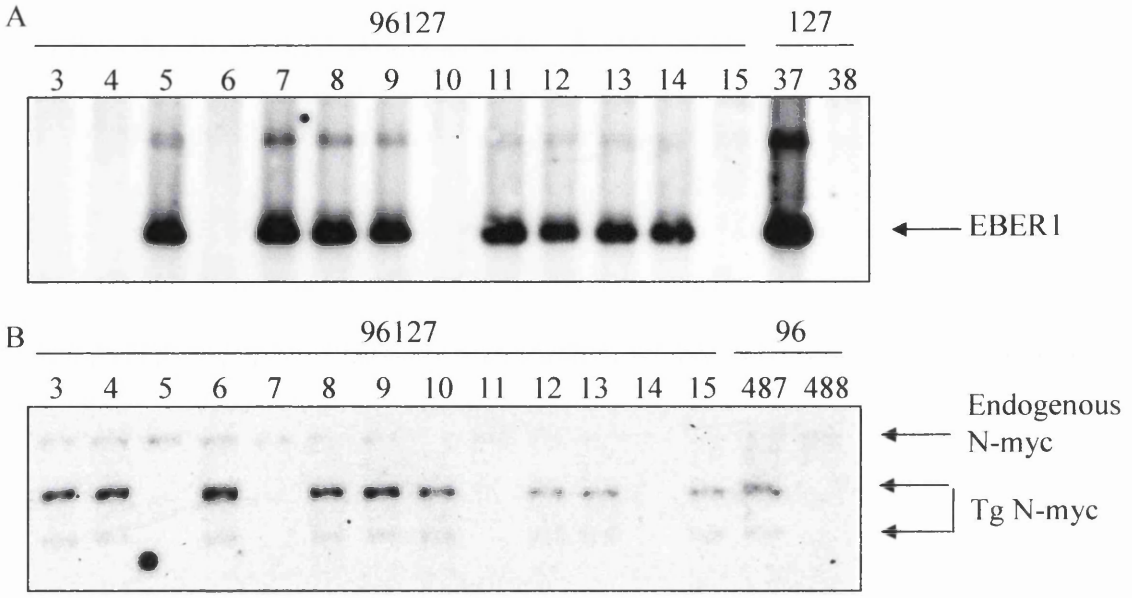

Figure 6.3: Southern blot from N-myc (line 96) and EBER1 (line 127) cross-breeding programme

Line 127 transgenic positive mice were crossed with line 96 transgenic positive mice. The offspring were genotyped and 5µg of gDNA was digested either with *Eco*RI (for EBER1) or with *Bam*HI (for N-myc). The digestion products were electrophoresed through a 0.8% agarose gel for the *Bam*HI products or through a 1% agarose gel for the *Eco*RI products and Southern blotted. The Southern blot was hybridised with either EBER1 radiolabelled probe at 60°C or N-myc radiolabelled probe at 65°C in Church buffer. A final hot wash was performed at 60°C (for EBER1) or at 65°C (for N-myc). Panel A shows the EBER1 blot and panel B shows the N-myc blot. The numbers shown above the tracks are the animal numbers either from lines 127 and 96 or the 96x127 cross. Number 127.37 was used as positive control and number 127.38 was used as negative control for EBER1. Numbers 96.487 and 96.488 were used as positive and negative controls for N-myc respectively. The endogenous N-myc, transgenic N-myc and EBER1 bands are indicated with arrows.

numbered 96127.5, 7, 11 and 14 were EBER1 positive and mice numbered 96127.8, 9, 12 and 13 were bi-transgenic. No 96127 negative mice were identified from this blot. A representative example of the genetic status of the 96137 offspring is also shown in figure 6.4. From this blot, mice numbered 96137.16, 18, 19 and 20 were N-myc positive, mouse number 96137.21 was EBER1 positive, mice numbered 96137.17 and 22 were bi-transgenic and mouse number 96137.23 was negative. A summary of the number of animals used in the 96127 and the 96137 studies and their status is presented in tables 6.2 and 6.3.

6.3.2. Phenotype and survival of the bi-transgenic EBER1/N-myc mice

The animals were monitored weekly for any sign of phenotype. Once the appearance of lymphoma (mainly observed by an enlargement of the peripheral lymph nodes in the N-myc animals) was detected, the mice were euthanised and tissues were collected. Tissues were also placed in formalin for subsequent histo-pathological analysis. Figure 6.5 shows a comparison between a wild-type mouse, an EBER1 127 positive mouse and an EBER1/N-myc bi-transgenic mouse, when the latter two developed lymphoma at 19 and 12 months of age respectively. For the bi-transgenic animal a clear enlargement of all the lymph nodes was observed as well as an expansion of the spleen, whereas for the EBER1 animal the spleen was enlarged and infiltrated and only the mesenteric lymph nodes were very enlarged (as described in Chapter 5). In the EBER1 mouse it was also noticed that the thymus was enlarged (not shown). For both animals (127 and 96127) the Peyer's patches were double the size of a wild-type Peyer's patch. These results indicate that the phenotype of the bi-transgenic mice resembles that of the Eμ N-myc mice which was described by Dildrop *et al* (1989) and observed in the N-myc mice in this study. From this study it was also noticed that the Eμ N-myc mice have a biphasic phenotype. The first phenotype is characterised by a thymoma (and previously noted for line 96 by Mark Drotar in the laboratory, unpublished observation) and the animals succumb at an early age whereas for the second type the animals succumb to expanded lymph nodes when older than 8 months of age, which is characteristic of the myc phenotype in B cells (shown in figure 6.5).

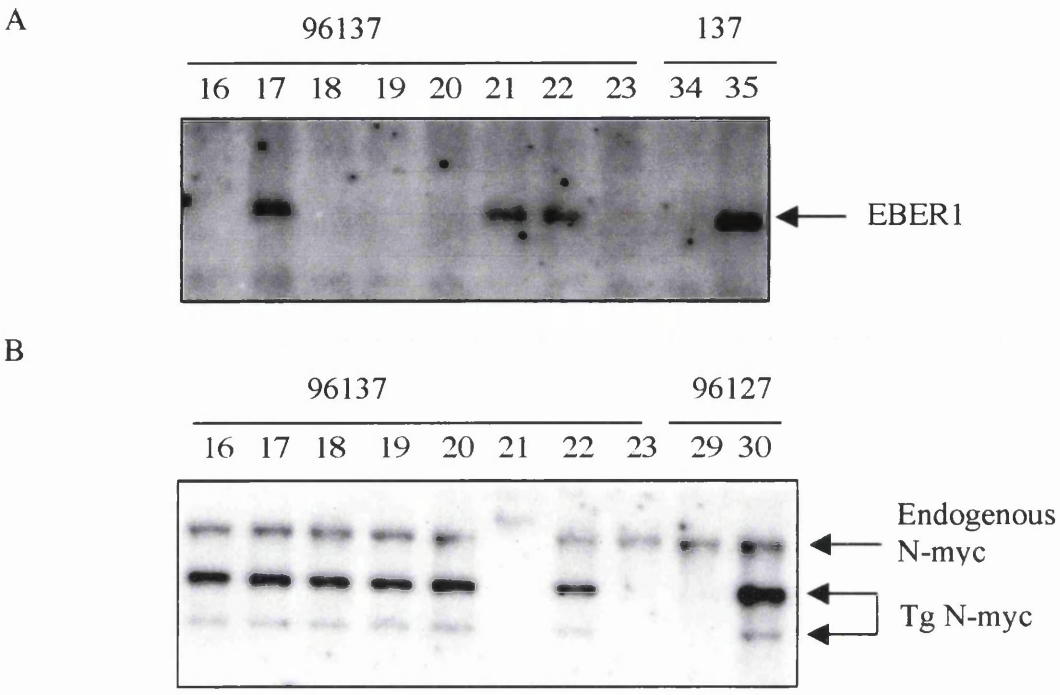

Figure 6.4: Southern blot from N-myc (line 96) and EBER1 (line 137) cross-breeding programme

Line 137 transgenic positive mice were crossed with line 96 transgenic positive mice. The offspring were genotyped and 5μg of gDNA was digested either with *Eco*RI (for EBER1) or with *Bam*HI (for N-myc). The digestion products were electrophoresed through a 0.8% agarose gel for the *Bam*HI products or through a 1% agarose gel for the *Eco*RI products and Southern blotted. The Southern blot was hybridised with either EBER1 radiolabelled probe at 60°C or N-myc radiolabelled probe at 65°C in Church buffer. A final hot wash was performed at 60°C (for EBER1) or at 65°C (for N-myc). Panel A shows the EBER1 blot and panel B shows the N-myc blot. The numbers shown above the tracks are the animal numbers either from lines 137 or 96137 and 96x127 crosses. Number 137.34 was used as negative control and number 137.35 was used as positive control for EBER1. Numbers 96127.29 and 96127.30 were used as negative and positive controls for N-myc respectively. The endogenous N-myc, transgenic N-myc and EBER1 bands are indicated with arrows.

Transgene	Number
N-myc	12
EBER1	5
N-myc and EBER1	12
Negative	14

Table 6.2: Summary of the 96127 cross-breed

Transgene	Number
N-myc	4
EBER1	5
N-myc and EBER1	6
Negative	8
Remain to be tested	11

Table 6.3: Summary of the 96137 cross-breed

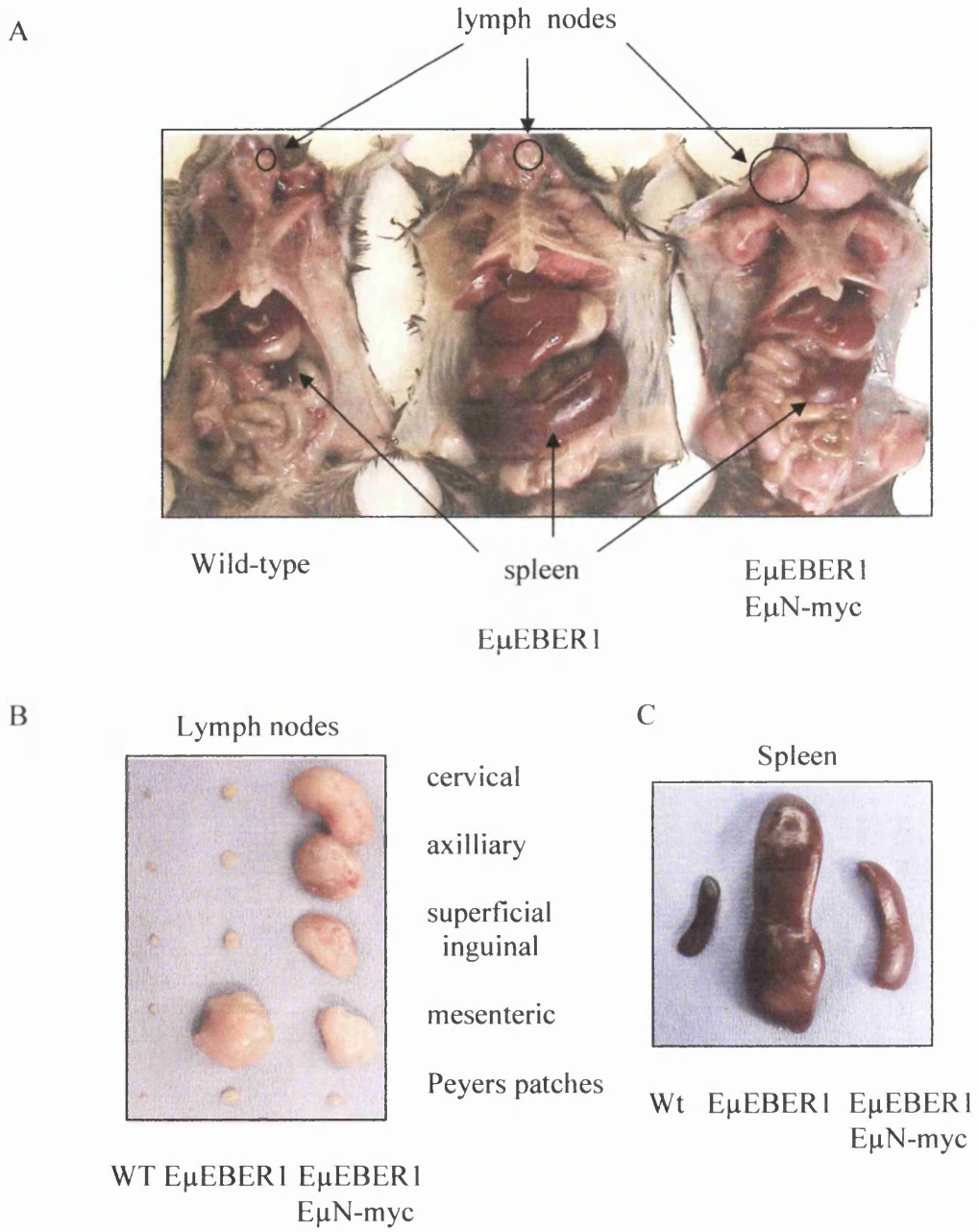

Figure 6.5: Phenotype of line 96127 bi-transgenic mice

Panel A shows a dissected wild-type mouse (12 months), an EBER1 positive mouse with a tumour (line 127, 19 months) and an EBER1/N-myc bi-transgenic mouse with a tumour (line 96127, 12 months). The spleen and a cervical lymph node in each are indicated with arrows. Panel B shows the different lymph nodes removed from these mice and panel C focuses on the spleens of these animals.

Kaplan Meier plots to explore the possible cooperation between EBER1 and N-myc are shown in figure 6.6. The study is still ongoing as not all the bi-transgenic (3 mice remaining) and N-myc (4 mice remaining) mice had succumbed to lymphoma at the time of writing. In the time frame of this study no EBER1 mice developed lymphoma; nor did any negative control. The first Kaplan Meier plot shows the lymphoma incidence of all the N-myc and bi-transgenic mice in the study (Figure 6.6A). 8/12 N-myc mice developed lymphoma between 104 and 406 days with a median age of 441.5 days. The bi-transgenic mice developed lymphoma faster than the N-myc mice, as is shown by their median age of 214 days compared to 441.5 days. Despite the apparent difference between the two curves, the P value is 0.1514, which is not statistically significant. However in this plot 2/12 N-myc mice succumbed to a thymoma at an early age (104 and 135 days). As this phenotype is different from that of the B-cell lymphoma a second Kaplan Meier plot was generated excluding these two mice from the percentages of B-cell lymphoma (Figure 6.6 B). In this plot the P value is 0.0481, showing a significant difference between the two curves. This suggests that EBER1 and N-myc may cooperate in B-cell lymphomagenesis. However, in order to support this approach, the two thymomas should be checked for T cell receptor rearrangement. Depending on the outcome of this analysis, the two animals will be included or removed from the plot. A T cell lymphoma was described by Dildrop *et al.*, (1989) in one mouse; however they do not state if it originated from a mouse with a thymoma or from a mouse with expanded lymph nodes, except for the fact that both kidneys were invaded by tumour cells.

For line 96137 the study is still ongoing as line 137 was established later. 2/12 N-myc animals succumbed to lymphoma at 83 and 250 days and 2/6 bi-transgenic animals succumbed to lymphoma at 194 and 210 days as represented by the Kaplan Meier plot (Figure 6.7 A). The P value between the two curves is 0.428, which is not statistically significant and the oldest mice for both N-myc and bi-transgenic are now 335 days old. However, a young N-myc mouse (83 days) had a thymoma and a second Kaplan Meier plot was generated excluding this animal (Figure 6.7 B) with a P value of 0.1815. So far none of the other animals in the study have developed disease.

A

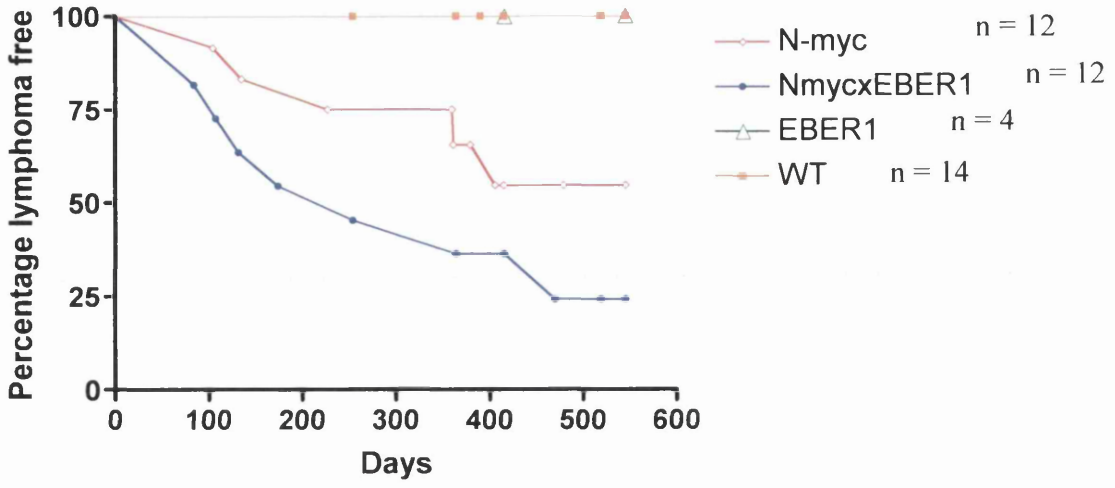

B

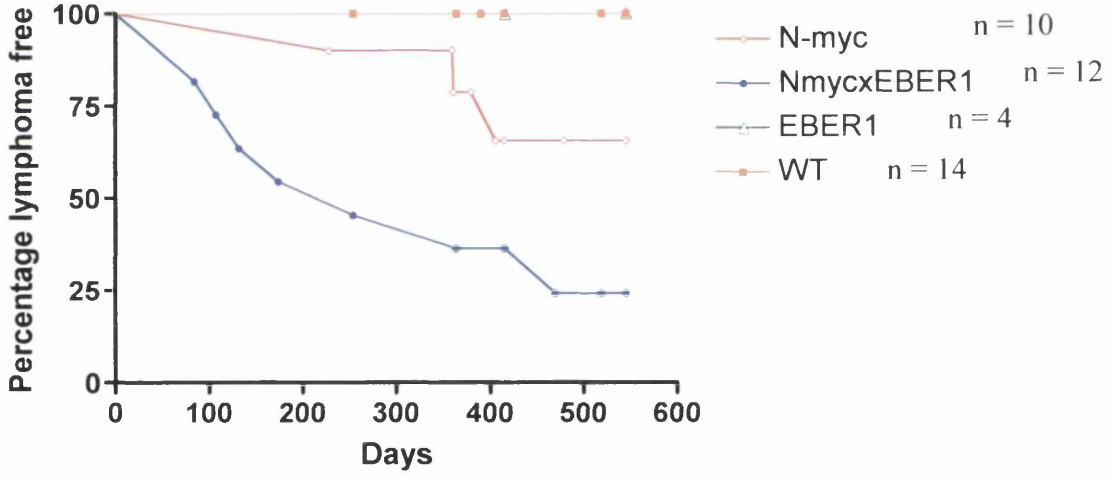

Figure 6.6: Kaplan Meier survival curves of line 96127 mice

The graphs show the proportion of mice succumbing to lymphoma (Y axis) over time (X axis). The graphs were generated and the data analysed for statistical significance with a log rank test using Graphpad Prism 4 software. Panel A shows the survival curve of all the offspring resulting from the 96x127 cross, whereas panel B shows the survival curve of the offspring from the same cross, omitting for the two N-myc transgenic positive mice which developed a thymoma at an early age.

A

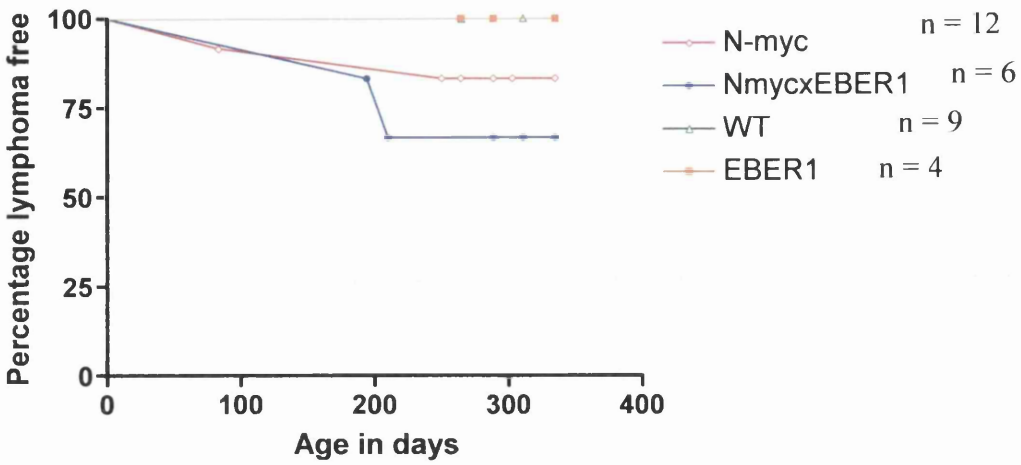

B

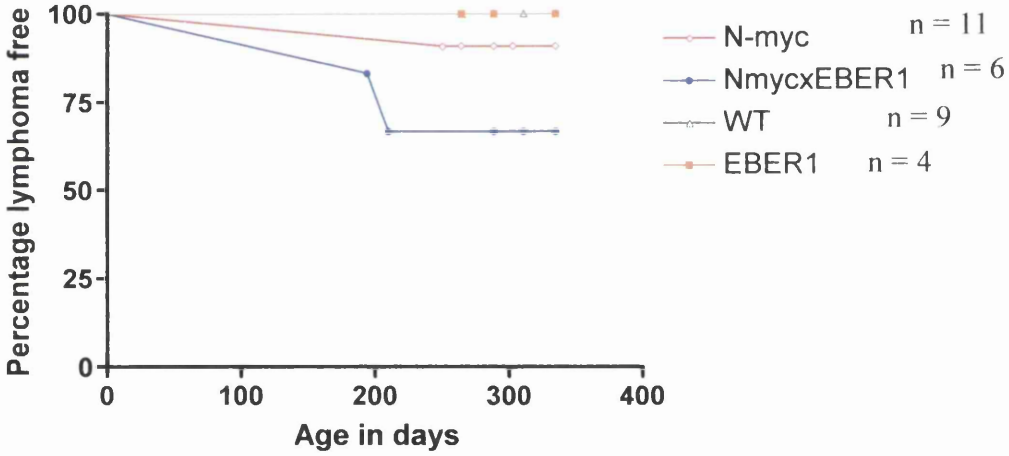

Figure 6.7: Kaplan Meier survival curves of line 96137 mice

The graph shows the proportion of mice succumbing to lymphoma (Y axis) over time (X axis). The graph was generated and the data analysed for statistical significance with a log rank test using Graphpad Prism 4 software. Panel A shows the survival curve of all the offspring resulting from the 96x137 cross (except for the mice that are not genotyped), whereas panel B shows the survival curve of the offspring from the same cross discounting the young N-myc transgenic positive mouse which developed a thymoma at an early age

.

6.3.3. Characterisation of the EBER1/N-myc bi-transgenic tumour tissues

6.3.3.1. Immunoglobulin gene rearrangement analysis

The tumour tissues were analysed for both immunoglobulin heavy chain (IgH) and T cell receptor (TCR) rearrangements to determine if the tumours were of B cell or T cell origin. Tumours arising in N-myc positive animals are reported to be of B cell origin, showing an IgH rearrangement (Dildrop *et al.*, 1989) (C57Bl/6 strain). gDNAs were extracted from different tumour tissues (liver, spleen, thymus, cervical lymph nodes and mesenteric lymph nodes) of two bi-transgenic 96127 mice, number 9 and 13. Two Southern blots were performed and one was probed with an IgH (J_H region) probe and the other with a TCR ($J_\beta 1$, constant region 1 fragment) probe. No TCR rearrangement was observed in any of the tissues tested for the two mice (data not shown). However, IgH rearrangements were observed in all the tissues tested (Figure 6.8). In both animals 9 and 13 the endogenous band was observed as well as additional bands. For animal 13 the additional band is smaller than the endogenous band (4.5kb) whereas for animal 9 the bands are larger (at 8 and 9kb) indicating that different rearrangements occurred in the two animals. However, within an animal these rearrangements are the same showing that the tumours are of clonal origin. For the thymus of animal 13 an extra band was also noticed (3.5kb) suggesting that tumour cells in this tissue had undergone an additional rearrangement of the second immunoglobulin heavy chain locus. Further analysis of tumour tissues from different bi-transgenic and N-myc mice also indicated that these tumours were of B cell origin. FACS analysis also supported this result showing an increase in $B220^+$, $CD3^-$ cells in the tissue compared to wild-type (Figure 6.9).

6.3.3.2. EBER1 and N-myc expression analysis

In order to explore if the apparent cooperation in B cell lymphomagenesis between line 127 and 96 was simply due to one transgene affecting the expression level of the other, expression analysis of both EBER1 and N-myc was undertaken. For EBER1 expression, RNA was extracted from the tumour tissues of single positive (line 127) and bi-transgenic (line 96127) mice and was followed by an RT-PCR using EBER1 specific primers. No

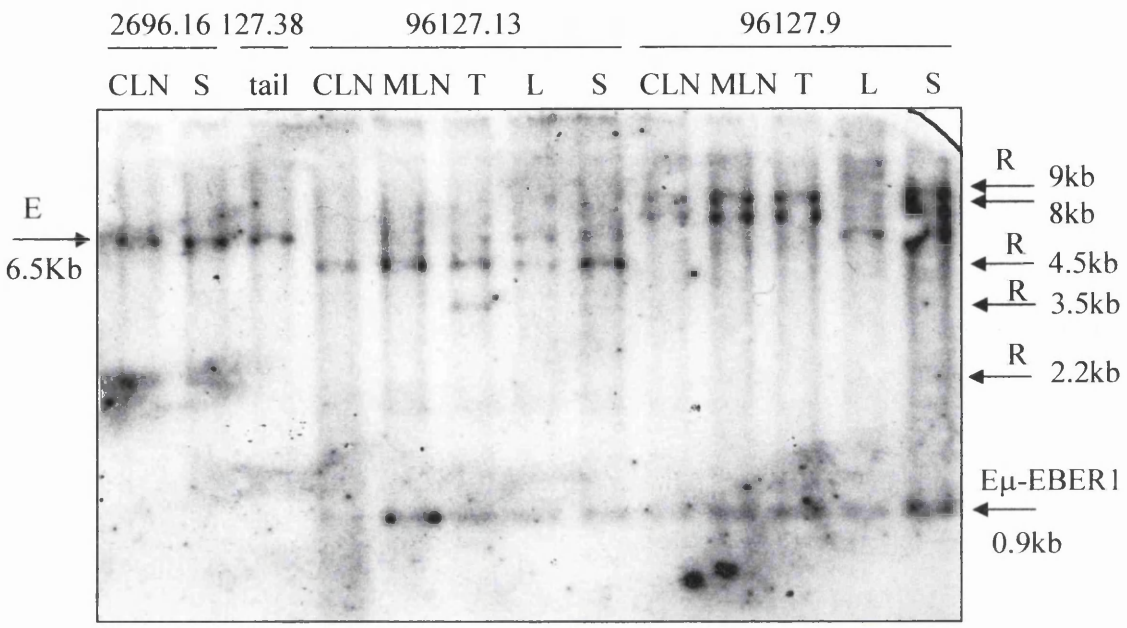

Figure 6.8: IgH rearrangements in line 96127 bi-transgenic mice

gDNA was extracted from tumour bearing tissues collected from line 96127 bi-transgenic mice. 5μg of gDNA digested with *Eco*RI was electrophoresed through a 0.8% agarose gel and Southern blotted. The blot was hybridised with an IgH probe at 65°C in Church buffer. A final hot wash was performed at 65°C. Tail gDNA from animal 127.38 was used as negative control for IgH rearrangements. gDNAs from 2696.16 were used as positive control for IgH rearrangements. The endogenous (E) band is shown with an arrow on the left hand-side whereas the rearranged (R) bands are shown with arrows on the right hand-side. As the EBER1 transgene is fused to Eμ an EμEBER1 band is also observed at 0.9kb and is indicated by an arrow. The tissues analysed were: CLN: cervical lymph nodes, S: spleen, MLN: mesenteric lymph nodes, T: thymus and L: liver.

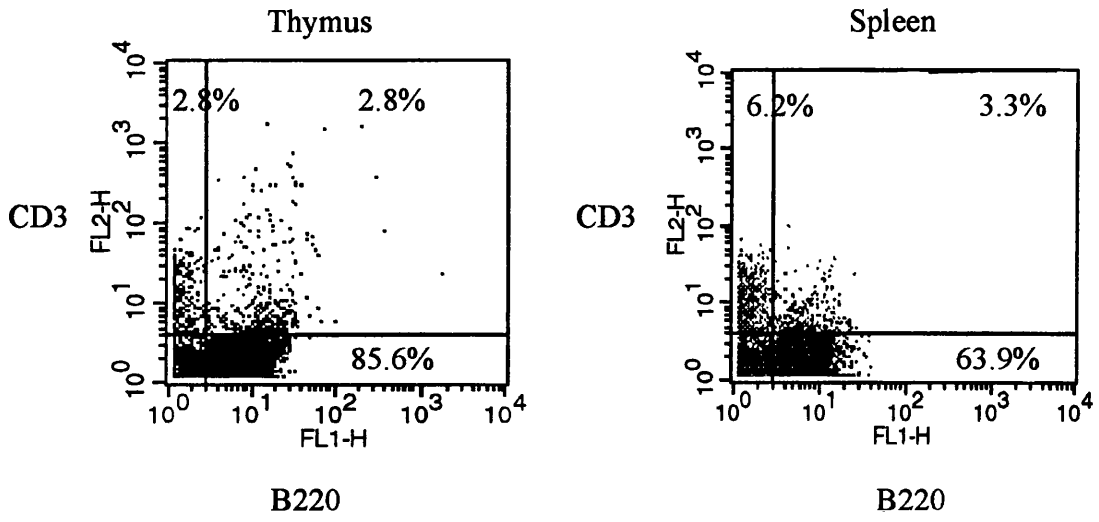

Figure 6.9: The tumour cells from a 96127 bi-transgenic mouse are mainly B cells

The spleen and thymus were collected from a 96127 bi-transgenic mouse with a tumour. Primary cells were isolated and 10^6 cells were stained with B220FITC and CD3PE. The percentage of the cells in each quadrant is indicated.

difference in EBER1 expression was observed between the different bi-transgenic tissues tested and two EBER1 tumour tissues (Figure 6.10). However, it should be noted that although relative expression levels can be seen by this technique, it is not an accurately quantitative method.

N-myc expression was examined by western analysis (Figures 6.11 A and 6.12). The study was performed on three bi-transgenic 96127 mice (Figures 6.11 and 6.12), two N-myc mice (Figure 6.12), an EBER1 mouse with a tumour and a wild-type control (Figure 6.12). A band of approximately the correct size for N-myc (67kDa) was clearly detected in the bi-transgenic samples along with several other bands (Figures 6.11 and 6.12). In order to confirm if this band was N-myc protein, the blot was re-probed with antibody plus the epitope peptide (Figure 6.11 B). From this it can be seen that the 67kDa band was blocked, and therefore is specific, confirming its identity as N-myc, but in addition a band migrating at around 120kDa also was blocked (band B on the figure). The identity of this protein or complex is not clear, but it is also specifically expressed in the N-myc only transgenic samples (Figure 6.12) and may represent a dimeric protein. Samples from two N-myc mice with tumours were used in this assay and both lymph nodes from mouse 41 showed a high level of expression of N-myc (67kDa), whereas the thymus from mouse 37 was low (Figure 6.12). This sample was extracted from a thymoma of a 4 month old animal showing the early thymoma phenotype described above. However, this sample showed high expression of the 120kDa molecular weight protein. The other two samples were from lymph nodes of a mouse succumbing to typical B-cell lymphoma. The expression level of N-myc in three different bi-transgenic mice was tested in lymph node tissues and was high and equivalent to N-myc positive animals. Two EBER1 tumour tissues from mouse number 127.49 were used and their level of N-myc expression was low. Together these results indicate that the cooperation phenotype of tumourigenesis seen in the bi-transgenic mice is not due to an increase of either EBER1 or N-myc expression.

6.3.3.3. Analysis of N-myc DNA binding activity

Another means by which EBER1 could cooperate with N-myc in tumourigenesis is by leading to increased N-myc activity by some unknown mechanism. To test this hypothesis indirectly, the DNA binding activity of N-myc was studied using an electrophoretic mobility shift assay (EMSA). The probe used in this assay was a myc

A

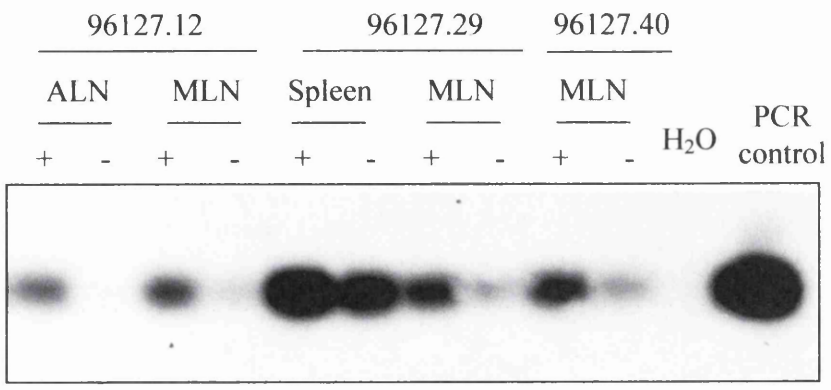

B

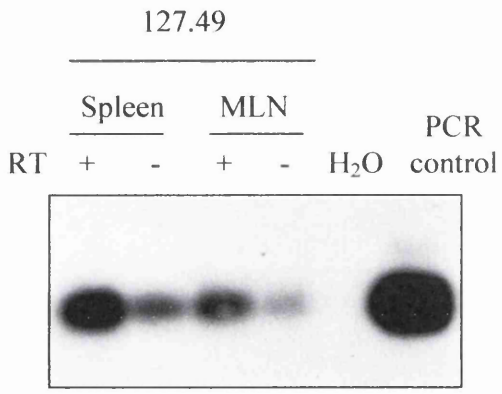

Figure 6.10: EBER1 expression in bi-transgenic 96127 mice

Lymphoid tumour tissues from three 96127 bi-transgenic mice (panel A) and from a line 127 tumour mouse (panel B) were collected. RNA extraction was performed followed by DNAse I treatment, acid phenol extraction and RT-PCR. The RT reaction was performed with an EBER1 specific primer (CR4) and 5μg of total RNA. For each sample a minus RT control was performed. The PCR was performed with $1/4^{th}$ of the RT reaction and CR8 and CR9 primers. A no DNA control (H_2O) and a positive plasmid DNA control (PCR control) were also performed for the PCR. The RT-PCR products were electrophoresed through an agarose gel followed by Southern blotting with an EBER1 probe. ALN: axillary lymph nodes, MLNs: mesenteric lymph nodes. Note the gDNA contamination in several samples: 96127.12 MLNs, 96127.29 spleen, MLN, 96127.10 MLN, 127.49 spleen and MLN.

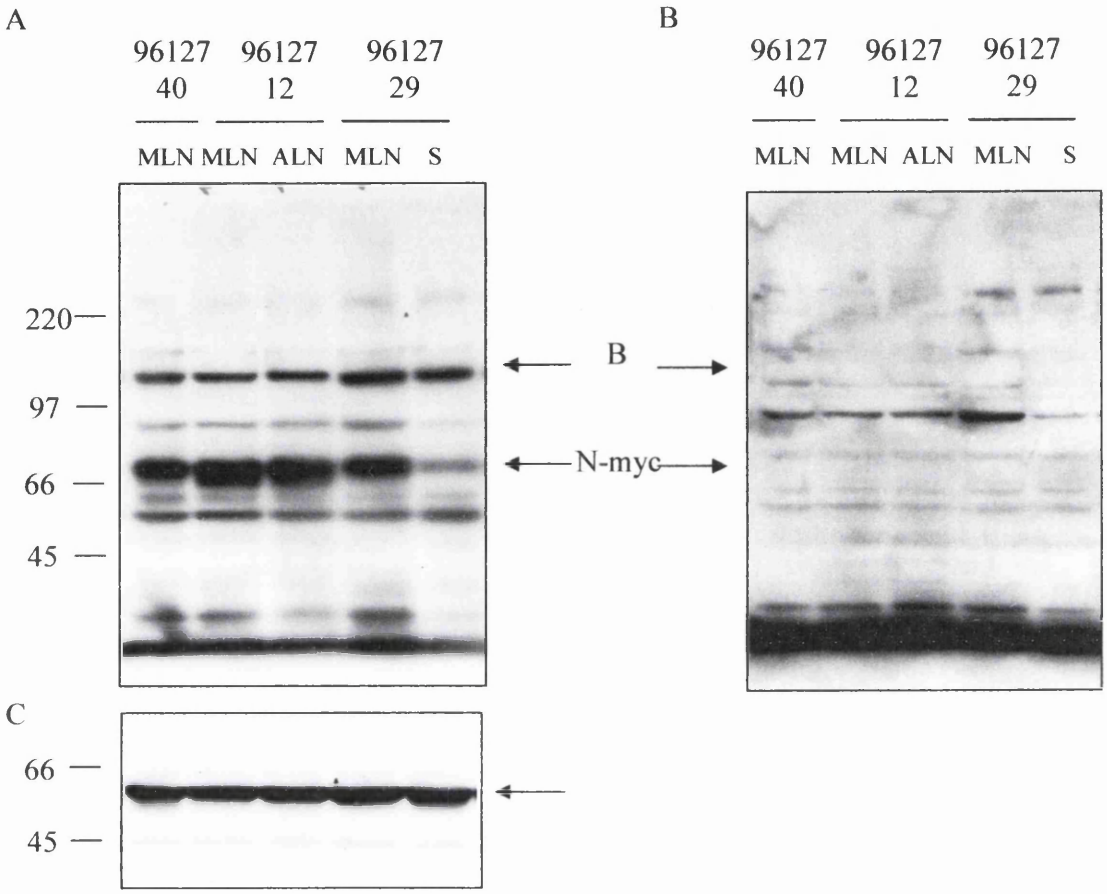

Figure 6.11: Western blot for N-myc and its blocking peptide in the bi-transgenic 96127 mice

Proteins from three different bi-transgenic EBER1/N-myc (line 96127) mice were extracted using the high salt nuclear extraction method. 100μg of proteins were separated by a 7.5% SDS-PAGE and the gel was western blotted. The membrane was probed with a rabbit anti-N-myc antibody (panel A) followed by a goat anti-rabbit IgG-HRP secondary antibody and visualised using ECL+. The membrane was stripped and reprobed with a rabbit anti-N-myc + N-myc blocking peptide (panel B) followed by a goat anti-rabbit IgG-HRP secondary antibody and visualised using ECL+. Finally, the membrane was stripped and reprobed with a rabbit anti-βtubulin antibody (panel C), as a loading control, followed by a goat anti-rabbit IgG-HRP secondary antibody and visualised using ECL+. The molecular weights according to the marker lane are shown. The N-myc specific band is indicated at approximately 67kDa. Band B indicates a protein running at 120kDa which was also blocked when using the blocking peptide. The βtubulin specific band is indicated by an arrow at 55kDa.

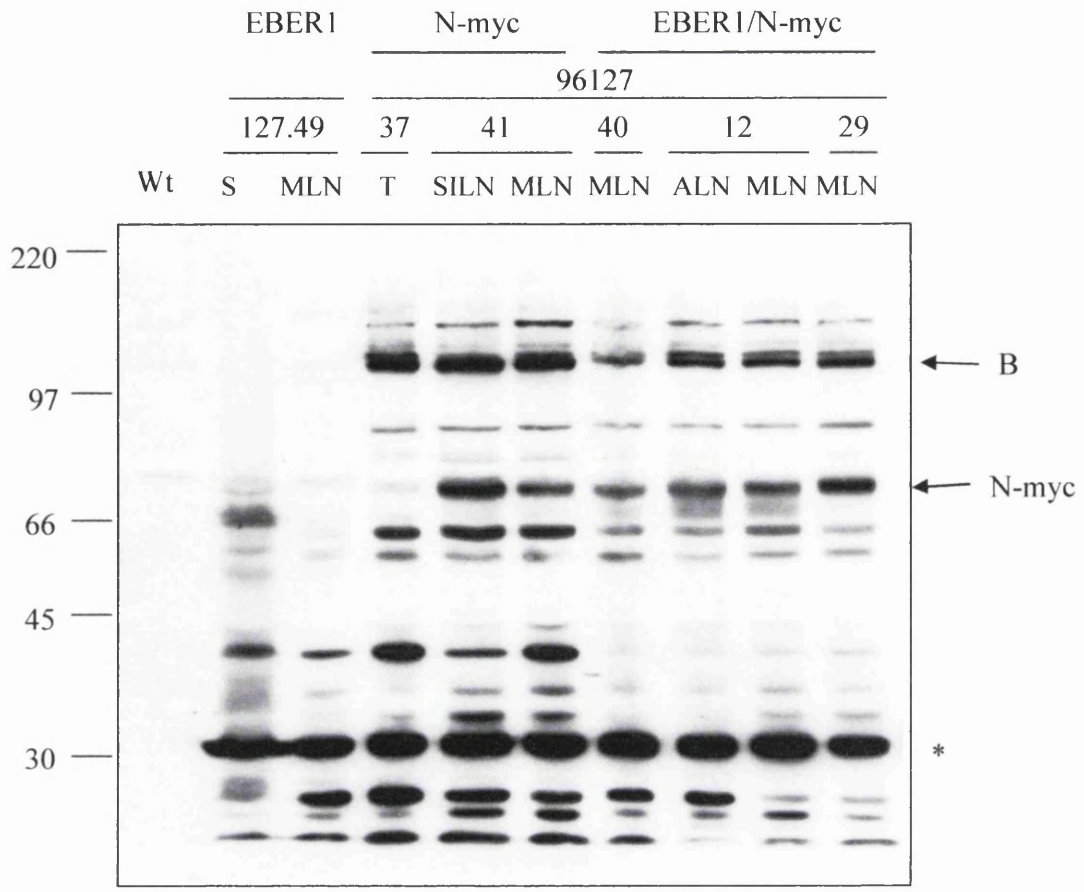

Figure 6.12: Western blot for N-myc expression in the bi-transgenic 96127 mice

Proteins from different tumour tissues of EBER1 positive (line 127) bi-transgenic EBER1/N-myc (line 96127) and N-myc positive mice (of the same cross) were extracted using the high salt nuclear extraction method. 100μg of proteins were separated by a 7.5% SDS-PAGE and the gel was western blotted. The membrane was probed with a rabbit anti-N-myc antibody followed by a goat anti-rabbit IgG-HRP secondary antibody and visualised using ECL+. A wild-type (Wt) control was used to determine the endogenous level of N-myc in the tissues. The molecular weights according to the marker lane are shown. The N-myc specific band is indicated at approximately 67kDa. Band B indicates another protein running at 120kDa which was not blocked when using the blocking peptide (Figure 6.11). The non-specific bands exemplified by the * sign show equal loading of the samples except for the Wt control. S: spleen, T: thymus, SILN: superficial inguinal lymph nodes, MLN: mesenteric lymph nodes and ALN: axillary lymph nodes.

binding site oligonucleotide comprising an E box (cacgtg) as the target binding site which is specific for all the members of the myc family. Therefore to determine if any shift observed was due to N-myc or c-Myc binding, supershift assays were also performed with the appropriate antibodies (Figure 6.13). Two EBER1 line 127 tumour tissues, an N-myc tumour tissue (line 96127.41) and a bi-transgenic tumour tissue (line 96127.29) were used for the assay, as well as a c-Myc tumour sample as a positive control (line 97) to assess c-Myc DNA binding. No obvious shift by either antibody was observed (even for the N-myc and c-Myc controls), suggesting that either the assay did not work or the antibodies were not effective, or the bands observed are not N-myc and c-Myc. Therefore it was not possible to determine which proteins are in the complex. The two 127 tumours showed different complexes as previously described in chapter 5. When using the same extracts with an Sp1 probe, the bi-transgenic sample and the N-myc and c-Myc samples appeared equally loaded (Figures 6.14 and 5.10). However the wild-type sample appeared underloaded or degraded and similar for the line 127 samples (as shown in Chapter 5, Figure 5.10). This could have been due to repeated freezing and thawing of the samples before performing the Sp1 EMSA. Nevertheless when the band from the bi-transgenic sample was compared to that of the N-myc sample they were of similar intensity. This result indicates that the cooperation between EBER1 and N-myc in tumourigenesis is not due to altered activity of Myc.

6.4. Does EBER1 cooperate with c-Myc in lymphomagenesis?

6.4.1. Generation of EμEBER1 and Eμc-myc bi-transgenic mice

EμEBER1 line 127 and line 136 mice were crossed with EμC-myc mice (Tables 6.4 and 6.5). Line 136 was chosen instead of line 137 (which was used for the N-myc cross-breed study) as it harbours the p670 transgene which incorporates a myc binding site 5' to EBER1 (Figure 3.1, Chapter 3). It was therefore hypothesised that this cross might lead to increased expression of the EBER1 transgene. The transgenic status of the 97127 offspring was assessed by Southern blot for EBER1 and by PCR for *c-myc* (representative examples shown in figure 6.15). From the Southern blot and the PCR results, mice numbered 39, 40, 45 and 47 were bi-transgenic, mice numbered 42 and 46 were EBER1 positive, mice numbered 41 and 44 were *c-myc* positive and finally mice numbered 37, 38

Figure 6.13: Myc DNA binding activity in the EBER1/N-myc bi-transgenic mouse tissues

Proteins were extracted from different tumour samples (two line 127 samples, one N-myc sample line 96127.41, one line 96127.29 bi-transgenic sample and a line 97 (c-Myc) sample) using the high salt nuclear extraction buffer. 10μg of protein extract was used for each sample. A sample from line 97 was used as positive control for c-Myc binding. Two, three or four reactions were prepared for each sample: one without and one with 200x unlabelled competitor (+ track competitor), one with 4μg of N-myc antibody (+ track N-myc antibody) and one with 4μg of c-Myc antibody (+ track c-Myc antibody). Labelled myc binding oligo was added to each sample and incubated for 20 minutes on ice before loading the samples on to a 6% polyacrylamide gel. For the supershift the antibody was incubated at room-temperature for 15 minutes with the extract before the addition of the labelled probe. A labelled oligo without extract was also used as control (P). The gel was electrophoresed for 3 hours before being dried and exposed on film for the required amount of time. Panel A shows a wild-type sample, a spleen line 127.37 tumour sample, a mesenteric lymph node (MLN) line 96127.29 tumour sample (bi-transgenic N-myc/EBER1) and a spleen line 97 tumour sample. Panel B shows the same wild-type sample as panel A, a mesenteric lymph node (MLN) line 127.49 tumour sample, a superficial inguinal lymph node (SILN) line 96127.41 tumour sample (N-myc positive only) and a spleen line 97 tumour sample. The arrow in panel A indicates the specific band, which is the same as band A in panel B. The B and C bands were only detected in this single EBER1 sample. All bands (A, B and C) are completely competed out with excess unlabelled oligonucleotide (+ tracks) demonstrating specificity.

A

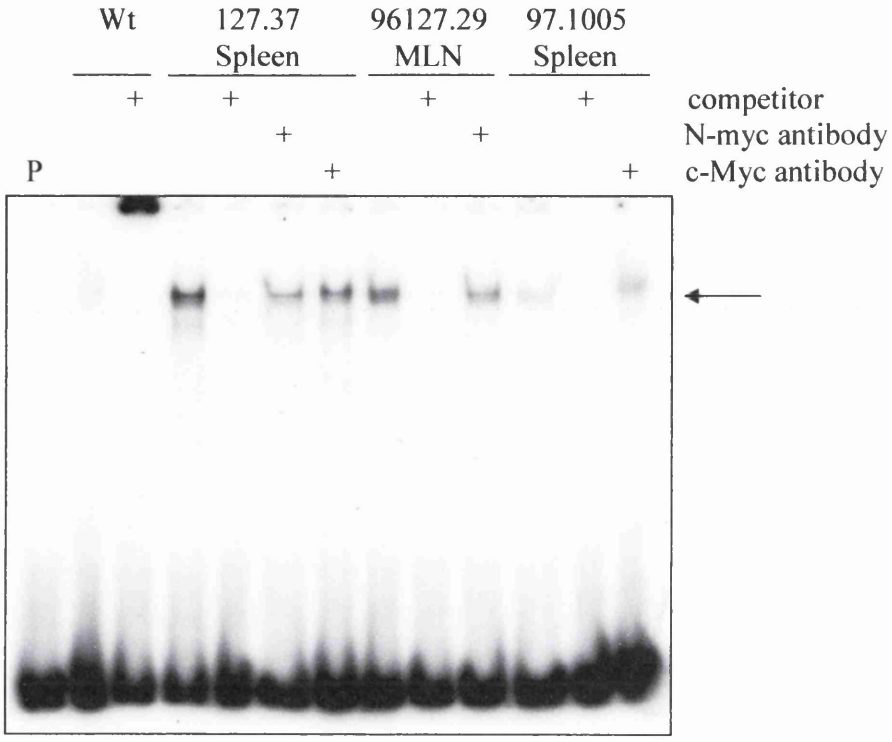
Wt
127.37
Spleen
96127.29
MLN
97.1005
Spleen
competitor
N-myc antibody
c-Myc antibody
P

B

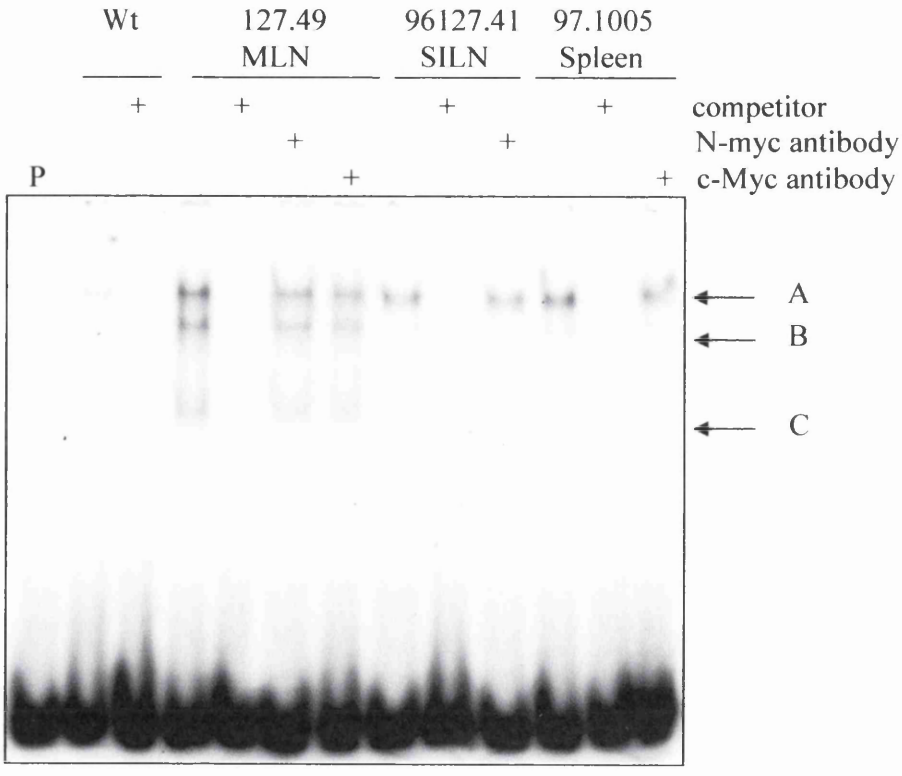
Wt
127.49
MLN
96127.41
SILN
97.1005
Spleen
competitor
N-myc antibody
c-Myc antibody
P
A
B
C

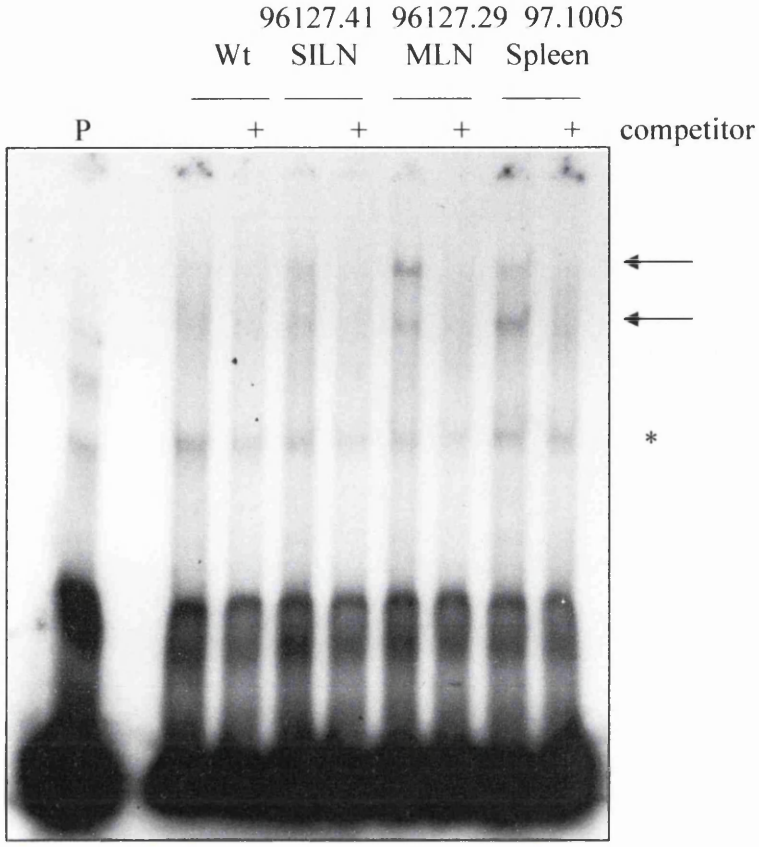

Figure 6.14: Sp1 DNA binding activity in the EBER1/N-myc bi-transgenic mouse tissues
Proteins were extracted from different tumour samples (two line 96127 bi-transgenic samples and a line 97 (c-Myc) sample) using the high salt nuclear extraction buffer. 10µg of protein extract was used for each sample. Two reactions were prepared for each sample: one without and one with 200x unlabelled competitor (+ track competitor). Labelled Sp1 binding oligo was added to each sample and incubated for 20 minutes on ice before loading the samples on to a 6% polyacrylamide gel. A labelled oligo without extract was also used as control (P). The gel was electrophoresed for 3 hours before being dried and exposed on film for the required amount of time. The arrows indicate specific bands which are competed out with excess unlabelled oligonucleotide (+ tracks) demonstrating specificity and the * sign shows a non-specific band.

Transgene	Number
c-Myc	19
EBER1	10
c-Myc and EBER1	19
Negative	7

Table 6.4: Summary of the 97127 cross-breed

Transgene	Number
c-Myc	11
EBER1	6
c-Myc and EBER1	4
Negative	8
Not tested	32

Table 6.5: Summary of the 97136 cross-breed

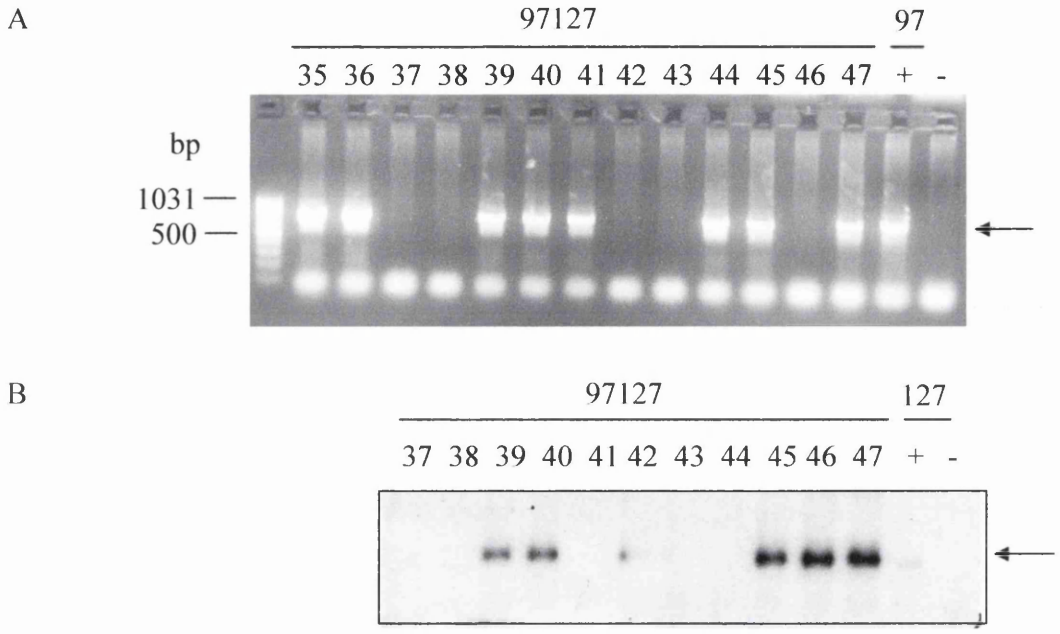

Figure 6.15: Genotype of line 97127 offspring

gDNAs were extracted from tails of line 97127 mice. In panel A, 300ng of gDNA was used as template for the PCR using *c-myc* primers. The gDNA from a c-Myc positive mouse (97) was used as positive control for the reaction and the track is labelled with a + sign. A reaction with water was used as negative control and the track is labelled with a - sign. The PCR products were electrophoresed through a 1.5% agarose gel and the O'GeneRuler™ 100bp DNA ladder was used as a marker for size. The sizes are indicated on the left hand-side of the gel. An arrow indicates the transgenic *c-myc* DNA fragment. In panel B, 5µg of gDNA was digested with *Eco*RI, electrophoresed through a 1% agarose gel and Southern blotted. The membrane was hybridised with an EBER1 specific probe. gDNAs from known EBER1 positive (+) and negative (-) line 127 mice were used as controls. The EBER1 band is indicated by an arrow. In both panels the numbers above the tracks indicate the animal number.

and 43 were negative. Animals numbered 35 and 36 were tested on a different Southern blot and number 35 was shown to be EBER1 positive whereas 36 was not; therefore number 35 was a bi-transgenic animal and 36 was *c-myc* positive. The transgenic status of the 97136 offspring was assessed by PCR for both EBER1 and *c-myc* (representative examples shown in figure 6.16). From the PCR results, mice numbered 18 and 21 were EBER1 positive, mice numbered 17, 20 and 22 were *c-myc* positive and finally mouse number 19 was negative.

6.4.2. Phenotype and survival of the bi-transgenic EBER1/c-Myc mice

The animals were monitored weekly for any sign of phenotype. Once the appearance of lymphoma was detected the mice were euthanised and tissues were collected. The phenotype for Eμc-myc mice has been described previously and is characterised by an expansion of the cervical lymph nodes and axillary lymph nodes that is externally obvious and has been described as a "water wings" phenotype (Adams *et al.*, 1985, Harris *et al.*, 1988). Tissues were also placed in formalin for subsequent pathological analysis. Figure 6.17 A shows a bi-transgenic (line 97127) mouse compared to a negative mouse and a c-Myc positive mouse. The phenotype in the EBER1/c-myc bi-transgenic mice was the same as that in c-Myc mouse. In the bi-transgenic animal a clear enlargement of the different lymph nodes was observed as well as in the spleen compared to that of the wild-type mouse. A comparison of the spleen and the different lymph nodes of a negative, a c-Myc and a bi-transgenic mouse (line 97127) is also presented (figure 6.17 B and C). The spleens of both the bi-transgenic mouse and the c-Myc positive mouse were enlarged compared to that of the wild-type and appeared of the same size. Similarly for the different lymph nodes, an enlargement was observed for the bi-transgenic and the c-Myc positive lymph nodes compared to that of the wild-type mouse, and also appeared of a similar size. The phenotype of the 97136 bi-transgenic mice was similar to that of c-Myc positive mice. The thymus was also markedly enlarged in 10/12 of the c-Myc mice that succumbed to lymphoma as well as in 13/13 of the bi-transgenic 97127 and 2/2 of the bi-transgenic 97136 mice, as was described by Adams *et al.*, (1985). Therefore, the bi-transgenic EBER1/c-Myc mice have the same phenotype as Eμc-myc mice.

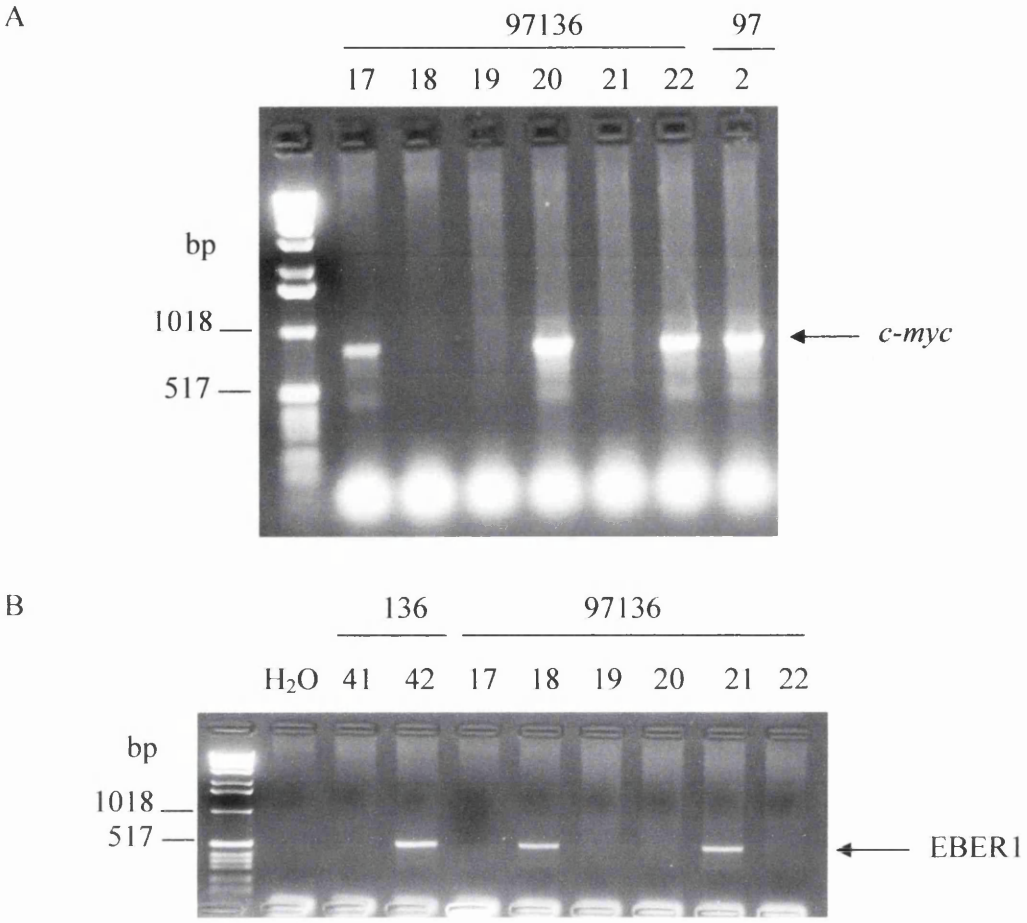

Figure 6.16: Genotype of line 97136 offspring

gDNAs were extracted from tails of line 97136 mice. 300ng of gDNA was used as template for the PCR using either *c-myc* primers (panel A) or EBER1 primers (panel B). In panel A, the gDNA from a c-Myc positive mouse (97) was used as positive control. In panel B, the gDNA from an EBER1 transgenic positive mouse (136.42) and a negative mouse (136.41) were used as positive and negative controls. The PCR products were electrophoresed through a 1.5% agarose gel and a 1kb DNA ladder was used as a marker for size. The sizes are indicated on the left hand-side of the gels. Arrows indicate the transgenic *c-myc* or EBER1 DNA fragments.

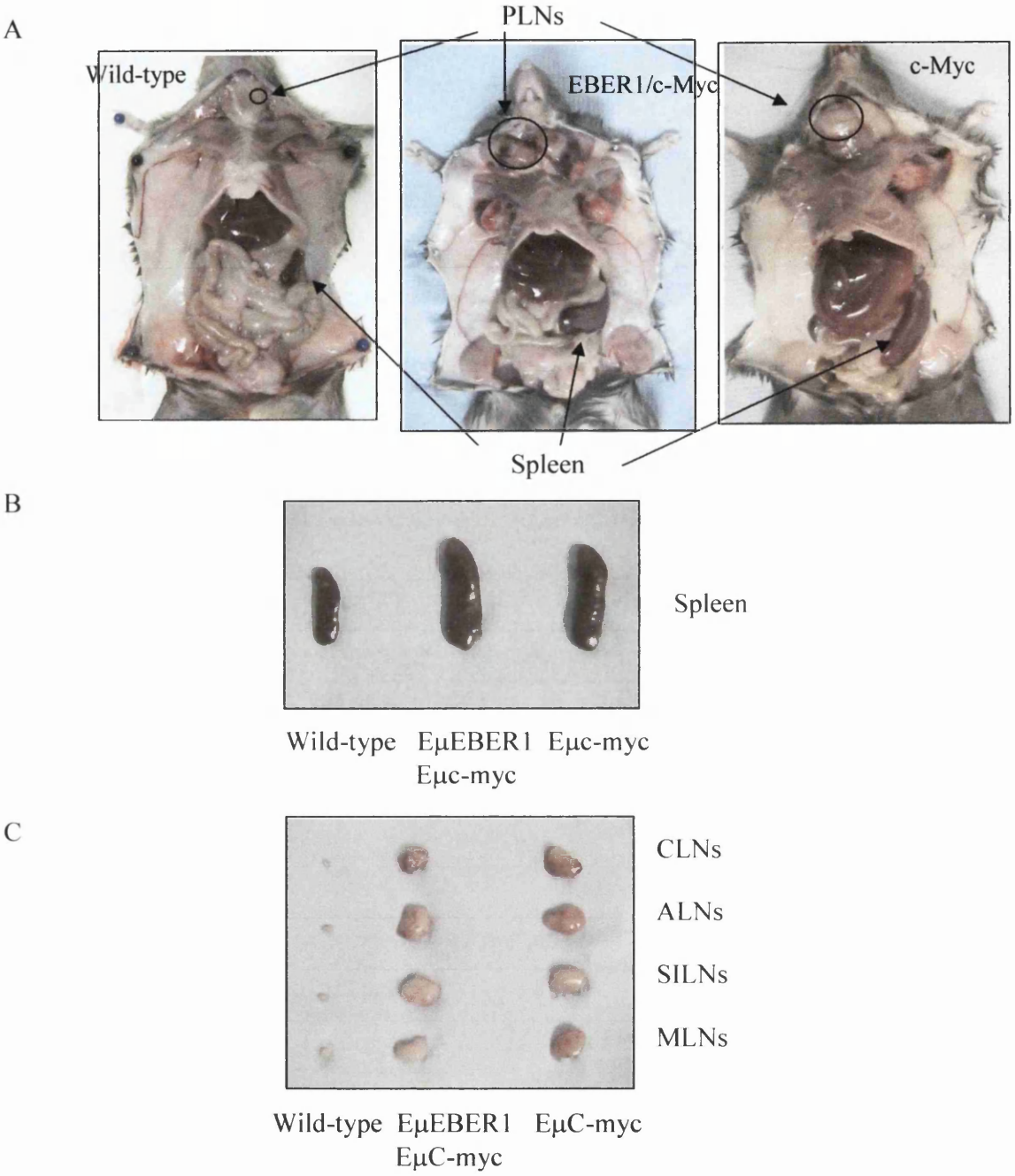

Figure 6.17: Phenotype of line 97127 bi-transgenic mice

Panel A shows a dissected wild-type mouse, an EBER1/c-Myc bi-transgenic mouse (line 97127) and a c-Myc mouse. Panel B shows the spleen of a wild-type mouse, an EBER1/c-Myc bi-transgenic mouse and a c-Myc positive mouse. Panel C shows the different lymph nodes of the same mice. CLNs: cervical lymph nodes, ALNs: axillary lymph nodes, SILNs: superficial inguinal lymph nodes and MLNs: mesenteric lymph nodes.

A Kaplan Meier plot to explore the possible cooperation between EBER1 and c-Myc is shown in figure 6.18 A. The study is still ongoing as not all the bi-transgenic (6 mice remaining) and c-Myc (7 mice remaining) mice had succumbed to lymphoma at the time of writing. In the time frame of this study no EBER1 mice developed lymphoma, nor did any of the negative controls. 12/19 c-Myc mice developed lymphoma between 60 and 158 days so far, with a median age of 129.5 days. 13/19 bi-transgenic mice have developed lymphoma between 57 and 150 days so far, with a median age of 113 days. The P value between the two curves is 0.5744, showing no significant difference in tumour onset between bi-transgenic 97127 mice and c-Myc mice. A Kaplan Meier plot was also generated for the 97136 mice (Figure 6.18 B) and the study is still ongoing as some of the mice have not been genotyped yet and not all the bi-transgenic (2 mice remaining) and c-Myc (6 mice remaining) mice have developed lymphoma. 5/11 c-Myc mice developed lymphoma between 79 and 117 days so far and 2/4 bi-transgenic mice developed lymphoma between 94 and 140 days so far. The P value between the two curves is 0.788, and like 97127 mice, the 97136 bi-transgenic mice have a similar tumour onset and phenotype as c-Myc mice. However more bi-transgenic mice should be included in the study to be able to draw any conclusion.

6.4.3. Characterisation of the EBER1/c-Myc bi-transgenic tumour tissues

6.4.3.1. Analysis of c-Myc DNA binding activity

The expression of c-Myc in the tumours was not investigated thoroughly as several antibodies were previously tried, some with their blocking peptides, using c-Myc only tumour samples and specific c-Myc bands could not be identified properly (Figure 5.7). For instance, several bands were observed at the expected size of c-Myc, and when the blocking peptide was used, it resulted in the disappearance of all the bands from the blot.

As an alternative to examining the c-Myc expression level, Myc DNA binding activity in the bi-transgenic mice was studied by EMSA in order to determine if this was altered compared to c-Myc positive mice. The probe used was same as the one used for the EMSA with the N-myc samples. A supershift was also attempted on these samples using an anti-c-Myc antibody (Figure 6.19). In this figure the unlabelled oligonucleotide

A

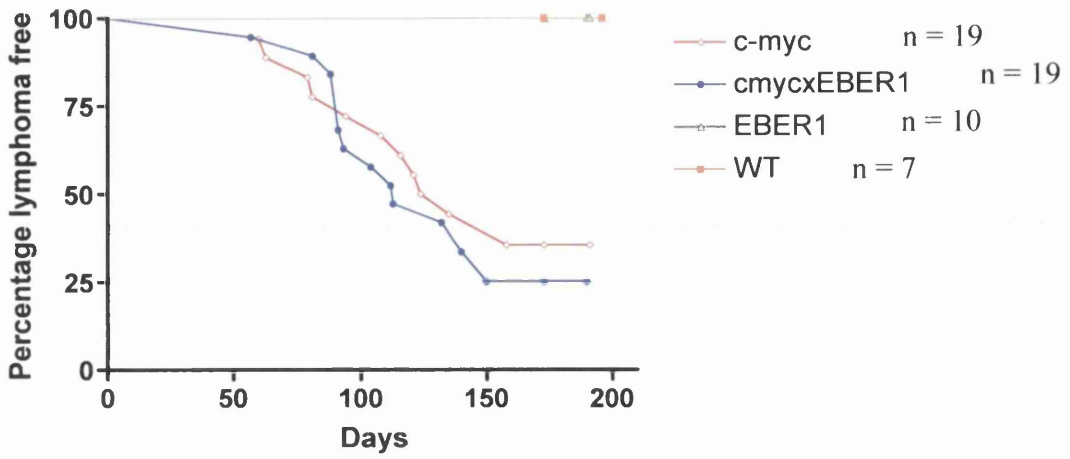

B

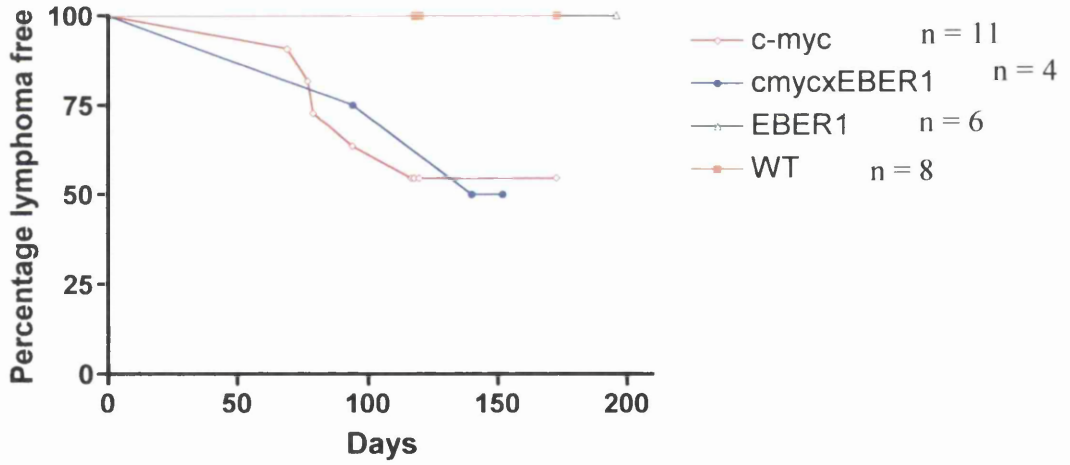

Figure 6.18: Kaplan Meier survival curves of line 97127 and 97136 mice

The graphs show the proportion of mice succumbing to lymphoma (Y axis) over time (X axis). The graphs were generated and the data analysed for statistical significance with a log rank test using Graphpad Prism 4 software. Panel A shows the survival curve of all the offspring resulting from the 97x127 cross and panel B shows the survival curve of all the offspring resulting from the 97x136 cross (except for the mice that are not yet genotyped).

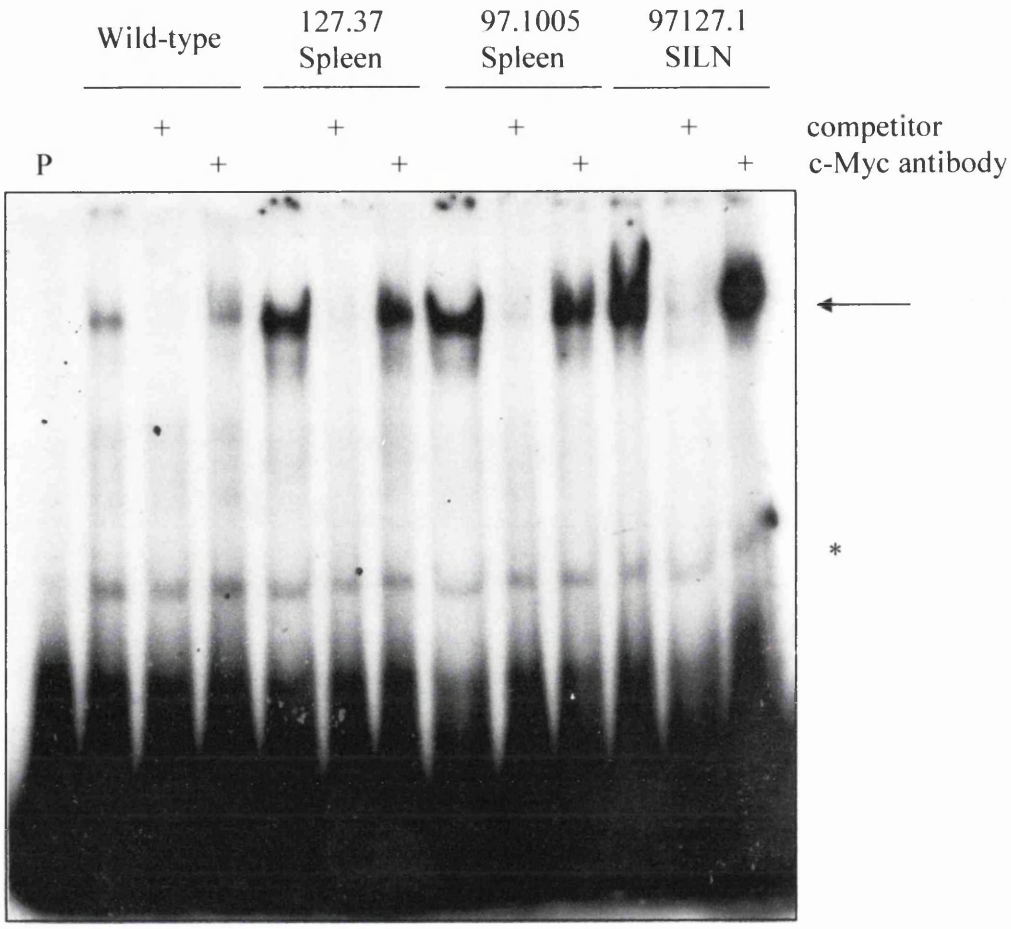

Figure 6.19: Myc DNA binding activity in the EBER1/c-Myc bi-transgenic mouse tissues
Proteins from a wild-type sample, an EBER1 tumour sample (line 127), a c-Myc tumour sample and an EBER1/c-Myc bi-transgenic tumour sample (line 97127) were extracted using the high salt nuclear extraction method. 10μg of protein extract was used for each sample. Three reactions were prepared for the different samples, one without and one with 200x unlabelled competitor (+ competitor track), and one with 4μg of anti-c-Myc antibody (+ c-Myc antibody tracks). Labeled Myc oligo was added to each sample and incubated for 20 minutes on ice before loading the samples on to a 6% polyacrylamide gel. For the supershift the antibody was incubated at room-temperature for 15 minutes with the extract before the addition of the labelled probe. A labelled oligo without extract was also used as control (P). The arrow indicates a specific band and the * sign indicates a non-specific band.

effectively competed for the observed band indicating that it is specific. The Myc DNA binding activity in the wild-type sample was low compared to that of the EBER line 127 extract. It was subsequently discovered that this sample was of not very good quality when an Sp1 EMSA was performed, which provides a normalising control for the quality and quantityof the samples (Figure 6.20). From the Sp1 EMSA, the EBER1 tumour sample was underloaded compared to the c-Myc and bi-transgenic samples which appeared of the same quality and quantity. The addition of anti-cMyc antibody did not appear to induce a mobility shift in the specific band, suggesting that it either did not work or the band observed is not c-Myc. Nevertheless, no difference in intensity was observed between the specific band in the c-Myc sample and the bi-transgenic sample, suggesting that the DNA binding activity of Myc is not increased in the bi-transgenic mice. As only one bi-transgenic tumour sample was tested by EMSA, the myc DNA binding activity should be explored further using different tumour samples in order to be able to fully conclude on this part.

6.4.3.2. Upregulation of Id2 in the bi-transgenic samples and EBER1 tumours

The protein level of Id2 was analysed in the EBER1 tumour samples by western blot using an anti-Id2 antibody (Figure 6.21). In order to identify the Id2 specific band, the membrane was stripped and re-probed with the anti-Id2 antibody and the Id2 blocking peptide. This blocked all bands and therefore specificity of Id2 could not be confirmed; however a band at the correct size (around 16kDa) was observed in some of the lanes. No Id2 signal was observed in the wild-type, the EBER1 positive young animal sample and also in the two tumour tissues of mouse 127.49 (previously described in chapter 5, figure 5.11). This tumour also showed a different Myc banding pattern on the EMSA (Figure 5.9, Chapter 5). However, a 16kDa band was observed for one EBER1 tumour (animal number 127.37), a pre-tumour sample (127.117), the two c-Myc tumour samples (97.1005 and 97127.13) and in the bi-transgenic tumour sample (97127.1), indicating that in these samples Id2 is upregulated and the signal appears of a similar intensity in these lanes. However, a loading control needs to be performed in order to conclude fully.

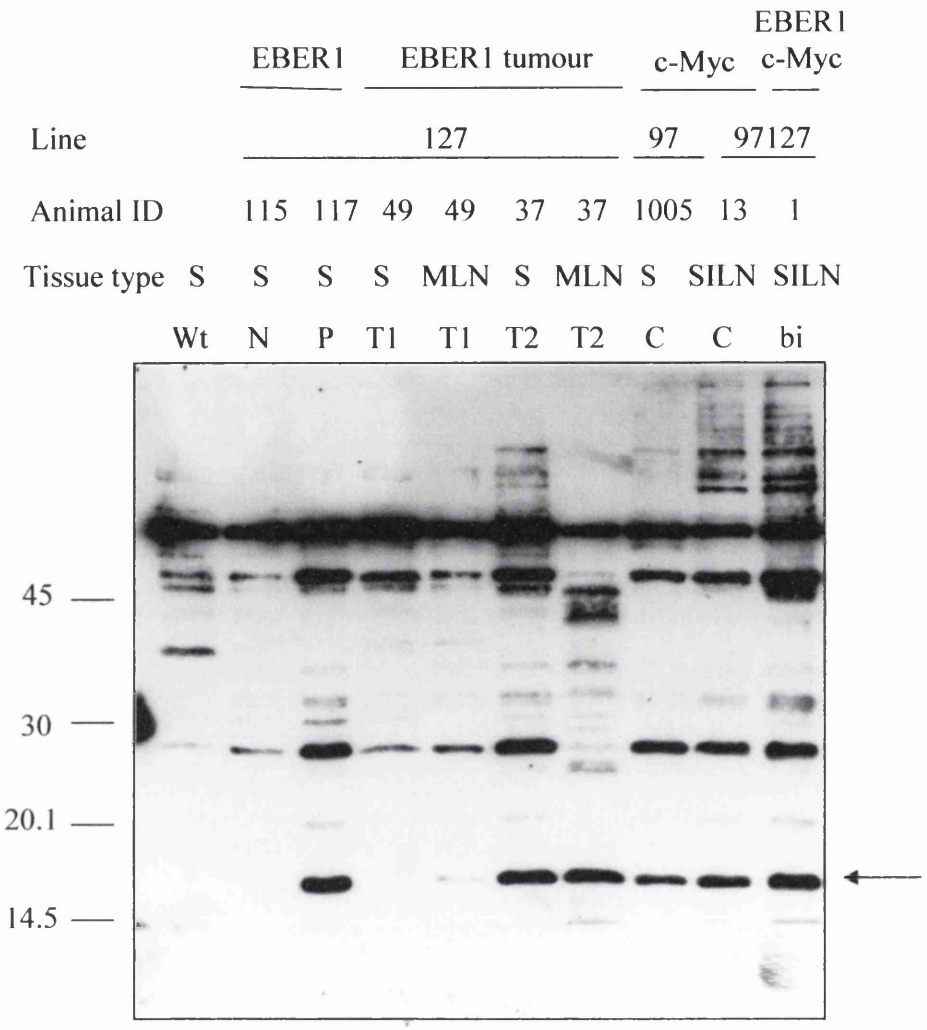

Figure 6.21: Id2 western blot of lines 127 and 97127 samples

Proteins from wild-type (Wt), EBER1 positive young animal (N) line 127, EBER1 pre-tumour (P) line 127, two EBER1 animals with tumours (T1 and T2), two different c-Myc tumour samples (C, line 97.1005 and 97127.13) and bi-transgenic tumour (bi) were extracted using the high salt nuclear extraction method. 100µg of proteins were separated by 12.5% SDS-PAGE and the gel was western blotted. The membrane was probed with a rabbit anti anti-Id2 antibody and followed by a goat anti-rabbit IgG-HRP secondary antibody and visualised using ECL+. The molecular weights according to the marker lane are shown. The Id2 band is indicated by an arrow and is running at 16kDa. S: spleen, MLN: mesenteric lymph nodes, SILN: superficial inguinal lymph nodes.

6.5. Summary

In this chapter, three cooperation studies are presented, which were undertaken in order to investigate if the tumours could develop more rapidly in bi-transgenic mice compared to EBER1 mice and also compared to the possible cooperating partner (EBNA1 or Myc). The first study involved EBNA1, another EBV latent gene which like EBER1 is expressed in all latencies. No cooperation was observed between EBNA1 and EBER1 in lymphomagenesis as the bi-transgenic mice have the same tumour onset as the EBNA1 mice. However the absence of the "tail" of the curve in the bi-transgenic mice compared to that of the EBNA1 mice suggests a possible additive effect between the two genes. The phenotype in the bi-transgenic EBER1/EBNA1 mice was the same as the one observed in the EBNA1 mice. This study was only undertaken with line 127.

EμEBER1 mice (lines 127 and 137) were crossed with EμN-myc mice, and the bi-transgenic mice succumbed to lymphoma on average at 214 days compared to 441.5 days for N-myc mice. It should be noted that a biphasic phenotype was observed for the N-myc animals, the first phase where a thymoma was detected (possibly indicative of a T cell lymphoma) when the mice were young and the second where lymphoma was observed in the lymph nodes and spleen, of B-cell type as previously described by Dildrop *et al.*, (1989) in older mice. The difference between the B-cell tumour onset of the bi-transgenic and the N-myc mice (excluding the presumed T-cell lymphoma) is statistically significant suggesting that the two genes cooperate in B-cell lymphomagenesis. The phenotype in the EBER1/N-myc bi-transgenic mice is the same as the one observed for the EμN-myc mice. It was also shown that the bi-transgenic tumours have a clonal IgH rearrangement, no TCR rearrangement and are B220 positive, indicating that they are of B cell origin (however the thymomas have not been tested for IgH or TCR rearrangement). The cooperation between EBER1 and N-myc is not due to either increased EBER1 or N-myc expression, nor to increased Myc DNA binding activity and therefore is due to complementarity in the actions of EBER1 and N-myc. No cooperation was yet observed between line 137 and EμN-myc; however it should be noted that mice of line 137 express EBER1 in the thymus.

The last cooperation study was between EμEBER1 (lines 127 and 136) and Eμc-myc. In these mice the two genes do not appear to cooperate in disease onset; however the studies were still underway at the time of submission. The phenotype observed in the bi-transgenic EBER1/c-Myc mice is the same as that of Eμc-myc mice. Following EMSA analysis the DNA binding activity of Myc was shown not to be increased in the bi-transgenic sample compared to the c-Myc sample tested. The expression of Id2 (a c-Myc regulated gene) was also similar in the bi-transgenic sample and the c-Myc samples.

Chapter 7. Discussion

The aim of the work presented in this thesis was to investigate the phenotypic consequences of expression of EBER1 *in vivo*. Before this project was started, reports demonstrated that transfection of EBERs into Akata EBV negative cells or BJAB rendered them malignant and resistant to apoptosis, suggesting a possible involvement of the EBERs in the disease process of EBV (Komano *et al.*, 1999, Yamamoto *et al.*, 2000). For this purpose, we sought to explore this hypothesis by generating transgenic mice expressing EBER1 and analysing their phenotype.

7.1. EBER1 transgenic mice

The design of the transgene was a critical step as the EBER1 gene promoter encompasses both RNA pol II and pol III elements (Howe and Shu, 1989). Therefore three different EBER1 constructs were generated. They each contain different promoter elements as it was unknown which construct would lead to *in vivo* expression. The expression of the transgene was targeted to the B cell compartment of the animal using the immunoglobulin heavy chain intronic enhancer Eμ. Expression of the three EBER1 constructs, either supercoiled plasmid or linear fragment, was observed in transient transfection assays of EBV negative B-cells. However the expression of EBER1 was higher from the supercoiled plasmids compared to that of the linear fragments as would be expected. This could be due to differences in transfection efficiencies, where transfection of a supercoil plasmid is more efficient than that of a linear fragment, or to the presence of the CMV promoter upstream of the Eμ in the supercoiled plasmids, which could lead to a higher expression level. However, these hypotheses were not tested, as this assay was performed to establish whether or not the constructs expressed EBER1. For both the supercoil and the linear fragments, the expression level of EBER1 was higher for constructs p670 and p671 compared to p672. This is in accordance with published work where it was shown that deletion of Sp1 and ATF sites dramatically reduced transcription of EBER1 following transfection assays (Wensing *et al.*, 2001).

Pronuclear microinjections of the three constructs were performed and 19 founders were generated (6 for p670, 3 for p671 and 10 for p672). For construct p670, 8.8% of the pups born were transgenic positive, for p671 5.2% pups born were transgenic positive and for p672, 9.8% pups born were transgenic positive. It has been estimated that 20% of pups born after pronuclear injections carry the transgene (Nagy *et al.*, 2003a). However, this does vary enormously depending on DNA concentration, lethality of the construct and experience of the individual. The low number of transgenic positive founders in this case, is reflective of the first few months of microinjection when the technique was learned and optimised. The number of founders increased once the technique was mastered.

For constructs p670 and p672, four founders (126, 128, 129 and 130) had a partial transgene when checked by PCR. It was subsequently determined that the two transgene preparations used for microinjection were partially degraded. New transgene preparations were then used for microinjections. The different transgene preparations were subsequently frequently checked for degradation.

68% of the founders were established into lines. It is usually estimated that between 20 to 30% of the founders are mosaïc (Wilkie *et al.*, 1986). This means that the transgene integrates after the cell started to divide; therefore not all the cells in the organism will carry the transgene. The mosaïc founders transmit the transgene at a lower frequency (which varies depending on the degree of mosaicism) compared to a non-mosaïc animal, which transmits the transgene to 50% of the offspring. The founders that were not established into lines include the four that had a partial transgene (126, 128, 129 and 130) and founders 140 and 144. However founder 144 was sterile as no offspring were generated when the mouse was set up in several breeding-pairs. The founders of lines 127 and 141 could also have been mosaics as only 32% and 11% of the offspring from the first generation were transgenic positive respectively.

When pronuclear microinjections are performed both the integration site and the copy number of the transgene cannot be controlled. The configuration of the integrated transgene is usually in head to tail tandem repeats and with multiple copies. The copy number for each line was determined using two different approaches. For lines 136, 141, 133 and 137 the copy number was found to be similar using both approaches. It was noted that the first approach had a maximum threshold and was under-estimating lines that had a

high copy number. Therefore this technique should be optimised (the enzyme quantity can be changed as well as the incubation time) in order to provide a more accurate copy number and the results compared to the numbers obtained with the second approach. Moreover, the samples could be electrophoresed longer in order to obtain better separation of the high molecular weight fragments.

7.2. Does the expression level of the transgene correlate with the construct?

The expression analysis was performed using total RNA extracted from different tissues followed by RT-PCR and Southern blotting, indicating that EBER1 expression in these lines is very low (Chapter 4). This was also observed in tissue culture assay following transient transfection of the linear fragments (Chapter 3). Line 133 is the only line tested where no expression of the transgene was detected, suggesting that in this line the transgene integrated into a "silent region", such as heterochromatin where the packing of the DNA is very dense and therefore proteins required for transcription cannot access these regions.

For all the other lines EBER1 expression was detected in the lymphoid tissues with different patterns and expression levels. Expression in the lymphoid tissues suggested that the Eμ enhancer was able to direct expression of a pol III transcript in a tissue specific fashion, especially for line 127 where expression was only observed in the lymphoid tissues and the brain. Although the data are not directly comparable and the method used to detect expression is not absolutely quantitative, the highest expressing lines from each construct were determined to be lines 136 and 142 for p670, 127 for p671, 131 and 137 for p672. A quantification of EBER1 expression level was then performed using the Peyer's patches and thymus samples of these lines. The results showed that the expression of EBER1 was not dependent on the construct; for example in the Peyer's patches, mice of line 127 (construct p671) have a higher expression level than mice of line 131 (construct p672) followed by mice of line 142 (construct p670), mice of line 137 (construct p672) and mice of line 136 (construct p670). This does not reflect the tissue culture observation where constructs p670 and p671 showed a higher level of EBER1 expression than construct p672 (Chapter 3) and also previously published data from transient transfection

assays using deletion mutants (Wensing *et al.*, 2001). Therefore in these mice, the level of EBER1 expression is independent of the different elements present on the promoter. This could be explained by the fact that the previous observations were only described following transient transfection assays as opposed to a "stable integration" in the mouse. It would be of interest to examine EBER1 expression level following stable transfections of the three constructs and determine if they are construct dependent or independent. In this assay it was also determined that the EBER1 expression level was lower than that of established BL cell lines.

7.3. Does the expression pattern of the transgene correlate with the construct?

For both lines of construct p670, the highest EBER1 expressing tissue was the thymus followed by the peripheral lymph nodes, mesenteric lymph nodes, bone marrow and Peyer's patches for line 136 and bone marrow, spleen and liver for line 142. In addition line 136 was shown to express EBER1 in several non-lymphoid tissues at a low level. Line 127 (construct p671) was shown to express EBER1 at a relatively high level in Peyer's patches followed by the thymus, peripheral lymph nodes and bone marrow and expression was also detected in the brain but not in any other non-lymphoid tissue tested. For line 145, the second p671 line, the highest EBER1 expressing tissue was the peripheral lymph nodes followed by mesenteric lymph nodes, spleen and thymus. For the p672 construct (lacking all the EBER1 upstream motifs apart from the TGTA box and only including the Eμ), the expression patterns were also very variable between the lines, with line 131 highest expressing tissues being the peripheral lymph nodes and mesenteric lymph nodes followed by bone marrow, spleen, thymus and Peyer's patches. Expression was also detected in several non-lymphoid tissues tested. Line 132 expression was medium in the thymus and low in the other lymphoid tissues tested. For line 134 EBER1 expression was high in the spleen and low in mesenteric lymph nodes and thymus, whereas line 135 only showed high expression in the thymus. The highest EBER1 expressing tissue for line 137 was the thymus and expression was very low in other lymphoid and non-lymphoid tissues tested. Line 138 was shown to express EBER1 at a relatively high level in peripheral lymph nodes followed by thymus. As expression was also detected in several non-lymphoid tissues for a few lines it could suggest that the transgene has integrated near a

cellular gene which could influence the expression pattern or that the transgene was not sufficiently lymphoid specific. However, expression in non-lymphoid tissues is not uncommon in Eμ transgenes and was also observed in other studies (Dildrop *et al.*, 1989, Wilson *et al.*, 1990, Alkema *et al.*, 1997). Although the Eμ enhancer was used to direct expression to the B cell compartment, several lines (127, 135, 137, 138) showed relatively high expression in the thymus and it is also not unsual for transgenic mice with an Eμ enhancer to express the transgene in T cells. For instance, EμLmyc mice and Eμ-IEX-1 mice develop T cell lymphomas and EμBim1 mice are highly susceptible to both T and B cell lymphomas (Moroy *et al.*, 1990, Zhang *et al.*, 2003, Alkema *et al.*, 1997). Despite this, lymphomas in 127 mice were shown to be of B-cell origin.

In conclusion, the pattern of expression was found to be variable within and between constructs, showing no correlation with the transgene construct.

7.4. Does EBER1 expression *in vivo* affect the dsRNA interferon response?

EBER1 was shown to have a role in the inhibition of the anti-viral effect of IFN. It was demonstrated that EBER1 could bind PKR and inhibit its activation both *in vitro* and *in vivo* (Clarke *et al.*, 1991, Sharp *et al.*, 1993, Yamamoto *et al.*, 2000, Nanbo *et al.*, 2002). Thus the possible involvement of EBER1 in the inhibition of an IFN response in the EμEBER1 mouse model was tested following injection of dsRNA (pIC) in the tail vein of the animal. In the spleen of line 127 transgenic positive mice a very slight activation of PKR was observed and considered negligable compared to that of wild-type mice, which is in accordance with previous reports. However, eIF2α, which is a PKR substrate, was shown to be phosphorylated in both wild-type and transgenic positive mice treated with pIC, suggesting that in this tissue EBER1 does not block phosphorylation of eIF2α. The DNA binding activity of NFκB remained unchanged following pIC treatment in both wild-type and transgenic positive mice, which was surprising as an increase in NFκB DNA binding activity was expected at least for the wild-type samples following treatment, suggesting that either the EMSA performed was not sufficiently sensitive or that the effect of PKR on NFκB occurs at a later time point than the one used for collecting the tissues. In order to explore this result further a western blot with an anti-total IκB antibody could be

performed, as IκB is a PKR substrate, and a decrease in the total level of IκB would imply activation of NFκB. Stat1, which is invoved in the IFN signalling pathway, was shown to be upregulated and activated following pIC treatment in both wild-type and transgenic positive mice. However a different result was observed when thymus protein extracts of mice of lines 127 and 137 were used. For instance, Stat1 was not upregulated and activated following pIC treatment in the transgenic positive samples when compared to wild-type. This would suggest that EBER1 is blocking Stat1 expression and activation by a yet unknown mechanism in this tissue. It should be noted that in the thymus of mice of both lines 127 and 137 EBER1 expression is higher and could explain the different result for Stat1 between the spleen and thymus of line 127. It would be interesting to determine the status of PKR and eIF2α in the thymic protein extracts. If both PKR and eIF2α are not phosphorylated it would suggest that EBER1 does inhibit the IFN response via PKR in this tissue and that a higher expression level of EBER1 is needed to achieve it. If they are both phosphorylated and the inhibition of Stat1 expression and activation is confirmed, it would suggest that EBER1 is able block the IFN signalling pathway via Stat1 by a yet unknown mechanism. A report was recently published showing that following IFNα treatment of both EBER positive and negative BL cells, PKR was upregulated and activated and eIF2α was also phosphorylated (Ruf *et al.*, 2005), suggesting that protection against IFNα apoptosis was not due to inhibition of PKR by EBERs and contradictory to previous findings by other groups. It could be possible, considering the results presented in this thesis, that induction of Stat1 was inhibited in Ruf and colleagues' assays and therefore lead to inhibition of apoptosis. However, Ruf and colleagues' experiments were performed following IFNα treatment as opposed to pIC treatment as described here. Thus it would be interesting to examine the results from the thymocyte and splenocyte explants for lines 127 and 137 following various treatments (pIC or IFNα) and determine if they follow the same trend as the one observed with the tissues. This assay would also enable the direct comparison between pIC and IFNα treatment and provide more insight into the relationship between PKR and EBER1.

In conclusion, following dsRNA treatment in the spleen of line 127 transgenic positive mice, EBER1 may be blocking PKR but this is not apparent in its substrates or Stat1 and therefore the IFN response might not be blocked in this tissue. However, with higher EBER1 expression in the thymus of lines 127 and 137 transgenic positive mice,

Stat1 induction is blocked, which may indicate a new mechanism of EBER1 action in the IFN response. However activation of PKR and its substrates has yet to be analysed in this tissue.

7.5. Does EBER1 expression *in vivo* predispose to tumourigenesis?

53% of the transgenic positive mice in the phenotype watch of line 127 animals developed lymphomas with a late onset compared to 12.5% in controls. The average age of tumour development was 18 months. The late onset could be due to the low expression of EBER1 in the tissues. However, the development of B-cell lymphomas in these mice suggests an oncogenic role for EBER1, independent of the presence of other viral genes and thus implicating EBER1 in the pathogenesis of EBV associated tumours at least in B-cell tumours. The development of lymphomas in other independent lines would further support this and the phenotype watches were still underway at the time of writing. As mice of line 127 have developed lymphomas so far, the hypothesis that the phenotype could be caused by an insertional mutation in this line cannot be excluded. The transgene could have inserted near an oncogene or have disrupted a gene. To investigate if this is the case, the site of insertion of the transgene could be determined and the genes in close proximity to the transgene which could potentially influence the phenotype observed would then be identified. Two known oncogenes, Araf and Elk1, and members of the Ras and myc families are located on the X chromosome and therefore could influence the phenotype in this line as the transgene was shown to be X-linked (Chapter 3).

The animals in the other lines under phenotype watches are now reaching the age of lymphoma onset of line 127 and so far one mouse has succumbed to lymphoma at 13.5 months of age for line 131. The repeated observation of lymphoid expansion in younger animals of lines 137 and 136, which is statistically significant (summary in table 7.1), is an encouraging sign and one could predict that animals in these 2 lines will develop lymphoma, as lymphoid expansion was also observed in young line 127 mice but not in any negative controls. In mice of line 145 a phenotype comprising of multiple lymph nodes at several locations (instead of the usual one) was observed in young animals (Table 7.1) and is statistically significant.

Line / Age months	127	131	132	134	135	136	137	138	142	145 *	Negative
> 19 – 24 ≤	5/8										1/12
> 14 - 19 ≤	4/5										1/6
> 10 – 14 ≤	3/5	1/1									0/9
> 6 – 10 ≤	10/16		0/3		1/1	4/8	6/6			2/3	0/26
> 3 – 6 ≤	2/15	0/5	0/2	0/2			5/8	0/2	1/2	0/1	0/30
≤ 3	4/6				0/1	2/2				2/2	0/7
P χ^2	<0.001					<0.001	<0.001				
P Fisher's exact		0.18			0.065				0.065	0.00007	

Table 7.1: Summary of the lymphoid pathology in several EμEBER1 lines

This table presents the number of transgenic positive animals which have either developed a lymphoma or shown signs of lymphoid expansion out of the total number of animals examined for different age categories. Each of the lines expressing EBER1 is presented as well as negative controls. The negatives were siblings combined from different lines but all with the same strain background. The majority of negative mice examined in the 19-24 months category were taken at 23/24 months at the end of study (tumour watch study). Generally mice examined under 1 year old were taken in cohort groups (without phenotypic selection) for particular studies (eg. Expression analysis). The * sign indicates that for line 145 an increase in the number of lymph nodes was observed but no expansion. The P values calculated from a chi squared (P χ^2) test or a Fisher's exact (P Fisher's exact) test are presented for some of the lines.

Cross-breeding studies have shown that EBER1 (line 127) cooperates with N-myc in B-cell lymphomagenesis, whereas no cooperation was observed between EBER1 (line 127) and EBNA1 or EBER1 (lines 127 and 136) and c-Myc.

Several approaches have been taken to investigate the mechanism of tumour formation in mice of line 127. It was shown that it was not likely to be due to increased EBER1 expression in the tumour samples, although the approach used was not fully quantitative. The expression level of c-Myc was shown to be unchanged in pre-tumour and line 127 tumour samples as compared to wild-type. No rearrangement in the c-Myc locus in the EμEBER1 tumours was observed. However, this technique only examines rearrangements in close proximity to the *myc* locus and therefore does not provide any information with respect to possible trisomy or translocation at greater distance from *myc*, which could have occurred. Trisomy of chromosome 15 (carrying *c-myc*) was previously observed with EμEBNA1 mice of line 26 (Drotar *et al.*, 2003). Despite no apparent increase in c-Myc expression levels, the DNA binding activity of Myc was increased in the two 127 tumour samples tested when compared to wild-type mice. However two different results were obtained; the DNA binding activity of sample 127.37 resembled that of the transgenic c-Myc control sample, whereas for sample 127.49 two extra specific bands were observed suggesting that in this tumour additional protein complexes, such as other members of the Myc family, Max, members of the Mad family and Mnt, bind to this oligo.

Id2 is a member of the Id family of genes which are basic helix-loop-helix proteins lacking a DNA binding domain (Perk *et al.*, 2005, for review). The Id proteins were found to be upregulated in many cancers including BL (Nilsson *et al.*, 2004). Id2 was shown to be the only member of the Id family able to bind to hypo-phosphorylated Rb and lead to cell cycle progression (Iavarone *et al.*, 1994). As Id2 was shown to be a transcriptional target of c-Myc (Lasorella *et al.*, 2000), Id2 expression was analysed in line 127 tumour samples. Id2 was found to be upregulated in the sample (127.37) with the same DNA binding profile as that of the c-Myc sample by EMSA, whereas no Id2 expression was detected for sample 127.49 with the extra EMSA bands. This suggests that for mouse 127.37 Id2 was implicated in the mechanism leading to tumour formation, possibly by enhancing cycle progression. Due to time limitations, other 127 tumour samples were not analysed for Id2 expression but it would be interesting to determine in which category they

fall. However, this result suggests that in some cases EBER1 expression could lead to upregulation of genes involved in cell cycle progression.

In order to assess if EBER1 and c-Myc cooperate in lymphomagenesis EμEBER1 mice (lines 127 and 136) were crossed with Eμc-myc mice. From the data obtained the two genes do not appear to cooperate in lymphomagenesis, thus indicating that either the two genes have redundant modes of action or that c-Myc is such a powerful oncogene in itself that only the presence of another strongly expressed oncogene with a complementary function would accelerate tumour onset, as described when Eμc-myc mice were crossed with EμBcl$_2$ mice (Strasser *et al.*, 1990). With the 97136 cross more bi-transgenic mice are needed in order to perform a thorough analysis, but so far the results indicate that the presence of the c-Myc binding site on the EBER1 promoter does not lead to increased tumour onset when c-Myc is over-expressed. However, it would be interesting to determine if EBER1 expression is changed in the 97136 bi-transgenic mice, which could provide more information on the involvement of the c-Myc binding site in EBER1 transcription. Analysis of a bi-transgenic 97127 tumour sample showed that Myc DNA binding activity and Id2 expression were unchanged when compared to a c-Myc (97) sample.

As EμN-myc mice develop B-cell lymphoma with a longer latency than Eμc-myc mice, a cross-breeding programme was undertaken between EμN-myc and EμEBER1 (lines 127 and 137) to determine if the two genes could cooperate in lymphomagenesis. A biphasic phenotype was observed for the N-myc animals, the first phase being a thymoma, possibly indicative of a T cell lymphoma, which was detected in young mice and the second one being a B-cell lymphoma involving enlargement of the lymph nodes and spleen as previously described by Dildrop *et al.*, (1989) in older mice. In their study, N-myc was found to be highly expressed in the spleen and to a lower extent in the thymus, which is indicative of both B and T cell expression. As N-myc is less oncogenic than c-Myc in B cells it could allow for a T cell phenotype to develop. In order to determine if the animals succumbing to a thymoma developed a T cell lymphoma, the samples should be analysed for T cell receptor rearrangement. The result from this experiment will be used to determine if these animals should be excluded from the B-cell lymphoma incidence in this study. If they are included the difference in tumour incidence between N-myc mice and bi-

transgenic mice (96127) was not found to be statistically significant, and therefore would indicate that the two genes do not cooperate in lymphomagenesis. However, it should be noted that the median age for both groups is very different with the bi-transgenic (96127) mice succumbing to lymphoma twice as fast as N-myc mice, which is indicative of an accelerated phenotype and would tend to suggest a possible cooperation between the two genes. This was supported when the mice with a thymoma were excluded from the B-cell lymphoma incidence as the difference between the two curves was found to be statistically significant. It would be interesting to compare these results with the 96137 study upon completion. If both studies show similar results it will be strongly indicative of a cooperation between EBER1 and N-myc in B-cell lymphomagenesis. The bi-transgenic 96127 tumours were shown to be of B cell origin as was previsouly described for N-Myc by Dildrop *et al.*, (1989). To investigate the mechanism of cooperation between the EBER1 and N-myc, expression of EBER1 was analysed in bi-transgenic samples and compared to EBER1 tumour samples and was shown to be unchanged, although the method used was not entirely quantitative. N-myc expression level was unchanged when the bi-transgenic and N-myc tumour samples were compared. It was noted that the expression level of the 66kDa protein in a thymoma (sample 37 T on the blot) was low, suggesting that the phenotype in this mouse arose by a different mechanism and would favour the removal of the mice succumbing with a thymoma from this study. However in order to conclude fully on this, N-myc expression should be analysed in different thymomas. A higher band was also observed on the blot (in all N-myc and bi-transgenic samples) and like the N-myc band was blocked with the N-myc blocking peptide. One hypothesis is that this band could be reflective of an N-myc (homo or hetero) dimer. It could also be an N-myc related protein of high molecular weight, as it is specific to the peptide. The Myc DNA binding activity was the same in the N-myc and bi-transgenic samples. These results suggest that the cooperation mechanism between EBER1 and N-myc is likely due to the complementary actions of both genes. One could imagine that EBER1 could complement the action of N-myc with an anti-apoptotic activity.

As mentioned previously, EBER1 and EBNA1 do not cooperate in lymphomagenesis, thus indicating that the two genes are redundant and possibly activate pathways of similar functions in the cell leading to the phenotype observed. It was previously shown in the laboratory that EBNA1 expression in transgenic mice lead to increased expression of Bcl_{XL} and increased survival via upregulation of a cytokine, IL2

(Tsimbouri *et al.*, 2002). It was previously observed that EBER expression led to increased Bcl_2 expression in BL (Komano *et al.*, 1999). Therefore, it is possible that in line 127 EBER1 could lead to the upregulation of an anti-apoptotic gene such as Bcl_2 or even Bcl_{XL}. Hence, it would be of interest to determine the expression level of these genes in different EBER1 tumours and compare it with pre-tumour samples. Expression of EBER1 in transgenic positive mice could lead to increased survival and also upregulate a B cell growth or survival factor. It was observed in BL cell lines that EBERs increased expression of IL10 (Kitagawa *et al.*, 2000). In the serum of mice of lines 127 and 137 several cytokines were tested and the results may indicate increased levels for some of them; however these results need to be confirmed with other serum samples. Amongst these cytokines, IL10 level was increased in samples from line 127 young animals and from older animals with tumours. This upregulation was not observed in the serum of mice of line 137. As IL10 is used as an autocrine growth factor for B-cells (Rousset *et al.*, 1992) it is possible that sustained IL10 secretion might promote tumour formation in B-cells. IL10 was shown to inhibit NFκB activity (Driessler *et al.*, 2004) in human monocytic cells and it is possible that a similar effect occurs in B-cells. If true, IL10 upregulation by EBER1 could lead to inhibition of IFNβ expression and also expression of other essential genes involved in apoptosis, for example, which contain an NFκB binding site in the promoter. An NFκB binding site was found in the p100 form of human 2'5'OAS (three 2'5'OAS isoforms have been identified, p40/46, p69/71 and p100) (Rebouillat *et al.*, 2000) and also in the promoter of the murine PKR gene (Tanaka and Samuel, 1994). Therefore, one can hypothesise that inhibition of NFκB by IL10 could block expression of both PKR and 2'5'OAS, which would then impair the IFN response. It would be interesting to determine by which mechanism EBER1 upregulates IL10 expression as it would give further insight into its oncogenic role.

Another possibility is via PKR, as it has been shown that EBER1 blocks PKR actions *in vitro* and *in vivo* (Clarke *et al.*, 1991, Sharp *et al.*, 1993, Yamamoto *et al.*, 2000, Nanbo *et al.*, 2002). This is supported by a report where a mutant PKR was shown to enhance tumourigenesis (Koromilas *et al.*, 1992, Meurs *et al.*, 1993). This mechanism could involve the extensive enhancement of protein synthesis from both cellular and viral mRNA. However, this has yet to be confirmed in the EμEBER1 mice as PKR activation following pIC treatment was inhibited (in the spleen of mice of line 127) but not

eIF2α phosphorylation. Moreover a recent report has suggested that the anti-apoptotic actions of EBER are not mediated by PKR (Ruf *et al.*, 2005), thus suggesting alternative mechanisms independent of PKR. This could be mediated via Stat1, as it was not induced or activated in the thymus of lines 127 and 137 following pIC treatment and its loss of expression has previously been implicated in oncogenesis (Kaplan *et al.*, 1998). A report showed that following dsRNA treatment, PKR induced phosphorylation of p38 (Silva *et al.*, 2004), which then leads to the activation of Stat1 (Ser 727) (Goh *et al.*, 1999). Therefore it is possible that EBER1 acts via p38 and inhibits its phosphorylation, leading to inhibition of Stat1 activation, which would promote anti-apoptotic effects. However p38 phosphorylation was not analysed in the samples following pIC treatment.

MicroRNA (miRNAs) are derived from long double-stranded transcripts (pri-miRNA) with a high degree of secondary structure and are processed by Drosha, an RNase III endonuclease, to generate a precursor miRNA (pre-miRNA), which is then exported to the cytoplasm. The pre-miRNA is then processed by Dicer (which is the same enzyme that processes dsRNA to siRNAs), another RNase III endonuclease, to generate a miRNA, which will be taken up by the RNA induced silencing complex (RISC) leading to either mRNA degradation or translation inhibition (Bartel, 2004, for review). A miRNA polycistron (*mir*-17-92) was recently reported to be acting like an oncogene. It was found amplified in different B lymphoma samples as compared to wild-type samples and was shown to cooperate with c-Myc to accelerate tumour onset (He *et al.*, 2005). As EBER1 is an RNA with a high degree of secondary structure and was shown to cooperate with N-myc in B-cell lymphomagenesis, it can be hypothesised that EBER1 could be the precursor of a miRNA. It is possible that the EBER1 miRNA could originate from the usual start or from the upstream start of EBER1. This was demonstrated in different EμEBER1 transgenic lines (127 and 131, possibly 137) and confirmed in Raji using an RT-PCR approach and to date has an unknown function (Chapter 4, Jat and Arrand, 1982, Arrand and Rymo, 1982). Therefore future work to test this would be to detect if EBER1 can lead to production of a miRNA and also if the level of this EBER1 miRNA increases between a pre-tumour tissue and a tumour tissue. If EBER1 is a miRNA it could also down-regulate the expression of genes which negatively regulate anti-apoptotic genes, thus leading to overexpression of these anti-apoptotic genes. A recent study has shown that two miRNAs, *miR-15a* and *miR-16-1*, act as tumour suppressor genes. In chronic lymphocytic leukaemia,

miR-15a and *miR-16-1* have been shown to either be down-regulated or deleted, which leads to the upregulation of Bcl2 (Cimmino *et al.*, 2005). A study using BL41/B95.8 cells reported the identification of 5 miRNAs expressed by EBV; however the EBERs were not included (Pfeffer *et al.*, 2004). The same group also reported the identification of miRNAs from several members of the herpesviridae (Pfeffer *et al.*, 2005).

The development of cancer involves a succession of events and therefore EBER1's actions as an oncogene could combine more than one mechanism suggested here.

7.6. How does EBER1 contribute to the actions of EBV in healthy individuals?

Following a viral infection dsRNA is produced, from viral replication and protein synthesis, which can trigger the induction of an immune response (eg IFN response) in the infected cell. This may lead to death of this cell and neighbouring cells. One of the best characterised functions of the EBERs is to block the IFN response via binding of PKR and inhibition of its autophosphorylation. This enables the virus to evade the IFN response and also to control protein synthesis, as one of the substrates of PKR is the translation initiation factor eIF2α. Therefore viral proteins can be expressed and the infected cell does not die. The EBERs have also been reported to inhibit apoptosis under other conditions (Nanbo *et al.*, 2002, Wong *et al.*, 2005) and therefore could promote survival of the virus infected cells. Recently the EBERs have been suggested to contribute to the immortalisation process using EBER-deleted virus and EBV Akata negative cells (Yajima *et al.*, 2005). This could be mediated by the expression of IL10, which could provide an autocrine growth factor to the infected cells and ensure their longer-lived status. IL10 also inhibits Th1 response and favours a Th2 response (Kidd, 2003, for review). As IFNγ is produced by differentiated Th1 cells (Murphy and Reiner, 2002, for review) one can hypothesise that the IL10 induced skew towards Th2 cells mediated by the EBERs would lead to a reduction in IFNγ production. Therefore, as well as restricting the production of IFNα and IFNβ the EBERs could also control the response mediated by IFNγ. For the virus, this would provide evasion from the IFN systems and thus contribute to establishing life-long viral persistence.

In this study it was also shown that the presence of EBER1 did not change the proportions of B and T cells or their status in the transgenic mice, suggesting that EBER1 does not interfere with B and T cell development (Chapter 5). However it should be noted that in the Peyer's patches of line 127 transgenic positive mice, there was a skew towards a possible B1 population when compared to wild-type animals. This increase in B1 cells was also described in LMP2A transgenic positive animals (Ikeda *et al.*, 2004). This skew in both cases could be due to the system used (eg expression in transgenic mice) rather than to a function that would manifest also during viral infection. However, if EBER1 and LMP2A favour the development of B1 cells as opposed to B2 cells following EBV infection, this could be advantageous for virus persistence as B1 cells are longer lived then B2 cells (Berland and Wortis, 2002, Martin and Kearney, 2001, for reviews).

It was recently demonstrated that adenovirus VAI and VAII RNA inhibited RNA interference (RNAi) resulting from small hairpin RNAs (shRNAs) and pre-miRNAs (Lu and Cullen, 2004, Andersson *et al.*, 2005). It was shown that this effect was mediated through competitive binding to both exportin 5 nuclear export factor and the RNase III Dicer. The VA RNAs were shown to be processed by Dicer into siRNAs and incorporated by RISC. As the EBERs share similar properties with the VAs (pol III transcripts with a high degree of secondary structure that bind and inhibit PKR) and were shown to functionally replace the VAs in a mutant Adenovirus lacking VA genes (Bhat and Thimmappaya, 1983, Bhat and Thimmappaya, 1985), one can hypothesise that the EBERs could also function as suppressors of RNAi in EBV infected cells and thereby contribute to the persistence of the infected cells.

7.7. Future directions

As this is the first report describing the generation of transgenic mice expressing a pol III gene following pronuclear microinjection, it is of particular importance to fully determine if the transgene produces a pol II or pol III transcript. An RT-PCR approach was undertaken and showed that the EBER1 transcript in different lines (127, 131, 134, 136 and 137) does not contain a polyA tail, therefore indicating that it could be a pol III transcript (Chapter 4). To further confirm this in the transgenic mice, a primer extension assay using an EBER1 specific reverse primer could be performed. A run on assay could

also be performed using nuclei isolated from an EBER1 transgenic mouse tissue with and without α-amanitin treatment. If EBER1 in the transgene mice is confirmed to be a pol III transcript this study would be the first report describing the generation of transgenic mice expressing a pol III gene.

As EBER1 was previously shown to bind to PKR and inhibit its activation, it would be of interest to analyse the kinase activity of PKR in EμEBER1 lines and possibly in the tumour samples. This would confirm if PKR is involved in the oncogenic properties of EBER1. However it should be noted that kinase activity of PKR might be increased in the samples, as it has been shown that L22 could regulate PKR activity through its ability to sequester EBER1 (Elia *et al.*, 2004). Therefore it would also be of interest to analyse L22 in these samples. EBER1 has also been shown to bind and activate 2'5'OAS *in vitro*. It would be of interest to assess 2'5'OAS activity in the transgenic positive mice and determine if it is also activated *in vivo*. This could be performed by monitoring RNase L activity, as RNase L is activated by 2'5'A which are synthesised by activated 2'5'OAS, using one of the protocols described by Player *et al.*, (1998).

The mechanism by which EBER1 exerts its actions remains largely unknown. To explore this, the establishement of an EBER1 expressing cell line derived from a tumour tissue would be a very useful tool. This has been attempted but has yet to be successful.

If the EBERs can act to suppress RNAi, as hypothesised in section 7.6, it is possible to imagine that EBER1 in line 127 mice could compete for Dicer binding and therefore inhibit the processing of some transcripts which would normally lead to inhibition of their target genes. In this case, the intact target genes would still be present in the cells and could therefore lead to a tumour phenotype. Moreover if the EBER1 can be processed into a functional siRNA, it could potentially target a tumour suppressor gene and lead to its mRNA degradation. Thus it would be interesting to determine if the activity of Dicer is changed in EBV positive BL cells as compared to EBV negative BL cells, as well as in the mice samples and if the EBERs can be processed into functional siRNAs. EBER1 could also regulate its own expression with this process, as its high expression could be toxic to the cells, and thus modulate its effects.

As EBER1 might be implicated in the disease process of the virus, it would be a good target for therapeutic purposes in EBV infected cells. Therefore the properties of EBER1 (and EBER2) can be used to develop assays to either inhibit their expression or to use their properties. For instance, one could imagine that the IFN response could be restored in EBV infected cells if EBER1/EBER2 expression is inhibited. siRNAs targeting both genes could be transfected into EBER expressing cells and followed by either IFNα or pIC treatment to induce an IFN response. If the EBERs are inhibited it could lead to apoptosis of the cells. If the proof of concept is validated in BL cell lines it can then be tested *in vivo* by injecting the EBER1 siRNA into the tail vein of EμEBER1 mice as described by Lewis *et al.*, (2002), followed by either IFNα or pIC treatment and analysis of the response in tissues expressing EBER1.

This project was conducted using EBER1 and no investigation into the role of EBER2 was performed. Due to the similarities between EBER1 and EBER2 one can hypothesise that they might act in a similar fashion. Therefore EBER2 could also have oncogenic properties in B-cells *in vivo*. To test this, one could generate EBER2 transgenic mice; however tumours might develop with a long latency as was observed for EBER1 (line 127). The generation of EBER1-EBER2 transgenic mice might provide more information on the properties of the EBERs *in vivo* and it might also lead to shorter tumour latency as the expression might be higher in the cells when both genes are present. The fact that both EBER1 and EBER2 are present in EBV infected cells (as are VAI and VAII in adenovirus infected cells) and also in EBV associated malignancies leads to the hypothesis that both genes are needed for a full phenotype. However, the presence of two slightly different genes having similar roles is intriguing and could suggest that they might have different functions. An upstream transcription start was detected for the EBER1 gene, which led to the expression of a minor EBER1 species (Chapter 4, Jat and Arrand, 1982, Arrand and Rymo, 1982). However Arrand and colleagues did not observe this minor species for EBER2. Therefore, the minor EBER1 species could provide other functions for EBER1 that EBER2 would not have. It would be of interest to test if EBER2 is a miRNA precursor and therefore can lead to the production of a miRNA. EBER2 could also act to suppress RNAi (like the VA RNAs). One could determine if EBER2 can compete for Dicer binding and can be processed into a functional siRNA.

References

Abbot, S.D., Rowe, M., Cadwallader, K., Ricksten, A., Gordon, J., Wang, F., Rymo, L. and Rickinson, A.B. (1990) Epstein-Barr virus nuclear antigen 2 induces expression of the virus-encoded latent membrane protein. *J Virol*, **64**, 2126-2134.

Adams, A. (1987) Replication of latent Epstein-Barr virus genomes in Raji cells. *J Virol*, **61**, 1743-1746.

Adams, J.M., Harris, A.W., Pinkert, C.A., Corcoran, L.M., Alexander, W.S., Cory, S., Palmiter, R.D. and Brinster, R.L. (1985) The c-myc oncogene driven by immunoglobulin enhancers induces lymphoid malignancy in transgenic mice. *Nature*, **318**, 533-538.

Adhikary, S. and Eilers, M. (2005) Transcriptional regulation and transformation by Myc proteins. *Nat Rev Mol Cell Biol*, **6**, 635-645.

Alkema, M.J., Jacobs, H., van Lohuizen, M. and Berns, A. (1997) Pertubation of B and T cell development and predisposition to lymphomagenesis in Emu Bmi1 transgenic mice require the Bmi1 RING finger. *Oncogene*, **15**, 899-910.

Allan, G.J., Inman, G.J., Parker, B.D., Rowe, D.T. and Farrell, P.J. (1992) Cell growth effects of Epstein-Barr virus leader protein. *J Gen Virol*, **73 (Pt 6)**, 1547-1551.

Allday, M.J. and Farrell, P.J. (1994) Epstein-Barr virus nuclear antigen EBNA3C/6 expression maintains the level of latent membrane protein 1 in G1-arrested cells. *J Virol*, **68**, 3491-3498.

Amon, W. and Farrell, P.J. (2005) Reactivation of Epstein-Barr virus from latency. *Rev Med Virol*, **15**, 149-156.

Andersson, M.G., Haasnoot, P.C., Xu, N., Berenjian, S., Berkhout, B. and Akusjarvi, G. (2005) Suppression of RNA interference by adenovirus virus-associated RNA. *J Virol*, **79**, 9556-9565.

Arrand, J.R. and Rymo, L. (1982) Characterization of the major Epstein-Barr virus-specific RNA in Burkitt lymphoma-derived cells. *J Virol*, **41**, 376-389.

Arrand, J.R., Young, L.S. and Tugwood, J.D. (1989) Two families of sequences in the small RNA-encoding region of Epstein- Barr virus (EBV) correlate with EBV types A and B. *J Virol*, **63**, 983-986.

Babcock, G.J., Hochberg, D. and Thorley-Lawson, A.D. (2000) The expression pattern of Epstein-Barr virus latent genes in vivo is dependent upon the differentiation stage of the infected B cell. *Immunity*, **13**, 497-506.

Bach, E.A., Tanner, J.W., Marsters, S., Ashkenazi, A., Aguet, M., Shaw, A.S. and Schreiber, R.D. (1996) Ligand-induced assembly and activation of the gamma interferon receptor in intact cells. *Mol Cell Biol*, **16**, 3214-3221.

Banerji, J., Olson, L. and Schaffner, W. (1983) A lymphocyte-specific cellular enhancer is located downstream of the joining region in immunoglobulin heavy chain genes. *Cell*, **33**, 729-740.

Bartel, D.P. (2004) MicroRNAs: genomics, biogenesis, mechanism, and function. *Cell*, **116**, 281-297.

Baumforth, K.R., Young, L.S., Flavell, K.J., Constandinou, C. and Murray, P.G. (1999) The Epstein-Barr virus and its association with human cancers. *Mol Pathol*, **52**, 307-322.

Berland, R. and Wortis, H.H. (2002) Origins and functions of B-1 cells with notes on the role of CD5. *Annu Rev Immunol*, **20**, 253-300.

Bhat, R.A., Domer, P.H. and Thimmappaya, B. (1985) Structural requirements of adenovirus VAI RNA for its translation enhancement function. *Mol Cell Biol*, **5**, 187-196.

Bhat, R.A. and Thimmappaya, B. (1983) Two small RNAs encoded by Epstein-Barr virus can functionally substitute for the virus-associated RNAs in the lytic growth of adenovirus 5. *Proc Natl Acad Sci U S A*, **80**, 4789-4793.

Biggin, M., Bodescot, M., Perricaudet, M. and Farrell, P. (1987) Epstein-Barr virus gene expression in P3HR1-superinfected Raji cells. *J Virol*, **61**, 3120-3132.

Birnboim, H.C. and Doly, J. (1979) A rapid alkaline extraction procedure for screening recombinant plasmid DNA. *Nucleic Acids Res*, **7**, 1513-1523.

Bochkarev, A., Barwell, J.A., Pfuetzner, R.A., Furey, W., Jr., Edwards, A.M. and Frappier, L. (1995) Crystal structure of the DNA-binding domain of the Epstein-Barr virus origin-binding protein EBNA 1. *Cell*, **83**, 39-46.

Borza, C.M. and Hutt-Fletcher, L.M. (2002) Alternate replication in B cells and epithelial cells switches tropism of Epstein-Barr virus. *Nat Med*, **8**, 594-599.

Bradford, M.M. (1976) A rapid and sensitive method for the quantitation of microgram quantities of protein utilizing the principle of protein-dye binding. *Anal Biochem*, **72**, 248-254.

Brinster, R.L., Chen, H.Y., Messing, A., van Dyke, T., Levine, A.J. and Palmiter, R.D. (1984) Transgenic mice harboring SV40 T-antigen genes develop characteristic brain tumors. *Cell*, **37**, 367-379.

Brinster, R.L., Chen, H.Y., Trumbauer, M., Senear, A.W., Warren, R. and Palmiter, R.D. (1981) Somatic expression of herpes thymidine kinase in mice following injection of a fusion gene into eggs. *Cell*, **27**, 223-231.

Brinster, R.L., Chen, H.Y., Trumbauer, M.E. and Avarbock, M.R. (1980) Translation of globin messenger RNA by the mouse ovum. *Nature*, **283**, 499-501.

Briscoe, J., Rogers, N.C., Witthuhn, B.A., Watling, D., Harpur, A.G., Wilks, A.F., Stark, G.R., Ihle, J.N. and Kerr, I.M. (1996) Kinase-negative mutants of JAK1 can sustain interferon-gamma-inducible gene expression but not an antiviral state. *Embo J*, **15**, 799-809.

Burdin, N., Rousset, F. and Banchereau, J. (1997) B-cell-derived IL-10: production and function. *Methods*, **11**, 98-111.

Burkitt, D. (1962) A children's cancer dependent on climatic factors. *Nature*, **194**, 232-234.

Butzler, C., Zou, X., Popov, A.V. and Bruggemann, M. (1997) Rapid induction of B-cell lymphomas in mice carrying a human IgH/c-mycYAC. *Oncogene*, **14**, 1383-1388.

Caldwell, R.G., Wilson, J.B., Anderson, S.J. and Longnecker, R. (1998) Epstein-Barr virus LMP2A drives B cell development and survival in the absence of normal B cell receptor signals. *Immunity*, **9**, 405-411.

Capoulade, C., Bressac-de Paillerets, B., Lefrere, I., Ronsin, M., Feunteun, J., Tursz, T. and Wiels, J. (1998) Overexpression of MDM2, due to enhanced translation, results in inactivation of wild-type p53 in Burkitt's lymphoma cells. *Oncogene*, **16**, 1603-1610.

Carbone, A., Gloghini, A., Zagonel, V. and Tirelli, U. (1996) Expression of Epstein-Barr virus-encoded latent membrane protein 1 in nonendemic Burkitt's lymphomas. *Blood*, **87**, 1202-1204.

Carel, J.C., Myones, B.L., Frazier, B. and Holers, V.M. (1990) Structural requirements for C3d,g/Epstein-Barr virus receptor (CR2/CD21) ligand binding, internalization, and viral infection. *J Biol Chem*, **265**, 12293-12299.

Cheung, W.C., Kim, J.S., Linden, M., Peng, L., Van Ness, B., Polakiewicz, R.D. and Janz, S. (2004) Novel targeted deregulation of c-Myc cooperates with Bcl-X(L) to cause plasma cell neoplasms in mice. *J Clin Invest*, **113**, 1763-1773.

Chomczynski, P. and Sacchi, N. (1987) Single-step method of RNA isolation by acid guanidinium thiocyanate-phenol-chloroform extraction. *Anal Biochem*, **162**, 156-159.

Chong, K.L., Feng, L., Schappert, K., Meurs, E., Donahue, T.F., Friesen, J.D., Hovanessian, A.G. and Williams, B.R. (1992) Human p68 kinase exhibits growth suppression in yeast and homology to the translational regulator GCN2. *Embo J*, **11**, 1553-1562.

Ciliberto, G., Raugei, G., Costanzo, F., Dente, L. and Cortese, R. (1983) Common and interchangeable elements in the promoters of genes transcribed by RNA polymerase iii. *Cell*, **32**, 725-733.

Cimmino, A., Calin, G.A., Fabbri, M., Iorio, M.V., Ferracin, M., Shimizu, M., Wojcik, S.E., Aqeilan, R.I., Zupo, S., Dono, M., Rassenti, L., Alder, H., Volinia, S., Liu, C.G., Kipps, T.J., Negrini, M. and Croce, C.M. (2005) miR-15 and miR-16 induce apoptosis by targeting BCL2. *Proc Natl Acad Sci U S A*, **102**, 13944-13949.

Clarke, P.A., Schwemmle, M., Schickinger, J., Hilse, K. and Clemens, M.J. (1991) Binding of Epstein-Barr virus small RNA EBER-1 to the double-stranded RNA-activated protein kinase DAI. *Nucleic Acids Res*, **19**, 243-248.

Clarke, P.A., Sharp, N.A. and Clemens, M.J. (1990) Translational control by the Epstein-Barr virus small RNA EBER-1. Reversal of the double-stranded RNA-induced inhibition of protein synthesis in reticulocyte lysates. *Eur J Biochem*, **193**, 635-641.

Clarke, P.A., Sharp, N.A. and Clemens, M.J. (1992) Expression of genes for the Epstein-Barr virus small RNAs EBER-1 and EBER-2 in Daudi Burkitt's lymphoma cells: effects of interferon treatment. *J Gen Virol*, **73 (Pt 12)**, 3169-3175.

Clemens, M.J. (1993) The small RNAs of Epstein-Barr virus. *Mol Biol Rep*, **17**, 81-92.

Clemens, M.J. (2006) Epstein-Barr virus: Inhibition of apoptosis as a mechanism of cell transformation. *Int J Biochem Cell Biol*, **38**, 164-169.

Clemens, M.J. and Elia, A. (1997) The double-stranded RNA-dependent protein kinase PKR: structure and function. *J Interferon Cytokine Res*, **17**, 503-524.

Coffman, R.L. (1982) Surface antigen expression and immunoglobulin gene rearrangement during mouse pre-B cell development. *Immunol Rev*, **69**, 5-23.

Cohen, J.I., Wang, F., Mannick, J. and Kieff, E. (1989) Epstein-Barr virus nuclear protein 2 is a key determinant of lymphocyte transformation. *Proc Natl Acad Sci U S A*, **86**, 9558-9562.

Cordier, M., Calender, A., Billaud, M., Zimber, U., Rousselet, G., Pavlish, O., Banchereau, J., Tursz, T., Bornkamm, G. and Lenoir, G.M. (1990) Stable transfection of Epstein-Barr virus (EBV) nuclear antigen 2 in lymphoma cells containing the EBV P3HR1 genome induces expression of B-cell activation molecules CD21 and CD23. *J Virol*, **64**, 1002-1013.

Dawson, C.W., Tramountanis, G., Eliopoulos, A.G. and Young, L.S. (2003) Epstein-Barr virus latent membrane protein 1 (LMP1) activates the phosphatidylinositol 3-kinase/Akt pathway to promote cell survival and induce actin filament remodeling. *J Biol Chem*, **278**, 3694-3704.

Der, S.D. and Lau, A.S. (1995) Involvement of the double-stranded-RNA-dependent kinase PKR in interferon expression and interferon-mediated antiviral activity. *Proc Natl Acad Sci U S A*, **92**, 8841-8845.

Dialynas, D.P., Quan, Z.S., Wall, K.A., Pierres, A., Quintans, J., Loken, M.R., Pierres, M. and Fitch, F.W. (1983) Characterization of the murine T cell surface molecule, designated L3T4, identified by monoclonal antibody GK1.5: similarity of L3T4 to the human Leu-3/T4 molecule. *J Immunol*, **131**, 2445-2451.

Dildrop, R., Ma, A., Zimmerman, K., Hsu, E., Tesfaye, A., DePinho, R. and Alt, F.W. (1989) IgH enhancer-mediated deregulation of N-myc gene expression in transgenic mice: generation of lymphoid neoplasias that lack c-myc expression. *Embo J*, **8**, 1121-1128.

Driessler, F., Venstrom, K., Sabat, R., Asadullah, K. and Schottelius, A.J. (2004) Molecular mechanisms of interleukin-10-mediated inhibition of NF-kappaB activity: a role for p50. *Clin Exp Immunol*, **135**, 64-73.

Drotar, M.E., Silva, S., Barone, E., Campbell, D., Tsimbouri, P., Jurvansu, J., Bhatia, P., Klein, G. and Wilson, J.B. (2003) Epstein-Barr virus nuclear antigen-1 and Myc cooperate in lymphomagenesis. *Int J Cancer*, **106**, 388-395.

Dykstra, M.L., Longnecker, R. and Pierce, S.K. (2001) Epstein-Barr virus coopts lipid rafts to block the signaling and antigen transport functions of the BCR. *Immunity*, **14**, 57-67.

Elia, A., Vyas, J., Laing, K.G. and Clemens, M.J. (2004) Ribosomal protein L22 inhibits regulation of cellular activities by the Epstein-Barr virus small RNA EBER-1. *Eur J Biochem*, **271**, 1895-1905.

Eliopoulos, A.G., Blake, S.M., Floettmann, J.E., Rowe, M. and Young, L.S. (1999a) Epstein-Barr virus-encoded latent membrane protein 1 activates the JNK pathway through its extreme C terminus via a mechanism involving TRADD and TRAF2. *J Virol*, **73**, 1023-1035.

Eliopoulos, A.G., Gallagher, N.J., Blake, S.M., Dawson, C.W. and Young, L.S. (1999b) Activation of the p38 mitogen-activated protein kinase pathway by Epstein-Barr virus-encoded latent membrane protein 1 coregulates interleukin-6 and interleukin-8 production. *J Biol Chem*, **274**, 16085-16096.

Eliopoulos, A.G. and Young, L.S. (2001) LMP1 structure and signal transduction. *Semin Cancer Biol*, **11**, 435-444.

Epstein, M.A., Achong, B.G. and Barr, Y.M. (1964) Virus particles in cultured lymphoblasts from Burkitt's lymphoma. *Lancet*, **1**.

Farrell, P.J., Allan, G.J., Shanahan, F., Vousden, K.H. and Crook, T. (1991) p53 is frequently mutated in Burkitt's lymphoma cell lines. *Embo J*, **10**, 2879-2887.

Fingeroth, J.D., Weis, J.J., Tedder, T.F., Strominger, J.L., Biro, P.A. and Fearon, D.T. (1984) Epstein-Barr virus receptor of human B lymphocytes is the C3d receptor CR2. *Proc Natl Acad Sci U S A*, **81**, 4510-4514.

Fitzgerald, K.A., Rowe, D.C., Barnes, B.J., Caffrey, D.R., Visintin, A., Latz, E., Monks, B., Pitha, P.M. and Golenbock, D.T. (2003) LPS-TLR4 signaling to IRF-3/7 and NF-kappaB involves the toll adapters TRAM and TRIF. *J Exp Med*, **198**, 1043-1055.

Fruehling, S. and Longnecker, R. (1997) The immunoreceptor tyrosine-based activation motif of Epstein-Barr virus LMP2A is essential for blocking BCR-mediated signal transduction. *Virology*, **235**, 241-251.

Fukuda, M. and Longnecker, R. (2005) Epstein-Barr virus (EBV) latent membrane protein 2A regulates B-cell receptor-induced apoptosis and EBV reactivation through tyrosine phosphorylation. *J Virol*, **79**, 8655-8660.

Gaidano, G., Carbone, A. and Dalla-Favera, R. (1998) Genetic basis of acquired immunodeficiency syndrome-related lymphomagenesis. *J Natl Cancer Inst Monogr*, 95-100.

Geiduschek, E.P. and Kassavetis, G.A. (2001) The RNA polymerase III transcription apparatus. *J Mol Biol*, **310**, 1-26.

Gires, O., Kohlhuber, F., Kilger, E., Baumann, M., Kieser, A., Kaiser, C., Zeidler, R., Scheffer, B., Ueffing, M. and Hammerschmidt, W. (1999) Latent membrane protein 1 of Epstein-Barr virus interacts with JAK3 and activates STAT proteins. *Embo J*, **18**, 3064-3073.

Gires, O., Zimber-Strobl, U., Gonnella, R., Ueffing, M., Marschall, G., Zeidler, R., Pich, D. and Hammerschmidt, W. (1997) Latent membrane protein 1 of Epstein-Barr virus mimics a constitutively active receptor molecule. *Embo J*, **16**, 6131-6140.

Glickman, J.N., Howe, J.G. and Steitz, J.A. (1988) Structural analyses of EBER1 and EBER2 ribonucleoprotein particles present in Epstein-Barr virus-infected cells. *J Virol*, **62**, 902-911.

Goh, K.C., Haque, S.J. and Williams, B.R. (1999) p38 MAP kinase is required for STAT1 serine phosphorylation and transcriptional activation induced by interferons. *Embo J*, **18**, 5601-5608.

Gomez-Roman, N., Grandori, C., Eisenman, R.N. and White, R.J. (2003) Direct activation of RNA polymerase III transcription by c-Myc. *Nature*, **421**, 290-294.

Goodbourn, S., Didcock, L. and Randall, R.E. (2000) Interferons: cell signalling, immune modulation, antiviral response and virus countermeasures. *J Gen Virol*, **81**, 2341-2364.

Gordon, J.W. and Ruddle, F.H. (1981) Integration and stable germ line transmission of genes injected into mouse pronuclei. *Science*, **214**, 1244-1246.

Gordon, J.W., Scangos, G.A., Plotkin, D.J., Barbosa, J.A. and Ruddle, F.H. (1980) Genetic transformation of mouse embryos by microinjection of purified DNA. *Proc Natl Acad Sci U S A*, 77, 7380-7384.

Grandori, C., Gomez-Roman, N., Felton-Edkins, Z.A., Ngouenet, C., Galloway, D.A., Eisenman, R.N. and White, R.J. (2005) c-Myc binds to human ribosomal DNA and stimulates transcription of rRNA genes by RNA polymerase I. *Nat Cell Biol*, 7, 311-318.

Grossman, S.R., Johannsen, E., Tong, X., Yalamanchili, R. and Kieff, E. (1994) The Epstein-Barr virus nuclear antigen 2 transactivator is directed to response elements by the J kappa recombination signal binding protein. *Proc Natl Acad Sci U S A*, **91**, 7568-7572.

Gulley, M.L., Ogata, L.C., Thorson, J.A., Dailey, M.O. and Kemp, J.D. (1988) Identification of a murine pan-T cell antigen which is also expressed during the terminal phases of B cell differentiation. *J Immunol*, **140**, 3751-3757.

Hammerschmidt, W. and Sugden, B. (1988) Identification and characterization of oriLyt, a lytic origin of DNA replication of Epstein-Barr virus. *Cell*, **55**, 427-433.

Harris, A.W., Pinkert, C.A., Crawford, M., Langdon, W.Y., Brinster, R.L. and Adams, J.M. (1988) The E mu-myc transgenic mouse. A model for high-incidence spontaneous lymphoma and leukemia of early B cells. *J Exp Med*, **167**, 353-371.

Hathcock, K.S., Hirano, H., Murakami, S. and Hodes, R.J. (1992) CD45 expression by B cells. Expression of different CD45 isoforms by subpopulations of activated B cells. *J Immunol*, **149**, 2286-2294.

He, L., Thomson, J.M., Hemann, M.T., Hernando-Monge, E., Mu, D., Goodson, S., Powers, S., Cordon-Cardo, C., Lowe, S.W., Hannon, G.J. and Hammond, S.M. (2005) A microRNA polycistron as a potential human oncogene. *Nature*, **435**, 828-833.

Heard, E. (2004) Recent advances in X-chromosome inactivation. *Curr Opin Cell Biol*, **16**, 247-255.

Hennessy, K., Wang, F., Bushman, E.W. and Kieff, E. (1986) Definitive identification of a member of the Epstein-Barr virus nuclear protein 3 family. *Proc Natl Acad Sci U S A*, **83**, 5693-5697.

Hiscott, J. and Lin, R. (2005) IRF-3 Releases Its Inhibitions. *Structure (Camb)*, **13**, 1235-1236.

Hochberg, D., Middeldorp, J.M., Catalina, M., Sullivan, J.L., Luzuriaga, K. and Thorley-Lawson, D.A. (2004) Demonstration of the Burkitt's lymphoma Epstein-Barr virus phenotype in dividing latently infected memory cells in vivo. *Proc Natl Acad Sci U S A*, **101**, 239-244.

Horvath, C.M. (2000) STAT proteins and transcriptional responses to extracellular signals. *Trends Biochem Sci*, **25**, 496-502.

Horvath, C.M., Stark, G.R., Kerr, I.M. and Darnell, J.E., Jr. (1996) Interactions between STAT and non-STAT proteins in the interferon-stimulated gene factor 3 transcription complex. *Mol Cell Biol*, **16**, 6957-6964.

Howe, J.G. and Shu, M.D. (1988) Isolation and characterization of the genes for two small RNAs of herpesvirus papio and their comparison with Epstein-Barr virus-encoded EBER RNAs. *J Virol*, **62**, 2790-2798.

Howe, J.G. and Shu, M.D. (1989) Epstein-Barr virus small RNA (EBER) genes: unique transcription units that combine RNA polymerase II and III promoter elements. *Cell*, **57**, 825-834.

Howe, J.G. and Shu, M.D. (1993) Upstream basal promoter element important for exclusive RNA polymerase III transcription of the EBER 2 gene. *Mol Cell Biol*, **13**, 2655-2665.

Howe, J.G. and Steitz, J.A. (1986) Localization of Epstein-Barr virus-encoded small RNAs by in situ hybridization. *Proc Natl Acad Sci U S A*, **83**, 9006-9010.

Huen, D.S., Fox, A., Kumar, P. and Searle, P.F. (1993) Dilated heart failure in transgenic mice expressing the Epstein-Barr virus nuclear antigen-leader protein. *J Gen Virol*, **74 (Pt 7)**, 1381-1391.

Huen, D.S., Henderson, S.A., Croom-Carter, D. and Rowe, M. (1995) The Epstein-Barr virus latent membrane protein-1 (LMP1) mediates activation of NF-kappa B and cell surface phenotype via two effector regions in its carboxy-terminal cytoplasmic domain. *Oncogene*, **10**, 549-560.

Humme, S., Reisbach, G., Feederle, R., Delecluse, H.J., Bousset, K., Hammerschmidt, W. and Schepers, A. (2003) The EBV nuclear antigen 1 (EBNA1) enhances B cell immortalization several thousandfold. *Proc Natl Acad Sci U S A*, **100**, 10989-10994.

Hurlin, P.J. and Dezfouli, S. (2004) Functions of myc:max in the control of cell proliferation and tumorigenesis. *Int Rev Cytol*, **238**, 183-226.

Hwang, S.Y., Hertzog, P.J., Holland, K.A., Sumarsono, S.H., Tymms, M.J., Hamilton, J.A., Whitty, G., Bertoncello, I. and Kola, I. (1995) A null mutation in the gene encoding a type I interferon receptor component eliminates antiproliferative and antiviral responses to interferons alpha and beta and alters macrophage responses. *Proc Natl Acad Sci U S A*, **92**, 11284-11288.

Iavarone, A., Garg, P., Lasorella, A., Hsu, J. and Israel, M.A. (1994) The helix-loop-helix protein Id-2 enhances cell proliferation and binds to the retinoblastoma protein. *Genes Dev*, **8**, 1270-1284.

Ikeda, A., Merchant, M., Lev, L., Longnecker, R. and Ikeda, M. (2004) Latent membrane protein 2A, a viral B cell receptor homologue, induces CD5+ B-1 cell development. *J Immunol*, **172**, 5329-5337.

Iordanov, M.S., Paranjape, J.M., Zhou, A., Wong, J., Williams, B.R., Meurs, E.F., Silverman, R.H. and Magun, B.E. (2000) Activation of p38 mitogen-activated protein kinase and c-Jun NH(2)-terminal kinase by double-stranded RNA and encephalomyocarditis virus: involvement of RNase L, protein kinase R, and alternative pathways. *Mol Cell Biol*, **20**, 617-627.

Iwakiri, D., Sheen, T.S., Chen, J.Y., Huang, D.P. and Takada, K. (2005) Epstein-Barr virus-encoded small RNA induces insulin-like growth factor 1 and supports growth of nasopharyngeal carcinoma-derived cell lines. *Oncogene*, **24**, 1767-1773.

Jaenisch, R. (1988) Transgenic animals. *Science*, **240**, 1468-1474.

Jat, P. and Arrand, J.R. (1982) In vitro transcription of two Epstein-Barr virus specified small RNA molecules. *Nucleic Acids Res*, **10**, 3407-3425.

Jenkins, P.J., Binne, U.K. and Farrell, P.J. (2000) Histone acetylation and reactivation of Epstein-Barr virus from latency. *J Virol*, **74**, 710-720.

Joseph, A.M., Babcock, G.J. and Thorley-Lawson, D.A. (2000) Cells expressing the Epstein-Barr virus growth program are present in and restricted to the naive B-cell subset of healthy tonsils. *J Virol*, **74**, 9964-9971.

Kaiser, C., Laux, G., Eick, D., Jochner, N., Bornkamm, G.W. and Kempkes, B. (1999) The proto-oncogene c-myc is a direct target gene of Epstein-Barr virus nuclear antigen 2. *J Virol*, **73**, 4481-4484.

Kang, M.S., Lu, H., Yasui, T., Sharpe, A., Warren, H., Cahir-McFarland, E., Bronson, R., Hung, S.C. and Kieff, E. (2005) Epstein-Barr virus nuclear antigen 1 does not induce lymphoma in transgenic FVB mice. *Proc Natl Acad Sci U S A*, **102**, 820-825.

Kaplan, D.H., Shankaran, V., Dighe, A.S., Stockert, E., Aguet, M., Old, L.J. and Schreiber, R.D. (1998) Demonstration of an interferon gamma-dependent tumor surveillance system in immunocompetent mice. *Proc Natl Acad Sci U S A*, **95**, 7556-7561.

Kapoor, P., Lavoie, B.D. and Frappier, L. (2005) EBP2 plays a key role in Epstein-Barr virus mitotic segregation and is regulated by aurora family kinases. *Mol Cell Biol*, **25**, 4934-4945.

Kassavetis, G.A., Braun, B.R., Nguyen, L.H. and Geiduschek, E.P. (1990) S. cerevisiae TFIIIB is the transcription initiation factor proper of RNA polymerase III, while TFIIIA and TFIIIC are assembly factors. *Cell*, **60**, 235-245.

Kaye, K.M., Izumi, K.M. and Kieff, E. (1993) Epstein-Barr virus latent membrane protein 1 is essential for B-lymphocyte growth transformation. *Proc Natl Acad Sci U S A*, **90**, 9150-9154.

Kennedy, G., Komano, J. and Sugden, B. (2003) Epstein-Barr virus provides a survival factor to Burkitt's lymphomas. *Proc Natl Acad Sci U S A*, **100**, 14269-14274.

Kerr, I.M. and Brown, R.E. (1978) pppA2'p5'A2'p5'A: an inhibitor of protein synthesis synthesized with an enzyme fraction from interferon-treated cells. *Proc Natl Acad Sci U S A*, **75**, 256-260.

Kidd, P. (2003) Th1/Th2 balance: the hypothesis, its limitations, and implications for health and disease. *Altern Med Rev*, **8**, 223-246.

Kieff, E., Rickinson, A.B. (2001) In Knipe, D.M., Howley, P.M., Griffin, D.E., Lamb, R.A., Martin, M.A., Roizman, B. and Straus S.E. (ed.), *Fields in Virology*. Lippincott Williams and Wilkins, Philadelphia, pp. 2511-2573.

Kilger, E., Kieser, A., Baumann, M. and Hammerschmidt, W. (1998) Epstein-Barr virus-mediated B-cell proliferation is dependent upon latent membrane protein 1, which simulates an activated CD40 receptor. *Embo J*, **17**, 1700-1709.

Kim, S.H., Cohen, B., Novick, D. and Rubinstein, M. (1997) Mammalian type I interferon receptors consists of two subunits: IFNaR1 and IFNaR2. *Gene*, **196**, 279-286.

King, W., Thomas-Powell, A.L., Raab-Traub, N., Hawke, M. and Kieff, E. (1980) Epstein-Barr virus RNA. V. Viral RNA in a restringently infected, growth-transformed cell line. *J Virol*, **36**, 506-518.

Kitagawa, N., Goto, M., Kurozumi, K., Maruo, S., Fukayama, M., Naoe, T., Yasukawa, M., Hino, K., Suzuki, T., Todo, S. and Takada, K. (2000) Epstein-Barr virus-encoded poly(A)(-) RNA supports Burkitt's lymphoma growth through interleukin-10 induction. *Embo J*, **19**, 6742-6750.

Klangby, U., Okan, I., Magnusson, K.P., Wendland, M., Lind, P. and Wiman, K.G. (1998) p16/INK4a and p15/INK4b gene methylation and absence of p16/INK4a mRNA and protein expression in Burkitt's lymphoma. *Blood*, **91**, 1680-1687.

Komano, J., Maruo, S., Kurozumi, K., Oda, T. and Takada, K. (1999) Oncogenic role of Epstein-Barr virus-encoded RNAs in Burkitt's lymphoma cell line Akata. *J Virol*, **73**, 9827-9831.

Koromilas, A.E., Roy, S., Barber, G.N., Katze, M.G. and Sonenberg, N. (1992) Malignant transformation by a mutant of the IFN-inducible dsRNA-dependent protein kinase. *Science*, **257**, 1685-1689.

Kovalchuk, A.L., Qi, C.F., Torrey, T.A., Taddesse-Heath, L., Feigenbaum, L., Park, S.S., Gerbitz, A., Klobeck, G., Hoertnagel, K., Polack, A., Bornkamm, G.W., Janz, S. and Morse, H.C., 3rd. (2000) Burkitt lymphoma in the mouse. *J Exp Med*, **192**, 1183-1190.

Kulwichit, W., Edwards, R.H., Davenport, E.M., Baskar, J.F., Godfrey, V. and Raab-Traub, N. (1998) Expression of the Epstein-Barr virus latent membrane protein 1 induces B cell lymphoma in transgenic mice. *Proc Natl Acad Sci U S A*, **95**, 11963-11968.

Kumar, A., Haque, J., Lacoste, J., Hiscott, J. and Williams, B.R. (1994) Double-stranded RNA-dependent protein kinase activates transcription factor NF-kappa B by phosphorylating I kappa B. *Proc Natl Acad Sci U S A*, **91**, 6288-6292.

Kumar, A., Yang, Y.L., Flati, V., Der, S., Kadereit, S., Deb, A., Haque, J., Reis, L., Weissmann, C. and Williams, B.R. (1997) Deficient cytokine signaling in mouse embryo fibroblasts with a targeted deletion in the PKR gene: role of IRF-1 and NF-kappaB. *Embo J*, **16**, 406-416.

Kuppers, R. (2003) B cells under influence: transformation of B cells by Epstein-Barr virus. *Nat Rev Immunol*, **3**, 801-812.

Kuppers, R. and Rajewsky, K. (1998) The origin of Hodgkin and Reed/Sternberg cells in Hodgkin's disease. *Annu Rev Immunol*, **16**, 471-493.

Laing, K.G., Elia, A., Jeffrey, I., Matys, V., Tilleray, V.J., Souberbielle, B. and Clemens, M.J. (2002) In vivo effects of the Epstein-Barr virus small RNA EBER-1 on protein synthesis and cell growth regulation. *Virology*, **297**, 253-269.

Lasorella, A., Noseda, M., Beyna, M., Yokota, Y. and Iavarone, A. (2000) Id2 is a retinoblastoma protein target and mediates signalling by Myc oncoproteins. *Nature*, **407**, 592-598.

Ledbetter, J.A. and Herzenberg, L.A. (1979) Xenogeneic monoclonal antibodies to mouse lymphoid differentiation antigens. *Immunol Rev*, **47**, 63-90.

Ledbetter, J.A., Rouse, R.V., Micklem, H.S. and Herzenberg, L.A. (1980) T cell subsets defined by expression of Lyt-1,2,3 and Thy-1 antigens. Two-parameter immunofluorescence and cytotoxicity analysis with monoclonal antibodies modifies current views. *J Exp Med*, **152**, 280-295.

Lee, T.G., Tang, N., Thompson, S., Miller, J. and Katze, M.G. (1994) The 58,000-dalton cellular inhibitor of the interferon-induced double-stranded RNA-activated protein kinase (PKR) is a member of the tetratricopeptide repeat family of proteins. *Mol Cell Biol*, **14**, 2331-2342.

Lerner, M.R., Andrews, N.C., Miller, G. and Steitz, J.A. (1981) Two small RNAs encoded by Epstein-Barr virus and complexed with protein are precipitated by antibodies from patients with systemic lupus erythematosus. *Proc Natl Acad Sci U S A*, **78**, 805-809.

Levitskaya, J., Coram, M., Levitsky, V., Imreh, S., Steigerwald-Mullen, P.M., Klein, G., Kurilla, M.G. and Masucci, M.G. (1995) Inhibition of antigen processing by the internal repeat region of the Epstein-Barr virus nuclear antigen-1. *Nature*, **375**, 685-688.

Levitskaya, J., Sharipo, A., Leonchiks, A., Ciechanover, A. and Masucci, M.G. (1997) Inhibition of ubiquitin/proteasome-dependent protein degradation by the Gly-Ala repeat domain of the Epstein-Barr virus nuclear antigen 1. *Proc Natl Acad Sci U S A*, **94**, 12616-12621.

Lewis, D.L., Hagstrom, J.E., Loomis, A.G., Wolff, J.A. and Herweijer, H. (2002) Efficient delivery of siRNA for inhibition of gene expression in postnatal mice. *Nat Genet*, **32**, 107-108.

Li, H.P. and Chang, Y.S. (2003) Epstein-Barr virus latent membrane protein 1: structure and functions. *J Biomed Sci*, **10**, 490-504.

Li, Q., Spriggs, M.K., Kovats, S., Turk, S.M., Comeau, M.R., Nepom, B. and Hutt-Fletcher, L.M. (1997a) Epstein-Barr virus uses HLA class II as a cofactor for infection of B lymphocytes. *J Virol*, **71**, 4657-4662.

Li, X., Leung, S., Burns, C. and Stark, G.R. (1998) Cooperative binding of Stat1-2 heterodimers and ISGF3 to tandem DNA elements. *Biochimie*, **80**, 703-710.

Li, X., Leung, S., Kerr, I.M. and Stark, G.R. (1997b) Functional subdomains of STAT2 required for preassociation with the alpha interferon receptor and for signaling. *Mol Cell Biol*, **17**, 2048-2056.

Liebowitz, D., Mannick, J., Takada, K. and Kieff, E. (1992) Phenotypes of Epstein-Barr virus LMP1 deletion mutants indicate transmembrane and amino-terminal cytoplasmic domains necessary for effects in B-lymphoma cells. *J Virol*, **66**, 4612-4616.

Lin, T.P. (1966) Microinjection of mouse eggs. *Science*, **151**, 333-337.

Lindstrom, M.S., Klangby, U. and Wiman, K.G. (2001) p14ARF homozygous deletion or MDM2 overexpression in Burkitt lymphoma lines carrying wild type p53. *Oncogene*, **20**, 2171-2177.

Lindstrom, M.S. and Wiman, K.G. (2002) Role of genetic and epigenetic changes in Burkitt lymphoma. *Semin Cancer Biol*, **12**, 381-387.

Longnecker, R. (2000) Epstein-Barr virus latency: LMP2, a regulator or means for Epstein-Barr virus persistence? *Adv Cancer Res*, **79**, 175-200.

Longnecker, R., Druker, B., Roberts, T.M. and Kieff, E. (1991) An Epstein-Barr virus protein associated with cell growth transformation interacts with a tyrosine kinase. *J Virol*, **65**, 3681-3692.

Longnecker, R. and Kieff, E. (1990) A second Epstein-Barr virus membrane protein (LMP2) is expressed in latent infection and colocalizes with LMP1. *J Virol*, **64**, 2319-2326.

Longnecker, R., Miller, C.L., Miao, X.Q., Tomkinson, B. and Kieff, E. (1993a) The last seven transmembrane and carboxy-terminal cytoplasmic domains of Epstein-Barr virus latent membrane protein 2 (LMP2) are dispensable for lymphocyte infection and growth transformation in vitro. *J Virol*, **67**, 2006-2013.

Longnecker, R., Miller, C.L., Tomkinson, B., Miao, X.Q. and Kieff, E. (1993b) Deletion of DNA encoding the first five transmembrane domains of Epstein-Barr virus latent membrane proteins 2A and 2B. *J Virol*, **67**, 5068-5074.

Lu, C.C., Wu, C.W., Chang, S.C., Chen, T.Y., Hu, C.R., Yeh, M.Y., Chen, J.Y. and Chen, M.R. (2004) Epstein-Barr virus nuclear antigen 1 is a DNA-binding protein with strong RNA-binding activity. *J Gen Virol*, **85**, 2755-2765.

Lu, S. and Cullen, B.R. (2004) Adenovirus VA1 noncoding RNA can inhibit small interfering RNA and MicroRNA biogenesis. *J Virol*, **78**, 12868-12876.

Luo, W., Van de Velde, H., von Hoegen, I., Parnes, J.R. and Thielemans, K. (1992) Ly-1 (CD5), a membrane glycoprotein of mouse T lymphocytes and a subset of B cells, is a natural ligand of the B cell surface protein Lyb-2 (CD72). *J Immunol*, **148**, 1630-1634.

Luscher, B. (2001) Function and regulation of the transcription factors of the Myc/Max/Mad network. *Gene*, **277**, 1-14.

Magrath, I. (1990) The pathogenesis of Burkitt's lymphoma. *Adv Cancer Res*, **55**, 133-270.

Malmgaard, L. (2004) Induction and regulation of IFNs during viral infections. *J Interferon Cytokine Res*, **24**, 439-454.

Malynn, B.A., de Alboran, I.M., O'Hagan, R.C., Bronson, R., Davidson, L., DePinho, R.A. and Alt, F.W. (2000) N-myc can functionally replace c-myc in murine development, cellular growth, and differentiation. *Genes Dev*, **14**, 1390-1399.

Mannick, J.B., Cohen, J.I., Birkenbach, M., Marchini, A. and Kieff, E. (1991) The Epstein-Barr virus nuclear protein encoded by the leader of the EBNA RNAs is important in B-lymphocyte transformation. *J Virol*, **65**, 6826-6837.

Maraia, R.J. and Intine, R.V. (2001) Recognition of nascent RNA by the human La antigen: conserved and divergent features of structure and function. *Mol Cell Biol*, **21**, 367-379.

Marinkovic, D., Marinkovic, T., Kokai, E., Barth, T., Moller, P. and Wirth, T. (2004) Identification of novel Myc target genes with a potential role in lymphomagenesis. *Nucleic Acids Res*, **32**, 5368-5378.

Martin, F. and Kearney, J.F. (2001) B1 cells: similarities and differences with other B cell subsets. *Curr Opin Immunol*, **13**, 195-201.

Maruo, S., Johannsen, E., Illanes, D., Cooper, A. and Kieff, E. (2003) Epstein-Barr Virus nuclear protein EBNA3A is critical for maintaining lymphoblastoid cell line growth. *J Virol*, 77, 10437-10447.

Maruo, S., Johannsen, E., Illanes, D., Cooper, A., Zhao, B. and Kieff, E. (2005) Epstein-Barr virus nuclear protein 3A domains essential for growth of lymphoblasts: transcriptional regulation through RBP-Jkappa/CBF1 is critical. *J Virol*, **79**, 10171-10179.

Mathews, M.B. and Francoeur, A.M. (1984) La antigen recognizes and binds to the 3'-oligouridylate tail of a small RNA. *Mol Cell Biol*, **4**, 1134-1140.

Mathews, M.B. and Shenk, T. (1991) Adenovirus virus-associated RNA and translation control. *J Virol*, **65**, 5657-5662.

Meijer, C.J., Jiwa, N.M., Dukers, D.F., Oudejans, J.J., de Bruin, P.C., Walboomers, J.M. and van den Brule, A.J. (1996) Epstein-Barr virus and human T-cell lymphomas. *Semin Cancer Biol*, 7, 191-196.

Menezes, J., Leibold, W., Klein, G. and Clements, G. (1975) Establishment and characterization of an Epstein-Barr virus (EBC)-negative lymphoblastoid B cell line (BJA-B) from an exceptional, EBV-genome-negative African Burkitt's lymphoma. *Biomedicine*, **22**, 276-284.

Meurs, E.F., Galabru, J., Barber, G.N., Katze, M.G. and Hovanessian, A.G. (1993) Tumor suppressor function of the interferon-induced double-stranded RNA-activated protein kinase. *Proc Natl Acad Sci U S A*, **90**, 232-236.

Meyer, T., Marg, A., Lemke, P., Wiesner, B. and Vinkemeier, U. (2003) DNA binding controls inactivation and nuclear accumulation of the transcription factor Stat1. *Genes Dev*, **17**, 1992-2005.

Miescher, G.C., Schreyer, M. and MacDonald, H.R. (1989) Production and characterization of a rat monoclonal antibody against the murine CD3 molecular complex. *Immunol Lett*, **23**, 113-118.

Miller, C.L., Burkhardt, A.L., Lee, J.H., Stealey, B., Longnecker, R., Bolen, J.B. and Kieff, E. (1995) Integral membrane protein 2 of Epstein-Barr virus regulates reactivation from latency through dominant negative effects on protein-tyrosine kinases. *Immunity*, **2**, 155-166.

Miller, C.L., Lee, J.H., Kieff, E. and Longnecker, R. (1994) An integral membrane protein (LMP2) blocks reactivation of Epstein-Barr virus from latency following surface immunoglobulin crosslinking. *Proc Natl Acad Sci U S A*, **91**, 772-776.

Moroy, T., Fisher, P., Guidos, C., Ma, A., Zimmerman, K., Tesfaye, A., DePinho, R., Weissman, I. and Alt, F.W. (1990) IgH enhancer deregulated expression of L-myc: abnormal T lymphocyte development and T cell lymphomagenesis. *Embo J*, **9**, 3659-3666.

Moroy, T., Verbeek, S., Ma, A., Achacoso, P., Berns, A. and Alt, F. (1991) E mu N- and E mu L-myc cooperate with E mu pim-1 to generate lymphoid tumors at high frequency in double-transgenic mice. *Oncogene*, **6**, 1941-1948.

Muller, M., Laxton, C., Briscoe, J., Schindler, C., Improta, T., Darnell, J.E., Jr., Stark, G.R. and Kerr, I.M. (1993) Complementation of a mutant cell line: central role of the 91 kDa polypeptide of ISGF3 in the interferon-alpha and -gamma signal transduction pathways. *Embo J*, **12**, 4221-4228.

Muller, U., Steinhoff, U., Reis, L.F., Hemmi, S., Pavlovic, J., Zinkernagel, R.M. and Aguet, M. (1994) Functional role of type I and type II interferons in antiviral defense. *Science*, **264**, 1918-1921.

Murphy, K.M. and Reiner, S.L. (2002) The lineage decisions of helper T cells. *Nat Rev Immunol*, **2**, 933-944.

Nagy, A., Gertsenstein, M., Vintersten, K. and Behringer R. (2003a) Production of transgenic mice. In press, C.S.H.l. (ed.), *Manipulating the Mouse Embryo*, Cold Spring Harbor, New York, Vol. 7, pp. 289-358.

Nagy, A., Gertsenstein, M., Vintersten, K. and Behringer, R. (2003b) Recovery and In vitro culture of pre-implantation stage embryos. In Cold Spring Harbour, l.p. (ed.), *Manipulating the mouse embryo, a laboratory manual*, Cold Spring Harbor, New York, Vol. 4, pp. 161-208.

Nagy, A., Gertsenstein, M., Vintersten, K. and Behringer, R. (2003c) Surgical procedures. In press, C.S.H.l. (ed.), *Manipulating the mouse embryo, a laboratory manual*, Cold Spring Harbor, New York, Vol. 6, pp. 251-287.

Nalesnik, M.A. (1998) Clinical and pathological features of post-transplant lymphoproliferative disorders (PTLD). *Springer Semin Immunopathol*, **20**, 325-342.

Nanbo, A., Inoue, K., Adachi-Takasawa, K. and Takada, K. (2002) Epstein-Barr virus RNA confers resistance to interferon-alpha-induced apoptosis in Burkitt's lymphoma. *Embo J*, **21**, 954-965.

Nanbo, A. and Takada, K. (2002) The role of Epstein-Barr virus-encoded small RNAs (EBERs) in oncogenesis. *Rev Med Virol*, **12**, 321-326.

Nanduri, S., Carpick, B.W., Yang, Y., Williams, B.R. and Qin, J. (1998) Structure of the double-stranded RNA-binding domain of the protein kinase PKR reveals the molecular basis of its dsRNA-mediated activation. *Embo J*, **17**, 5458-5465.

Nemerow, G.R., Houghten, R.A., Moore, M.D. and Cooper, N.R. (1989) Identification of an epitope in the major envelope protein of Epstein-Barr virus that mediates viral binding to the B lymphocyte EBV receptor (CR2). *Cell*, **56**, 369-377.

Nemerow, G.R., Mold, C., Schwend, V.K., Tollefson, V. and Cooper, N.R. (1987) Identification of gp350 as the viral glycoprotein mediating attachment of Epstein-Barr virus (EBV) to the EBV/C3d receptor of B cells: sequence homology of gp350 and C3 complement fragment C3d. *J Virol*, **61**, 1416-1420.

Neri, A., Barriga, F., Knowles, D.M., Magrath, I.T. and Dalla-Favera, R. (1988) Different regions of the immunoglobulin heavy-chain locus are involved in chromosomal translocations in distinct pathogenetic forms of Burkitt lymphoma. *Proc Natl Acad Sci U S A*, **85**, 2748-2752.

Nguyen, K.B., Watford, W.T., Salomon, R., Hofmann, S.R., Pien, G.C., Morinobu, A., Gadina, M., O'Shea, J.J. and Biron, C.A. (2002) Critical role for STAT4 activation by type 1 interferons in the interferon-gamma response to viral infection. *Science*, **297**, 2063-2066.

Niedobitek, G., Agathanggelou, A., Rowe, M., Jones, E.L., Jones, D.B., Turyaguma, P., Oryema, J., Wright, D.H. and Young, L.S. (1995) Heterogeneous expression of Epstein-Barr virus latent proteins in endemic Burkitt's lymphoma. *Blood*, **86**, 659-665.

Niller, H.H., Salamon, D., Ilg, K., Koroknai, A., Banati, F., Bauml, G., Rucker, O., Schwarzmann, F., Wolf, H. and Minarovits, J. (2003) The in vivo binding site for oncoprotein c-Myc in the promoter for Epstein-Barr virus (EBV) encoding RNA (EBER) 1 suggests a specific role for EBV in lymphomagenesis. *Med Sci Monit*, **9**, HY1-9.

Nilsson, J.A., Nilsson, L.M., Keller, U., Yokota, Y., Boyd, K. and Cleveland, J.L. (2004) Id2 is dispensable for myc-induced lymphomagenesis. *Cancer Res*, **64**, 7296-7301.

Nitsche, F., Bell, A. and Rickinson, A. (1997) Epstein-Barr virus leader protein enhances EBNA-2-mediated transactivation of latent membrane protein 1 expression: a role for the W1W2 repeat domain. *J Virol*, **71**, 6619-6628.

Nucifora, G., Begy, C.R., Erickson, P., Drabkin, H.A. and Rowley, J.D. (1993) The 3;21 translocation in myelodysplasia results in a fusion transcript between the AML1 gene and the gene for EAP, a highly conserved protein associated with the Epstein-Barr virus small RNA EBER 1. *Proc Natl Acad Sci U S A*, **90**, 7784-7788.

Palmiter, R.D. and Brinster, R.L. (1986) Germ-line transformation of mice. *Annu Rev Genet*, **20**, 465-499.

Park, S.S., Kim, J.S., Tessarollo, L., Owens, J.D., Peng, L., Han, S.S., Tae Chung, S., Torrey, T.A., Cheung, W.C., Polakiewicz, R.D., McNeil, N., Ried, T., Mushinski, J.F., Morse, H.C., 3rd and Janz, S. (2005) Insertion of c-Myc into Igh induces B-cell and plasma-cell neoplasms in mice. *Cancer Res*, **65**, 1306-1315.

Parker, G.A., Crook, T., Bain, M., Sara, E.A., Farrell, P.J. and Allday, M.J. (1996) Epstein-Barr virus nuclear antigen (EBNA)3C is an immortalizing oncoprotein with similar properties to adenovirus E1A and papillomavirus E7. *Oncogene*, **13**, 2541-2549.

Paule, M.R. and White, R.J. (2000) Survey and summary: transcription by RNA polymerases I and III. *Nucleic Acids Res*, **28**, 1283-1298.

Pelicci, P.G., Knowles, D.M., 2nd, Magrath, I. and Dalla-Favera, R. (1986) Chromosomal breakpoints and structural alterations of the c-myc locus differ in endemic and sporadic forms of Burkitt lymphoma. *Proc Natl Acad Sci U S A*, **83**, 2984-2988.

Perk, J., Iavarone, A. and Benezra, R. (2005) Id family of helix-loop-helix proteins in cancer. *Nat Rev Cancer*, **5**, 603-614.

Pfeffer, S., Sewer, A., Lagos-Quintana, M., Sheridan, R., Sander, C., Grasser, F.A., van Dyk, L.F., Ho, C.K., Shuman, S., Chien, M., Russo, J.J., Ju, J., Randall, G., Lindenbach, B.D., Rice, C.M., Simon, V., Ho, D.D., Zavolan, M. and Tuschl, T. (2005) Identification of microRNAs of the herpesvirus family. *Nat Methods*, **2**, 269-276.

Pfeffer, S., Zavolan, M., Grasser, F.A., Chien, M., Russo, J.J., Ju, J., John, B., Enright, A.J., Marks, D., Sander, C. and Tuschl, T. (2004) Identification of virus-encoded microRNAs. *Science*, **304**, 734-736.

Player, M.R., Wondrak, E.M., Bayly, S.F. and Torrence, P.F. (1998) Ribonuclease L, a 2-5A-dependent enzyme: purification to homogeneity and assays for 2-5A binding and catalytic activity. *Methods*, **15**, 243-253.

Polyak, S.J., Tang, N., Wambach, M., Barber, G.N. and Katze, M.G. (1996) The P58 cellular inhibitor complexes with the interferon-induced, double-stranded RNA-dependent protein kinase, PKR, to regulate its autophosphorylation and activity. *J Biol Chem*, **271**, 1702-1707.

Prota, A.E., Sage, D.R., Stehle, T. and Fingeroth, J.D. (2002) The crystal structure of human CD21: Implications for Epstein-Barr virus and C3d binding. *Proc Natl Acad Sci U S A*, **99**, 10641-10646.

Pulvertaft, J.V. (1965) A Study of Malignant Tumours in Nigeria by Short-Term Tissue Culture. *J Clin Pathol*, **18**, 261-273.

Qureshi, S.A., Leung, S., Kerr, I.M., Stark, G.R. and Darnell, J.E., Jr. (1996) Function of Stat2 protein in transcriptional activation by alpha interferon. *Mol Cell Biol*, **16**, 288-293.

Raab-Traub, N. (1992) Epstein-Barr virus and nasopharyngeal carcinoma. *Semin Cancer Biol*, **3**, 297-307.

Radkov, S.A., Bain, M., Farrell, P.J., West, M., Rowe, M. and Allday, M.J. (1997) Epstein-Barr virus EBNA3C represses Cp, the major promoter for EBNA expression, but has no effect on the promoter of the cell gene CD21. *J Virol*, **71**, 8552-8562.

Rao, M., Lee, W.T. and Conrad, D.H. (1987) Characterization of a monoclonal antibody directed against the murine B lymphocyte receptor for IgE. *J Immunol*, **138**, 1845-1851.

Rawlins, D.R., Milman, G., Hayward, S.D. and Hayward, G.S. (1985) Sequence-specific DNA binding of the Epstein-Barr virus nuclear antigen (EBNA-1) to clustered sites in the plasmid maintenance region. *Cell*, **42**, 859-868.

Rebouillat, D., Hovnanian, A., David, G., Hovanessian, A.G. and Williams, B.R. (2000) Characterization of the gene encoding the 100-kDa form of human 2',5' oligoadenylate synthetase. *Genomics*, **70**, 232-240.

Rickinson, A.B., and Kieff, E. (2001) In Knipe, D.M., Howley, P.M., Griffin, D.E., Lamb, R.A., Martin, M.A., Roizman, B. and Straus, S.E. (ed.), *Fields in Virology*. Lippincott Williams and Wilkins, Philadelphia, pp. 2575-2627.

Robertson, E.S., Lin, J. and Kieff, E. (1996) The amino-terminal domains of Epstein-Barr virus nuclear proteins 3A, 3B, and 3C interact with RBPJ(kappa). *J Virol*, **70**, 3068-3074.

Rochford, R., Miller, C.L., Cannon, M.J., Izumi, K.M., Kieff, E. and Longnecker, R. (1997) In vivo growth of Epstein-Barr virus transformed B cells with mutations in latent membrane protein 2 (LMP2). *Arch Virol*, **142**, 707-720.

Rooney, C.M., Rowe, D.T., Ragot, T. and Farrell, P.J. (1989) The spliced BZLF1 gene of Epstein-Barr virus (EBV) transactivates an early EBV promoter and induces the virus productive cycle. *J Virol*, **63**, 3109-3116.

Rosa, M.D., Gottlieb, E., Lerner, M.R. and Steitz, J.A. (1981) Striking similarities are exhibited by two small Epstein-Barr virus-encoded ribonucleic acids and the adenovirus-associated ribonucleic acids VAI and VAII. *Mol Cell Biol*, **1**, 785-796.

Rothenberger, S., Burns, K., Rousseaux, M., Tschopp, J. and Bron, C. (2003) Ubiquitination of the Epstein-Barr virus-encoded latent membrane protein 1 depends on the integrity of the TRAF binding site. *Oncogene*, **22**, 5614-5618.

Rothenberger, S., Rousseaux, M., Knecht, H., Bender, F.C., Legler, D.F. and Bron, C. (2002) Association of the Epstein-Barr virus latent membrane protein 1 with lipid rafts is mediated through its N-terminal region. *Cell Mol Life Sci*, **59**, 171-180.

Rousset, F., Garcia, E., Defrance, T., Peronne, C., Vezzio, N., Hsu, D.H., Kastelein, R., Moore, K.W. and Banchereau, J. (1992) Interleukin 10 is a potent growth and differentiation factor for activated human B lymphocytes. *Proc Natl Acad Sci U S A*, **89**, 1890-1893.

Ruf, I.K., Lackey, K.A., Warudkar, S. and Sample, J.T. (2005) Protection from interferon-induced apoptosis by Epstein-Barr virus small RNAs is not mediated by inhibition of PKR. *J Virol*, **79**, 14562-14569.

Ruf, I.K., Rhyne, P.W., Yang, C., Cleveland, J.L. and Sample, J.T. (2000) Epstein-Barr virus small RNAs potentiate tumorigenicity of Burkitt lymphoma cells independently of an effect on apoptosis. *J Virol*, **74**, 10223-10228.

Sample, J., Liebowitz, D. and Kieff, E. (1989) Two related Epstein-Barr virus membrane proteins are encoded by separate genes. *J Virol*, **63**, 933-937.

Samuel, C.E. (2001) Antiviral actions of interferons. *Clin Microbiol Rev*, **14**, 778-809, table of contents.

Sato, M., Suemori, H., Hata, N., Asagiri, M., Ogasawara, K., Nakao, K., Nakaya, T., Katsuki, M., Noguchi, S., Tanaka, N. and Taniguchi, T. (2000) Distinct and essential roles of transcription factors IRF-3 and IRF-7 in response to viruses for IFN-alpha/beta gene induction. *Immunity*, **13**, 539-548.

Schaadt, E., Baier, B., Mautner, J., Bornkamm, G.W. and Adler, B. (2005) Epstein-Barr virus latent membrane protein 2A mimics B-cell receptor-dependent virus reactivation. *J Gen Virol*, **86**, 551-559.

Schindler, C. and Brutsaert, S. (1999) Interferons as a paradigm for cytokine signal transduction. *Cell Mol Life Sci*, **55**, 1509-1522.

Schlee, M., Krug, T., Gires, O., Zeidler, R., Hammerschmidt, W., Mailhammer, R., Laux, G., Sauer, G., Lovric, J. and Bornkamm, G.W. (2004) Identification of Epstein-Barr virus (EBV) nuclear antigen 2 (EBNA2) target proteins by proteome analysis: activation of EBNA2 in conditionally immortalized B cells reflects early events after infection of primary B cells by EBV. *J Virol*, **78**, 3941-3952.

Schwemmle, M., Clemens, M.J., Hilse, K., Pfeifer, K., Troster, H., Muller, W.E. and Bachmann, M. (1992) Localization of Epstein-Barr virus-encoded RNAs EBER-1 and EBER-2 in interphase and mitotic Burkitt lymphoma cells. *Proc Natl Acad Sci U S A*, **89**, 10292-10296.

Sharma, S., tenOever, B.R., Grandvaux, N., Zhou, G.P., Lin, R. and Hiscott, J. (2003) Triggering the interferon antiviral response through an IKK-related pathway. *Science*, **300**, 1148-1151.

Sharp, T.V., Raine, D.A., Gewert, D.R., Joshi, B., Jagus, R. and Clemens, M.J. (1999) Activation of the interferon-inducible (2'-5') oligoadenylate synthetase by the Epstein-Barr virus RNA, EBER-1. *Virology*, **257**, 303-313.

Sharp, T.V., Schwemmle, M., Jeffrey, I., Laing, K., Mellor, H., Proud, C.G., Hilse, K. and Clemens, M.J. (1993) Comparative analysis of the regulation of the interferon-inducible protein kinase PKR by Epstein-Barr virus RNAs EBER-1 and EBER-2 and adenovirus VAI RNA. *Nucleic Acids Res*, **21**, 4483-4490.

Shimizu, N., Tanabe-Tochikura, A., Kuroiwa, Y. and Takada, K. (1994) Isolation of Epstein-Barr virus (EBV)-negative cell clones from the EBV-positive Burkitt's lymphoma (BL) line Akata: malignant phenotypes of BL cells are dependent on EBV. *J Virol*, **68**, 6069-6073.

Shire, K., Ceccarelli, D.F., Avolio-Hunter, T.M. and Frappier, L. (1999) EBP2, a human protein that interacts with sequences of the Epstein-Barr virus nuclear antigen 1 important for plasmid maintenance. *J Virol*, **73**, 2587-2595.

Shuai, K. and Liu, B. (2003) Regulation of JAK-STAT signalling in the immune system. *Nat Rev Immunol*, **3**, 900-911.

Silins, S.L. and Sculley, T.B. (1994) Modulation of vimentin, the CD40 activation antigen and Burkitt's lymphoma antigen (CD77) by the Epstein-Barr virus nuclear antigen EBNA-4. *Virology*, **202**, 16-24.

Silva, A.M., Whitmore, M., Xu, Z., Jiang, Z., Li, X. and Williams, B.R. (2004) Protein kinase R (PKR) interacts with and activates mitogen-activated protein kinase kinase 6 (MKK6) in response to double-stranded RNA stimulation. *J Biol Chem*, **279**, 37670-37676.

Sinclair, A.J., Palmero, I., Peters, G. and Farrell, P.J. (1994) EBNA-2 and EBNA-LP cooperate to cause G0 to G1 transition during immortalization of resting human B lymphocytes by Epstein-Barr virus. *Embo J*, **13**, 3321-3328.

Snudden, D.K., Hearing, J., Smith, P.R., Grasser, F.A. and Griffin, B.E. (1994) EBNA-1, the major nuclear antigen of Epstein-Barr virus, resembles 'RGG' RNA binding proteins. *Embo J*, **13**, 4840-4847.

Spano, J.P., Busson, P., Atlan, D., Bourhis, J., Pignon, J.P., Esteban, C. and Armand, J.P. (2003) Nasopharyngeal carcinomas: an update. *Eur J Cancer*, **39**, 2121-2135.

Speck, S.H., Chatila, T. and Flemington, E. (1997) Reactivation of Epstein-Barr virus: regulation and function of the BZLF1 gene. *Trends Microbiol*, **5**, 399-405.

Steven, N.M. (1996) Infectious Mononucleosis. *Epstein-Barr Virus Report*, **3**, 91-95.

Stevenson, D., Charalambous, C. and Wilson, J.B. (2005) Epstein-Barr virus latent membrane protein 1 (CAO) up-regulates VEGF and TGF alpha concomitant with hyperlasia, with subsequent up-regulation of p16 and MMP9. *Cancer Res*, **65**, 8826-8835.

Strasser, A., Harris, A.W., Bath, M.L. and Cory, S. (1990) Novel primitive lymphoid tumours induced in transgenic mice by cooperation between myc and bcl-2. *Nature*, **348**, 331-333.

Subramanian, C., Knight, J.S. and Robertson, E.S. (2002) The Epstein Barr nuclear antigen EBNA3C regulates transcription, cell transformation and cell migration. *Front Biosci*, 7, d704-716.

Sugawara, Y., Mizugaki, Y., Uchida, T., Torii, T., Imai, S., Makuuchi, M. and Takada, K. (1999) Detection of Epstein-Barr virus (EBV) in hepatocellular carcinoma tissue: a novel EBV latency characterized by the absence of EBV-encoded small RNA expression. *Virology*, **256**, 196-202.

Swaminathan, S., Tomkinson, B. and Kieff, E. (1991) Recombinant Epstein-Barr virus with small RNA (EBER) genes deleted transforms lymphocytes and replicates in vitro. *Proc Natl Acad Sci U S A*, **88**, 1546-1550.

Szekely, L., Selivanova, G., Magnusson, K.P., Klein, G. and Wiman, K.G. (1993) EBNA-5, an Epstein-Barr virus-encoded nuclear antigen, binds to the retinoblastoma and p53 proteins. *Proc Natl Acad Sci U S A*, **90**, 5455-5459.

Takada, K. (1984) Cross-linking of cell surface immunoglobulins induces Epstein-Barr virus in Burkitt lymphoma lines. *Int J Cancer*, **33**, 27-32.

Takada, K., Horinouchi, K., Ono, Y., Aya, T., Osato, T., Takahashi, M. and Hayasaka, S. (1991) An Epstein-Barr virus-producer line Akata: establishment of the cell line and analysis of viral DNA. *Virus Genes*, **5**, 147-156.

Takada, K. and Nanbo, A. (2001) The role of EBERs in oncogenesis. *Semin Cancer Biol*, **11**, 461-467.

Tanaka, H. and Samuel, C.E. (1994) Mechanism of interferon action: structure of the mouse PKR gene encoding the interferon-inducible RNA-dependent protein kinase. *Proc Natl Acad Sci U S A*, **91**, 7995-7999.

Taniguchi, T. and Takaoka, A. (2001) A weak signal for strong responses: interferon-alpha/beta revisited. *Nat Rev Mol Cell Biol*, **2**, 378-386.

Taniguchi, T. and Takaoka, A. (2002) The interferon-alpha/beta system in antiviral responses: a multimodal machinery of gene regulation by the IRF family of transcription factors. *Curr Opin Immunol*, **14**, 111-116.

Tarkowski, A.K. (1959) Experiments on the development of isolated blastomers of mouse eggs. *Nature*, **184**, 1286-1287.

Thierfelder, W.E., van Deursen, J.M., Yamamoto, K., Tripp, R.A., Sarawar, S.R., Carson, R.T., Sangster, M.Y., Vignali, D.A., Doherty, P.C., Grosveld, G.C. and Ihle, J.N. (1996) Requirement for Stat4 in interleukin-12-mediated responses of natural killer and T cells. *Nature*, **382**, 171-174.

Thorley-Lawson, D.A. and Gross, A. (2004) Persistence of the Epstein-Barr virus and the origins of associated lymphomas. *N Engl J Med*, **350**, 1328-1337.

Toczyski, D.P., Matera, A.G., Ward, D.C. and Steitz, J.A. (1994) The Epstein-Barr virus (EBV) small RNA EBER1 binds and relocalizes ribosomal protein L22 in EBV-infected human B lymphocytes. *Proc Natl Acad Sci U S A*, **91**, 3463-3467.

Toczyski, D.P. and Steitz, J.A. (1991) EAP, a highly conserved cellular protein associated with Epstein-Barr virus small RNAs (EBERs). *Embo J*, **10**, 459-466.

Toczyski, D.P. and Steitz, J.A. (1993) The cellular RNA-binding protein EAP recognizes a conserved stem-loop in the Epstein-Barr virus small RNA EBER 1. *Mol Cell Biol*, **13**, 703-710.

Tomkinson, B. and Kieff, E. (1992) Use of second-site homologous recombination to demonstrate that Epstein-Barr virus nuclear protein 3B is not important for lymphocyte infection or growth transformation in vitro. *J Virol*, **66**, 2893-2903.

Tomkinson, B., Robertson, E. and Kieff, E. (1993) Epstein-Barr virus nuclear proteins EBNA-3A and EBNA-3C are essential for B-lymphocyte growth transformation. *J Virol*, **67**, 2014-2025.

Tornell, J., Farzad, S., Espander-Jansson, A., Matejka, G., Isaksson, O. and Rymo, L. (1996) Expression of Epstein-Barr nuclear antigen 2 in kidney tubule cells induce tumors in transgenic mice. *Oncogene*, **12**, 1521-1528.

Tsimbouri, P., Drotar, M.E., Coy, J.L. and Wilson, J.B. (2002) bcl-xL and RAG genes are induced and the response to IL-2 enhanced in EmuEBNA-1 transgenic mouse lymphocytes. *Oncogene*, **21**, 5182-5187.

Tsuji-Takayama, K., Aizawa, Y., Okamoto, I., Kojima, H., Koide, K., Takeuchi, M., Ikegami, H., Ohta, T. and Kurimoto, M. (1999) Interleukin-18 induces interferon-gamma production through NF-kappaB and NFAT activation in murine T helper type 1 cells. *Cell Immunol*, **196**, 41-50.

Tsurumi, T., Fujita, M. and Kudoh, A. (2005) Latent and lytic Epstein-Barr virus replication strategies. *Rev Med Virol*, **15**, 3-15.

Verbeek, S., van Lohuizen, M., van der Valk, M., Domen, J., Kraal, G. and Berns, A. (1991) Mice bearing the E mu-myc and E mu-pim-1 transgenes develop pre-B-cell leukemia prenatally. *Mol Cell Biol*, **11**, 1176-1179.

Visvanathan, K.V. and Goodbourn, S. (1989) Double-stranded RNA activates binding of NF-kappa B to an inducible element in the human beta-interferon promoter. *Embo J*, **8**, 1129-1138.

Vousden, K.H., Crook, T. and Farrell, P.J. (1993) Biological activities of p53 mutants in Burkitt's lymphoma cells. *J Gen Virol*, **74 (Pt 5)**, 803-810.

Vuyisich, M., Spanggord, R.J. and Beal, P.A. (2002) The binding site of the RNA-dependent protein kinase (PKR) on EBER1 RNA from Epstein-Barr virus. *EMBO Rep*, **3**, 622-627.

Wagner, T.E., Hoppe, P.C., Jollick, J.D., Scholl, D.R., Hodinka, R.L. and Gault, J.B. (1981) Microinjection of a rabbit beta-globin gene into zygotes and its subsequent expression in adult mice and their offspring. *Proc Natl Acad Sci U S A*, **78**, 6376-6380.

Waldschmidt, T.J., Conrad, D.H. and Lynch, R.G. (1988) The expression of B cell surface receptors. I. The ontogeny and distribution of the murine B cell IgE Fc receptor. *J Immunol*, **140**, 2148-2154.

Waldschmidt, T.J. and Tygrett, L.T. (1992) The low affinity IgE Fc receptor (CD23) participates in B cell activation. *Adv Exp Med Biol*, **323**, 149-156.

Walker, W., Zhou, Z.Q., Ota, S., Wynshaw-Boris, A. and Hurlin, P.J. (2005) Mnt-Max to Myc-Max complex switching regulates cell cycle entry. *J Cell Biol*, **169**, 405-413.

Wang, D., Liebowitz, D. and Kieff, E. (1985) An EBV membrane protein expressed in immortalized lymphocytes transforms established rodent cells. *Cell*, **43**, 831-840.

Wang, F., Gregory, C.D., Rowe, M., Rickinson, A.B., Wang, D., Birkenbach, M., Kikutani, H., Kishimoto, T. and Kieff, E. (1987) Epstein-Barr virus nuclear antigen 2 specifically induces expression of the B-cell activation antigen CD23. *Proc Natl Acad Sci U S A*, **84**, 3452-3456.

Wang, F., Tsang, S.F., Kurilla, M.G., Cohen, J.I. and Kieff, E. (1990) Epstein-Barr virus nuclear antigen 2 transactivates latent membrane protein LMP1. *J Virol*, **64**, 3407-3416.

Wang, J. and Boxer, L.M. (2005) Regulatory elements in the immunoglobulin heavy chain gene 3'-enhancers induce c-myc deregulation and lymphomagenesis in murine B cells. *J Biol Chem*, **280**, 12766-12773.

Wang, X. and Hutt-Fletcher, L.M. (1998) Epstein-Barr virus lacking glycoprotein gp42 can bind to B cells but is not able to infect. *J Virol*, **72**, 158-163.

Wells, S.M., Kantor, A.B. and Stall, A.M. (1994) CD43 (S7) expression identifies peripheral B cell subsets. *J Immunol*, **153**, 5503-5515.

Wen, Z., Zhong, Z. and Darnell, J.E., Jr. (1995) Maximal activation of transcription by Stat1 and Stat3 requires both tyrosine and serine phosphorylation. *Cell*, **82**, 241-250.

Wensing, B., Stuhler, A., Jenkins, P., Hollyoake, M., Karstegl, C.E. and Farrell, P.J. (2001) Variant chromatin structure of the oriP region of Epstein-Barr virus and regulation of EBER1 expression by upstream sequences and oriP. *J Virol*, **75**, 6235-6241.

Whittingham, D.G. (1968) Fertilization of mouse eggs in vitro. *Nature*, **220**, 592-593.

Wilkie, T.M., Brinster, R.L. and Palmiter, R.D. (1986) Germline and somatic mosaicism in transgenic mice. *Dev Biol*, **118**, 9-18.

Williams, B.R. (1999) PKR; a sentinel kinase for cellular stress. *Oncogene*, **18**, 6112-6120.

Wilson, J.B. (1997) transgenic Mouse Models of Disease and Epstein-Barr Virus. *Epstein-Barr Virus Report*, **4**, 63-72.

Wilson, J.B., Bell, J.L. and Levine, A.J. (1996) Expression of Epstein-Barr virus nuclear antigen-1 induces B cell neoplasia in transgenic mice. *Embo J*, **15**, 3117-3126.

Wilson, J.B. and Levine, A.J. (1992) The oncogenic potential of Epstein-Barr virus nuclear antigen 1 in transgenic mice. *Curr Top Microbiol Immunol*, **182**, 375-384.

Wilson, J.B., Weinberg, W., Johnson, R., Yuspa, S. and Levine, A.J. (1990) Expression of the BNLF-1 oncogene of Epstein-Barr virus in the skin of transgenic mice induces hyperplasia and aberrant expression of keratin 6. *Cell*, **61**, 1315-1327.

Wong, H.L., Wang, X., Chang, R.C., Jin, D.Y., Feng, H., Wang, Q., Lo, K.W., Huang, D.P., Yuen, P.W., Takada, K., Wong, Y.C. and Tsao, S.W. (2005) Stable expression of EBERs in immortalized nasopharyngeal epithelial cells confers resistance to apoptotic stress. *Mol Carcinog*, **44**, 92-101.

Wu, T.C., Mann, R.B., Epstein, J.I., MacMahon, E., Lee, W.A., Charache, P., Hayward, S.D., Kurman, R.J., Hayward, G.S. and Ambinder, R.F. (1991) Abundant expression of EBER1 small nuclear RNA in nasopharyngeal carcinoma. A morphologically distinctive target for detection of Epstein-Barr virus in formalin-fixed paraffin-embedded carcinoma specimens. *Am J Pathol*, **138**, 1461-1469.

Yagita, H., Nakamura, T., Karasuyama, H. and Okumura, K. (1989) Monoclonal antibodies specific for murine CD2 reveal its presence on B as well as T cells. *Proc Natl Acad Sci U S A*, **86**, 645-649.

Yajima, M., Kanda, T. and Takada, K. (2005) Critical role of Epstein-Barr Virus (EBV)-encoded RNA in efficient EBV-induced B-lymphocyte growth transformation. *J Virol*, **79**, 4298-4307.

Yamamoto, N., Takizawa, T., Iwanaga, Y. and Shimizu, N. (2000) Malignant transformation of B lymphoma cell line BJAB by Epstein-Barr virus-encoded small RNAs. *FEBS Lett*, **484**, 153-158.

Yang, L., Aozasa, K., Oshimi, K. and Takada, K. (2004) Epstein-Barr virus (EBV)-encoded RNA promotes growth of EBV-infected T cells through interleukin-9 induction. *Cancer Res*, **64**, 5332-5337.

Yates, J.L., Warren, N. and Sugden, B. (1985) Stable replication of plasmids derived from Epstein-Barr virus in various mammalian cells. *Nature*, **313**, 812-815.

Young, L.S. and Rickinson, A.B. (2004) Epstein-Barr virus: 40 years on. *Nat Rev Cancer*, **4**, 757-768.

Yukawa, K., Kikutani, H., Inomoto, T., Uehira, M., Bin, S.H., Akagi, K., Yamamura, K. and Kishimoto, T. (1989) Strain dependency of B and T lymphoma development in immunoglobulin heavy chain enhancer (E mu)-myc transgenic mice. *J Exp Med*, **170**, 711-726.

Zacny, V.L., Wilson, J. and Pagano, J.S. (1998) The Epstein-Barr virus immediate-early gene product, BRLF1, interacts with the retinoblastoma protein during the viral lytic cycle. *J Virol*, **72**, 8043-8051.

Zamanian-Daryoush, M., Mogensen, T.H., DiDonato, J.A. and Williams, B.R. (2000) NF-kappaB activation by double-stranded-RNA-activated protein kinase (PKR) is mediated through NF-kappaB-inducing kinase and IkappaB kinase. *Mol Cell Biol*, **20**, 1278-1290.

Zhang, L. and Pagano, J.S. (2002) Structure and function of IRF-7. *J Interferon Cytokine Res*, **22**, 95-101.

Zhang, Y., Finegold, M.J., Porteu, F., Kanteti, P. and Wu, M.X. (2003) Development of T-cell lymphomas in Emu-IEX-1 mice. *Oncogene*, **22**, 6845-6851.

Zhou, A., Paranjape, J., Brown, T.L., Nie, H., Naik, S., Dong, B., Chang, A., Trapp, B., Fairchild, R., Colmenares, C. and Silverman, R.H. (1997) Interferon action and apoptosis are defective in mice devoid of 2',5'-oligoadenylate-dependent RNase L. *Embo J*, **16**, 6355-6363.

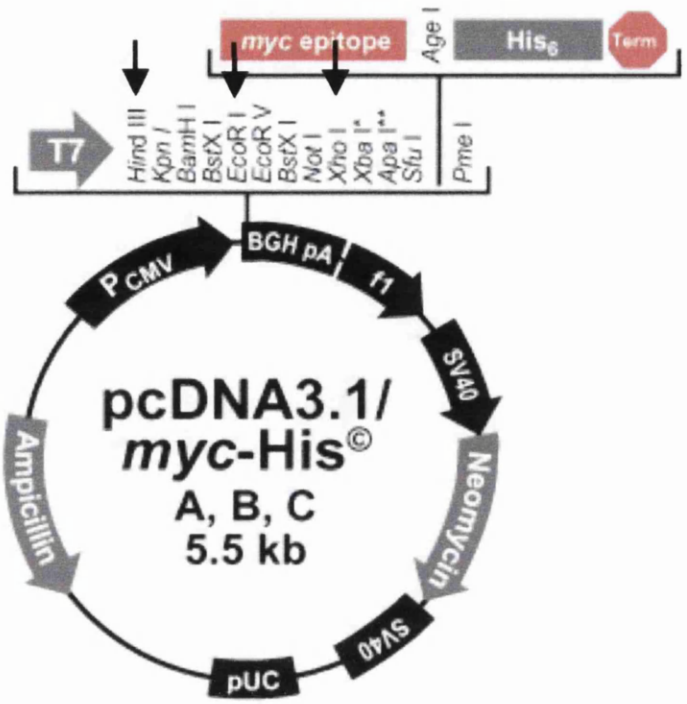

Appendix 1: pcDNA3.1 vector from Invitrogen

The figure shows the pcDNA3.1 vector which was used to clone the three different EBER1 inserts. The Eμ was first cloned using *Hind*III and *Eco*RI restriction sites and the different EBER1 inserts were cloned using *Eco*RI and *Xho*I restriction sites. These sites are indicated by arrows. The figure of the vector was taken from Invitrogen's website.